Drug targeting to tumors using HPMA copolymers

- revisiting PK1 and partners -

Twan Lammers

Drug targeting to tumors using HPMA copolymers

PhD thesis with a summary in Dutch

Twan Lammers
Department of Pharmaceutics, Utrecht University, Utrecht, The Netherlands
Department of Innovative Cancer Diagnosis and Therapy, Clinical Cooperation Unit Radiotherapeutic Oncology, German Cancer Research Center, Heidelberg, Germany

ISBN: 978-90-393-5114-7

Printed by Ipskamp Drukkers B.V., Enschede, The Netherlands

Drug targeting to tumors using HPMA copolymers

HPMA copolymeren voor tumor-gericht geneesmiddeltransport

(met een samenvatting in het Nederlands)

Proefschrift

ter verkrijging van de graad van doctor aan de Universiteit Utrecht
op gezag van de rector magnificus, prof. dr. J.C. Stoof,
ingevolge het besluit van het college voor promoties
in het openbaar te verdedigen op maandag 21 september 2009 des middags te 4.15 uur

door

Twan Gerardus Gertrudis Maria Lammers

geboren op 30 augustus 1979 te Vlodrop

Promotoren: Prof. dr. G. Storm
Prof. dr. ir. W.E. Hennink

all that we see or seem
is but a dream within a dream

Edgar Allen Poe (1809-1849)

Table of contents

Appendices

Chapter 1

Introduction:
Drug targeting to tumors using HPMA copolymers

Twan Lammers[a,b]

[a] Department of Pharmaceutics, Utrecht Institute for Pharmaceutical Sciences, Utrecht University, Sorbonnelaan 16, 3584 CA Utrecht, The Netherlands
[b] Department of Innovative Cancer Diagnosis and Therapy, Clinical Cooperation Unit Radiotherapeutic Oncology, German Cancer Research Center, Im Neuenheimer Feld 280, 69120 Heidelberg, Germany

Adv. Drug Deliv. Rev. (in preparation: 2010)

Abstract

The work described in this thesis deals with drug targeting to tumors using HPMA copolymers, and with the use of long-circulating and passively tumor-targeted polymeric nanomedicines for improving the efficacy of combined modality anticancer therapy. In this initial chapter, the basic aspects of cancer, cancer therapy, drug targeting and drug targeting to tumors using HPMA copolymers are briefly introduced, and the aims of our efforts are outlined.

Cancer is a complex disease. Not only is it difficult to understand and to treat cancer, it is even difficult to define cancer. Cancer is an umbrella term, used to describe a large number of different disease states all characterized by excessive cell growth (Figure 1). This rapid and uncontrolled cellular expansion results from (a series of) inherited and/or acquired genetic and epigenetic changes, giving rise a phenotype which I) is self-sufficient in providing growth signals; II) is insensitive to anti-growth signals; III) has limitless replicative potential; IV) evades apoptosis; V) induces angiogenesis; and VI) stimulates invasion and metastasis [1]. Cancers generally develop gradually, from relatively slowly growing benign lesions, to millimiter-sized non-vascularized nodules, to vascularized in situ tumors, to rapidly expanding primary tumors, to tumors infiltrating neighboring tissues, and to metastatic lesions developing in distant organs. Cancers kill by colonizing and damaging the tissues in which they develop, and by disrupting vital organ functions. Cancer affects hundreds of millions of people worldwide, and it accounts for eight million deaths annually [2].

Treatments for cancer rely on (combinations of) surgery, radiotherapy and chemotherapy. To a lesser extent, also hormone therapy, hyperthermia, immunotherapy and stem cell therapy are used. The success rate of anticancer therapy strongly depends on disease stage at the time of diagnosis. If detected early, many malignancies can be treated relatively well, using surgery to locally remove as many tumor cells as possible. If tumors cannot be resected, or if only part of the lesion can be removed surgically, radio- and chemotherapy are used. Depending on the nature, location and stage of the malignancy, various different types of radio- and chemotherapy can be administered. Radiotherapy can be given as external beam radiotherapy, as brachytherapy and as radio-immunotherapy. Brachytherapy relies on the local (i.e. intratumoral) implantation of sealed seeds loaded with radionuclides, and radio-immunotherapy relates to the intravenous injection of radionuclide-labeled antibodies, which selectively bind (and kill) cancer cells. The most effective (and by far most often used) form of radiotherapy is external beam radiotherapy. External beam radiotherapy relies on the use of an external (i.e. extracorporal) source of radiation, such as a linear accelerator, or cesium- or cobalt-containing devices. By means of multi-leaf collimators and computers, the generated rays of photons (or particles) can be delivered to tumors with extremely high levels of spatial specificity. By at the same time administering radiotherapy in fractions (i.e. at low doses, on every weekday, for several consecutive weeks) and from various different angles (i.e.

intensity-modulated radiotherapy), damage to tumor cells can be optimized, while toxicity towards healthy tissues can be attenuated. Radiotherapy is an effective means for treating various different types of tumors, but there are also cases in which it is not very helpful, e.g. in case of hematological malignancies, in case of radioresistant cancers, and in case of metastases. Radiotherapy is used in about 50% of all patients, and it is often combined with surgery and with chemotherapy.

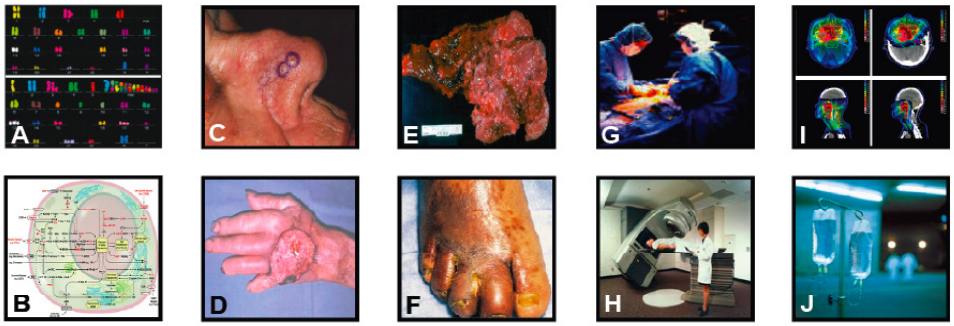

Figure 1: Cancer and cancer therapy. Cancer is a complex disease, resulting from changes at the genetic (A: chromosomal aberrations in cancer cells (bottom panel) versus normal cells (top panel) visualized using fluorescent in-situ hybridization) and signaling level (B: schematic overview of key pathways deregulated in cancer (see [1] for details)). The phenotypic appearance of cancer can be very diverse, ranging from barely detectable malignant melanomas (C), to more obvious squamous cell carcinomas (D), lung carcinomas (E) and Kaposi Sarcomas (F). Treatments for cancer primarily rely on (combinations of) surgery (G), radiotherapy (H-I) and chemotherapy (J). See page 225.

As opposed to radiotherapy, **chemotherapy** is generally administered systemically. It can, however, also be given locally (i.e. intratumorally), for instance in case of aggressively growing brain tumors, like glioblastoma. Systemic chemotherapy is used to treat inoperable tumors, secondary malignancies, radioresistant tumors, circulating tumor cells and metastatic lesions. It is generally combined with surgery and with radiotherapy, and in such settings, it is given either as adjuvant chemotherapy (after surgical and/or radiotherapeutic intervention; to remove residual tumor cells and to avoid recurrence), or as neoadjuvant chemotherapy (prior to surgery and/or radiotherapy; to reduce tumor masses). Routinely used chemotherapeutic agents include the intercalating agent doxorubicin, the alkylating agent cisplatin, the microtubule inhibitor paclitaxel and the antimetabolite gemcitabine. Such prototypic anticancer agents all inhibit cell growth by inhibiting processes involved in DNA duplication and cell division, and they are therefore only able to

discriminate between tumor cells and healthy cells on the basis of their proliferative index. Consequently, 'classical' chemotherapeutic drugs not only kill cancer cells, but all rapidly dividing cells, and besides in tumor growth inhibition, their intravenous administration generally also results in bone marrow depression, in damage to the gastrointestinal mucosa and in death of hair cells.

Significant progress has been made over the years in understanding the principles of malignant transformation and tumorigenesis. These improved insights into the genetic and (patho-) physiological processes contributing to cancer have resulted in the development of several novel (classes of) anticancer agents. Such '**targeted therapeutics**', like the growth factor receptor inhibitor Herceptin, the proteasome inhibitor Velcade, the histone deacetylase inhibitor Vorinostat and the anti-angiogenic agent Avastin, all more selectively interfere with certain 'hallmarks of cancer' [1], like with the overexpression of growth factors and growth factor receptors, with the altered balance between apoptosis and anti-apoptosis, with the numerous genetic and epigenetic changes that are present in cancer cells, and with the development of a dense vascular network, needed to provide tumours with oxygen and nutrients. By means of their pharmacologically and/or physiologically more optimal mechanism of action, such 'molecularly targeted therapeutics' have been shown to more preferentially kill cancer cells, both in vitro and in vivo, and to improve the balance between the efficacy and the toxicity of systemic anticancer therapy [3-5].

An important, but often neglected property that such second-generation therapeutics share with their first generation DNA-damaging counterparts, however, is that upon **intravenous administration**, their pharmacokinetics and their tissue distribution tend to be far from optimal. Because of their low molecular weight, for instance, the vast majority of routinely used anticancer agents are rapidly cleared from the circulation (by means of renal filtration), and they do not accumulate well in tumours and in tumour cells. Also, because of their small size and their (generally) high hydrophobicity, drug molecules often have a large volume of distribution, and they tend to accumulate in (and cause toxicity towards) many different healthy tissues. In addition to this, as outlined in Table 1, a large number of other barriers need to be overcome before an i.v. applied agent can elicit antitumor efficacy, related e.g. to enzymatic and hepatic degradation, to the high interstitial fluid pressure that is typical of tumors, to cellular and nuclear membranes, and to the presence of drug efflux pumps.

Barriers to drug delivery to tumors			
Chemical barriers	**Biological barriers**	**Physical barriers**	**Clinical barriers**
Low solubility	Renal filtration	Vascular endothelium	Low efficacy
Low stability	Hepatic degradation	Perivascular space	High toxicity
Low molecular weight	High tumor cell density	Cellular membrane	Need for hospitalization
Large volume of distribution	High interstitial fluid pressure	Nuclear membrane	Frequent administration
Charge interactions	Drug efflux pumps	Blood brain barrier	Low cost-effectiveness

Table 1. Overview of factors limiting the delivery of i.v. applied anticancer agents to tumors. Note that several barriers are inter-related, and that not all barriers apply to all types of (chemo-) therapeutics.

To assist i.v. applied anticancer agents in overcoming such barriers, and to improve the balance between their efficacy and their toxicity, a large number of **drug delivery systems** have been developed over the years, ranging in nature from 'simple' liposomes [6-8], polymers [9-11] and micelles [12-14], to bacterially derived 'Minicells' [15] and temporally targeted 'Nanocells' [16]. The majority of these systems essentially intend to improve the circulation time of the conjugated or entrapped active agent and, by doing so, to enable it to exploit the physiological fact that solid tumors tend to present with a tortuous and poorly differentiated vasculature, that in contrast to the vasculature in healthy tissues, allows for the extravasation of (carrier) materials with sizes of up to several hundreds of nanometers [17-19]. Together with the fact that solid tumors tend to lack functional lymphatics, and therefore are unable to eliminate extravasated (carrier) materials, this increase in vascular leakiness allows long-circulating nanomedicines to effectively accumulate in tumors over time, by means of a mechanism known as the Enhanced Permeability and Retention (EPR) effect [20-22]. The exploitation of the EPR effect is arguably the most important strategy for improving the delivery of low molecular weight (chemo-) therapeutic agents to tumors, and because of the fact that it essentially only relies on the pathophysiological properties of the target tissue, it is generally referred to as passive drug targeting [23-25]. Active drug targeting, on the other hand, relies on the use of targeting ligands, like antibodies and peptides, which specifically recognize receptor structures expressed at the target site, and which are used to improve target site accumulation and/or target cell uptake [26-28]. The principles of passive and active drug targeting, and several clinically relevant examples of tumor-targeted nanomedicines, are depicted schematically in Figure 2.

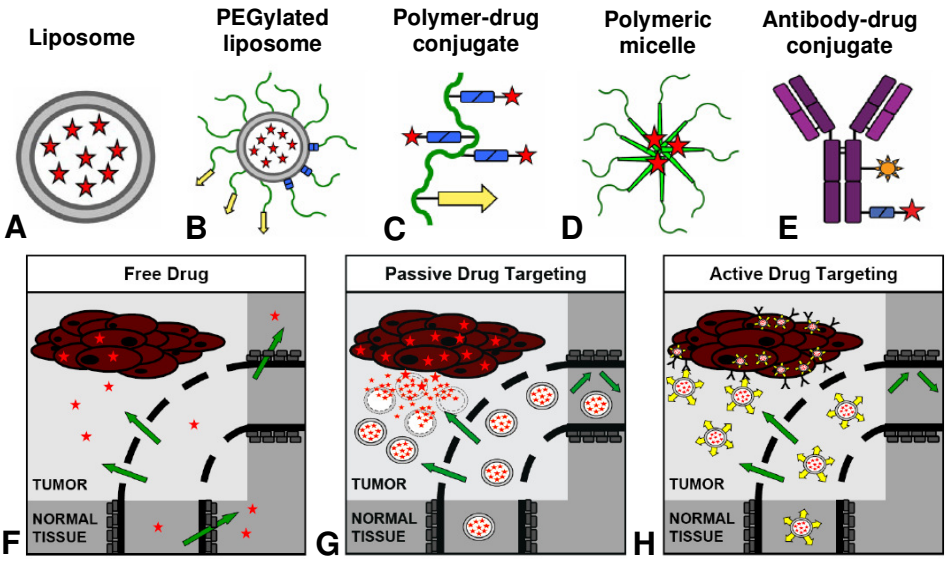

Figure 2: Drug delivery systems and drug targeting strategies. A-E: Examples of clinically used tumor-targeted nanomedicines. Liposomes and liposomal bilayers are depicted in grey, polymers and polymer-coatings in green, linkers allowing for drug release and for sheddable stealth coatings in blue (rectangles), targeting ligands in yellow (arrows), antibodies and antibody fragment in purple, radionuclides in orange (suns) and conjugated or entrapped active agents in red (stars). F-H: Principles of passive and active drug targeting to tumors. F: Upon i.v. injection, a low molecular weight anticancer agent is generally rapidly cleared from the circulation, and only low levels of the drug accumulate in tumors and in tumor cells. At the same, due to its small size, high hydrophobicity and/or large volume of distribution, significant levels of the agent accumulate in healthy tissues. G: Upon encapsulation in (or conjugation to) a long-circulating and passively tumor-targeted drug delivery system, the concentration of the active agent in tumors can be increased substantially (by means of Enhanced Permeability and Retention (EPR)), while its accumulation in healthy tissues can be attenuated. H: Upon the incorporation of targeting ligands, like antibodies and peptides, the interaction between the drug and/or drug delivery system and cancer cells can be improved, resulting in a more selective target site localization and/or target cell uptake. See page 225.

Of the passively targeted nanomedicine systems developed thus far, most progress has been made with **liposomes**. Liposomes are self-assembling colloid structures composed of lipid bilayers, and they can encapsulate a wide variety of pharmacologically active agents in their aqueous interiors. Myocet and Caelyx (Doxil in the US) were the first of such lipid formulations to be approved by the regulatory authorities. Both products contain doxorubicin, but differ particularly in the presence of a ‘stealth’ coating: the former refers to doxorubicin entrapped in uncoated liposomes, and the latter to liposomes surface-modified (or ‘sterically stabilized’) with poly(ethylene glycol), to reduce recognition by the

reticuloendothelial system, and to prolong circulation times [29,30]. The pharmacokinetic benefits of liposomal drug targeting (and of polymeric stealth coatings) can be illustrated as follows: for doxorubicin, an elimination half-life time of 0.2 h and a clearance of 45 l/h were found in patients, as compared to 2.5 h and 5 l/h for Myocet, and to 55 h and 0.02 l/h for Caelyx [31]. The resulting AUC's (i.e. area under the curve; reflecting drug availability in blood) were 4, 45 and 900 µg/ml*h, respectively. Both in animal models and in patients, such improvements in AUC have been shown to result in significant improvements in EPR-mediated drug targeting to tumours, and both PEGylated and non-PEGylated liposomes have been shown to be able to improve the balance between the efficacy and the toxicity of drug therapy.

Ten years after the first report on liposomes [32], and coinciding with the appreciation of their clinical potential [33], Helmut Ringsdorf proposed in 1975 that also natural and synthetic **polymers** might hold potential for passive drug targeting [34]. As depicted schematically in Figure 3A, he envisioned that a pharmacologically active agent can be conjugated to a long-circulating macromolecular drug carrier by means of a linker that is stable in blood, but labile in the acidic and/or enzymatic conditions typical for e.g. the tumor microenvironment or for certain intracellular compartments.

Based on the concept proposed by Ringsdorf, in the late 1970-ies and early 1980-ies, Jindrich Kopecek and colleagues at the Institute of Macromolecular Chemistry at the Czech Academy of Sciences in Prague started synthesizing polymer-drug conjugates based on **HPMA** (*N*-(2-hydroxypropyl)methacrylamide; see Figure 3). They choose to use polymers based on HPMA as these had already been developed as plasma expanders for infusion solutions, and as they were known to be non-immunogenic and non-toxic, and to reside in the circulation well [35,36]. In initial proof-of-principle experiments, together with Pavla Kopeckova, Ruth Duncan, Karel Ulbrich and several others, methods were developed for reproducibly synthesizing HPMA copolymers, and for functionalizing them with drugs [37-41]. Based on De Duve's concept of lysosomotropic drug delivery [42], oligopeptide sequences were identified which are stable in blood and extracellularly, but which effectively release the attached active agent upon endocytosis and exposure to lysosomal enzymes [43-46]. The tetrapeptide spacer GFLG, which is cleaved by lysosomal cathepsins at low pH, was identified as a suitable spacer, and doxorubicin was selected as a drug.

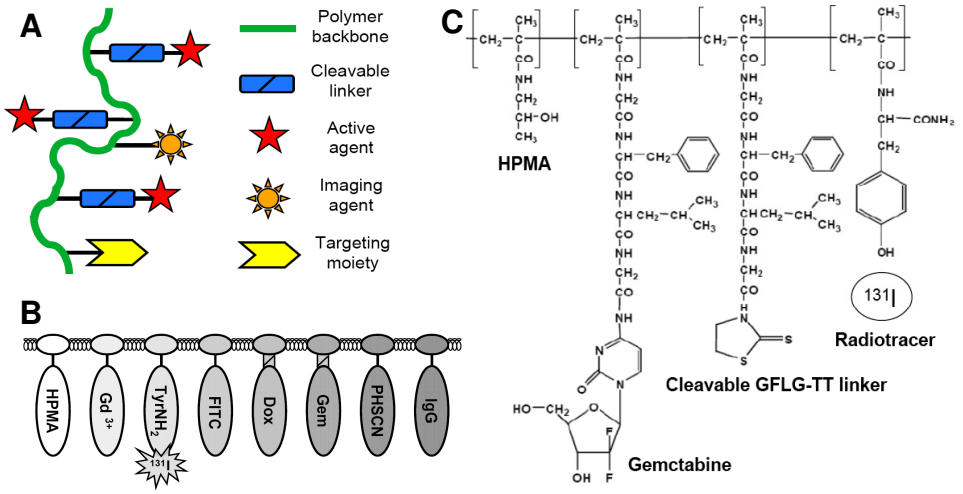

Figure 3: Polymer-drug conjugates based on HPMA. A: Schematic overview of the components routinely used in polymer therapeutics. B: Examples of imaging agents (gadolinium and radioactive iodine), fluorophores (fluorescein isothiocyanate), drug molecules (doxorubicin and gemcitabine) and targeting ligands (oligopeptides and antibodies) incorporated into HPMA copolymers. C: Chemical structure of an exemplary HPMA copolymer, functionalized with tyrosinamide (for radiolabeling), with GFLG-gemcitabine (for drug delivery and release), and with remaining GFLG-TT reactive groups (for attaching additional components, like a targeting moiety). The chemical formula of this copolymer is poly(HPMA-co-MA-GFLG-gemcitabine-co-MA-GFLG-TT-co-MA-TyrNH$_2$). On average, HPMA copolymers contain 80-95 wt-% of HPMA, 5-10 wt-% of drug and 1-2 wt-% of tyrosinamide and imaging agent. See page 226.

In initial in vitro experiments, doxorubicin release from GFLG spacers was confirmed, and **poly(HPMA-co-MA-GFLG-doxorubicin)** was shown to effectively kill cancer cells [47,48]. In subsequent in vivo analyses, the conjugate was shown to circulate for prolonged periods of time, and to effectively accumulate in tumors by means of EPR. In mice bearing B16F10 melanomas, for instance, the total amount of doxorubicin delivered to tumors within the first 48 h after i.v. injection was found to be up to 75 times higher upon the administration of poly(HPMA-co-MA-GFLG-doxorubicin) than upon the administration of the free drug [49]. Experiments with radiolabeled polymeric prodrugs substantiated these findings, as did ex vivo microscopy studies and HPLC analyses, demonstrating that HPMA copolymers present with a very beneficial biodistribution, and accumulate in tumors both effectively and selectively [50-52]. Low levels of the copolymer were found in the majority of healthy tissues, and high levels were essentially only detected in tumors and in organs of the reticulo-endothelial system (like liver and spleen), which are known

to be involved are in the clearance of long-circulating nanomedicines. Additional analyses demonstrated that HPMA copolymers are able to attenuate the accumulation of doxorubicin in the heart, which is particularly sensitive to treatment with this drug, reducing its peak concentration by more than two orders of magnitude [53]. As a result of this beneficial biodistribution, in experiments addressing the therapeutic potential of poly(HPMA-co-MA-GFLG-doxorubicin), the passively tumor-targeted polymeric prodrug was not only found to be more effective, but also to be less toxic than free doxorubicin. Regarding efficacy, improvements in growth inhibition were achieved in several different tumors models, including e.g. in L1210 leukemia, B16F10 melanoma, M5076 sarcoma and LS174T colon carcinoma, as well as in doxorubicin-resistant A2780/AD ovarian carcinoma (which does not respond to treatment with free doxorubicin) [49,54-56]. Regarding toxicity, the maximum tolerated dose of poly(HPMA-co-MA-GFLG-doxorubicin) was found to be 4-5 times higher than that of free doxorubicin, and the targeted agent induced less cardiomyopathy and less weight loss [57,58].

Following these promising proof-of-principle findings in animal models, in 1994, poly(HPMA-co-MA-GFLG-doxorubicin) became the first passively tumor-targeted polymeric prodrug to enter clinical trials [59,60]. The conjugate was termed **PK1**, i.e. Prague-Keele 1, it had an average molecular weight of ~28 kDa (corresponding to a hydrodynamic diameter of ~5 nm), and it contained ~8 weight-% of doxorubicin [61]. This rather small size – liposomes tend to be 100-150 nm and micelles 20-80 nm – was selected because it is just large enough to enable passive drug targeting, but at the same also just small enough to allow for renal excretion. Renal excretion was considered to be required as the polymeric backbone of PK1 is non-biodegradable, and as the threshold for kidney clearance is ~45 kDa. A total of 100 cycles of PK1 were administered in this trial, at doses ranging from 20 to 320 mg/m^2, to 36 heavily pretreated patients with various different types of tumors [60]. Using an iodine-131-labeled version of PK1 and γ-scintigraphy, in 21 of these patients, the biodistribution and the tumor accumulation of the polymeric prodrug were visualized, and some initial 'image-guided' insights into the passive targeting potential of HPMA copolymers were provided. The initial half-life time (i.e. $t_{1/2\alpha}$) of PK1 was found to be 2.7 h, as compared to less than 10 minutes for free doxorubicin [62], and effective drug targeting to tumors could be demonstrated in several different cases [60]. Two partial and two minor responses were observed, in patients with

non-small cell lung cancer, colorectal cancer and doxorubicin-resistant breast cancer, and no increases in toxicity were observed, in spite of the high overall doses administered [60]. The maximum tolerated dose of PK1 was found to be higher than that of free doxorubicin (320 mg/m^2 vs. 60-80 mg/m^2), and even at cumulative doses of up to 1680 mg/m^2, no signs of cardiotoxicity were observed. Dose-limiting toxicities were neutropenia and mucositis, and the recommended phase II dose was 280 mg/m^2.

Not long after completing the phase I study on PK1, **PK2** entered clinical trials [63,64]. PK2 was the first actively targeted polymeric prodrug to be evaluated in patients, and it remains to be the only one to date. In PK2, galactosamine was used as a targeting ligand, to improve drug delivery to the liver (i.e. to hepatocytes, which express high levels of the asialoglycprotein receptor, to which galactosamine binds [65,66]). The biodistribution of PK2 was visualized by means of γ-scintigraphy and SPECT, and as expected, the targeted agent effectively accumulated in the liver [64]. Somewhat disappointingly, however, it was also observed that the levels of PK2 in liver tumors (3±6 % of the injected dose) were substantially lower than its levels in healthy liver tissue (17±4 %ID), which can be explained by taking the smaller size of liver tumors as compared to healthy livers into account, as well as the fact that liver tumors tend to be less well-perfused and less well-vascularized. Antitumor responses were observed in several patients with advanced liver carcinomas, and included two partial remissions lasting for more than two years [64]. Dose-limiting side effects were comparable to those of PK1, and included myelosuppresion and mucositis. The maximum tolerated dose of PK2 was found to be lower than that of PK1 (160 mg/m^2 vs. 320 mg/m^2, respectively), and a dose of 120 mg/m^2 was suggested for phase II analysis.

Besides PK2, several other **partners of PK1** have been evaluated over the years (Table 2). Efforts in this regard have on the one hand focused on improving the delivery of drugs other than doxorubicin, as well as, on the other hand, on improving the targeting properties of the copolymers (generally using doxorubicin as a model drug). Concerning the former, most progress has thus far been made with an HPMA-based polymeric prodrug of paclitaxel (PNU166945), and with two different platinum-containing copolymers (AP5280 and AP5346), which have all three been evaluated in patients. The phase study I on PNU166945 was halted prematurely, after having treated 12 patients with

refractory solid malignancies (1 partial response; 1 case of grade III neutoxicity), because of severe neurotoxicity observed in parallel rat studies [67]. The platinum-containing compounds AP5280 and AP5346, which differ in linker structure (i.e. GFLG vs. GGG) and in platinum complex (i.e. diamine (cisplatin-derivative) vs. diaminocyclohexane (oxaliplatin)), have both completed phase I trials, and have been shown to be able improve the pharmacokinetics of the attached active agent, and to be tolerated well [68-71]. The most effective of these two compounds, i.e. AP5346, produced two partial responses, in patients with metastatic melanoma and advanced ovarian carcinoma, and under the new name ProLindac, it has recently entered phase II analysis [72]. At the preclinical level, a large number of additional HPMA-based polymeric nanomedicines have been evaluated, carrying besides standard chemotherapeutic drugs also more recently developed (and more sophisticatedly acting) agents, such as the heat shock protein inhibitor geldanamycin [73,74] and the anti-angiogenic agent TNP-470 [75,76]. The latter formulation, i.e. Caplostatin, has been developed by Ronit Satchi-Fainaro and colleagues at the Folkman lab, and because of the fact that it improved the efficacy of TNP-470 and reduced its (neuro-) toxicity, it is currently being considered for phase I evaluation [77].

Acronym	Description	Phase	Ref
PK1	HPMA copolymer-bound doxorubicin; Prague-Keele-1; GFLG-spacer	II	59-61
PK2	Galactosamine-modified PK1; GFLG-spacer ; for liver targeting	I	63,64
PK3	Tyrosinamide-modified PK1; for cancer diagnosis	I	60
PNU166945	Polymer-bound paclitaxel; GFLG-spacer; halted because of neurotoxicity in rats	I	67
AP5280	Polymer-bound cisplatin; GFLG-spacer; well-tolerated; moderately active	I	68,69
AP5346	Polymer-bound oxaliplatin; GGG-spacer; well-tolerated; moderately active	II	70,71
Caplostatin	Polymer-bound TNP-470; GFLG-spacer; for anti-angiogenic therapy	P / I	75,76
P-GDM	Polymer-bound geldanamycin ; GFLG-spacer ; for heat shock protein-inhibition	P	73,74
P-CPT	Polymer-bound camptothecin; GFLG-spacer; for topo-isomerase I inhibition	P	142
P-MCE6	Polymer-bound mesochlorin e_6; GFLG-spacer; for photodynamic therapy	P	128,129
P-IgG	HuIg-modified PK1; for passive targeting and immunomodulation	P / I	97,98
P-HMW	GFLG-crosslinked high molecular weight graft of PK1: for passive targeting	P	81
P-STAR	Star-shaped, antibody- or protein-containing construct; for passive targeting	P	143
P-B1	B1-antibody-targeted copolymer; for cancer cell targeting and immunomodulation	P	100,101
P-TF	Transferrin-targeted copolymer; for cancer cell targeting	P	91,92
P-RGD	RGD-oligopeptide-targeted copolymer; for endothelial cell targeting	P	87,88
P-TAT	TAT-oligopeptide-targeted copolymer; for improving cellular uptake	P	93,94
P-HYD	HPMA copolymer-bound doxorubicin; pH-sensitive hydrazone spacer	P / I	105,106
P-HYD-IgG	Star-shaped, IgG-modified P-HYD; for passive targeting and immunomodulation	P	109
P-HYD-HMW	GFLG-crosslinked high molecular weight graft of P-HYD; for passive targeting	P	82
P-HYD-B1	B1-antibody-targeted P-HYD; for cancer cell targeting and immunomodulation	P	101

Table 2. Overview of the properties of PK1 and several of its partners.

Besides in establishing novel polymer-drug combinations, significant efforts in this area of research have also been invested in optimizing the properties of the copolymers, aiming e.g. to improve passive and active drug targeting, to enhance drug release and to induce anti-tumor immunity. Regarding **passive drug targeting**, based on the notion that larger HPMA copolymers circulate longer and accumulate in tumors stronger than do shorter copolymers [78-80], but at the same time also need to be small enough to be excreted renally, several biodegradable high molecular weight grafts have been developed, which initially exploit their large size to accumulate in tumors (more) effectively, and subsequently are degraded to fragments smaller than ~45 kDa (i.e. the renal clearance threshold), and are excreted renally [81,82]. As compared to a standard, 22 kDa-sized analogue of PK1, for instance, which prolonged the circulation half-life time of doxorubicin in mice from less than 15 min to 2.6 h, GFLG-crosslinked high molecular weight grafts of PK1, with sizes of 160 kDa and 1230 kDa, were retained in systemic circulation significantly more effectively, as evidenced by half-life times of 4.3 and 13.9 h, respectively [81]. As a result of this, the total amount of doxorubicin delivered to tumors within the first week after i.v. injection (i.e. the AUC_{0-168}) could be improved by a factor 6 and 12, respectively, and tumor growth inhibition could be induced significantly more effectively [81]. Alternative methods for improving passive drug targeting to tumors using HPMA copolymers, based e.g. on combinations with hyperthermia, with radiotherapy or with (anti-) vascular therapies, such as angiotensin, prostaglandins and anti-angiogenic agents, have not yet been evaluated.

Regarding **active drug targeting**, various different targeting moieties have been conjugated to HPMA copolymers over the years, including besides aminosugars such as galactosamine also e.g. hormones, antibodies and peptides. Large numbers of in vitro and in vivo analyses have been published on actively targeted HPMA copolymers, aiming not only to demonstrate the added value of active (over passive) drug targeting, but also to optimize factors such as ligand-structure, ligand-binding and ligand-density. Analyses in this regard have focused both on improving the tumor accumulation of the copolymers (using e.g. monoclonal antibodies for tumor cell targeting [83-86], or RGD-based oligopeptides for targeting to the tumor vasculature [87-90]), and on enhancing their uptake (using e.g. cell penetrating peptides, like TAT [91-93], or transferrin [94,95]). In the vast majority of cases, active drug targeting has rendered more favorable results than passive drug targeting, and the use of targeting ligands

has been shown to be able to improve both uptake and cytotoxicity in vitro, and both tumor accumulation and antitumor efficacy in vivo. Comparably beneficial findings have been reported for a number of other actively targeted nanomedicine formulations, including e.g. for antibody- and peptide-targeted liposomes. In spite of these promising findings, however, apart from about a dozen or so antibody-drug conjugates, only very few actively targeted nanomedicines have been evaluated in patients, including besides PK2 essentially only an antibody- (GAH-) targeted version of PEGylated liposomal doxorubicin [27,96]. It is expected in this regard, however, that because of the significant advances made at the preclinical level, and the sometimes spectacular response rates observed (e.g. upon modifying HPMA copolymers with tumor cell-specific immunomodulating antibodies, like B1; see below), several additional actively targeted nanomedicines will soon enter clinical trials.

Besides possessing a beneficial biodistribution and a favorable toxicological profile, HPMA copolymers have recently also been shown to possess **immunomodulatory properties**. The most significant progress in this regard has been made with a human immunoglobin- (HuIg-) modified version of PK1, which has been evaluated in four end-stage patients in the Czech Republic [97,98]. Improvements in disease parameters in blood were observed in several cases, and in all four patients, evidence for an activation of lymphocyte activated killer (LAK) cells and nuclear killer (NK) cells could be obtained [98]. At the preclinical level, similar immunostimulatory effects have been reported for a number of other HPMA-based polymer therapeutics, including e.g. for anti-Thy1.2-, anti-CD71- and B1-targeted versions of PK1 [99-101]. It is furthermore interesting to note in this regard that in addition to producing cures in up to 100% of mice, several of these antibody-targeted polymer-drug conjugates have been shown to be able to induce antitumor immunity (i.e. relatively long-lasting immunoprotection), as exemplified by the fact that significant percentages of these cured mice were found to be resistant to rechallenge with a second (lethal) dose of cancer cells [101-104]). In spite of these promising findings and interesting insights, however, industrial interest in immunomodulating polymer therapeutics has been low, and clinical progress consequently slow. This is considered to be due to IP (intellectual property) issues and expired patents, and to the fact that no investors are available for sponsoring clinical trials.

More marketable progress with regard to drug targeting to tumors using HPMA copolymers has recently been made by developing **novel drug linkers**, and by establishing more optimal methods for enabling tumor-selective drug release. As compared to the enzymatically cleavable GFLG linker, for instance, which is used in PK1 and which even under optimal conditions releases doxorubicin only very slowly, the pH-sensitive hydrazone spacer releases doxorubicin much more rapidly, and it much more strongly inhibits tumor growth [105-108]. In spite of these high release and response rates, the hydrazone-based polymeric prodrug was found to be tolerated remarkably well, as exemplified by the fact that its maximum tolerated dose was more than threefold higher than that of PK1, and more than ten times as high as that of free doxorubicin [107,108]. In line with this, also when used in biodegradable high molecular weight grafts, in HuIg-targeted polymer-drug conjugates and in B1-targeted polymeric prodrugs, the hydrazone spacer was found to be more effective and less toxic than the GFLG spacer [82,101,109]. Experimental evidence in favor of the hydrazone spacer over the GFLG spacer has now been obtained in several different tumor models, and a ~25 kDa-sized hydrazone-based polymeric prodrug of doxorubicin is currently being considered for clinical trials. Additional drug linkers evaluated over the years include oligopeptide sequences other than GFLG [43-46], and other pH-sensitive spacers, such as polyacetals and cis-aconityls [110-112].

Additional important issues to take into account with regard to **drug targeting to tumors using HPMA copolymers** relate to the use of the copolymers for overcoming multi-drug resistance [113-116], the use of the copolymers as coating materials for viral and non-viral gene delivery systems [117-120], the use of the copolymers for imaging purposes [121-124], and the use of the copolymers for making block copolymer micelles, which can be core-crosslinked to improve their circulation times [125-128]. Notable advances have also been made by combining HPMA copolymer-based chemotherapeutics with other treatment modalities, e.g. with photodynamic therapy [129,130], with standard chemotherapy [131] and with each other [132-135]. And furthermore, HPMA copolymers have recently also been used to treat non-cancerous diseases, such as rheumatoid arthritis [136-138] and bacterial infections [139-141], which are also characterized by leaky blood vessels and a strong inflammation component, and which are also highly amenable to EPR-mediated passive drug targeting.

Taking the above insights and efforts into account, the **aim of the present thesis** is to investigate, understand, improve and extend drug targeting to tumors using HPMA copolymers. To provide a proper theoretical framework for investigating drug targeting to tumors, in **Chapter 2**, the basic principles of passive and active drug targeting are summarized, and several clinically relevant examples of tumor-targeted nanomedicines are highlighted. To better understand drug targeting to tumors, in **Chapter 3**, the circulation kinetics, the biodistribution and the tumor accumulation of thirteen physicochemically different HPMA copolymers are described. In **Chapter 4**, based on the notion that HPMA copolymers circulate for prolonged periods of time, a gadolinium-containing contrast agent is developed for MR angiography, i.e. for imaging blood vessels. In **Chapter 5**, to provide some initial indications in favor of the combination of polymeric nanomedicines with surgery, the impact of intratumoral injection on the biodistribution and the therapeutic potential of HPMA copolymer-based drug delivery systems is investigated. To actively improve passive drug targeting, in **Chapter 6**, the effects of different doses of radiotherapy and hyperthermia on the tumor accumulation of HPMA copolymers are evaluated. In **Chapter 7**, drug targeting to tumors using HPMA copolymers is extended, showing both for doxorubicin and for gemcitabine that long-circulating and passively tumor-targeted polymeric drug carriers are able to improve the efficacy of radiochemotherapy. In **Chapter 8**, using an HPMA copolymer co-functionalized both with doxorubicin and with gemcitabine, evidence is provided showing that polymers, as e.g. liposomes, can be used to deliver two different drugs to tumors simultaneously, and to mprove the efficacy of chemotherapy combinations. And finally, in **Chapter 9**, the insights provided and the evidence obtained are summarized and discussed, and several general conclusions are drawn. Together, the work described in this thesis demonstrates that HPMA copolymers are suitable systems for passive drug targeting to tumors, and that long-circulating and passively tumor-targeted polymeric nanomedicines are suitable systems for improving the efficacy of combined modality anticancer therapy.

References

1. D. Hanahan, R.A. Weinberg, The hallmarks of cancer, Cell 100 (2000) 57-70.
2. http://www.who.int/cancer.
3. D.S. Krause. R.A. Van Etten, Tyrosine kinases as targets for cancer therapy, New England Journal of Medicine 353 (2005) 172-187.
4. R.M. Sharkey, D.M. Goldenberg, Targeted therapy of cancer: new prospects for antibodies and immunoconjugates, CA - A Cancer Journal for Clinicians 56 (2006) 226-243.
5. I. Collins, P. Workman, New approaches to molecular cancer therapeutics, Nature Chemical Biology 2 (2006) 689-700.
6. D.C. Drummond, O. Meyer, K. Hong, D.B. Kirpotin, D. Papahadjopoulos, Optimizing liposomes for delivery of chemotherapeutic agents to solid tumours. Pharmacological Reviews 51 (1999) 691-743.
7. G. Storm, D.J.A. Crommelin, Liposomes: Quo vadis?, Pharmaceutical Science and Technology Today 1 (1998) 19-31.
8. V.P. Torchilin, Recent advances with liposomes as pharmaceutical carriers, Nature Reviews Drug Discovery, 4 (2005) 145-160.
9. J. Kopecek. P. Kopeckova, T. Minko, Z.R. Lu, C.M. Peterson, Water soluble polymers in tumor targeted delivery, Journal of Controlled Release 74 (2001) 147-158.
10. R. Duncan, Polymer conjugates as anticancer nanomedicines. Nature Reviews Cancer 6 (2006) 688-701.
11. R. Haag, F. Kratz, Polymer Therapeutics: Concepts and applications, Angewandte Chemie - International Edition 45 (2006) 1198-1215.
12. K Kataoka, H. Harada, Y. Nagasaki, Block copolymer micelles for drug delivery: design, characterization and biological significance, Advanced Drug Delivery Reviews 41 (2001) 113-131.
13. V.P. Torchilin, Micellar nanocarriers: Pharmaceutical perspectives, Pharmaceutical Research 24 (2007), 1-16.
14. M.C. Jones, J.C. Leroux, Polymeric micelles - A new generation of colloidal drug carriers, European Journal of Pharmaceutics and Biopharmaceutics 48 (1999) 101-111.
15. J.A. MacDiarmid, N.B. Mugridge, J.C. Weiss, L. Phillips, A.L. Burn, R. Paulin, J.E. Haasdyk, K.A. Dickson, V.N. Brahmbhatt, S.T. Pattison, A.C. James, G. Al Bakri, R.C. Straw, B. Stillman, R.M. Graham, H. Brahmbatt, Bacterially derived 400 nm particles for encapsulation and cancer cell targeting of chemotherapeutics, Cancer Cell 11 (2007) 431-445.
16. S. Sengupta, D. Eavarone, I. Capila, G. Zhao, N. Watson, T. Kiziltepe, R. Sasisekharan, Temporal targeting of tumor cells and neovasculature with a nanoscale delivery system. Nature 436 (2005) 568-572.
17. F. Yuan, M. Dellian, D. Fukumura, M. Leunig, D.A. Berk, V.P. Torchilin, R.K. Jain, Vascular permeability in a human tumor xenograft: Molecular size dependence and cutoff size, Cancer Research 55 (1995) 3752-3756.
18. S.K. Hobbs, W.L. Monsky, F. Yuan, W.G. Roberts, L. Griffith, V.P. Torchilin, R.K. Jain, Regulation of transport pathways in tumor vessels: Role of tumor type and microenvironment, Proceedings of the National Academy of Sciences of the United States of America 95 (1998) 4607-4612.
19. G. Kong, R.D. Braun, M.W. Dewhirst, Hyperthermia enables tumor-specific nanoparticle delivery: effect of particle size, Cancer Research 60 (2000) 4440-4445.
20. H. Maeda, Y. Matsumura, A new concept for macromolecular therapeutics in cancer chemotherapy: mechanism of tumoritropic accumulation of proteins and the antitumor agent Smancs, Cancer Research 46 (1986) 6387-6392.
21. H. Maeda, J. Wu, T. Sawa, Y. Matsumura, K. Hori, Tumour vascular permeability and the EPR effect in macromolecular therapeutics: a review, Journal of Controlled Release 65 (2000) 271-284.
22. H. Maeda, The enhanced permeability and retention (EPR) effect in tumor vasculature: The key role of tumor-selective macromolecular drug targeting, Advances in Enzyme Regulation 41 (2001) 189-207.
23. L.W. Seymour, Passive tumor targeting of soluble macromolecules and drug conjugates, Critical Reviews in Therapeutic Drug Carrier Systems 9 (1992) 135-187.
24. V.P. Torchilin, Drug targeting, European Journal of Pharmaceutical Sciences 11 (2000) S81-S91.
25. S.M. Moghimi, A.C. Hunter, J.C. Murray, Long-circulating and target-specific nanoparticles: theory to practice, Pharmacological Reviews 53 (2001) 283-318.

26. D.J.A. Crommelin, G. Scherphof, G. Storm, Active targeting with particulate carrier systems in the blood compartment, Advanced Drug Delivery Reviews 17 (1995) 49-60.
27. T.M. Allen, Ligand-targeted therapeutics in anticancer therapy, Nature Reviews Cancer 2 (2002) 750-763.
28. F. Marcucci, L. Lefoulon, Active targeting with particulate drug carriers in tumor therapy: fundamentals and recent progress, Drug Discovery Today 9 (2004) 219-228.
29. D. Papahadjopoulos, T.M. Allen, A. Gabizon, E. Mayhew, K. Matthay, S.K. Huang, K.D. Lee, M.C. Woodle, D.D. Lasic, C. Redemann, Sterically stabilized liposomes: Improvements in pharmacokinetics and antitumor therapeutic efficacy, Proceedings of the National Academy of Sciences of the United States of America 88 (1991) 11460-11464.
30. A. Gabizon, R. Catane, B. Uziely, B. Kaufman, R. Cohen, F. Martin, A. Huang, Y. Barenholz, Prolonged circulation time and enhanced accumulation in malignant exudates of doxorubicin encapsulated in polyethylene-glycol coated liposomes, Cancer Research 54 (1994) 987-992.
31. R.D. Hofheinz, S.U. Gnad-Vogt, U. Beyer, A. Hochhaus, Liposomal encapsulated anti-cancer drugs, Anticancer Drugs 16 (2005) 691 – 707.
32. A.D. Bangham, M.M. Standish, J.C. Watkins, Diffusion of univalent ions across the lamellae of swollen phospholipids, Journal of Molecular Biology 13 (1965) 238-252.
33. G. Gregoriadis, The carrier potential of liposomes in biology and medicine, New England Journal of Medicine 295 (1976) 765-770.
34. H. Ringsdorf, Structure and properties of pharmacologically active polymers, Journal of Polymer Science: Polymer Symposia 51 (1975) 135-153.
35. J. Kopecek, L. Sprincl, D. Lim, New types of synthetic infusion solutions. I. Investigation of the effect of solutions of some hydrophilic polymers on blood, Journal of Biomedical Materials Research 7 (1973) 179-191.
36. L. Sprincl, J. Exner, O. Sterba, J. Kopecek, New types of synthetic infusion solutions. III. Elimination and retention of poly[N-(2-hydroxypropyl)methacrylamide] in a test organism, Journal of Biomedical Materials Research 10 (1976), 953-963.
37. J. Kopecek, H. Bazilova, Poly[N-(2-hydroxypropyl)methacrylamide]. I. Radical polymerization and copolymerization, European Polymer Journal 9 (1973), 7-14.
38. M. Bohdanecky, H. Bazilova, J. Kopecek, Poly[N-(2-hydroxypropyl)methacrylamide]. II. Hydrodynamic properties of diluted polymer solutions, European Polymer Journal 10 (1974) 405-410.
39. V. Chytry, A. Vrana, J. Kopecek, Synthesis and activity of a polymer which contains insulin covalently bound on a copolymer of N-(2-hydroxypropyl)methacrylamide and N-methacryloylglycylglycine 4-nitrophenyl ester, Makromolekulare Chemie 179 (1978) 329-336.
40. R. Duncan, J. Kopecek, J.B. Lloyd, Development of HPMA copolymers as carriers of therapeutic agents, Polymer Science and Technology 23 (1983) 97-113.
41. M.V. Solovskij, K. Ulbrich, J. Kopecek, Synthesis of N-(2-hydroxypropyl)methacrylamide copolymers with antimicrobial activity, Biomaterials 4 (1983) 44-48.
42. C. De Duve, T. De Barsy, B. Poole, A. Trouet, P. Tulkens, F van Hoof, Lysosomotropic agents. Biochemical Pharmacology 23 (1974) 2495-2531.
43. J. Kopecek, I. Cifkova, P. Rejmanova, J. Strohalm, B. Obereigner, K. Ulbrich, Polymers containing enzymatically degradable bonds. 4. Preliminary experiments in vivo, Makromolekulare Chemie 182 (1981) 2941-2949.
44. R. Duncan, H.C. Cable, J.B. Lloyd, P. Rejmanova, J. Kopecek, Polymers containing enzymatically degradable bonds. 7. Design of oligopeptide side-chains in poly[N-(2-hydroxypropyl)methacrylamide] copolymers to promote efficient degradation by lysosomal enzymes, Makromolekulare Chemie 184 (1983) 1997-2008.
45. P. Rejmanová, J. Pohl, M. Baudy, V. Kostka, J. Kopecek, Polymers containing enzymatically degradable bonds. 8. Degradation of oligopeptide sequences in N-(2-hydroxypropyl)methacrylamide copolymers by bovine spleen cathepsin B, Makromolekulare Chemie 184 (1983) 2009-2020.
46. P. Rejmanová, J. Kopecek, R. Duncan, J.B. Lloyd, Stability in rat plasma and serum of lysosomally degradable oligopeptide sequences in N-(2-hydroxypropyl)methacrylamide copolymers. Biomaterials 6 (1985) 45-48.
47. R. Duncan, P. Kopeckova-Rejmanova, J. Strohalm, Anticancer agents coupled to N-(2-hydroxypropyl)methacrylamide copolymers. I. Evaluation of daunomycin and puromycin conjugates in vitro, British Journal of Cancer 55 (1987) 165-174.
48. J. Kopecek, P. Rejmanova, R. Duncan, J.B. Lloyd, Controlled release of drug model from N-(2-hydroxypropyl)-methacrylamide, Annals of the New York Academy of Sciences 446 (1985) 93-104.

49. L. Seymour, K. Ulbrich, P. Steyger, M. Brereton, V. Subr, J. Strohalm, R. Duncan, Tumour tropism and anti-cancer efficacy of polymer-based doxorubicin prodrugs in the treatment of subcutaneous murine B16F10 melanoma, British Journal of Cancer 70 (1994) 636-641.
50. R. Duncan, L.W. Seymour, K. Ulbrich, J. Kopecek, Soluble synthetic polymers for targeting and controlled release of anticancer agents, particularly anthracycline antibiotics, Journal of Bioactive and Compatible Polymers 3 (1988) 4-15.
51. M.V. Pimm, A.C. Perkins, R. Duncan, K. Ulbrich, Targeting of N-(2-hydroxypropyl)methacrylamide copolymer-doxorubicin conjugate to the hepatocyte galactose-receptor in mice: visualisation and quantification by gamma scintigraphy as a basis for clinical targeting studies, Journal of drug targeting 1 (1983) 125-131.
52. M.V. Pimm, A.C. Perkins, J. Strohalm, K. Ulbrich, R. Duncan, Gamma scintigraphy of the biodistribution of 123I-labelled N-(2-hydroxypropyl)methacrylamide copolymer-doxorubicin conjugates in mice with transplanted melanoma and mammary carcinoma, Journal of Drug Targeting 3 (1996) 375-383.
53. L.W. Seymour, K. Ulbrich, J. Strohalm, J. Kopecek, R. Duncan. The pharmacokinetics of polymer-bound adriamycin. Biochemical Pharmacology 39 (1990) 1125-1131.
54. R. Duncan, I.C. Hume, P Kopeckova, K. Ulbrich, J. Strohalm, J. Kopecek, Anticancer agents coupled to HPMA copolymers. 3. Evaluation of adriamycin conjugates against mouse leukaemia L1210 in vivo, Journal of Controlled Release 10 (1989) 51-63.
55. R. Duncan, L.W. Seymour, K.B. O'Hare, P.A. Flanagan, S. Wedge, I.C. Hume, K. Ulbrich, J. Strohalm, V. Subr, F. Spreafico, M. Grandi, M. Ripamonti, M. Farao, A. Suarato, Preclinical evaluation of polymer-bound doxorubicin, Journal of Controlled Release 19 (1992) 331-346.
56. T. Minko, P. Kopeckova, J. Kopecek, Efficacy of chemotherapeutic action of HPMA copolymer-bound doxorubicin in a solid tumor model of ovarian carcinoma, International Journal of Cancer 86 (2000) 108-117.
57. T.K. Yeung, J.W. Hopewell, R.H. Simmonds, L.W. Seymour, R. Duncan, O. Bellini, M. Grandi, F. Spreafico, J. Strohalm, K. Ulbrich, Reduced cardiotoxicity of doxorubicin given in the form of N-(2-hydroxypropyl)methacrylamide conjugates: and experimental study in the rat, Cancer Chemotherapy and Pharmacology 29 (1991) 105-111.
58. R. Duncan, J.K. Coatsworth, S. Burtles, Preclinical toxicology of a novel polymeric antitumour agent: HPMA copolymer-doxorubicin (PK1), Human and Experimental Toxicology 17 (1998) 93-104.
59. P.A. Vasey, R. Duncan, S.B. Kaye, J. Cassidy, Clinical phase I trial of PK1 (HPMA co-polymer doxorubicin), European Journal of Cancer 31A (1995) S193.
60. P.A. Vasey, S.B. Kaye, R. Morrison, C. Twelves, P. Wilson, R. Duncan, A.H. Thomson, L.S. Murray, T.E. Hilditch, T. Murray, S. Burtles, D. Fraier, E. Frigerio, J. Cassidy, Cancer Research Campaign Phase I/II Committee, Phase I clinical and pharmacokinetic study of PK1 [N-(2-hydroxypropyl)methacrylamide copolymer doxorubicin]: first member of a new class of chemotherapeutic agents-drug-polymer conjugates, Clinical Cancer Research 5 (1999) 83-94.
61. V. Bilim, Technology evaluation: PK1, Pfizer/Cancer Research UK, Current Opinion in Molecular Therapeutics 5 (2003) 326-330.
62. A.H. Thomson, P.A. Vasey, L.S. Murray, J. Cassidy, D. Fraier, E. Frigerio, C. Twelves, Population pharmacokinetics in phase I drug development: A phase I study of PK1 in patients with solid tumours, British Journal of Cancer 81 (1999) 99-107.
63. P.J. Julyan, L.W. Seymour, D.R. Ferry, S. Daryani, C.M. Boivin, J. Doran, M. David, D. Anderson, C. Christodoulou, A.M. Young, S. Hesslewood, D.J. Kerr. Preliminary clinical study of the distribution of HPMA copolymers bearing doxorubicin and galactosamine. Journal of Controlled Release 57 (1999) 281-290.
64. L.W. Seymour, D.R. Ferry, D. Anderson, S. Hesslewood, P.J. Julyan, R. Poyner, J. Doran, A.M. Young, S. Burtles, D.J. Kerr, Cancer Research Campaign Phase I/II Clinical Trials committee, Hepatic drug targeting: phase I evaluation of polymer-bound doxorubicin, Journal of Clinical Oncology 20 (2002) 1668-1676.
65. L.W. Seymour, K. Ulbrich, S.R. Wedge, I.C. Hume, J. Strohalm, R. Duncan, N-(2-hydroxypropyl)methacrylamide copolymers targeted to the hepatocyte galactose-receptor: pharmacokinetics in DBA2 mice, British Journal of Cancer 63 (1991) 859-866.
66. M.V. Pimm, A.C. Perkins, J. Strohalm, K. Ulbrich, R. Duncan, Gamma scintigraphy of a 123I-labelled N-(2-hydroxypropyl)methacrylamide copolymer-doxorubicin conjugate containing galactosamine following intravenous administration to nude mice bearing hepatic human colon carcinoma, Journal of Drug Targeting 3 (1996) 385-390.

67. J.M. Meerum Terwogt, W.W. ten Bokkel Huinink, J.H. Schellens, M. Schot, I.A. Mandjes, M.G. Zurlo, M. Rocchetti, H. Rosing, F.J. Koopman, J.H. Beijnen, Phase I clinical and pharmacokinetic study of PNU166945, a novel water-soluble polymer-conjugated prodrug of paclitaxel, Anticancer Drugs 12 (2001) 315-323.
68. X. Lin, Q. Zhang, J.R. Rice, D.R. Stewart, D.P. Nowotnik, S.B. Howell, Improved targeting of platinum chemotherapeutics. the antitumour activity of the HPMA copolymer platinum agent AP5280 in murine tumour models, European Journal of Cancer 40 (2004) 291-297.
69. J.M. Rademaker-Lakhai, C. Terret, S.B. Howell, C.M. Baud, R.F. De Boer, D. Pluim, J.H. Beijnen, J.H. Schellens, J.P. Droz, A Phase I and pharmacological study of the platinum polymer AP5280 given as an intravenous infusion once every 3 weeks in patients with solid tumors, Clinical Cancer Research 10 (2004) 3386-3395.
70. J.R. Rice, J.L. Gerberich, D.P. Nowotnik, S.B. Howell, Preclinical efficacy and pharmacokinetics of AP5346, a novel diaminocyclohexane-platinum tumor-targeting drug delivery system Clinical Cancer Research 12 (2006) 2248-2254.
71. M. Campone, J.M. Rademaker-Lakhai, J. Bennouna, S.B. Howell, D.P. Nowotnik, J.H. Beijnen, J.H. Schellens, Phase I and pharmacokinetic trial of AP5346, a DACH-platinum-polymer conjugate, administered weekly for three out of every 4 weeks to advanced solid tumor patients, Cancer Chemothererapy and Pharmacology 60 (2007) 523-533.
72. D.P. Nowotnik, E. Cvitkovic, ProLindac (AP5346): A review of the development of an HPMA DACH platinum polymer therapeutic. Advanced Drug Delivery Reviews (in press).
73. Y. Kasuya, Z.R. Lu, P. Kopeckova, T. Minko, S.E. Tabibi, J. Kopecek, Synthesis and characterization of HPMA copolymer-aminopropylgeldanamycin conjugates, Journal of Controlled Release 74 (2001) 203-211.
74. N. Nishiyama, A. Nori, A. Malugin, Y. Kasuya, P. Kopeckova, J. Kopecek J, Free and HPMA copolymer-bound geldanamycin derivative induce different stress responses in A2780 human ovarian carcinoma cells, Cancer Research 63 (2003) 7876-7882.
75. R. Satchi-Fainaro, M. Puder, J.W. Davies, H.T. Tran, D.A. Sampson, A.K. Greene, G. Corfas, J. Folkman, Targeting angiogenesis with a conjugate of HPMA copolymer and TNP-470, Nature Medicine 10 (2004) 255-261.
76. R. Satchi-Fainaro, R. Mamluk, L. Wang, S.M. Short, J.A. Nagy, D. Feng, A.M. Dvorak, H.F. Dvorak, M. Puder, D. Mukhopadhyay, J. Folkman, Inhibition of vessel permeability by TNP-470 and its polymer conjugate, caplostatin, Cancer Cell 3 (2005) 251-261.
77. http://www.syndevrx.com/documentsSynDevRxExecutiveSummaryJuly2008_003.pdf
78. L.W. Seymour, R. Duncan, J. Strohalm, J. Kopecek, Effect of molecular weight (Mw) of N-(2-hydroxypropyl)methacrylamide copolymers on body distribution and rate of excretion after subcutaneous, intraperitoneal, and intravenous administration to rats, J. Biomed. Mater. Res. 21 (1987) 1341-1358.
79. L.W. Seymour, Y. Miyamoto, H. Maeda, M. Brereton, J. Strohalm, K. Ulbrich, R. Duncan, Influence of molecular weight on passive tumour accumulation of a soluble macromolecular drug carrier, Eur. J. Cancer. 31A (1995) 766-70
80. T. Lammers, R. Kuhnlein, M. Kissel, V. Subr, T. Etrych, R. Pola, M. Pechar, K. Ulbrich, G. Storm, P. Huber, P. Peschke, Effect of physicochemical modification on the biodistribution and tumor accumulation of HPMA copolymers, Journal of Controlled Release 110 (2005) 103-118.
81. J.G. Shiah, M. Dvorak, P. Kopeckova, Y. Sun, C.M. Peterson, J. Kopecek, Biodistribution and antitumour efficacy of long-circulating N-(2-hydroxypropyl)methacrylamide copolymer-doxorubicin conjugates in nude mice, Eur. J. Cancer 37 (2001) 131-139.
82. T. Etrych, P. Chytil, T. Mrkvan, M. Sirova, B. Rihova, K. Ulbrich. Conjugates of doxorubicin with graft HPMA copolymers for passive tumor targeting, Journal of Controlled Release 132 (2008) 184-192.
83. M. Jelinkova, J. Strohalm, D. Plocova, V. Subr, M. St'astny, K. Ulbrich, B. Rihova, Targeting of human and mouse T-lymphocytes by monoclonal antibody-HPMA copolymer-doxorubicin conjugates directed against different T-cell surface antigens. Journal of Controled Release, 52 (1998) 253-270.
84. B. Rihova, Receptor-mediated targeted drug or toxin delivery, Advanced Drug Delivery Reviews 29 (1998) 273-289.
85. V. Omelyanenko, P. Kopeckova, C. Gentry, J. Kopecek, Targetable HPMA copolymer-adriamycin conjugates. Recognition, internalization, and subcellular fate, Journal of Controlled Release, 53 (1998) 25-37
86. Z.R. Lu, P Kopeckova, J. Kopecek, Polymerizable Fab' antibody fragments for targeting of anticancer drugs, Nature Biotechnology 17 (1999) 1101-4.

87. A. Mitra, T. Coleman, M. Borgman, A. Nan, H. Ghandehari H, B.R. Line, Polymeric conjugates of mono- and bi-cyclic alphaVbeta3 binding peptides for tumor targeting.Journal of Controlled Release 114 (2006) 175-183.
88. A. Mitra, J. Mulholland, A. Nan, E. McNeill, H. Ghandehari, B.R. Line, Targeting tumor angiogenic vasculature using polymer-RGD conjugates, Journal of Controlled Release 102 (2005) 191-201.
89. A. Mitra, A. Nan, J. Papadimitriou, H. Ghandehari, B.R. Line, Polymer-peptide conjugates for angiogenesis targeted tumor radiotherapy, Nuclear Medicine and Biology 33 (2006) 43-52.
90. M.P. Borgman, A. Ray, R.B. Kolhatkar, E.A. Sausville, A.M. Burger, H. Ghandehari, Targetable HPMA Copolymer-Aminohexylgeldanamycin Conjugates for Prostate Cancer Therapy.Pharmaceutical Research (in press)
91. A. Nori, K.D. Jensen, M. Tijerina, P. Kopeckova, J. Kopecek, Tat-conjugated synthetic macromolecules facilitate cytoplasmic drug delivery to human ovarian carcinoma cells, Bioconjugate Chemistry 14 (2003) 44-50.
92. A. Nori, K.D. Jensen, M. Tijerina, P. Kopeckova, J. Kopecek, Subcellular trafficking of HPMA copolymer-Tat conjugates in human ovarian carcinoma cells, Journal of Controlled Release 91 (2003) 53-59.
93. A. Nori, J. Kopecek, Intracellular targeting of polymer-bound drugs for cancer chemotherapy, Advanced Drug Delivery Reviews 57 (2005) 609-636.
94. P.A. Flanagan, P. Kopeckova, J. Kopecek, R. Duncan, Evaluation of protein-N-(2-hydroxypropyl)methacrylamide copolymer conjugates as targetable drug carriers. 1. Binding, pinocytic uptake and intracellular distribution of transferrin and anti-transferrin receptor antibody conjugates, Biochimica et Biophysica Acta 993 (1989) 83-91.
95. M. Kovar, J. Strohalm, K. Ulbrich, B. Rihova, In vitro and in vivo effect of HPMA copolymer-bound doxorubicin targeted to transferrin receptor of B-cell lymphoma 38C13, Journal of Drug Targeting 10 (2002) 23-30.
96. Y. Matsumura, M. Gotoh, K. Muro, Y. Yamada, K. Shirao, Y. Shimada, M. Okuwa, S. Matsumoto, Y. Miyata, H. Ohkura, K. Chin, S. Baba, T. Yamao, A. Kannami, Y. Takamatsu, K. Ito, K. Takahashi. Phase I and pharmacokinetic study of MCC-465, a doxorubicin (DXR) encapsulated in PEG immunoliposome, in patients with metastatic stomach cancer. Annals of Oncology 15 (2004) 517-525
97. B. Rihova, J. Strohalm, K. Kubackova, M. Jelinkova, L Rozprimova, M. Sirova, D. Plocova, T. Mrkvan, M. Kovar, J. Pokorna, T. Etrych, K. Ulbrich. Drug-HPMA-HuIg conjugates effective against human solid cancer. Advances in Experimental Medicine and Biology 519 (2003) 125-43.
98. B. Rihova, J. Strohalm, J. Prausova, K. Kubackova, M. Jelinkova, L Rozprimova, M. Sirova, D. Plocova, T. Etrych, V. Subr, T. Mrkvan, M. Kovar, K. Ulbrich, Cytostatic and immunomobilizing activities of polymer-bound drugs: experimental and first clinical data, Journal of Controlled Release 91 (2003) 1-16.
99. B. Rihova, J. Strohalm, K. Kubackova, M. Jelinkova, O. Hovorka, M. Kovar, D. Plocova, M. Sirova, M. St'astny, L. Rozprimova, K. Ulbrich, Acquired and specific immunological mechanisms co-responsible for efficacy of polymer-bound drugs. Journal of Controlled Release 78 (2002) 97-114.
100. M. Kovar, T. Mrkvan, J. Strohalm, T. Etrych, K. Ulbrich, M Stastny, B. Rihova, HPMA copolymer-bound doxorubicin targeted to tumor-specific antigen of BCL1 mouse B cell leukemia, Journal of Controlled Release 92 (2003) 315-30.
101. M. Kovar, J. Tomala, H. Chmelova, L. Kovar, T. Mrkvan, R. Joskova, Z. Zakostelska, T. Etrych, J. Strohalm, K. Ulbrich, M. Sirova, B. Rihova, Overcoming immunoescape mechanisms of BCL1 leukemia and induction of CD8+ T-cell-mediated BCL1-specific resistance in mice cured by targeted polymer-bound doxorubicin, Cancer Research 68 (2008) 9875-9883.
102. B. Rihova, Immunomodulating activities of soluble synthetic polymer-bound drugs, Advanced Drug Delivery Reviews 12 (2002) 653-674
103. B. Rihova, J. Strohalm, M. Kovar, T. Mrkvan, V. Subr, O. Hovorka, M. Sirova, L. Rozprimova L, K. Kubackova, K. Ulbrich, Induction of systemic antitumour resistance with targeted polymers, Scandinavian Journal of Immunology 62 (2005) 100-105
104. M. Sirova, J. Strohalm, V. Subr, D. Plocova, P. Rossmann, T. Mrkvan, K. Ulbrich, B. Rihova, Treatment with HPMA copolymer-based doxorubicin conjugate containing human immunoglobulin induces long-lasting systemic anti-tumour immunity in mice, Cancer Immunology Immunotherapy 56 (2007) 35-47.

105. T. Etrych, M. Jelinkova, B. Rihova, K. Ulbrich, New HPMA copolymers containing doxorubicin bound via pH-sensitive linkage: synthesis and preliminary in vitro and in vivo biological properties, Journal of Controlled Release 73 (2001) 89-102.
106. B. Rihova, T. Etrych, M. Pechar, M. Jelinkova, M. Stastny, O. Hovorka, M. Kovar, K. Ulbrich, Doxorubicin bound to a HPMA copolymer carrier through hydrazone, Journal of Controlled Release 74 (2001) 225-32
107. K. Ulbrich, T. Etrych, P. Chytil, M. Pechar, M. Jelinkova, B. Rihova, Polymeric anticancer drugs with pH-controlled activation, International Journal of Pharmaceutics 277 (2004) 63-72.
108. K. Ulbrich, V. Subr, Polymeric anticancer drugs with pH-controlled activation, Advanced Drug Delivery Reviews 56 (2004) 1023-1050.
109. T. Etrych, T. Mrkvan, B. Rihova, K. Ulbrich, Star-shaped immunoglobulin-containing HPMA-based conjugates with doxorubicin for cancer therapy, Journal of Controlled Release. 122 (2007) 31-38.
110. R. Tomlinson, J. Heller, S. Brocchini, R. Duncan R, Polyacetal-doxorubicin conjugates designed for pH-dependent degradation, Bioconjugate Chemistry 14 (2003) 1096-1106.
111. W.C. Shen, H.J.P. Ryser, Cis-aconityl spacer between daunomycin and macromolecular carriers: a model of pH sensitive linkage releasing drug from a lysosomotropic conjugate, Biochemical and Biophysical Research Communications 102 (1981) 1048-1054.
112. W.M. Choi, P. Kopecková, T. Minko, J. Kopecek, Synthesis of HPMA copolymer containing adriamycin bound via an acid-labile spacer and its activity toward human ovarian carcinoma cells. Journal of Bioactive and Compatible Polymers 14 (1999) 447–556.
113. T Minko, P. Kopeckova, V. Pozharov, J. Kopecek, HPMA copolymer bound adriamycin overcomes MDR1 gene encoded resistance in a human ovarian carcinoma cell line, J ournal of Controlled Release 54 (1998) 223-233.
114. T Minko, P. Kopeckova, J. Kopecek, Chronic exposure to HPMA copolymer-bound adriamycin does not induce multidrug resistance in a human ovarian carcinoma cell line, Journal of Controlled Release 59 (1999) 133-148.
115. M. Tijerina, K.D. Fowers, P. Kopeckova, J. Kopecek, Chronic exposure of human ovarian carcinoma cells to free or HPMA copolymer-bound mesochlorin e6 does not induce P-glycoprotein-mediated multidrug resistance, Biomaterials (2000) 2203-2210.
116. T Minko, P. Kopeckova, J. Kopecek, Preliminary evaluation of caspases-dependent apoptosis signaling pathways of free and HPMA copolymer-bound doxorubicin in human ovarian carcinoma cells, Journal of Controlled Release 71 (2001) 227-237.
117. P.R. Dash, M.L. Read, K.D. Fisher, K.A. Howard, M. Wolfert, D. Oupicky, V. Subr, J. Strohalm, K. Ulbrich, L.W. Seymour, Decreased binding to proteins and cells of polymeric gene delivery vectors surface modified with a multivalent hydrophilic polymer and retargeting through attachment of transferrin, Journal of Biological Chemistry 275 (2000) 3793-3802.
118. K.D. Fisher, Y. Stallwood, N.K. Green, K. Ulbrich, V. Mautner, L.W. Seymour, Polymer-coated adenovirus permits efficient retargeting and evades neutralising antibodies, Gene Therapy 8 (2001) 341-348.
119. D. Oupicky, M. Ogris, K.A. Howard, P.R. Dash, K. Ulbrich, L.W, Seymour, Importance of lateral and steric stabilization of polyelectrolyte gene delivery vectors for extended systemic circulation, Mol Therapy 5 (2002) 463-472.
120. N.K. Green, C.W. Herbert, S.J. Hale, A.B. Hale, V. Mautner, R. Harkins T. Hermiston, K. Ulbrich, K.D. Fisher, L.W. Seymour, Extended plasma circulation time and decreased toxicity of polymer-coated adenovirus, Gene Therapy 11 (2004) 1256-1263
121. F. Kiessling, M. Heilmann, T. Lammers, K. Ulbrich, V. Subr, P. Peschke, B. Waengler, W. Mier, H.H. Schrenk, M. Bock, L. Scha, W. Semmler, Synthesis and characterization of HE-24.8: a polymeric contrast agent for magnetic resonance angiography. Bioconjugate Chemistry 17 (2006) 42-51.
122. B. Zarabi, A. Nan, J. Zhuo, R. Gullapalli, H. Ghandehari, Macrophage targeted N-(2-hydroxypropyl)methacrylamide conjugates for magnetic resonance imaging, Zarabi B, Nan A, Zhuo J, Gullapalli R, Ghandehari H, Molecular Pharmaceutics 3 (2006) 550-557.
123. Y. Wang, F. Ye, E.K. Jeong, Y. Sun, D.L. Parker, Z.R. Lu, Noninvasive visualization of pharmacokinetics, biodistribution and tumor targeting of poly[N-(2-hydroxypropyl)methacrylamide] in mice using contrast enhanced MRI, Pharmaceutical Research 24 (2007) 1208-1216.
124. B. Zarabi, M.P. Borgman, J. Zhuo, R. Gullapalli, H. Ghandehari, Noninvasive Monitoring of HPMA Copolymer-RGDfK Conjugates by Magnetic Resonance Imaging, Pharmaceutical Research 26 (2009) 1121-1129.

125. M. Hruby, C. Konak, K. Ulbrich, Polymeric micellar pH-sensitive drug delivery system for doxorubicin, Journal of Controlled Release 103 (2005) 137-148.
126. O. Soga, C.F. van Nostrum, M. Fens, C.J. Rijcken, R.M. Schiffelers, G. Storm, W.E. Hennink, Thermosensitive and biodegradable polymeric micelles for paclitaxel delivery, Journal of Controlled Release 103 (2005) 341-353.
127. C.J. Rijcken, C.J. Snel, R.M. Schiffelers, C.F. van Nostrum, W.E. Hennink, Hydrolysable core-crosslinked thermosensitive polymeric micelles: synthesis, characterisation and in vivo studies, Biomaterials 28 (2007) 5581-5593.
128. Z. Jia, L. Wong, T.P. Davis, V. Bulmus, One-pot conversion of RAFT-generated multifunctional block copolymers of HPMA to doxorubicin conjugated acid- and reductant-sensitive crosslinked micelles, Biomacromolecules 9 (2008) 3106-3113.
129. M Tijerina, P. Kopeckova, J. Kopecek, Mechanisms of cytotoxicity in human ovarian carcinoma cells exposed to free Mce6 or HPMA copolymer-Mce6 conjugates, Photochemistry and Photobiology 77 (2003) 645-652.
130. C.M. Peterson, J.G. Shiah, Y. Sun, C.A. P. Kopeckova, T. Minko, R.C. Straight, J. Kopecek, HPMA copolymer delivery of chemotherapy and photodynamic therapy in ovarian cancer, Advances in Experimental Medicine and Biology 519 (2003) 101-123.
131. J. Hongrapipat, P Kopeckova, S. Prakongpan S, Kopecek J, Enhanced antitumor activity of combinations of free and HPMA copolymer-bound drugs, International Journal of Pharmaceutics 351 (2008) 259-270.
132. C.M. Peterson, J.M. Lu, Y. Sun, C.A. Peterson, J.G. Shiah, R.C. Straight, J. Kopecek, Combination chemotherapy and photodynamic therapy with N-(2-hydroxypropyl) methacrylamide copolymer-bound anticancer drugs inhibit human ovarian carcinoma heterotransplanted in nude mice, Cancer Research 56 (1996) 3980-3985.
133. J.G. Shiah, Y. Sun, C.M. Peterson, R.C. Straight, J. Kopecek, Antitumor activity of N-(2-hydroxypropyl) methacrylamide copolymer-Mesochlorine e6 and adriamycin conjugates in combination treatment, Clinical Cancer Research 6 (2000) 1008-1015.
134. J.G. Shiah, Y. Sun, P. Kopeckova, C.M. Peterson, R.C. Straight, J. Kopecek, Combination chemotherapy and photodynamic therapy of targetable N-(2-hydroxypropyl)methacrylamide copolymer-doxorubicin/mesochlorin e(6)-OV-TL 16 antibody immunoconjugates, Journal Controlled Release 74 (2001) 249-253.
135. J. Hongrapipat, P. Kopeckova, J. Liu, S. Prakongpan, J. Kopecek, Combination chemotherapy and photodynamic therapy with fab' fragment targeted HPMA copolymer conjugates in human ovarian carcinoma cells, Molecular Pharmaceutics 5 (2008) 696-709.
136. D. Wang, S.C. Miller, M. Sima, D. Parker, H. Buswell, K.C. Goodrich, P. Kopeckova, J. Kopecek, The arthrotropism of macromolecules in adjuvant-induced arthritis rat model: a preliminary study, Pharmaceutical Research 21 (2004) 1741-1749.
137. D. Wang, S.C. Miller, X.M. Liu, B. Anderson, X.S. Wang, S.R. Goldring SR, Novel dexamethasone-HPMA copolymer conjugate and its potential application in treatment of rheumatoid arthritis, Arthritis Research Therapy 9 (2007) R2.
138. X.M. Liu, L.D. Quan, J. Tian, Y. Alnouti, K. Fu, G.M. Thiele, D. Wang, Synthesis and evaluation of a well-defined HPMA copolymer-dexamethasone conjugate for effective treatment of rheumatoid arthritis, Pharmaceutical Research 25 (2008) 2910-2919.
139. A. Nan, N.P. Nanayakkara, L.A. Walker, V. Yardley, S.L. Croft, H. Ghandehari, N-(2-hydroxypropyl)methacrylamide (HPMA) copolymers for targeted delivery of 8-aminoquinoline antileishmanial drugs, Journal of Controlled Release 77 (2001) 233-243.
140. A. Nan, S.L. Croft, V. Yardley, H. Ghandehari,Targetable water-soluble polymer-drug conjugates for the treatment of visceral leishmaniasis, Journal of Controlled Release 94 (2004) 115-127.
141. S. Nicoletti, K. Seifert K, I.H. Gilbert, N-(2-hydroxypropyl)methacrylamide-amphotericin B (HPMA-AmB) copolymer conjugates as antileishmanial agents, International Journal of Antimicrobial Agents 33 (2009) 441-448.
142. V.R. Caiolfa, M. Zamai, A. Fiorino, E. Frigerio, C. Pellizzoni, R. d'Argy, A. Ghiglieri, M.G. Castelli, M. Farao, E. Pesenti, M. Gigli, F. Angelucci, A. Suarato A, polymer-bound camptothecin: initial biodistribution and antitumour activity studies, Journal of Controlled Release 65 (2000) 105-119.
143. M. Kovar, J. Strohalm, T. Etrych, K. Ulbrich, B. Rihova, Star structure of antibody-targeted HPMA copolymer-bound doxorubicin: a novel type of polymeric conjugate for targeted drug delivery with potent antitumor effect, Bioconjugate Chemistry 13 (2002) 13: 206-215.

Chapter 2

Tumour-targeted nanomedicines: principles and practice

Twan Lammers[a], Wim E. Hennink[a], Gert Storm[a]

[a] Department of Pharmaceutics, Utrecht Institute for Pharmaceutical Sciences, Utrecht University, Sorbonnelaan 16, 3584 CA Utrecht, The Netherlands

Brit. J. Cancer 99: 392-397 (2008)

Abstract

Drug targeting systems are nanometre-sized carrier materials designed for improving the biodistribution of systemically applied (chemo)therapeutics. Various different tumour-targeted nanomedicines have been evaluated over the years, and clear evidence is currently available for substantial improvement of the therapeutic index of anticancer agents. Here, we briefly summarise the most important targeting systems and strategies, and discuss recent advances and future directions in the development of tumour-targeted nanomedicines.

1. Introduction

Over the past few decades, our knowledge on the aetiology of cancer has increased exponentially [1]. This improved understanding of the processes that are at the heart of malignant transformation and tumorigenesis has resulted in the development of several new classes of antitumour therapeutics. In addition to classical chemotherapeutic agents (like doxorubicin, cisplatin and paclitaxel), these so-called 'molecularly targeted therapeutics' (like growth factor receptor inhibitors, proteasome inhibitors, histone deacetylase inhibitors and anti-angiogenic agents) have enriched the therapeutic armoury with their ability to more selectively interfere with certain 'hallmarks of cancer'. An important, but often neglected property that such second-generation agents share with classical chemotherapeutic drugs, however, is their unfavourable biodistribution upon intravenous administration: the agents are generally rapidly cleared from the circulation, and only a very small fraction reaches the tumour site. Moreover, in certain situations, reaching the tumour is not enough: the drug may be cleared from the tumour too rapidly and may not be available long enough to display a strong therapeutic effect. Also, the physicochemical properties of the agent may make it difficult for the drug to enter the target cells. Tumour-targeted nanomedicines are drug delivery systems being developed in oncology to improve drug performance by overcoming such limitations (Table 1). Their most striking feature is their ability to target a drug to the tumour site, thereby enhancing tumoral drug levels (site-specific delivery; aiming for enhanced antitumour activity), and/or to direct a drug away from those body sites that are particularly sensitive to the toxic effects of the drug (site-avoidance delivery; aiming for reduced damage to normal tissues). In this review, we briefly address the most important nanomedicine systems and strategies, summarise the current clinical status and highlight several potential future directions.

Characteristics of an ideal tumour-targeted nanomedicine
1: Increase drug localisation in the tumour (through passive or active targeting)
2: Decrease drug accumulation in sensitive, non-target tissues
3: Ensure minimal drug leakage during transit to target
4: Protect the drug from degradation and from premature clearance
5: Retain the drug at the target site for the desired period of time
6: Facilitate cellular uptake and intracellular trafficking
7: Biocompatible and biodegradable

Table 1. Characteristics of an ideal tumour-targeted nanomedicine. Note that not all characteristics apply to all types of nanomedicines.

2. Passive drug targeting

Tumour-targeted nanomedicines currently in clinical use are shown in Figure 1. Most of these systems utilise the so-called 'passive targeting' concept, with the exception of antibodies and their fragments, which use a receptor recognition motif for improving the delivery of the drug (through 'active targeting'). By designing the systems such that a long circulation time is achieved, significant accumulation in tumours is obtained, especially in those tumour areas with active angiogenesis. Passive targeting refers to the substantial extravasation of the nanomedicine-associated drug into the interstitial fluid at the tumour site, exploiting the locally increased vascular permeability (Figure 2B). In addition, solid tumours tend to lack functional lymphatics, and extravasated (nano)materials are retained within the tumour for prolonged periods of time. The exploitation of this so-called 'enhanced permeability and retention' (EPR) effect is currently the most important strategy for improving the delivery of low molecular weight (chemo)therapeutic agents to tumours [2-4].

2.1. Liposomes

Liposomes are frontrunners among the nanomedicine systems developed so far [5,6]. Liposomes are self-assembling colloid structures composed of lipid bilayers surrounding (an) aqueous compartment(s), and can encapsulate a wide variety of (chemo)therapeutic agents. Myocet and Caelyx (Doxil in the US) were among the first of such lipid self-assemblies to be approved by the regulatory authorities (Table 2). Both products contain doxorubicin, but differ particularly in the presence of a 'stealth' coating: the former refers to doxorubicin entrapped in uncoated liposomes, and the latter to liposomes surface-modified (or 'sterically stabilized') with poly(ethylene glycol) (PEG), to reduce rapid recognition by the reticuloendothelial system, and thereby to prolong circulation time [3,7].

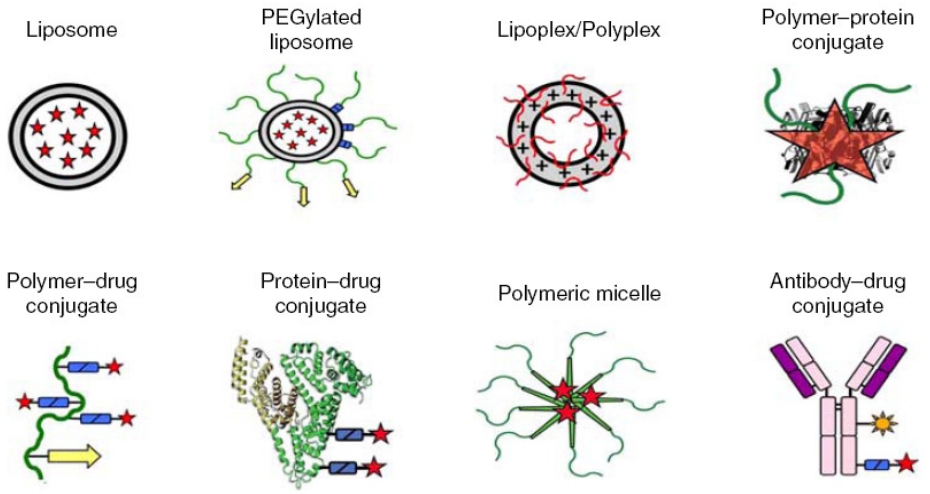

Figure 1. Representative examples of clinically used tumour-targeted nanomedicines. Liposomal bilayers are depicted in grey, polymers and polymer-coatings in green, biodegradable linkers (for releasing drugs and polymer coatings) in blue, targeting ligands in yellow, antibody fragments in purple, radionuclides in orange, and conjugated or entrapped active agents in red. See page 226.

The pharmacokinetic benefits of liposomal drug encapsulation can be illustrated as follows: for free doxorubicin, an elimination half-life time of 0.2 h and an AUC (area under the curve) of 4 μg h ml^{-1} were found in patients, as compared with 2.5 h and 45 μg h ml^{-1} for Myocet, and with 55 h and 900 μg h ml^{-1} for Caelyx, respectively [8]. Both in animal models and in patients, such (liposome-mediated) improvements in AUC have been shown to result in significant improvements in (EPR-mediated) drug targeting to tumours [3,7]. Thus far, however, the primary justification for approving liposomal anthracyclines has been their ability to attenuate drug-related toxicity (e.g. cardiomyopathy, bone marrow depression, alopecia and nausea), rather than to enhance antitumour efficacy. A phase III head-to-head comparison of free doxorubicin vs Myocet in patients with metastatic breast cancer, for instance, demonstrated in this regard that at comparable response rates (RR: 26% for both) and progression-free survival times (PFS: 4 months for both), the incidence of cardiac events (29 vs 13%) and of congestive heart failure (8 vs 2%) were significantly lower for Myocet [9]. Also for Caelyx, significantly reduced cardiomyopathy was observed, whereas its response rates, its progression-free survival times and its overall survival times were always at least comparable with those of the free drug [3,7,9]. In certain specific cases, e.g. in patients suffering from AIDS-related

Kaposi's sarcomas, which are characterized by a dense and highly permeable vasculature, Caelyx not only reduced the toxicity of the intervention but also substantially improved its efficacy: as compared to the formerly standard combination regimen ABV (i.e. adriamycin (doxorubicin), bleomycin and vincristine), which produced a partial response in 31 out of 125 patients (RR: 25%), Caelyx achieved 1 complete response and 60 partial responses (RR: 46%) [10]. Caelyx has consequently been approved for Kaposi's sarcoma, and it is currently also marketed for metastatic breast cancer, for advanced ovarian cancer and for multiple myeloma.

Besides Myocet and Caelyx, several other liposomal nanomedicines have been evaluated over the years, including e.g. non-PEGylated liposomal daunorubicin (DaunoXome) and vincristine (Onco-TCS), PEGylated liposomal cisplatin (SPI-77) and lurtotecan (OSI-211), and lipoplexes, such as Allovectin and LErafAON, in which cationic lipids are used to complex, carry, protect and deliver genetic material, such as plasmid DNA and antisense oligonucleotides (Table 2). Thermodox, a temperature-sensitive version of liposomal doxorubicin (that can be triggered to release its contents; see Figure 2E), has also recently entered clinical trials. At the preclinical level, numerous additional liposomal nanomedicines have been tested, aiming not only to establish novel carrier–drug combinations [11], but also to improve the efficacy of already existing formulations, e.g. by optimising the composition of the lipid bilayer [7], or the nature or density of the polymeric stealth coatings [12].

2.2. Polymers

Ten years after the first report on liposomes [5], and coinciding with the acceptance of their clinical potential [6], natural and synthetic polymers started attracting attention as drug delivery systems. Conceptualised by Ringsdorf in 1975, it was envisioned that polymeric macromolecules can be conjugated to pharmacologically active agents by means of linkers that are stable in blood, but labile in the acidic and/or enzymatic conditions typical for e.g. the tumour microenvironment or for certain intracellular compartments [13]. These so-called 'polymer therapeutics' have been shown to passively accumulate in tumours by means of the EPR effect, and to be able to beneficially affect the therapeutic index of attached low molecular weight agents [2,4].

In 1994, a conjugate called PK1 was the first tumour-targeted polymeric prodrug to enter clinical trials. In PK1, doxorubicin is conjugated to the prototypic polymeric drug carrier PHPMA (poly(*N*-(2-hydroxypropyl)methacrylamide) through an enzymatically cleavable tetrapeptide spacer (GFLG). Like Myocet and Caelyx, PK1 primarily improved the therapeutic index of doxorubicin by attenuating its (cardio)toxicity [4]. This is exemplified by the remarkably high maximum tolerated dose observed for PK1 in clinical trials, being more than 5 times higher than that determined for free doxorubicin (320 vs 60 mg m^{-2}) [14]. Following this proof of principle, PK1 progressed into phase II evaluation, and several additional polymer therapeutics entered clinical trials (Table 2).

In 2005, Abraxane (i.e. albumin-based paclitaxel) was the first passively tumour-targeted polymeric nanomedicine to gain FDA approval. Evidence for an advantage of Abraxane over the standard, Cremophor-formulated version of paclitaxel has been provided by a large phase III trial in which more than 400 women with metastatic breast cancer were randomized to receive either Abraxane (260 mg m^{-2}; given as a 30-min infusion; without premedication) or the free drug (i.e. Taxol; 175 mg m^{-2}; given as a 3-h infusion; with standard steroid and antihistamine premedication). As compared with Taxol, Abraxane significantly improved both the response rate (33 vs 19%) and the progression-free survival time (23 vs 17 weeks) of systemic taxane treatment [15], and at the same time, it also attenuated its toxicity: the incidence of grade 4 neutropenias was significantly lower for Abraxane (9 vs 22%), despite the 50% higher dose, and no hypersensitivity reactions were observed, despite the absence of premedication [15].

Besides Abraxane and PK1, a number of additional polymeric nanomedicines have been evaluated clinically (Table 2). Oncaspar, for instance, in which the polymer PEG is conjugated to the protein L-asparaginase (to decrease allergic reactions and frequency of administration), has been used for treating patients with acute lymphoblastic leukemia for more than 10 years now; Zinostatin, i.e. PSMA-bound neocarcinostatin, has been approved in Japan for the treatment of liver cancer; and Xyotax, i.e. PLGA-conjugated paclitaxel, is in phase III evaluation for ovarian and non-small-cell lung cancer. In addition to such conventional polymer–drug, polymer–protein and protein–drug conjugates, several novel types of polymeric nanomedicines have also recently entered clinical trials, including cationic polyplexes for DNA and siRNA delivery [16,17], dendrimers [18], and polymeric micelles [19].

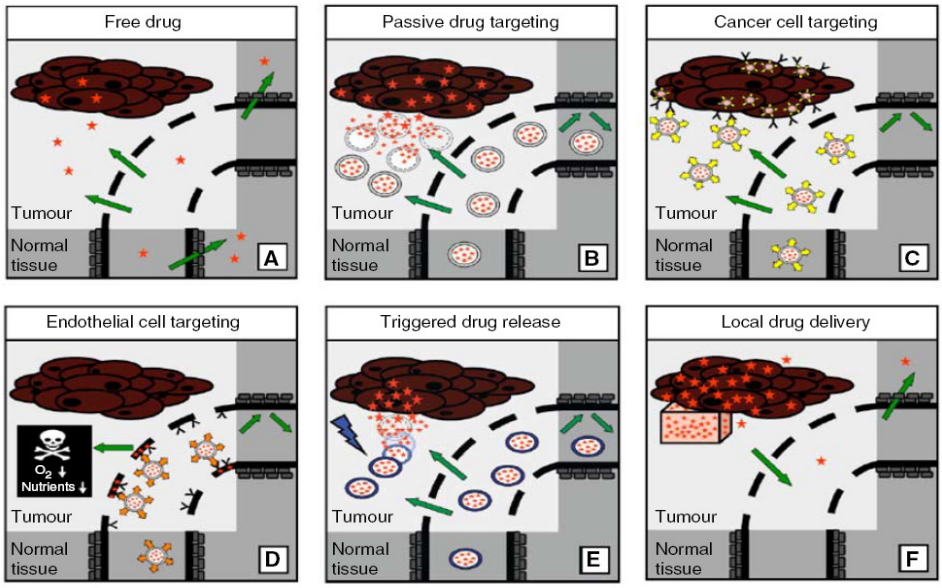

Figure 2. Overview of the clinically most relevant drug targeting strategies. A: Upon the i.v. injection of a low molecular weight (chemo)therapeutic agent, which is often rapidly cleared from blood, only low levels of the drug accumulate in tumours and in tumour cells, whereas their localisation to certain healthy organs and tissues can be relatively high. B: Upon the implementation of a passively targeted drug delivery system, by means of the enhanced permeability and retention (EPR) effect, the accumulation of the active agent in tumours and in tumour cells can be increased substantially. C: Active drug targeting to internalisation-prone cell surface receptors (over)expressed by cancer cells generally intends to improve the cellular uptake of the nanomedicine systems, and can be particularly useful for the intracellular delivery of macromolecular drugs, such as DNA, siRNA and proteins. D: Active drug targeting to receptors (over)expressed by angiogenic endothelial cells aims to reduce blood supply to tumours, thereby depriving tumour cells from oxygen and nutrients. E: Stimuli-sensitive nanomedicines, such as Thermodox, can be activated (i.e. induced to release their contents) by externally applied physical triggers, such as hyperthermia, ultrasound, magnetic fields and light. F: In cases in which tumours are easily accessible, e.g. during surgery, sustained-release delivery devices can be implanted or injected directly into (the irresectable parts of the) tumours. See page 227.

3. Active drug targeting

In active drug targeting, targeting ligands are attached to drugs and drug delivery systems to act as homing devices for binding to receptor structures expressed at the target site [20,21]. Antibody–drug conjugates targeted to e.g. CD20, CD25 and CD33, which are (over)expressed in non-Hodgkin's lymphoma, T-cell lymphoma and acute myeloid leukaemia, respectively, have been successfully used for delivering radionuclides (Zevalin), immunotoxins (Ontak) and antitumour antiobiotics (Mylotarg) more selectively to tumour cells (Table 2).

Antibodies, antibody fragments and peptides have also been used as targeting moieties for drug delivery systems. Clinical evidence in support of this strategy, however, is scarce, and has to date only been provided for galactosamine-targeted PHPMA-doxorubicin (PK2) [22] and for GAH-targeted doxorubicin-containing immunoliposomes (MCC-4650) [23]: for the former, responses were observed in 3 out of 31 patients with liver cancer (with one partial remission lasting for more than 47 months), and for the latter, disease stabilisation was detected in 10 out of 18 patients with gastric cancer (but no obvious reductions in tumour size).

Compound	Name	Indication	Status
Liposomal Doxorubicin	Myocet, Caelyx (Doxil)	Breast, Ovarian, KS	Approved
Liposomal Daunorubicin	Daunoxome	Kaposi's Sarcoma	Approved
Liposomal Vincristine	Onco-TCS	Non-Hodgkin Lymphoma	Approved
Liposomal Cisplatin	SPI-77	Lung	Phase II
Liposomal Lurtotecan	OSI-221	Ovarian	Phase II
Cationic Liposomal c-Raf AON	LErafAON	Various	Phase I / II
Cationic Liposomal E1A pDNA	PLD-E1A	Breast, Ovarian	Phase I / II
Thermosensitive Liposomal Doxorubicin	ThermoDox	Breast, Liver	Phase I
Albumin-Paclitaxel	Abraxane	Breast	Approved
Albumin-Methotrexate	MTX-HSA	Kidney	Phase II
Dextran-Doxorubicin	DOX-OXD	Various	Phase I
PEG-L-Asparaginase	Oncaspar	Leukaemia	Approved
PEG-IFNα2a / -IFNα2b	PegAsys / PegIntron	Melanoma, Leukaemia	Phase I / II
PHPMA-Doxorubicin	PK1	Breast, Lung, Colon	Phase II
Galactosamine-targeted PK1	PK2	Liver	Phase I / II
PGA-Paclitaxel	Xyotax	Lung, Ovarian	Phase III
Paclitaxel-containing Polymeric Micelles	Genexol-PM	Breast, Lung	Phase II
Cisplatin-containing Polymeric Micelles	Nanoplatin	Various	Phase I
Doxorubicin-containing Polymeric Micelles	NK911	Various	Phase I
SN38-containing Polymeric Micelles	LE-SN38	Colon, Colorectal	Phase I
^{90}Yttrium-Ibritumomab Tiuxetan (α-CD20)	Zevalin	Non-Hodgkin Lymphoma	Approved
DTA-IL2 fusion protein (α-CD25)	Ontak	T-Cell Lymphoma	Approved
Ozogamycin-Gemtuzumab (α-CD33)	Mylotarg	Leukaemia	Approved
Doxorubicin-cBR96 (α-CD174)	SGN-15	Lung, Prostate, Breast	Phase II

Table 2. Examples of clinically used tumour-targeted nanomedicines.

Preclinically, a much larger number of studies have dealt with actively targeted nanomedicines, and several general principles have emerged. In most cases in which the nanosized carrier materials were targeted to receptors (over)expressed by cancer cells, for instance, the observed improvements in antitumour efficacy were found to be due to an enhanced cellular internalisation of the agents, rather than to an increased tumour accumulation (Figure 2C) [21,24]. The fact that improving cellular internalisation can – at least under certain circumstances – improve the efficacy of systemic anticancer therapy has resulted in the design of delivery systems targeted to endocytosis-prone surface receptors, such as the transferrin receptor, the folate receptor and EGFR [3,4,20]. In addition, it has stimulated research into the use of cell-penetrating peptides and protein-transduction domains, such as oligo-arginine and TAT, to enable the internalisation of agents that would otherwise not be taken up effectively by cancer cells [25].

Destruction of the endothelium in solid tumours can result in the death of tumour cells induced by the lack of oxygen and nutrients. This observation, together with the high accessibility of luminal surface receptors, has led to the design of nanomedicines actively targeted to tumour endothelial cells (Figure 2D). Ligands used to target drugs and/or drug delivery systems to tumour blood vessels include the antibody fragment L19 [26], which uses the EDB domain of the oncofetal protein fibronectin to home to angiogenic vasculature, and several cyclic and linear derivatives of the oligopeptides RGD and NGR, which bind to angiogenic endothelium through the integrins α2bβ3, αvβ3 and α5β1, and through aminopeptidase-N, respectively. Recent data obtained in our group with RGD-targeted liposomes containing vascular targeting agents showed widespread central necrosis in established experimental tumours [27]. Opposite to the short-lasting antitumour effects obtained with the free agent, endothelial cell-targeted liposomal delivery halted tumour progression for significantly prolonged periods of time. Further preclinical and clinical studies on the efficacy of tumour vasculature-targeted nanomedicines are eagerly awaited. If such nanomedicines ultimately prove in the clinic to be efficacious with manageable side effects, combination therapies together with radiation, chemotherapeutic agents and/or antiangiogenic drugs are anticipated to attack the thin film of viable tumour cells in the periphery of the tumour, which usually survives when vascular targeting agents are applied as anticancer therapeutics.

4. Future directions

In this review, we have primarily restricted ourselves to tumour-targeted nanomedicines designed for improving the delivery of already established, low molecular weight chemotherapeutic agents. Many of the new drugs arising from advances in biotechnology, however, are macromolecules, such as proteins and nucleic acids. The clinical development of these challenging and often fragile molecules will likely also profit substantially from the attributes of targeted nanomedicines, providing these complex molecules e.g. with protection against degradation and elimination, and with improved access to target cells and tissues.

In the document 'Forward Look on Nanomedicine 2005', the European Science Foundation included in their definition of the discipline of nanomedicine not only the use of nanometer-sized materials for the treatment, but also for the diagnosis of diseases. Regarding the latter aspect, the development of high-resolution imaging techniques (such as, MRI and PET) for the rapid, noninvasive monitoring of the in vivo fate and performance of targeted nanomedicines is currently receiving intense attention, and will certainly facilitate the implementation of imaging-guided drug delivery to promote the optimal use of (tumour-) targeted nanomedicines.

Additional areas likely to receive considerable attention in the years to come are:

1) the design of systems that are able to respond to externally applied stimuli, such as hyperthermia, ultrasound, light and magnetic fields, and that can be triggered to release their contents (like Thermodox; Figure 2E);

2) the targeting of agents other than conventional chemotherapeutic drugs to tumours, such as anti-inflammatory agents (like corticosteroids) to inhibit tumour-associated inflammation [11], and siRNA to reduce the expression of proteins essential for tumour progression [17];

3) the development of systems that are able to simultaneously deliver multiple therapeutic agents to tumours, such as temporally targeted 'nanocells', which first release the anti-angiogenic agent combrestatin and subsequently the chemotherapeutic agent doxorubicin [28];

4) the translation of the insights obtained and the experiences gained in oncology into applications for improving the treatment of other diseases, such as rheumatoid arthritis, Crohn's disease, autoimmune diseases and infections, which are all highly amenable to EPR-mediated drug targeting [11];

5) the establishment of treatment regimens in which tumour-targeted nanomedicines are combined with other clinically relevant treatment modalities, such as with surgery, with radiotherapy and with chemotherapy.

For obvious reasons, the latter of the above strategies has thus far received the most clinical attention. During surgery, for instance, sustained-release delivery devices, such as Gliadel (i.e. carmustine-containing polymeric wafers), can be implanted into those parts of glioblastoma lesions that cannot be removed surgically (see Figure 2F). In addition to this, also systems originally intended for systemic administration, such as polymers and liposomes, have been shown to hold potential for such local interventions [29]. Regarding radiotherapy, preclinical and early clinical evidence suggest that tumour-targeted nanomedicines and radiotherapy interact synergistically, with radiotherapy improving the tumour accumulation of the delivery systems, and with the delivery systems improving the interaction between radiotherapy and chemotherapy [30-32]. And regarding chemotherapy, both Myocet and Caelyx have been successfully included in several different combination chemotherapy trials [8], and also for Abraxane, initial results obtained in combination regimens are promising. Combinations of molecularly targeted therapeutics with tumour-targeted therapeutics have also already been evaluated, showing, for example, that the combination of Avastin (Bevacizumab) with Abraxane produced an overall response rate of almost 50% in heavily pretreated breast cancer patients [33].

Since the approval, in 1995, of the first tumour-targeted anticancer nanomedicine (Caelyx/Doxil, i.e. stealth liposomal doxorubicin), targeted nanomedicines have become an established addition to the anticancer drug arsenal, with several formulations presently on the market. A major limitation impeding the entry of targeted nanomedicines onto the market is that new concepts and innovative research ideas within academia are not being developed and exploited in collaboration with the pharmaceutical industry. An integrated 'bench-to-clinic' approach, realised within a structural collaboration between industry and academia, would strongly stimulate the progression of tumour-targeted nanomedicines towards clinical application.

References

1. Hanahan D, Weinberg RA (2000) The hallmarks of cancer. *Cell* **100**: 57–70
2. Maeda H, Wu J, Sawa T, Matsumura Y, Hori K (2000) Tumour vascular permeability and the EPR effect in macromolecular therapeutics: a review. *J Control Release* **65**: 271–284
3. Torchilin VP (2005) Recent advances with liposomes as pharmaceutical carriers. *Nat Rev Drug Discov* **4**: 145–160
4. Duncan R (2006) Polymer conjugates as anticancer nanomedicines. *Nat Rev Cancer* **6**: 688–701
5. Bangham AD, Standish MM, Watkins JC (1965) Diffusion of univalent ions across the lamellae of swollen phospholipids. *J Mol Biol* **13**: 238–252
6. Gregoriadis G (1976) The carrier potential of liposomes in biology and medicine. *N Engl J Med* **295**: 765–770
7. Drummond DC, Meyer O, Hong K, Kirpotin DB, Papahadjopoulos D (1999) Optimizing liposomes for delivery of chemotherapeutic agents to solid tumours. *Pharmacol Rev* **51**: 691–743
8. Hofheinz RD, Gnad-Vogt SU, Beyer U, Hochhaus A (2005) Liposomal encapsulated anti-cancer drugs. *Anticancer Drugs* **16**: 691–707
9. Harris L, Batist G, Belt R, Rovira D, Navari R, Azarnia N, Welles L, Winer E (2002) Liposome-encapsulated doxorubicin compared with conventional doxorubicin in a randomized multicenter trial as first-line therapy of metastatic breast carcinoma. *Cancer* **94**: 25–36
10. Northfelt DW, Dezube BJ, Thommes JA, Miller BJ, Fischl MA, Friedman-Kien A, Kaplan LD, Du Mond C, Mamelok RD, Henry DH (1998) Pegylated-liposomal doxorubicin versus doxorubicin, bleomycin, and vincristine in the treatment of AIDS-related Kaposi's sarcoma: results of a randomized phase III clinical trial. *J Clin Oncol* **16**: 2445–2451
11. Schiffelers RM, Banciu M, Metselaar JM, Storm G (2006) Therapeutic application of long-circulating liposomal glucocorticoids in auto-immune diseases and cancer. *J Liposome Res* **16**: 185–194
12. Romberg B, Hennink WE, Storm G (2007) Sheddable coatings for long-circulating nanoparticles. Sheddable coatings for long-circulating nanoparticles. *Pharm Res* **25**: 55–71
13. Ringsdorf H (1975) Structure and properties of pharmacologically active polymers. *J Polymer Sci Polymer Symp* **51**: 135–153
14. Vasey PA, Kaye SB, Morrison R, Twelves C, Wilson P, Duncan R, Thomson AH, Murray LS, Hilditch TE, Murray T (1999) Phase I clinical and pharmacokinetic study of PK1 [N-(2-hydroxypropyl)methacrylamide copolymer doxorubicin]: first member of a new class of chemotherapeutic agents-drug-polymer conjugates. *Clin Cancer Res* **5**: 83–94
15. Gradishar WJ, Tjulandin S, Davidson N, Shaw H, Desai N, Bhar P, Hawkins M, O'Shaughnessy J (2005) Phase III trial of nanoparticle albumin-bound paclitaxel compared with polyethylated castor oil-based paclitaxel in women with breast cancer. *J Clin Oncol* **23**: 7794–7803
16. De Smedt SC, Demeester J, Hennink WE (2001) Cationic polymer based gene delivery systems. *Pharm Res* **17**: 113–126
17. Schiffelers RM, Ansari A, Xu J, Zhou Q, Tang Q, Storm G, Molema G, Lu PY, Scaria PV, Woodle MC (2004) Cancer siRNA therapy by tumour selective delivery with ligand-targeted sterically stabilized nanoparticle. *Nucleic Acids Res* **32**: e14
18. Bai S, Thomas C, Rawat A, Ahsan F (2006) Recent progress in dendrimer-based nanocarriers. *Crit Rev Ther Drug Carrier Syst* **23**: 437–495
19. Nishiyama N, Kataoka K (2006) Current state, achievements, and future prospects of polymeric micelles as nanocarriers for drug and gene delivery. *Pharmacol Ther* **112**: 630–648
20. Allen TM (2002) Ligand-targeted therapeutics in anticancer therapy. *Nat Rev Cancer* **2**: 750–763
21. Park JW, Benz CC, Martin FJ (2004) Future directions of liposome- and immunoliposome-based cancer therapeutics. *Semin Oncol* **31-S13**: 96–205
22. Seymour LW, Ferry DR, Anderson D, Hesslewood S, Julyan PJ, Poyner R, Doran J, Young AM, Burtles S, Kerr DJ (2002) Hepatic drug targeting: phase I evaluation of polymer-bound doxorubicin. *J Clin Oncol* **20**: 1668–1676
23. Matsumura Y, Gotoh M, Muro K, Yamada Y, Shirao K, Shimada Y, Okuwa M, Matsumoto S, Miyata Y, Ohkura H, Chin K, Baba S, Yamao T, Kannami A, Takamatsu Y, Ito K, Takahashi K (2004) Phase I and pharmacokinetic study of MCC-465, a doxorubicin (DXR).

encapsulated in PEG immunoliposome, in patients with metastatic stomach cancer. *Ann Oncol* **15**: 517–525

24. Kirpotin DB, Drummond DC, Shao Y, Shalaby MR, Hong K, Nielsen UB, Marks JD, Benz CC, Park JW (2006) Antibody targeting of long-circulating lipidic nanoparticles does not increase tumour localisation but does increase internalization in animal models. *Cancer Res* **66**: 6732–6740
25. Gupta B, Levchenko TS, Torchilin VP (2005) Intracellular delivery of large molecules and small particles by cell-penetrating proteins and peptides. *Adv Drug Deliv Rev* **57**: 637–651
26. Neri D, Bicknell R (2005) Tumour vascular targeting. *Nat Rev Cancer* **5**: 436–446
27. Fens MH, Hill KJ, Issa J, Ashton SE, Westwood FR, Blakey DC, Storm G, Ryan AJ, Schiffelers RM (2008) Liposomal encapsulation enhances the antitumour efficacy of the vascular disrupting agent ZD6126 in murine B16.F10 melanoma. *Br J Cancer* **99**: 1256-1264
28. Sengupta S, Eavarone D, Capila I, Zhao G, Watson N, Kiziltepe T, Sasisekharan R (2005) Temporal targeting of tumour cells and neovasculature with a nanoscale delivery system. *Nature* **436**: 568–572
29. Lammers T, Peschke P, Kühnlein R, Subr V, Ulbrich K, Huber P, Hennink W, Storm G (2006) Effect of intratumoral injection on the biodistribution and the therapeutic potential of HPMA copolymer-based drug delivery systems. *Neoplasia* **8**: 788–795
30. Li C, Ke S, Wu QP, Tansey W, Hunter N, Buchmiller LM, Milas L, Charnsangavej C, Wallace S (2000) Tumor irradiation enhances the tumor-specific distribution of poly(L-glutamic acid)-conjugated paclitaxel and its antitumor efficacy. *Clin Cancer Res* **6**: 2829–2834
31. Dipetrillo T, Milas L, Evans D, Akerman P, Ng T, Miner T, Cruff D, Chauhan B, Iannitti D, Harrington D, Safran H (2006) Paclitaxel poliglumex (PPX-Xyotax) and concurrent radiation for esophageal and gastric cancer: a phase I study. *Am J Clin Oncol* **29**: 376–379
32. Lammers T, Subr V, Peschke P, Kühnlein R, Hennink WE, Ulbrich K, Kiessling F, Heilmann M, Debus J, Huber PE, Storm G (2008) Image-guided and passively tumor-targeted polymeric nanomedicines for radiochemotherapy. *Br J Cancer* **99**: 900-910
33. Link JS, Waisman JR, Nguyen B, Jacobs CI (2007) Bevacizumab and albumin-bound Paclitaxel treatment in metastatic breast cancer. *Clin Breast Cancer* **7**: 779–783

Chapter 3

Effect of physicochemical modification on the biodistribution and the tumor accumulation of HPMA copolymers

Twan Lammers[a,b], Rainer Kühnlein[a], Maria Kissel[a], Vladimir Subr[c], Tomas Etrych[c], Robert Pola[c], Michal Pechar[c], Karel Ulbrich[c], Gert Storm[b], Peter Huber[a], Peter Peschke[a]

[a] Department of Innovative Cancer Diagnosis and Therapy, Clinical Cooperation Unit Radiotherapeutic Oncology, German Cancer Research Center, Im Neuenheimer Feld 280, 69120 Heidelberg, Germany

[b] Department of Pharmaceutics, Utrecht Institute for Pharmaceutical Sciences, Utrecht University, Sorbonnelaan 16, 3584 CA Utrecht, The Netherlands

[c] Institute of Macromolecular Chemistry, Academy of Sciences of the Czech Republic, Heyrovsky Square 2, 162 06 Prague 6, Czech Republic

J. Control. Release 110: 103-118 (2005)

Abstract

Copolymers of *N*-(2-hydroxypropyl)methacrylamide (HPMA) are prototypic and well-characterized polymeric drug carriers that have been broadly implemented in the delivery of anticancer therapeutics. To better predict the in vivo potential of the copolymers and to describe the biodistributional consequences of functionalization, thirteen physicochemically different HPMA copolymers were synthesized, varying in molecular weight and in the nature and amount of functional groups introduced. Upon radiolabeling, the copolymers were injected i.v., and their circulation kinetics, tissue distribution and tumor accumulation were monitored in rats bearing subcutaneous Dunning AT1 tumors. It was found that increasing the average molecular weight of HPMA copolymers resulted in prolonged circulation times and in increased tumor concentrations. The conjugation of carboxyl and hydrazide groups, as well as the introduction of spacer, drug and peptide moieties, reduced the long-circulating properties of the copolymers and as a result, lower levels were found in tumors and in all organs other than kidney. Interestingly, however, in spite of the reduced (absolute) tumor concentrations, hardly any reduction in the relative levels localizing to tumors was found. Tumor-to-organ ratios were comparable to those of unmodified controls for the majority of chemically modified copolymers, indicating that functionalization does not necessarily affect the tumor targeting ability of the copolymers, and suggesting that HPMA copolymer-based drug delivery systems may prove to be attractive tools for more effectively treating various forms of advanced solid malignancy.

1. Introduction

Copolymers of *N*-(2-hydroxypropyl)methacrylamide (HPMA) are prototypic and well-characterized drug carriers that hold significant promise for implementation in anticancer therapy [1-4]. With their long-circulating properties, HPMA copolymers are able to localize to tumors relatively effectively by means of the enhanced permeability and retention (EPR) effect [5]. EPR relies on the notion that the tumor vasculature tends to be significantly more leaky than normal, continuous endothelium [6]. Long-circulating macromolecular drug carriers use this enhanced vascular permeability to extravasate into the tumor interstitium, and because of the lack of a functional lymphatic drainage system within solid tumors, they tend to accumulate there (passively) over time [2-6].

Currently, several HPMA-based chemotherapeutic agents are being evaluated clinically. PK1, an HPMA copolymer in which doxorubicin is coupled to the polymeric backbone by means of an enzymatically cleavable tetrapeptide (GFLG) spacer, was the first conjugate to enter phase I trials [7-9]. Based on the relatively promising results obtained for PK1, a few years later, PK2 was designed, in which galactose moieties were included to actively and more specifically target hepatocytes [10,11]. In parallel, a number of other HPMA copolymer-based anticancer agents were designed, carrying both classical chemotherapeutics, like cisplatinum [12-14] and paclitaxel [15], as well as more recently discovered drugs, like the heat shock protein inhibitor geldanamycin [16,17] and the angiogenesis inhibitor TNP-470 [18,19]. In addition, HPMA copolymers have been shown to be able to improve the tumor-targeted delivery of proteins, like ribonucleases [20] and β-lactamase [21], and to allow for the design of polymer-based imaging agents, in which tracers like 131-iodine [11], 99-technetium [22] and gadolinium [23] are used to visualize tumors, metastases and tumor vasculature.

The conjugation of most, if not of all, of the abovementioned agents to HPMA copolymers is expected to have significant impact on the physicochemical properties of the copolymers. Up to now, however, hardly any study has directly delineated how the functionalization of HPMA copolymers affects their biodistribution and their tumor targeting ability. Hypothesizing that parental (i.e. chemically unmodified) HPMA copolymers reside in the most optimal random coil conformation, that they thus possess the most optimal long-circulating

properties, and that they are therefore more effective in targeting solid tumors than are HPMA copolymers carrying e.g. drugs, spacers and/or tracers, we have here set out to investigate the effects of functionalization by synthesizing thirteen different HPMA copolymers (see Table 1). In four sequentially performed sets of experiments, the copolymers were radiolabeled and injected i.v., and their kinetics, their tissue distribution and their tumor accumulation were monitored in Copenhagen rats bearing subcutaneously transplanted Dunning AT1 tumors [24]. In the first set of experiments, to validate previous findings from us and others suggesting that increasing the average molecular weight of HPMA copolymers increases their ability to localize to tumors [25-28], copolymers with weights ranging from 23 kD to 65 kD were analyzed. Then, HPMA copolymers bearing 3 mol% and 8 mol% of carboxyl (COOH) and hydrazide ($NHNH_2$) groups were studied, in order to investigate the impact of both the nature and the amount of functional groups introduced. Third, HPMA copolymers conjugated to doxorubicin were analyzed, to describe the effect of the introduction of a low molecular weight chemotherapeutic drug. And fourth, the effect of the conjugation of a peptide moiety was assessed, by synthesizing and analyzing three differently spaced HPMA copolymers carrying the (potentially therapeutic) pentapeptide PHSCN [29,30].

2. Materials and Methods

2.1. Materials

Methacryloyl chloride, methacrylic acid (MAA), 1-aminopropan-2-ol, tyrosinamide, glycylglycine, glycylphenylalanine, leucylglycine, 4-nitrophenol, hydrazine hydrate, *N,N'*-dicyclohexylcarbodiimide (DCC), 2,2'-azobis(isobutyronitrile) (AIBN), *N,N*-dimethylformamide (DMF), dimethylsulfoxide (DMSO), tetrahydrofurane (THF), triethylamine (Et_3N), doxorubicin hydrochloride (DOX.HCl) and trinitrobenzenesulfonic acid (TNBSA) were purchased from Fluka. Fmoc-Asn(Trt)-OH, Fmoc-Cys(Trt)-OH, Fmoc-Ser(tBu)-OH, Fmoc-His(Trt)-OH, Fmoc-Pro-OH, Fmoc-AHX-OH, Fmoc-PEG-COOH and Sieber amide resin were obtained from Novabiochem. All chemicals and solvents were of analytical grade, and all amino acids were of L-configuration (unless stated otherwise).

2.2. Synthesis of the monomers

N-(2-hydroxypropyl)methacrylamide (HPMA) was prepared by reaction of methacryloyl chloride with 1-aminopropan-2-ol in methylene chloride [31]. *N*-Methacryloylglycylglycine (Ma-GlyGly-OH) was prepared by Schotten-Baumann acylation of glycylglycine with methacryloyl chloride in an aqueous alkaline medium [32]. *N*-Methacryloylglycylglycine 4-nitrophenyl ester (Ma-GlyGly-ONp) and *N*-methacryloylglycyl-DL-phenylalanylleucylglycine 4-nitrophenyl ester (Ma-Gly-DL-PheLeuGly-ONp) were prepared by the reaction of corresponding *N*-methacryloylated oligopeptide with 4-nitrophenol in the presence of *N*,*N'*-dicyclohexylcarbodiimide in DMF or THF [31,32]. *N*-methacryloylglycyl-DL-phenylalanylleucylglycine (Ma-Gly-DL-PheLeuGly-OH) was prepared as described earlier [33]. *N*-Methacryloyl tyrosinamide (Ma-TyrNH_2) was prepared by reaction of methacryloyl chloride with tyrosinamide in distilled water [28].

2.3. Synthesis of the copolymers

The copolymers poly(HPMA-co-Ma-TyrNH_2) (**I**, **II** and **III**; see Table 1) were prepared by radical copolymerization of HPMA and Ma-TyrNH_2 in methanol at 60 °C for 24 h [28]. Terpolymers bearing carboxylic groups and tyrosinamide residue in the side chains (**IV**, **VI** and **IX**; Table 1) were prepared by terpolymerization of HPMA, Ma-TyrNH_2 and methacrylic acid (MAA) or Ma-Gly-DL-PheLeuGly-OH in methanol at 60 °C for 24 h. Narrow distribution of molecular weight was obtained by fractionation of the polymers on Sepharose 4B/6B column (5.3 x 100 cm) in 0.3M sodium acetate buffer (pH 6.5) containing 0.5 g/L sodium azide. The main fraction was dialyzed against distilled water for two days, filtered on a Sephadex G-25 column in water and lyophilized. Polymeric precursors bearing 4-nitrophenyl reactive groups and tyrosinamide residue in the side chains were prepared by precipitation radical terpolymerization of HPMA, Ma-TyrNH_2 and corresponding *N*-methacryloylated oligopeptide 4-nitrophenyl ester in acetone at 50 °C for 24 h [34]. Polymeric precursors bearing hydrazide groups and tyrosinamide residue in the side chains (**V**, **VII**; Table 1) were prepared by the reaction of HPMA copolymers bearing 4-nitrophenyl reactive groups and tyrosinamide residue in the side chains with hydrazine monohydrate (10-fold molar excess of hydrazine monohydrate, relative to the amount of ONp) in methanol [35]. Finally, precursors carrying glycylglycine were prepared by radical copolymerization of HPMA and Ma-GlyGly-ONp.

Polymer	Identity	Size (kD)	Polydispersity	Functional Group (Y)	$TyrNH_2$
I	Poly(HPMA)	23.4	1.40	–	0.44 mol%
II	Poly(HPMA)	30.5	1.32	–	0.83 mol%
III	Poly(HPMA)	64.5	1.23	–	0.33 mol%
IV	Poly(HPMA) : 3%–	33.6	1.54	3.45 mol% -COOH	0.29 mol%
V	Poly(HPMA) : 3%+	29.0	2.00	3.05 mol% $-NHNH_2$	1.02 mol%
VI	Poly(HPMA) : 8%–	21.0	1.56	8.00 mol% -COOH	0.30 mol%
VII	Poly(HPMA) : 8%+	19.0	1.77	7.55 mol% $-NHNH_2$	1.08 mol%
VIII	Poly(HPMA)-GG-Dox	30.8	1.20	7.2 mol% -GlyGly-Dox	0.47 mol%
IX	Poly(HPMA)-GFLG-Dox	29.5	1.25	6.25 mol% -GlyPheLeuGly-Dox	0.50 mol%
X	Poly(HPMA)-GG-Dox	25.5	1.50	5.07 mol% -GlyPheLeuGly-OH	0.61 mol%
XI	Poly(HPMA)-GFLG-NN-Dox	22.0	1.57	6.47 mol% -GFLG-NHNH-Dox	0.85 mol%

Table 1. Identities and characteristics of the thirteen HPMA copolymers synthesized.

2.4. Synthesis of the polymer-doxorubicin conjugates

The polymer-Dox conjugates were prepared by reaction of the polymer precursor bearing ONp reactive groups with Dox.HCl in DMSO in the presence of Et_3N [36]. The precursors (0.5 g, 1.98 x 10^{-4} mol ONp) were dissolved in DMSO (3 mL) and Dox.HCl (0.050 g, 8.62 x 10^{-5} mol) was added, followed by the addition of Et_3N (15 μL, 9.5 x 10^{-5}mol) in two portions during 30 min. The reaction mixture was stirred for 4 h at 25 °C. Then 10 μL 1-aminopropan-2-ol were added and the mixture was precipitated into aceton : diethylether (3:1). The polymer-Dox conjugate was filtered off, dried in vacuum and purified on a Sephadex LH-20 column in methanol to remove free doxorubicin. Finally, to obtain narrow polydispersities, conjugates **VIII** and **X** were purified on a Sephadex LH-60 column in methanol (Table 1).

2.5. Synthesis of PHSCN peptides

The protected peptides Pro-His(Trt)-Ser(tBu)-Cys(Trt)-Asn(Trt)-OH, Ahx- Pro-His(Trt)-Ser(tBu)-Cys(Trt)-Asn(Trt)-OH and PEG- Pro-His(Trt)-Ser(tBu)-Cys(Trt)-Asn(Trt)-OH were prepared by manual solid phase peptide synthesis using 9-fluorenylmethoxycarbonyl/tertiary butyl (Fmoc/tBu) strategy on Sieber amide

resin [37]. The following amino acid derivatives were used in the synthesis: Fmoc-Asn(Trt)-OH, Fmoc-Cys(Trt)-OH, Fmoc-Ser(tBu)-OH, Fmoc-His(Trt)-OH, Fmoc-Pro-OH, Fmoc-Ahx-OH and Fmoc-PEG-COOH. The elongation cycle consisted of Fmoc removal with 20% piperidine in DMF (2×5 min) and condensation with the appropriate N-Fmoc protected amino acid (3 eq.) activated with PyBOP (3 eq.) and HOBt (3 eq.) in DMF in presence of DIEA (0.86 mL, 5 mmol) under N_2 (15–45 min). The completion of each acylation step was verified with a ninhydrin test. After the last condensation, the N-terminal Fmoc was removed with 20% piperidine and the partially protected peptide amide was cleaved from the resin with 1 % TFA in dichloromethane and filtered into 10 % pyridine in methanol. The filtrate was concentrated under vacuum, precipitated with water, filtered and dried under vacuum. In case of the PEG-derivative the product was soluble in water; therefore it was extracted with dichloromethane from the aqueous solution, dried and triturated with diethyl ether. Homogeneity of the partially protected peptide derivatives was checked by HPLC using a reversed phase column, Nucleosil C18, 250×4 mm (Watrex, Czech Republic) and linear gradient water-acetonitrile, 0-100% acetonitrile in presence of 0.1% TFA, 1 mL/min, UV detector 220 nm (>90 %). Identity of the peptide derivatives was confirmed by matrix-assisted laser desorption-ionization time-of-flight mass spectroscopy (MALDI-TOF MS) performed on Bruker Biflex III mass spectrometer: PHSCN (protected) 1360.55 (M+Na), AHX-PHSCN (protected) 1473.61 (M+Na), PEG-PHSCN (protected) 1959.79 (M+Na).

2.6. Preparation of the polymer-PHSCN conjugates

The precursors (100 mg, 0.052 mmol ONp), the partially protected peptides (0.013 mmol) and tyrosinamide (1.1 mg, 0.006 mmol) were dissolved in DMF (2 mL). Then DIEA (0.02 mL, 0.12 mmol) was added. After 16 hrs at 25ºC, the reaction was terminated by addition of (*R,S*)-1-aminopropan-2-ol and the polymer conjugate was isolated by precipitation with diethyl ether followed by centrifugation. The precipitate was dissolved in a mixture of 94% TFA, 2.5% H_2O, 2.5% ethandithiol and 1% triisopropylsilane to remove the protecting groups. Then the polymer was precipitated with diethyl ether, redissolved in acetic acid, once more precipitated and dried. Finally, the conjugate was dissolved in water, purified by chromatography on Sephadex G 25 in water (PD 10 column, Pharmacia) and freeze dried to yield 83 mg of peptide-polymer conjugate **XI, XII** and **XIII** (Table 1).

2.7. Characterization of the copolymers

The weight- and number-average molecular weights (M_w and M_n) and the polydispersity (M_w/M_n) of the copolymers were determined by size exclusion chromatography on an Äkta Explorer (Amersham Biosciences) with a Superose 6^{TM} or a Superose 12^{TM} column equipped with UV, a differential refractometer (Shodex R-72, Japan) and a multiangle light scattering detector DAWN DSP-F (Wyatt Technology Corp., USA). 0.3M Sodium acetate buffer (pH 6.5) containing 0.5 g/L sodium azide was used as the mobile phase. The flow rate was 0.5 mL/min. The content of carboxylic groups in copolymers containing MAA was determined by titration with 0.05 M NaOH on an automatic titrator Tim900 (Radiometry, Copenhagen). The composition and content of PHSCN oligopeptide and the amount of tyrosinamide were determined on a HPLC amino acid analyzer (LDC Analytical, USA) with a reverse-phase column Nucleosil 120-3 C_{18} (Macherey-Nagel, 125 x 4 mm) using precolumn derivatization with phthalaldehyde and a fluorescence detector (excitation at 229 nm, emission at 450 nm). Gradient elution was used: 10–100 % of solvent B within 65 min and flow rate 0.5 mL/min (solvent A: 0.05 M sodium acetate buffer, pH 6.5; solvent B: 300 mL of 0.17 M sodium acetate and 700 mL of methanol). Prior to analysis, the copolymer samples were hydrolyzed with 6 N HCl at 115 °C for 18 h in sealed ampule. The content of DOX and ONp reactive groups was determined spectrophotometrically on a UV/VIS spectrophotometer (HEλIOS α, Thermospectronic, UK; Dox-methanol, εB_{484} = 13500 L mol^{-1} cm^{-1}; ONp–DMSO, ε_{274} = 9500 L mol^{-1} cm^{-1P}). The content of hydrazide-terminated side chains was determined by a modified TNBSA assay. Briefly, a stock solution of copolymer containing hydrazide groups (10 mg/mL) was prepared in a borate buffer (0.1 M $Na_2B_4O_7H_2O$, pH 9.3). 25 Microliters of this solution were added to a cuvette (l = 1cm, V = 1 mL) containing 950 μL of borate buffer and 25 μL of 0.03 M TNBSA solution. After 100 min of incubation, the absorbance was measured at λ = 500 nm. A molar absorption coefficient ε_{500} = 14100 L mol^{-1} cm^{-1} estimated for the model reaction of ethyl carbazate with TNBSA was used.

2.8. Radiolabeling

131-Iodine was obtained from Amersham. All copolymers were radiolabeled using the mild oxidizing agent 1,3,4,6-tetrachloro-3 alpha,6 alpha-diphenyl glycoluril (i.e. by means of the Iodogen-method) [38]. Free iodine was removed using a Biogel-P6 column.

2.9. Animal model

All experiments involving animals were approved by an external committee for animal welfare and were performed according to the guidelines for laboratory animals established by the German government. Experiments were performed on 6 to 12 month old male Copenhagen rats (Charles River, Germany), using the syngeneic Dunning R3327-AT1 prostate carcinoma model [24]. Experimental groups consisted of 3 to 6 animals. During all experimental procedures, the animals were anaesthetized using Ethrane (Enfluran). Fresh pieces of tumor tissue (≈ 10 mm^3) were prepared from a donor AT1 tumor and were transplanted subcutaneously into the right thigh of the rats. Tumors were grown for 12 to 18 days, until they reached diameters ranging from 10 to 15 millimeters, corresponding to a wet weight of 0.5 to 2 grams.

2.10. Kinetics and tissue distribution

For analyzing the biodistribution of the copolymers, 500 µl of a 0.1 mM solution (based on copolymer concentration and corresponding to a radioactivity of 150 to 300 µCi) were injected intravenously into the lateral tail vein of the rats. At 0.5, 24, 72 and 168 hours post i.v. injection, biodistribution was monitored two dimensionally using a Searle-Siemens scintillation camera. In the scintigrams, signals detected for thyroid were considered to correspond to released radioactive iodine, rather than to radiolabeled HPMA copolymer. Under physiological conditions, a small amount of iodine is liberated from the tyrosine groups (~2% per 24 h). Most of the released label is rapidly eliminated by means of renal filtration, a significant portion, however, is taken up specifically by sodium-iodine symporter-expressing thyroid cells. At various time points post injection, 20 or 50 µL of blood were collected to determine the concentrations of the copolymers in blood. The amounts of radiolabeled copolymer in systemic circulation were approximated by assuming that the complete blood pool equals 6% of the body weight of the rats. One week post i.v. injection, the animals were sacrificed, and tumors and organs were collected. Residual amounts of radioactivity in tissues were determined using a gamma counter (Canberra Packard), they were corrected for radioactive decay and they were expressed as percent of the total injected dose per gram tissue.

2.11. Statistical analysis

All results are expressed as average ± standard deviation. The unpaired student's *t*-test was used to assess if the differences observed between the various experimental groups were statistically significant ($p<0.05$).

3. Results

3.1. Characterization of the copolymers

A general backbone structure of the HPMA copolymers synthesized is presented in Figure 1. In this Figure, x indicates the relative amount of HPMA monomer units, y indicates the amount of functionalized side chain groups introduced and z represents the amount of methacryloyl tyrosinamide, included to allow for radiolabeling. The identities and physicochemical characteristics of the thirteen copolymers are summarized in Table 1. For each of the copolymers, chemical composition, average molecular weight, polydispersity (Mw/Mn) and molar contents of side chain groups introduced are listed. It can be seen that the polydispersities were generally low, indicating a narrow distribution of the average molecular weight, and a reproducible synthesis and fractionation.

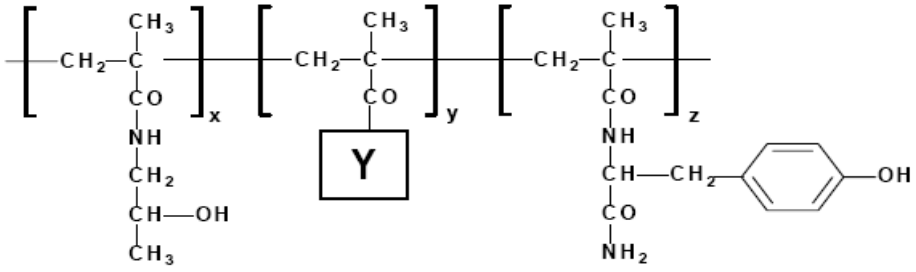

Figure 1. Basic chemical structure of an HPMA copolymer carrying a functional group (Y) and tyrosinamide. x = molar content of HPMA units; y = molar content of (functional) side chain groups introduced; z = molar content of monomers containing tyrosinamide. See table 1 for specifications.

3.2. Effect of molecular weight

In the first set of experiments, in order to assess the effect of increasing the average molecular weight of HPMA copolymers, the pharmacokinetics, tumor accumulation and tissue distribution were compared for copolymers **I**, **II** and **III** (corresponding to weights of 23 kD, 31 kD and 65 kD respectively; see Table 1). Figure 2A shows that the half-life time of the copolymers in circulation increased as the average molecular weight increased. Up to 168 hours post i.v. injection (p.i.), concentrations in blood were always significantly higher for copolymers with higher average weights: at 24 hours, for instance, 23.7±1.2 %ID, 11.2±0.7 %ID and 5.8±0.7 %ID were found for 65 kD, 31 kD and 23 kD poly(HPMA), respectively.

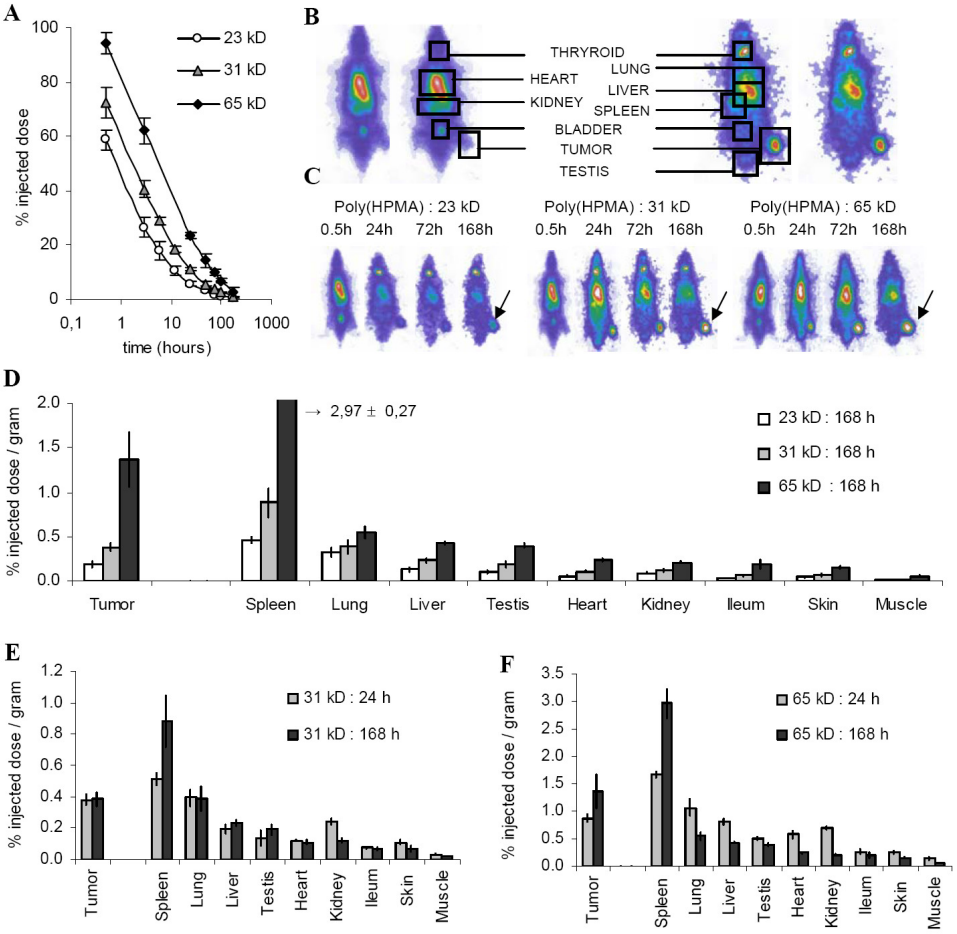

Figure 2. Effect of (increasing) the average molecular weight of HPMA copolymers on their biodistribution. A: Percentage of the injected dose remaining in circulation after i.v. injection of radiolabeled HPMA copolymers with different average molecular weights. B: Schematic representation of the regions of interest (and the corresponding organs) used in scintigraphic analysis. C: Scintigraphic analysis of biodistribution and tumor accumulation (solid arrows) for the three HPMA copolymers. D: Amounts of radiolabeled HPMA copolymer retrieved per gram tissue upon dissection at 168 hours post i.v. injection. E: Tumor and organ levels for 31 kD poly(HPMA) at 24 and 168 h p.i. F: Tumor and organ levels for 65 kD poly(HPMA) at 24 and 168 h p.i. See page 227.

To visualize the biodistribution and the tumor accumulation of the copolymers, scintigraphic images were obtained at 0.5, 24, 72 and 168 hours p.i. In Figure 2B, for a proper interpretation of the images, several regions of interest and the corresponding organs are displayed. In the scintigrams in Figure 2C, biodistributional patterns are presented for 23 kD, 31 kD and 65 kD poly(HPMA).

Figure 2C clearly shows that the copolymers concentrated in tumors both effectively and selectively (solid arrows). It also shows that tumor accumulation correlated well to the weight of the copolymers, with higher average molecular weights rendering higher tumor concentrations. And furthermore, Figure 2C shows that the copolymer concentrations in tumors increased over time. Levels at 168 hours were found to be higher than levels at 72 hours, and levels at 72 hours were generally higher than levels at 24 hours.

Quantification of the tumor and organ concentrations at 168 hours p.i. then confirmed two of these three observations. First, as shown in Figure 2D, the concentrations of the copolymers in tumors were indeed found to be significantly higher than their levels in the majority of healthy organs, demonstrating that tumor accumulation was indeed relatively effective and selective. And second, the Figure 2D demonstrates that the tumor concentrations of the copolymers indeed correlated well with their average molecular weight; for 23 kD, 31 kD and 65 kD poly(HPMA), levels in tumors were 0.19±0.03 %ID/g, 0.38±0.04 %ID/g and 1.37±0.31 %ID/g, respectively.

Subsequently, to address the third observation, i.e. to investigate if tumor concentrations indeed increase over time, we also quantified tumor and healthy tissue levels at 24 hours p.i. Figure 2E shows that for 31 kD poly(HPMA), in contrast to what had been observed in the scintigrams, no measurable increase in tumor concentration could be noted (0.38±0.03 %ID/g vs. 0.38±0.04 %ID/g). For 65 kD poly(HPMA), on the other hand, the amount of copolymer concentrating in tumors increased by more than half over time, from 0.87±0.06 %ID/g at 24 hours p.i. to 1.37±0.31%ID/g at 168 hours p.i. (Figure 2F).

In Figures 2E and 2F, several other observations can be made. First, at both time points, overall biodistributional patterns appeared to be well comparable for the two copolymers. Spleen, tumor and lung always accumulated the highest amounts per gram tissue, and levels in ileum, skin and muscle were always found to be lowest. Second, the two figures demonstrate that only for spleen, significant increases over time were observed. For both copolymers, concentrations at 168 hours p.i. were almost twice as high as concentrations at 24 hours p.i.: for 31 kD poly(HPMA), levels were 0.89±0.16 %ID/g and 0.52±0.04 %ID/g, respectively, and for 65 kD poly(HPMA), levels were 2.97±0.27 %ID/g and 1.67±0.06 %ID/g, respectively. And third, Figures 2E and

2F show that for 65 kD poly(HPMA), levels in all organs other than tumor and spleen had decreased over time. For 31 kD poly(HPMA), on the other hand, concentrations in most organs did not change significantly between 24 and 168 hours p.i. (Figure 2E). Only in kidney, skin and muscle, levels had decreased significantly over time, indicating that the smaller (31 kD) HPMA copolymer reaches its 'EPR-extravasation-equilibrium' earlier on in time than the larger (65 kD) copolymer. The latter (65 kD) is still present at high concentrations in the vascular compartment of the analyzed organs at 24 hours p.i., and it is thus still able to feed EPR-driven extravasation, as exemplified by the increases over time that were observed for the two typical EPR-tissues tumor and spleen.

3.3. Effect of chemical modification

Next, to examine the effect of chemical modification of HPMA copolymers, and also to investigate the in vivo behaviour (accumulation – elimination) of the carriers after the drug and/or spacer is released, the biodistribution was compared for copolymers bearing different amounts of carboxyl (COOH) and hydrazide ($NHNH_2$) groups (**IV**-**VII**; see Table 1). Both chemical entities have been used repetitively as precursors or intermediates in the synthesis of HPMA copolymer-drug conjugates, and both can be considered to be the polymeric end-products after cleavage of drugs and/or spacers. Carboxyl-containing copolymers likely present upon enzymatic hydrolysis of tetrapeptide spacers (like -GFLG-), and hydrazide-containing copolymers likely result from the pH-dependent release of drugs from conjugates carrying hydrazone spacers [35].

In Figures 3A and 3B, the kinetics of the HPMA copolymers containing carboxyl and hydrazide groups (**IV**-**VII**) are compared to the kinetics of unmodified HPMA copolymers of comparable molecular weight (**I** and **II**). The Figures show that elimination from systemic circulation was found to be induced significantly for all four chemically modified HPMA copolymers. For copolymers containing hydrazide groups, reductions were found to be much more substantial than for copolymers carrying carboxyl groups. At 30 minutes p.i., for instance, less than half and less than one third of the blood concentration of control was found for 3 mol% and 8 mol% of hydrazide groups, respectively (Figures 3A and 3B). For copolymers carrying 3 mol% and 8 mol% of carboxyl groups, levels were also reduced significantly, but in this case, the effect of chemical modification was found to be much more moderate. As compared to control, levels at 30 minutes p.i. were only reduced by approximately one sixth and one fourth, respectively.

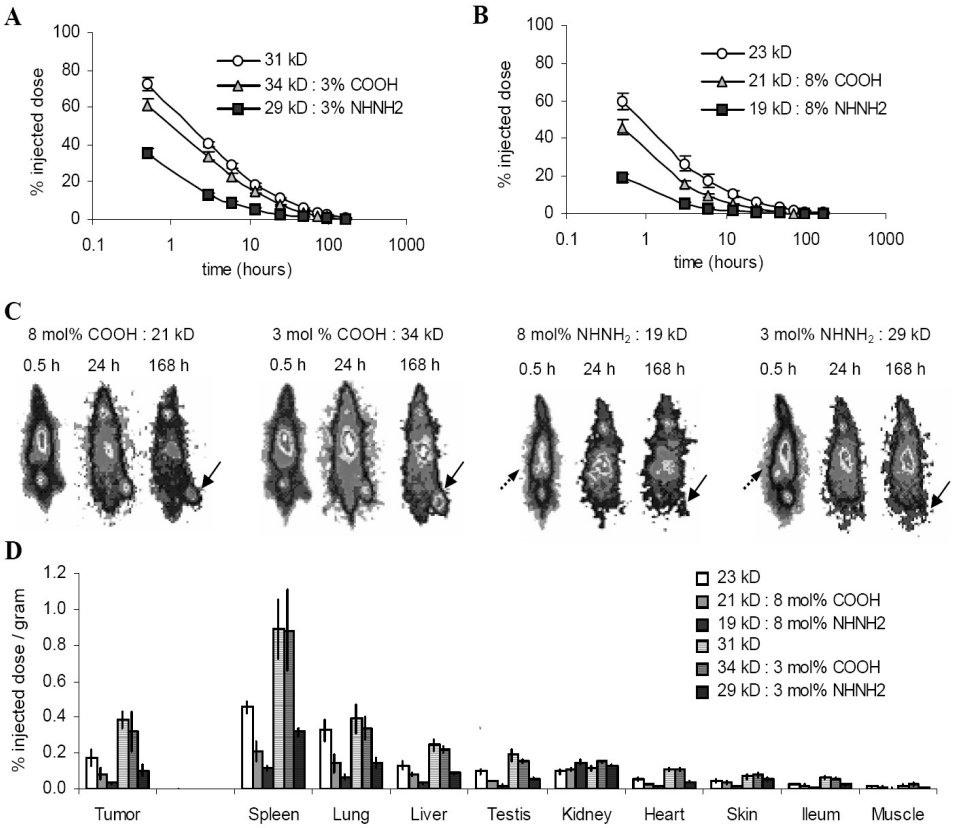

*Figure 3. Effect of (the amount of) carboxyl and hydrazide groups on the biodistribution of HPMA copolymers. A: Percentage injected dose remaining in systemic circulation upon the i.v. injection of HPMA copolymers carrying 3 mol% of groups (**IV** and **V**; see table I). B: Percentage injected dose remaining in circulation upon the i.v. injection of HPMA copolymers carrying 8 mol% of groups (**VI** and **VII**; see table I). C: Scintigraphic imaging of the biodistribution and the tumor accumulation of HPMA copolymers carrying 3 mol% and 8 mol% of carboxyl and hydrazide groups. Solid arrows indicate tumor accumulation, dashed arrows indicate kidney accumulation. D: Tumor and tissue concentrations for chemically modified HPMA copolymers at 168 h p.i.*

The scintigrams in Figure 3C confirm this observation, showing that for HPMA copolymers carrying hydrazide groups, kidney accumulation was induced at 30 minutes p.i. (indicating an increased renal elimination; dashed arrows) and levels localizing to heart were reduced (confirming a more pronounced clearance from circulation). In addition, the scintigrams show that the tumor concentrations of the $NHNH_2$-containing copolymers were reduced significantly as compared to control, while the levels of the COOH-containing copolymers appeared to be comparable to those of control (Figure 3C; solid arrows).

Quantification at 168 hours p.i. then showed that tumor and tissue concentrations were indeed reduced significantly for chemically modified copolymers. As predicted, reductions were much more substantial for $NHNH_2$-containing copolymers than for copolymers carrying COOH. For the former, lower levels were detected both for 8 mol% and 3 mol% of groups, while for the latter, reductions were only found to be significant for 8 mol% of groups. For 8 mol% and 3 mol% of hydrazide groups, tumor concentrations were 0.04±0.01 %ID/g and 0.09±0.03 %ID/g, respectively. For 8 mol% and 3 mol% of carboxyl groups, levels were 0.10±0.03 %ID/g and 0.32±0.11 %ID/g, respectively, and for size-matched control copolymers, levels were 0.19±0.03%ID/g and 0.38±0.04 %ID/g, respectively (Figure 3D). For the majority of other organs, levels were also found to be reduced significantly upon chemical modification, and only for kidney, increased concentrations were found.

When examining Figure 3 more closely, it can furthermore be seen that the amount of groups introduced correlates with the biodistribution of the copolymers. In Figure 3A, which presents the kinetics for 3 mol% of groups, the differences in concentration (between chemically modified and control copolymers) are clearly smaller than the differences displayed in Figure 3B, which presents the kinetics for 8 mol% of groups. Thus, HPMA copolymers carrying 8 mol% of chemical groups are cleared from circulation more rapidly than HPMA copolymers carrying 3 mol% of groups. Analogously, Figure 3D shows that for copolymers carrying 8 mol% of groups, concentrations in tumors and organs were always reduced much more substantially (as compared to control) than the concentrations found for the copolymers carrying 3 mol% of groups. These observations confirm the assumption that the higher the amount of functional groups introduced into an HPMA copolymer is, the more it reflects on the biodistribution and the tumor accumulation of the copolymer.

3.4. Effect of conjugation of doxorubicin

In the third set of experiments, HPMA copolymers **VIII**-**X** were analyzed (see Table 1). Copolymer **VIII**, in which doxorubicin was conjugated to poly(HPMA) by means of the small and uncleavable glycylglycine (-GG-) spacer, served to assess the impact of introducing a relevant drug. Copolymer **IX**, carrying the tetrapeptide glycyl-DL-phenylalanylleucylglycine terminating in a carboxyl group (-GFLG-OH), was used to assess the effect of a relevant spacer. Upon cellular

internalization, this spacer enables cleavage by the cysteine protease cathepsin B, and thus allows for the release of attached active agents in the lysosomes. And third, to assess the effect of the conjugation of both spacer and drug, poly(HPMA)-GFLG-doxorubicin was synthesized (copolymer **X**). With an average molecular weight of 30 kD and a drug loading density of ~6 mol% (see Table 1), this HPMA copolymer compares well to clinically used PK1, except for the fact that it contains tyrosinamide, included to allow for radiolabeling.

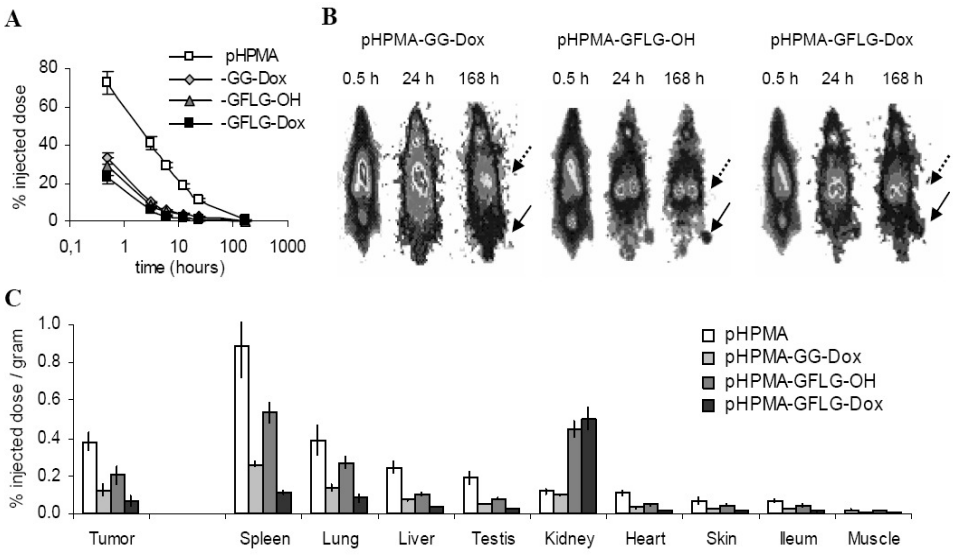

*Figure 4. Effect of introducing drug and/or spacer moieties on the biodistribution of HPMA copolymers. A: Percentage of the injected dose remaining in systemic circulation after the i.v. injection of radiolabeled HPMA copolymers **VIII**-**X**, carrying -GG-Dox, -GFLG-OH and -GFLG-Dox, respectively (see table 1). B: Scintigraphic analysis of the biodistribution and the tumor accumulation of HPMA copolymers **VIII**-**X**. Solid arrows indicate tumor accumulation, dashed arrows kidney accumulation. C: Tumor and tissue concentrations for copolymers **VIII**-**X** at 168 h p.i.*

Figure 4A shows that the introduction of drug and spacer groups reduced the long-circulating properties of the copolymers. As had been observed for hydrazide-containing HPMA copolymers (Figures 3A-C), early renal elimination appeared to be induced for the three copolymers carrying drug and/or spacer. Already at 30 minutes p.i., levels in blood were found to be reduced substantially. This notion was again confirmed by scintigraphic analysis, which clearly indicated increased kidney concentrations (Figure 4B; dashed arrows).

This increase in kidney accumulation was found to depend on the chemical nature of the spacer used, with -GFLG- causing a much stronger retention in kidney than -GG-. Figure 4B also shows that levels localizing to tumors were reduced as a result of the conjugation of drug and/or spacer moieties (solid arrows). One week post i.v. injection, tumor and tissue concentrations were then quantified, and as predicted by the scintigrams, concentrations in tumors and in all organs other than kidney were found to be decreased significantly (Figure 4C). In tumors, 0.12±0.03 %ID/g was found for pHPMA-GG-Dox, 0.20±0.04 %ID/g for pHPMA-GFLG-OH and 0.07±0.03 %ID/g for pHPMA-GFLG-Dox, as compared to 0.38±0.04 %ID/g for control. In kidney, levels were 0.10±0.004 %ID/g, 0.45±0.04 %ID/g and 0.50±0.06 %ID/g, respectively, as compared to 0.12±0.04 %ID/g for control.

3.5. Effect of conjugation of PHSCN

Fourth, to investigate the impact of the introduction of a peptide moiety, three conjugates carrying the (potentially therapeutic [29, 30]) pentapeptide PHSCN were synthesized (see Table 1). In copolymer **XI**, PHSCN was conjugated to poly(HPMA) by means of a glycylglycine (-GG-) spacer, in copolymer **XII**, glycylglycine coupled to aminohexanoic acid (-GG-AHX) was used as a spacer, and in copolymer **XIII,** glycylglycine coupled to a 0.5 kD fragment of poly(ethyleneglycol) (-GG-PEG-) was used.

Figure 5A shows that for all three PHSCN-carrying HPMA copolymers, moderate but significant decreases in the concentrations in circulation were observed. The scintigraphic images in Figure 5B again demonstrate that for functionalized HPMA copolymers, levels localizing to kidney were increased substantially (dashed arrows). They also points towards an increase in thyroid accumulation (solid arrows), as well as to a substantial decrease in tumor accumulation. The increased localization of radioactive signal to thyroid likely indicates an increase in the release of 131-iodine, part of which then accumulates specifically in thyroid cells expressing the sodium-iodide symporter. Possible explanations for an increase in the release of radiolabel are an increase in unspecific binding of 131-iodine to PHSCN, an increase in the internalization (rate) of the conjugates and an increase in the degree of degradation.

Figure 5C shows that when quantifying the tumor and tissue levels for the three PHSCN-containing HPMA copolymers, concentrations in all organs other than kidney were found to be reduced dramatically. On average, levels were decreased by >90%, likely to some extent as a result of the abovementioned increase in the release of radiolabel. In tumors, 0.016±0.003, 0.014±0.001 and 0.042±0.008 %ID/g were found for pHPMA-GG-PHSCN, pHPMA-GG-AHX-PHSCN and pHPMA-GG-PEG-PHSCN, respectively, as compared to 0.38±0.04 %ID/g for control. In kidney, on the other hand, concentrations were again found to be increased upon the introduction of functional groups; 0.25±0.01 %ID/g was found for pHPMA-GG-PHSCN, 0.31±0.002 %ID/g for pHPMA-GG-AHX-PHSCN and 0.70±0.09 %ID/g for pHPMA-GG-PEG-PHSCN, respectively, as compared to 0.12±0.01 %ID/g for control.

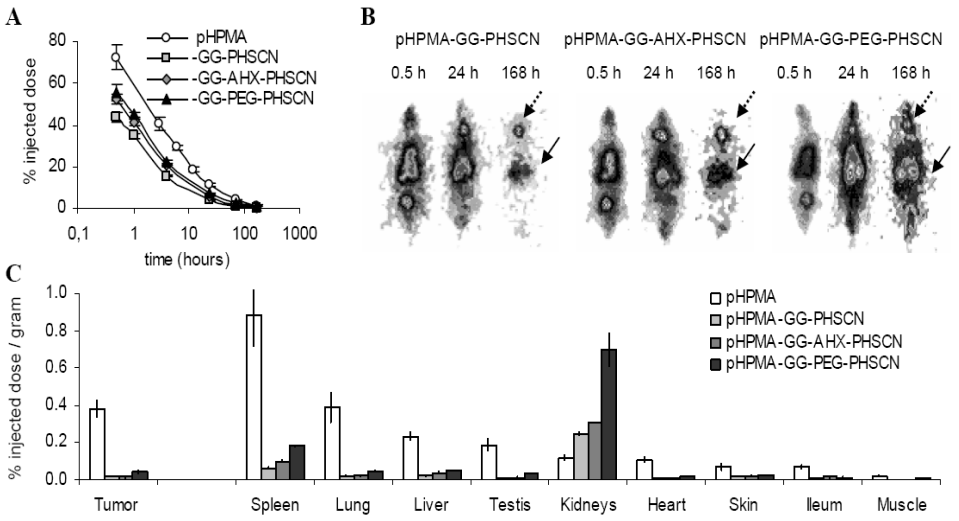

*Figure 5. Effect of introducing a peptide moiety (PHSCN) on the biodistribution of HPMA copolymers. A: Percentage of the injected dose remaining in systemic circulation after the i.v. injection of radiolabeled HPMA copolymers **XI**-**XIII**, carrying -GG-PHSCN, -GG-AHX-PHSCN and -GG-PEG-PHSCN respectively (see Table 1). B: Scintigraphic imaging of the biodistribution of copolymers **XI**-**XIII**. Solid arrows indicate kidney accumulation, dashed arrows indicate thyroid accumulation (of released 131-iodine). C: Tumor and tissue concentrations for copolymers **XI**-**XIII** at 168 h p.i.*

3.6. Tumor targeting ability

Finally, to evaluate the targeting potential of HPMA copolymers, their ability to specifically localize to tumors was investigated. By dividing the tumor concentration of a given HPMA copolymer by its concentrations in healthy organs and tissues, tumor-to-organ ratios were calculated, and they were used to allow for a more direct and cross-sectional comparison of the tumor targeting abilities of the thirteen copolymers (Table 2). A tumor-to-organ ratio >1 indicates that accumulation in tumor tissue was more effective, and a ratio <1 indicates an enhanced localization to healthy tissue.

A	**I : pHPMA 23 kD**	**II : pHPMA 31 kD**	**III : pHPMA 65 kD**	**IV : 3% -COOH 34kD**	**V : 3% -$NHNH_2$ 29 kD**	**VI : 8% -COOH 21kD**	**VII : 8% -$NHNH_2$ 19kD**
Tumor	1	1	1	1	1	1	1
Spleen	0.4	0.4	0.5	0.4	0.3	0.4	0.3
Lung	0.6	1.0	2.4	1.0	0.7	0.6	0.5
Kidney	2.0	3.3	6.4	2.1	0.8	0.8	0.2
Liver	1.4	1.6	3.1	1.5	1.1	1.0	1.0
Testis	1.9	2.0	3.4	2.1	1.8	1.8	2.3
Heart	3.4	3.5	5.5	2.9	2.6	3.1	2.4
Skin	3.9	5.5	8.9	4.1	1.8	2.3	1.7
Ileum	6.3	5.7	7.1	5.7	3.9	4.2	3.4
Muscle	13.0	20.1	22.4	11.7	9.3	7.8	3.3

B	**II : Control pHPMA**	**VIII : pHPMA - GG-Dox**	**IX : pHPMA - GFLG-OH**	**X: pHPMA - GFLG-Dox**	**XI : pHPMA-GG-PHSCN**	**XII : pHPMA-GG-AHX-PHSCN**	**XIII : pHPMA-GG-PEG-PHSCN**
Tumor	1	1	1	1	1	1	1
Spleen	0.4	0.5	0.4	0.6	0.3	0.1	0.2
Lung	1.0	0.9	0.8	0.8	0.8	0.6	0.9
Kidney	3.3	1.2	0.5	0.1	0.06	0.04	0.06
Liver	1.6	1.7	2.0	1.9	0.7	0.4	0.8
Testis	2.0	2.4	2.5	2.9	1.8	1.4	2.4
Heart	3.5	3.7	4.2	4.6	1.3	1.2	1.2
Skin	5.5	4.4	4.6	4.3	0.9	0.6	1.6
Ileum	5.7	5.3	4.6	4.5	2.4	1.0	3.9
Muscle	20.1	12.6	12.6	12.1	4.4	3.6	6.3

Table 2. Evaluation of the tumor targeting ability of the HPMA copolymers studied. Tumor-to-organ ratios were calculated by dividing the tumor concentration of a given HPMA copolymer (in %ID per gram) at 168 hours p.i. by the concentrations of the copolymer in the indicated healthy organs. A tumor-to-organ ratio >1 thus indicates a preferred localization to tumor, a ratio <1 indicates an enhanced accumulation in healthy tissue. The tumor-to-organ ratios allow for a more direct and cross-sectional comparison of the tumor targeting abilities of the thirteen HPMA copolymers.

When comparing the tumor-to-organ ratios listed in Table 2, several observations can be made. First, when interpreting all ratios macroscopically, it can be seen that for the majority of the thirteen copolymers, a proper tumor targeting ability was found. Except for the three HPMA copolymers carrying PHSCN, tumor-to-organ ratios were always found to be >1 for liver, testis, heart, skin, ileum and muscle (Tables 2A and 2B). Only for spleen, ratios were always <1, confirming the role of the spleen (and splenic macrophages) in clearing long-circulating drug delivery systems. Second, in Table 2A, it can be seen that the tumor-to-organ ratios were always clearly higher for higher molecular weight copolymers. This confirms the assumption that increasing the average molecular weight of HPMA copolymers increases their ability to target solid tumors. Third, when comparing the tumor-to-organ ratios found for copolymers **IV**-**VII** to the ratios found for copolymers **I** and **II**, it can be seen that introduction of carboxyl and hydrazide groups reduced the tumor targeting ability of the copolymers (Table 2A). It can also be seen, however, that it did so only relatively moderately, with only for kidney, levels dropping from >1 to <1. Fourth, in Table 2A, it can be seen that this modification-induced reduction in tumor targeting ability depended both on the nature of the groups introduced (hydrazide vs. carboxyl; compare **IV** vs. **V**, and **VI** vs. **VII**), as well as on the amount of groups introduced (3 mol% vs. 8 mol%; compare **IV** vs. **VI**, and **V** vs. **VII**). Fifth, in Table 2B, it can be seen that, as compared to control**,** hardly any reduction in tumor targeting ability was found for copolymers **VIII**-**X**, carrying -GG-Dox, -GFLG-OH and -GFLG-Dox respectively. Only for kidney (and to a lesser extent also for muscle) reduced tumor-to-organ ratios were found, indicating that even though the three copolymers were cleared from the circulation more rapidly than parental (control) copolymers (Figure 4A), they were virtually equally effective as controls in localizing to tumors specifically. Remarkably, for heart, testis, spleen and liver, i.e. for organs potentially suffering from the implementation of (polymer-based) anthracycline therapy, tumor-to-organ ratios were even found to be higher (Table 2B). And sixth, Table 2B shows that the introduction of another potential anticancer agent, the pentapeptide PHSCN, reduced the tumor targeting ability of copolymers substantially: for all organs analyzed, the tumor-to-organ ratios of the copolymers carrying PHSCN were much lower than the ratios found for the other ten HPMA copolymers. For copolymer **XIII**, these reductions were somewhat less substantial than the reductions observed for copolymers **XI** and **XII**, indicating that of the three spacers tested, -GG-PEG_{500}- appears to be the most effective spacer for delivering peptides to tumors.

4. Discussion

Many previous reports have addressed the biocompatibility, the versatility and the therapeutic potential of HPMA copolymers [3-23, and references therein]. Only few, however, have addressed the biodistributional consequences of physicochemical modification [25-28], and even less have directly delineated the impact of functionalization (e.g. with spacers, drugs, proteins and peptides) on the biodistribution of the copolymers. When examining the effects of the conjugation of an active agent to a polymeric drug carrier, pharmacokinetics, tumor accumulation and tissue distribution are generally only being compared for the drug moiety, and hardly ever for the carrier moiety. We therefore decided to investigate how the incorporation of chemically and functionally diverse groups reflects on the biodistribution and the tumor targeting potential of HPMA copolymers. To this end, thirteen physicochemically different HPMA copolymers were synthesized and analyzed, varying in average molecular weight, in the nature of functional groups introduced, and in the amount of groups introduced.

First, the effect of increasing the average molecular weight of HPMA copolymers was investigated. Figure 2 showed that, as predicted by previous reports [25-28], circulation times, tumor concentrations and organ levels were higher for copolymers with higher average molecular weights. Also in line with these reports was the observation that for larger HPMA copolymers, relative biodistributional patterns were more advantageous than for smaller HPMA copolymers, which was exemplified by the fact that the tumor-to-organ ratios were always found to be higher for copolymers with higher average molecular weights (Table 2A). Increasing the size of HPMA copolymers thus increases both their circulation time and their tumor targeting ability. This indicates that the size of the polymer-drug conjugates that are currently being evaluated clinically (~20-30 kD) may be suboptimal [2,3], and that it might be worthwhile to investigate if the therapeutic index of the conjugates can be improved simply by increasing the average molecular weight of copolymer. How such an increase in size reflects on the biodistribution of the active agent, and how it affects its efficacy and its toxicity, could be assessed relatively easily, using the data obtained and the experiences gained in the past two decades [3-5,7-19].

Second, to investigate how the introduction of functional groups affects the biodistribution and the tumor accumulation of HPMA copolymers, three different sets of chemically modified copolymers were analyzed (see Table 1). As compared to unmodified controls, all ten functionalized HPMA copolymers were shown to be eliminated from systemic circulation more rapidly (Figures 3A, 3B, 4A and 5A). Tissue concentrations correlated well with the observed kinetics in blood, and as a consequence, levels in tumors and in all organs other than kidney were found to be lower for functionalized HPMA copolymers than for control copolymers (Figures 3D, 4C and 5C). In kidney, relatively independent of the nature of the groups introduced, concentrations were always found to be increased significantly upon functionalization. This indicates that concentrations in kidney are minimal for chemically unmodified HPMA copolymers, and that the introduction of functional groups in general results in an increase in kidney accumulation.

The fact that only kidney concentrations were found to be directly affected by chemical modification indicates that, in principle, functionalized HPMA copolymers are able to retain the predominant part of the spatial targeting specificity of parental HPMA copolymers. Table 2 clearly shows that except for the three conjugates carrying PHSCN, all copolymers displayed a proper ability to localize to tumors. Relative levels were always higher for tumors than for six out of nine healthy tissues (liver, testis, heart, skin, ileum and muscle), and only for spleen, the accumulation of the copolymers was found to be more specific than for tumors. Relative levels in lung were generally comparable to levels in tumor, and levels in kidney were, as discussed above, always higher for functionalized copolymers.

Though a (more) pronounced localization to spleen, to kidney and to lung may intuitively seem disadvantageous, this could also be used to argue for a broader implementation of HPMA copolymers in the treatment of advanced solid malignancies. Because the carrier constructs tend to concentrate in lung tissue relatively effectively, HPMA copolymer-based anticancer agents may well provide more effective means for treating both primary and metastatic lung lesions. In addition, primary and secondary lesions of the liver, which also tends to accumulate the copolymers relatively effectively, may prove to be good targets for investigating the potential of HPMA copolymer-based chemotherapeutics. The same is true for kidney cancer (i.e. renal cell

carcinoma), which in spite of extensive research efforts remains to be one of the most lethal malignancies [40]. Functionalized HPMA copolymers were shown to possess an intrinsic ability to accumulate in kidney. It can therefore be expected that they will be able to increase the (long-term) levels of therapeutic agents in the kidney substantially. Copolymers conjugated to the anti-invasive and antimetastatic PHSCN peptide, for instance, as well as standard HPMA copolymer-doxorubicin conjugates, were shown to localize to kidney both effectively and selectively, indicating that these (and physicochemically comparable) constructs may be interesting tools for improving the treatment of renal cell carcinoma [41].

5. Conclusion

Taken together, the results presented here show that the physicochemical modification (and functionalization) of HPMA copolymers substantially affects the pharmacokinetics, the tissue distribution and the tumor accumulation of HPMA copolymers. They also show that even though absolute levels in blood and in tumors decrease significantly upon the introduction of chemical (functional) groups, the predominant part of the tumor targeting ability of parental HPMA copolymers can be retained. These findings confirm the potential of HPMA copolymers as long-circulating and tumor-targeted drug carriers, and they indicate that polymer-based drug delivery systems may prove to be interesting and useful modalities for more effectively treating various forms of advanced solid malignancy.

References

1. T. Reynolds, Polymers help guide cancer drugs to tumor targets--and keep them there, J. Natl. Cancer Inst. 87 (1995) 1582-4
2. R. Duncan, The dawning era of polymer therapeutics, Nat. Rev. Drug Discov. 2 (2003) 347-60
3. J. Kopecek, P. Kopeckova P., T. Minko, Z.R. Lu, C.M. Peterson, Water soluble polymers in tumor targeted delivery, J. Control. Release 74 (2001) 147-58
4. B. Rihova, K. Kubackova, Clinical implications of N-(2-hydroxypropyl)methacrylamide copolymers, Curr. Pharm. Biotechnol. 4 (2003) 311-22
5. J. Kopecek, P. Kopeckova, T. Minko, Z. Lu, HPMA copolymer-anticancer drug conjugates: design, activity, and mechanism of action, Eur. J. Pharm. Biopharm. 50 (2000) 61-81.
6. H. Maeda, J. Wu, T. Sawa, Y. Matsumura, K. Hori, Tumor vascular permeability and the EPR effect in macromolecular therapeutics: a review, J. Control. Release 65 (2000) 271-84
7. P.A. Vasey, S.B. Kaye, R. Morrison, C. Twelves, P. Wilson, R. Duncan, A.H. Thomson, L.S. Murray, T.E. Hilditch, T. Murray, S. Burtles, D. Fraier, E. Frigerio, J. Cassidy, Phase I clinical and pharmacokinetic study of PK1 [N-(2-hydroxypropyl)methacrylamide copolymer doxorubicin]: first member of a new class of chemotherapeutic agents-drug-polymer conjugates. Cancer Research Campaign Phase I/II Committee, Clin. Cancer Res. 5 (1999) 83-94
8. A.H. Thomson, P.A. Vasey, L.S. Murray, J. Cassidy, D. Fraier, E. Frigerio, C. Twelves, Population pharmacokinetics in phase I drug development: a phase I study of PK1 in patients with solid tumours, Br. J. Cancer. 81 (1999) 99-107
9. V. Bilim, Technology evaluation: PK1, Pfizer/Cancer Research UK, Curr. Opin. Mol. Ther. 5 (2003) 326-30
10. P.J. Julyan, L.W. Seymour, D.R. Ferry, S. Daryani, C.M. Boivin, J. Doran, M. David, D. Anderson, C. Christodoulou, A.M. Young, S. Hesslewood, D.J. Kerr, Preliminary clinical study of the distribution of HPMA copolymers bearing doxorubicin and galactosamine, J. Control. Release 57(1999) 281-90
11. L.W. Seymour, D.R. Ferry, D. Anderson, S. Hesslewood, P.J. Julyan, R. Poyner, J. Doran, A.M. Young, S. Burtles, D.J. Kerr, Hepatic drug targeting: phase I evaluation of polymer-bound doxorubicin, J. Clin. Oncol. 20 (2002) 1668-76
12. E. Gianasi, M. Wasil, E.G. Evagorou, A. Keddle, G. Wilson, R. Duncan, HPMA copolymer platinates as novel antitumour agents: in vitro properties, pharmacokinetics and antitumour activity in vivo, Eur. J. Cancer 35 (1999) 994-1002
13. X. Lin, Q. Zhang, J.R. Rice, D.R. Stewart, D.P. Nowotnik, S.B. Howell, Improved targeting of platinum chemotherapeutics. the antitumour activity of the HPMA copolymer platinum agent AP5280 in murine tumour models, Eur. J. Cancer 40 (2004) 291-7
14. J.M. Rademaker-Lakhai, C. Terret, S.B. Howell, C.M. Baud, R.F. De Boer, D. Pluim, J.H. Beijnen, J.H. Schellens, J.P. Droz, A Phase I and pharmacological study of the platinum polymer AP5280 given as an intravenous infusion once every 3 weeks in patients with solid tumors, Clin. Cancer Res. 10 (2004) 3386-95
15. J.M. Meerum Terwogt, W.W. ten Bokkel Huinink, J.H. Schellens, M. Schot, I.A. Mandjes, M.G. Zurlo, M. Rocchetti, H. Rosing, F.J. Koopman, J.H. Beijnen, Phase I clinical and pharmacokinetic study of PNU166945, a novel water-soluble polymer-conjugated prodrug of paclitaxel, Anticancer Drugs 12 (2001) 315-23
16. Y. Kasuya, Z.R. Lu, P. Kopeckova, T. Minko, S.E. Tabibi, J. Kopecek, Synthesis and characterization of HPMA copolymer-aminopropylgeldanamycin conjugates, J. Control. Release 74 (2001) 203-11
17. N. Nishiyama, A. Nori, A. Malugin, Y. Kasuya, P. Kopeckova, J. Kopecek, Free and N-(2-hydroxypropyl)methacrylamide copolymer-bound geldanamycin derivative induce different stress responses in A2780 human ovarian carcinoma cells, Cancer Res. 63 (2003) 7876-82
18. R. Satchi-Fainaro, M. Puder, J.W. Davies, H.T. Tran, D.A. Sampson, A.K. Greene, G. Corfas, J. Folkman, Targeting angiogenesis with a conjugate of HPMA copolymer and TNP-470, Nat. Med. 10 (2004) 255-61
19. R. Satchi-Fainaro, R. Mamluk, L. Wang, S.M. Short, J.A. Nagy, D. Feng, A.M. Dvorak, H.F. Dvorak, M. Puder, D. Mukhopadhyay, J. Folkman, Inhibition of vessel permeability by TNP-470 and its polymer conjugate, caplostatin, Cancer Cell 3(2005) 251-61
20. P. Pouckova, M. Zadinova, D. Hlouskova, J. Strohalm, D. Plocova, M. Spunda, T. Olejar, M. Zitko, J. Matousek, K. Ulbrich, J. Soucek, Polymer-conjugated bovine pancreatic and seminal ribonucleases inhibit growth of human tumors in nude mice, J. Control. Release 95 (2004) 83-92

21. R. Satchi-Fainaro, H. Hailu, J.W. Davies, C. Summerford, R. Duncan, PDEPT: polymer-directed enzyme prodrug therapy. 2. HPMA copolymer-beta-lactamase and HPMA copolymer-C-Dox as a model combination, Bioconjug. Chem. 14(2003) 797-804
22. A. Mitra, A. Nan, H. Ghandehari, E. McNeill, J. Mulholland, B.R. Line, Technetium-99m-Labeled N-(2-Hydroxypropyl) methacrylamide copolymers: synthesis, characterization, and in vivo biodistribution, Pharm. Res. 21 (2004) 1153-9
23. F. Kiessling, M. Heilmann, T. Lammers, K. Ulbrich, V. Subr, P. Peschke, B. Wängler, W. Mier, H. Schrenk, M. Bock, L. Schad, W. Semmler, Characterization of HE-24.8: a polymeric contrast agent for Magnetic Resonance Angiography, Bioconjug. Chem. 17 (2006) 42-51
24. D.M. Lubaroff, L. Canfield, T.L. Feldbush, W.W. Bonney, R3327 adenocarcinoma of the Copenhagen rat as a model for the study of the immunologic aspects of prostate cancer J. Natl. Cancer Inst. 58 (1977) 1677-89.
25. L.W. Seymour, R. Duncan, J. Strohalm, J. Kopecek, Effect of molecular weight (Mw) of N-(2-hydroxypropyl)methacrylamide copolymers on body distribution and rate of excretion after subcutaneous, intraperitoneal, and intravenous administration to rats, J. Biomed. Mater. Res. 21 (1987) 1341-58
26. L.W. Seymour, Y. Miyamoto, H. Maeda, M. Brereton, J. Strohalm, K. Ulbrich, R. Duncan, Influence of molecular weight on passive tumour accumulation of a soluble macromolecular drug carrier, Eur. J. Cancer 31A (1995) 766-70
27. Y. Noguchi, J. Wu, R. Duncan, J. Strohalm, K. Ulbrich, T. Akaike, H. Maeda, Early phase tumor accumulation of macromolecules: a great difference in clearance rate between tumor and normal tissues, Jpn. J. Cancer Res. 89 (1998) 307-14
28. M. Kissel, P. Peschke, V. Subr, K. Ulbrich, J. Schuhmacher, J. Debus, E. Friedrich, Synthetic macromolecular drug carriers: biodistribution of poly[(N-2-hydroxypropyl)methacrylamide] copolymers and their accumulation in solid rat tumors, PDA J. Pharm. Sci. Technol. 55 (2001) 191-201
29. D.L. Livant, R.K. Brabec, K.J. Pienta, D.L. Allen, K. Kurachi, S. Markwart, A. Upadhyaya, Anti-invasive, antitumorigenic, and antimetastatic activities of the PHSCN sequence in prostate carcinoma, Cancer Res. 60 (2000) 309-20
30. K.L. Van Golen, L. Bao, G.J. Brewer, K.J. Pienta, J.M. Kamradt, D.L. Livant, S.D. Merajver, Suppression of tumor recurrence and metastasis by a combination of the PHSCN sequence and the antiangiogenic compound tetrathiomolybdate in prostate carcinoma, Neoplasia 4 (2002) 373-9
31. K.Ulbrich, V.Šubr, J.Strohalm, D.Plocová, M.Jelínková, B.Říhová, Polymeric drugs based on conjugates of synthetic and natural macromolecules I. Synthesis and physico-chemical characterisation, J. Control. Release 64 (2000) 63-79
32. J. Drobnik, J. Kopecek, J. Labsky, J. Rejmanova, J. Exner, V. Saudek, J. Kalal, Enzymatic cleavage of side chains of synthetic water-soluble polymers, Makromol. Chem. 177 (1976) 2833-48
33. B. Rihova, M. Bilej, V. Vetvicka, K. Ulbrich, J. Strohalm, J. Kopecek, R. Duncan, Biocompatibility of HPMA copolymers containing adriamycin. Immunogenicity, and effect on haematopoietic stem cells in bone marrow in vivo and mouse splenocytes and human peripheral blood lymphocytes in vitro, Biomaterials 10(1989) 335-42
34. J. Strohalm, J. Kopecek, Poly-[N-(2-hydroxypropyl)methacrylamide]. IV. Heterogeneous polymerization, Angew Makromol. Chem. 70 (1978) 109-118
35. T. Etrych, M. Jelinkova, B. Rihova, K. Ulbrich, New HPMA copolymers containing doxorubicin bound via pH-sensitive linkage: synthesis and preliminary in vitro and in vivo biological properties, J. Control. Release 73(2001) 89-102
36. L.W. Seymour, K. Ulbrich, J. Strohalm, J. Kopecek, R. Duncan, The pharmacokinetics of polymer-bound adriamycin, Biochem. Pharmacol. 39 (1990) 1125-31.
37. W.C. Chan, P.D. White, Fmoc solid phase peptide synthesis: A practical approach, Oxford University Press 2000
38. P.R. Salacinski, C. McLean, J.E. Sykes, V.V. Clement-Jones, P.J. Lowry, Iodination of proteins, glycoproteins, and peptides using a solid-phase oxidizing agent, 1,3,4,6-tetrachloro-3 alpha,6 alpha-diphenyl glycoluril (Iodogen), Anal. Biochem. 117 (1981) 136-46
39. P.K. Singal, N. Iliskovic, Doxorubicin-induced cardiomyopathy, N. Engl. J. Med. 339 (1998) 900-5
40. B.D. Curti, Renal cell carcinoma, JAMA 292 (2004) 97-100
41. M.B. Atkins, D.E. Avigan, R.M. Bukowski, R.W. Childs, J.P. Dutcher, T.G. Eisen, R.A. Figlin, J.H. Finke, R.C. Flanigan, D.J. George, S.N. Goldberg, M.S. Gordon, O. Iliopoulos, W.G. Kaelin Jr, W.M. Linehan, A. Lipton, R.J. Motzer, A.C. Novick, W.M. Stadler, B.T. Teh, J.C. Yang, L. King, Innovations and challenges in renal cancer: consensus statement from the first international conference, Clin. Cancer. Res. 10 (2004) S6277-81

Chapter 4

Synthesis and characterization of HE-24.8: a polymeric contrast agent for magnetic resonance angiography

Fabian Kiessling[a], Melanie Heilmann[a], Twan Lammers[b,d], Karel Ulbrich[e], Vladimir Subr[e], Peter Peschke[b], Bjoern Waengler[a], Walter Mier[f], Hans-Herrmann Schrenk[c], Michael Bock[a], Lothar Schad[a], Wolfhard Semmler[a]

[a-c] Departments of [a] Medical Physics in Radiology, [b] Radiation Oncology and [c] Molecular Toxicology, German Cancer Research Center, Im Neuenheimer Feld 280, 69120 Heidelberg, Germany

[d] Department of Pharmaceutics, Utrecht Institute for Pharmaceutical Sciences, Utrecht University, Sorbonnelaan 16, 3584 CA Utrecht, The Netherlands

[e] Institute of Macromolecular Chemistry, Academy of Sciences of the Czech Republic, Heyrovsky Square 2, 162 06 Prague 6, Czech Republic

[f] Department of Nuclear Medicine, Heidelberg University, Im Neuenheimer Feld 110, 69120 Heidelberg, Germany

Bioconjug. Chem. 17: 42-51 (2006)

Abstract

The physical and biological properties of a novel water-soluble polymeric contrast agent based on a complex of N-(2-hydroxypropyl)methacrylamide copolymer with gadolinium (HE-24.8) were investigated, and its potential for experimental magnetic resonance (MR) angiography was assessed. The relaxivities of Gd-DTPA-BMA, Gd-DTPA-HSA (human serum albumin), and HE-24.8 were determined at 1.5 T. The thermic stability and the biocompatibility of HE-24.8 were assessed in vitro and by analyzing kinetics and organ distribution in rats for up to 2 weeks. For comparison, HE-24.8- and Gd-DTPA-HSA-enhanced micro-MR angiographies of brain, chest and subcutaneous tumors in rats were performed. The T1 relaxivity of HE-24.8 (21.3±1.1 $mM^{-1}s^{-1}$) was found to be 5-fold higher than that of Gd-DTPA-BMA (4.1±0.1 $mM^{-1}s^{-1}$), and twice as high as that of Gd-DTPA-HSA (12.4±0.2 $mM^{-1}s^{-1}$). Varying the molecular weight of the copolymer (15-46 kDa) did not significantly alter its T1 relaxivity. In rats, 20 and 10% of the injected dose of HE-24.8 were detected at 24 and 168 h post i.v. injection, respectively. Upon a relatively rapid initial renal clearance, no specific retention in any organ was noted, with some exception for organs of the reticulo-endothelial system, like liver and spleen. No measurable release of gadolinium from the polymer-Gd complex and no cytotoxicity was observed. An excellent display of rat and tumor vascularization could be achieved both with Gd-DTPA-HSA and with HE-24.8; vessel contrast, however, was found to be significantly higher for the latter. These findings demonstrate that gadolinium-labeled HPMA copolymers are highly suitable systems for experimental MR angiography.

1. Introduction

Clinically approved contrast agents for magnetic resonance imaging (MRI) are small chelates of gadolinium often complexed with diethylenetriamine-pentaacetic acid (DTPA) [1,2]. They are characterized by an early extravasation, a fast renal clearance, and a low toxicity [1,2]. This makes them suitable for many clinical applications, such as the detection and delineation of pathologically altered tissue [3-5] or first-pass angiographies of larger vessels [6-8]. However, their use for studying micro-vascularization often is problematic: for visualizing microvessels, long scanning times are required to achieve a suitable signal-to-noise ratio, and these are not compatible with the kinetics of small gadolinium chelates. Furthermore, in functional experiments on tissue vascularization, the fast extravasation interferes with the ability to delineate differences in vessel permeability in a reliable manner [9,10].

To overcome such limitations, attempts have been made to design contrast agents with larger molecular sizes [11,12]. First attempts included the labeling of plasma proteins, such as albumin, with gadolinium complexes [13,14]. These gadolinium-labeled albumin compounds were characterized by long circulation times and by a high degree of hepatic metabolism of the altered proteins, which make clinical implementation questionable. As a consequence, with the outlook to a clinical assessment, dendrimeric contrast agents with a medium molecular size, like Gadomer [15], and contrast agents with affinity to plasma proteins, such as MS325 [16], were designed, which show a moderate intravascular half-life of several minutes and are largely cleared by the kidneys [11,15]. Indeed, these contrast agents show the potential to improve functional studies on tumor vascularization including the assessment of vessel permeability during anti-angiogenic treatments [10,17] and to visualize microvessels in vivo [18,19]. An alternative is the use of labeled polymers, such as the PGC-derivates [20]. As an advantage, these can be synthesized with variable configurations and molecular sizes, thus enabling optimization of their pharmacokinetic properties to the biological target [20]. Furthermore, contrast-giving agents can be easily connected to these molecules, and double or triple labeling can be performed, e.g. with a fluorescent dye, a radioactive isotope and/or a superparamagnetic agent [21,22].

Copolymers based on *N*-(2-hydroxypropyl)methacrylamide (HPMA) are water-soluble, biocompatible and nonimmunogenic macromolecular carrier materials that have been used as potential drug delivery systems for a variety of low molecular weight drugs, such as doxorubicin [23], campthotecin [24], paclitaxel [25] and platinates [26]. Conjugates of this highly biocompatible polymer with cytotoxic drugs have already been used in clinical trials [27-29]. It has been shown that the uptake of HPMA-based copolymers in tumors depends on the molecular weight of the copolymer [29-31]. In contrast, in the molecular weight range up to 60 kDa, the distribution of HPMA copolymers in normal organs was quite similar [31]. The synthesis and properties of HPMA copolymers labeled with ^{99m}Tc used for scintigraphic imaging have been described in [32], and HPMA copolymer-linked nitroxides have been used as MR agents in [33]. It was shown that organ biodistribution of the copolymer significantly depends on its molecular weight, that the ^{99m}Tc complexes are relatively stable, and that polymer nitroxides exhibit higher relaxivity than does Gd-DTPA-BMA.

Taking the advantages of the high flexibility in polymer synthesis, and the existing preclinical and clinical experiences with HPMA copolymers into account, the aim of this study was to use HPMA copolymers as carriers of gadolinium-based MR contrast agents. As compared with the results of Wang et al [34], who have presented initial results with Gd-containing HPMA copolymers, in this study, an alternative method for integrating gadolinium was chosen. Several Gd-containing HPMA polymers with different molecular weights were synthesized. Of those, a copolymer with an average molecular weight of 24.8 kDa (named HE-24.8) was used to obtain preclinical proof-of-principle, addressing e.g. its cell toxicity in vitro, its blood half-life time, and its organ distribution. Furthermore, first results using HE-24.8 as a MR contrast agent are presented, including the determination of the T1 and T2 relaxation times and its in vivo use as a contrast agent for micro-MR angiography. The HE-24.8-enhanced MR angiographies were also compared with those performed after administration of Gd-DTPA-HSA (human serum albumin), the latter being a standard experimental contrast agent with a long blood half-life.

2. Materials and methods

2.1. Materials

Methacryloyl chloride, 1-aminopropan-2-ol, 6-aminohexanoic acid, L-aspartic acid, di-*tert*-butyl dicarbonate ($(Boc)_2O$), thionyl chloride, triethylamine (Et_3N) *N,N*-dicyclohexylcarbodiimide (DCC), isobutyl chloroformate, 2,2'-azobis(isobutyronitrile) (AIBN), and trifluoroacetic acid (TFA) were purchased from Fluka, and L-tyrosinamide was from Sigma-Aldrich. All chemicals and solvents were of appropriate analytical grade.

2.2. Synthesis of monomers and copolymers

N-(2-Hydroxypropyl)methacrylamide (HPMA) was synthesized as described in the literature [35]. *N*-Methacryloyl tyrosinamide (Ma-TyrNH_2) was prepared by the reaction of methacryloyl chloride with tyrosinamide in distilled water, as described in [36].

2.3. Synthesis and characterization of Ma-Acap-Asp-[(Asp-$(OMe)_2$]$_2$

Synthesis of N-tert-Butyloxycarbonyl-L-aspartic Acid (Boc-L-Asp-OH). L-Aspartic acid (10 g; 0.075 mol) and sodium hydroxide (6.0 g; 0.15 mol) were dissolved in distilled water (100 mL). The solution was cooled to 0 °C, and dioxane (100 mL) was added. $(Boc)_2O$ (18.0 g; 0.083 mol) was added dropwise during 1 h. The reaction mixture was stirred in an ice bath for 2 h and then for another 2 h at room temperature. The reaction mixture was concentrated on a vacuum evaporator. The unreacted $(Boc)_2O$ was removed by extraction into diethyl ether. The aqueous layer was separated and acidified to pH 2 with a saturated solution of sodium hydrogen sulfate, and the product was extracted into ethyl acetate. The organic phase was separated, dried with sodium sulfate, and concentrated on a vacuum evaporator. Boc-L-Asp-OH was crystallized from a mixture of ethyl acetate/hexane. Yield: 13.4 g (76.5%), mp 116-118 °C.

Synthesis of L-Aspartic Acid Bis-methylester Hydrochloride (HCl.Asp-$(OMe)_2$). Methanol (100 mL), dried with calcium hydride, was put into a round-bottom flask equipped with a stirrer and condenser. Methanol was cooled to -10 °C, and the thionyl chloride (was added dropwise during 30 min. L-Aspartic acid (15.0 g; 0.112 mol) was added, and the reaction mixture was stirred and refluxed for 5 h. The reaction mixture was cooled to room temperature and concentrated on a vacuum evaporator. The final product was crystallized from a mixture of methanol/diethyl ether. Yield: 18.3 g (82.5%); mp: 115-117 °C.

Synthesis of TFA.Asp-[Asp-(OMe)$_2$]$_2$. Boc-Asp-OH (1.475 g; 6.33 mmol), HCl.Asp-(OMe)$_2$ (2.5 g; 12.66 mmol), and Et_3N (1.77 mL; 6.33 mmol) were mixed in 50 mL of tetrahydrofurane (THF), and the suspension was cooled to -10 ºC. DCC (3.12 g; 15.1 mmol) was dissolved in 20 mL of THF, and the solution was cooled to -10 ºC. The cool solution of DCC was added to the suspension, and the reaction mixture was kept at -10 ºC for 1 h and then overnight at 5 ºC without mixing. The reaction mixture was warmed to room temperature, acetic acid (0.1 mL) was added, and the mixture was stirred for 30 min at room temperature. Precipitated *N,N'*-dicyclohexylurea (DCU) and triethylamine hydrochloride (Et_3N.HCl) were filtered off, and the filtrate was concentrated on a vacuum evaporator. The resulting oily residue was diluted with ethyl acetate (100 mL) and gradually extracted with 2 wt % aqueous sodium hydrogen carbonate (50 mL), 0.5 wt % citric acid (50 mL), and water (50 mL) in a last step. The organic layer was dried with sodium sulfate, and the product was crystallized from a mixture ethyl acetate/hexane. Yield: 2.1 g (64.5%); mp: 115-116 ºC, TLC: (silica gel, ethyl acetate, R_f = 0.54). Elemental analysis: calcd/found C = 48.55/48.85; H = 6.40/6.50; N = 8.09/8.05. The Boc protection group was removed by TFA. Boc-Asp-[Asp-(OMe)$_2$]$_2$ (2.0 g) was dissolved in TFA (8.0 mL) and stirred for 30 min at room temperature. The excess TFA was evaporated, the mixture was diluted three times with dry methanol, and the solvent was evaporated again. The oily residue was triturated with diethyl ether to form crystals of TFA.Asp-[Asp-(OMe)$_2$]$_2$.

Synthesis of N-methacryloyl-6-amino Hexanoic Acid (Ma-Acap-OH). The Schotten-Baumann acylation method with methacryloyl chloride in an aqueous alkaline medium was used for the methacryloylation of 6-aminohexanoic acid [37]. (mp: 52-53 ºC; elemental analysis: calculated/found C 60.28/60.43; H 8.60/8.37; N 7.03/6.98).

Synthesis of Ma-Acap-Asp-[(Asp-(OMe)$_2$]$_2$. N-Methacryloyl 6-aminohexanoic acid (0.5 g; 2.51 mmol) and Et_3N (0.385 mL; 2.76 mmol) were dissolved in THF (5 mL). The solution was cooled to -10 ºC, and isobutyl chloroformate (0.36 mL; 2.76 mmol) was added. After 10 min, the reaction mixture was added to a cooled mixture of TFA.Asp-[Asp-(OMe)$_2$]$_2$ (1.47 g; 2.76 mmol) and Et_3N (0.424 mL; 3.04 mmol) in THF (5 mL). The reaction mixture was stirred for 4 h at room temperature. The precipitated Et_3N.HCl was filtered off, and THF was evaporated in vacuum. The residue was dissolved in ethyl acetate (20 mL) and

gradually extracted with 2 wt % aqueous sodium hydrogen carbonate (5 mL), 0.5 wt % citric acid (5 mL), and water (5 mL). The organic layer was dried with sodium sulfate, and the product was crystallized from a mixture of ethyl acetate/hexane. Yield 0.5 g (33%); mp: 110-113 °C; elemental analysis: Calculated/found C = 51.99/50.31; H = 6.71/6.34; N = 9.33/8.93.

Synthesis and Characterization of the Copolymer P-Acap-Asp-[(Asp-(OH)$_2$]$_2$. The copolymer was prepared by solution radical copolymerization of HPMA with Ma-Acap-Asp-[(Asp-(OMe)$_2$]$_2$ in methanol at 60 ºC. HPMA (1.0 g; 6.98 mmol) and Ma-Acap-Asp-[(Asp-(OMe)$_2$]$_2$ (0.221 g; 0.368 mmol) were dissolved in methanol (7.0 mL), and the initiator AIBN (0.068 g; 0.41 mmol) was added. The solution was transferred into a glass ampule and bubbled with nitrogen. The ampule was sealed, and the polymerization was carried out at 60 °C for 24 h. The polymer was isolated by precipitation into a mixture of acetone and diethyl ether (3:1), filtered off, washed with acetone and diethyl ether, and dried in vacuum. The HPMA copolymer used for kinetic and biodistribution studies (HE-radiolabel) was prepared analogously, i.e. by the terpolymerization of HPMA (1.0 g; 6.98 mmol), Ma-TyrNH$_2$ (0.037 g; 0.15 mmol), Ma-Acap-Asp-[(Asp-(OMe)$_2$]$_2$ (0.221 g; 0.368 mmol), and AIBN (0.070 g; 0.42 mmol) in methanol (7.0 mL) at 60 °C for 24 h.

The methyl ester groups from both copolymers mentioned above were removed by alkaline hydrolysis. Briefly, the copolymer (0.8 g) was dissolved in distilled water, and the pH of the solution was maintained at 11.5 with addition of 0.1 M NaOH for 6 h at room temperature. Then, the pH was lowered to 2 with diluted hydrochloric acid, and the copolymer was dialyzed in a Visking dialysis tube with a molecular weight cut off of 3.5 kDa for 2 days and lyophilized.

The weight average molecular weight (M_w) and polydispersity (M_w/M_n) of the copolymers were determined by size exclusion chromatography on the ÄKTA explorer HPLC system (Amersham Biosciences) equipped with a DAWN DSP-F multiangle light scattering detector (Wyatt Technolology) on Superose 6 column.

The side chain (amino acids) content was determined after hydrolysis of polymers HE 24.8 and HE-radiolabel with 6 N HCl at 115 °C for 16 h using an HPLC amino acid analyzer (LDC Analytical, USA) with a reverse-phase column Nucleosil 120-3 C_{18} (Macherey-Nagel, 125 x 4 mm) using precolumn

derivatization with phthaldialdehyde, and detection with a fluorescence detector (excitation at 229 nm; emission at 450 nm). Gradient elution: 0-100% of solvent B within 65 min and flow rate 0.5 mL min^{-1} (solvent A: 0.05 M sodium acetate buffer, pH 6.5; solvent B: 300 mL of 0.17 M sodium acetate and 700 mL of methanol).

HPMA copolymers differing in chemical composition and molecular weight could be easily prepared by changing monomer ratios, initiator concentration, monomer concentrations in the polymerization mixture, and polymerization temperature. Several copolymers with a content of Ma-Acap-Asp-$[(Asp\text{-}(OMe)_2]_2$ up to 30% and molecular weights between 15 and 200 kDa were prepared. From these, gadolinium-containing HPMA polymers with an average weight of 16.2, 21.7, 22.2, 24.8, 27.7, 43.9, and 45.6 kDa were used for comparison of T_1 relaxivities.

Synthesis of P-Acap-Asp-[Asp-$(OH)_2]_2$ Gadolinium Complex HE-24.8). HPMA copolymer P-Acap-Asp-$[Asp\text{-}(OH)_2]_2$ (0.45 g) was dissolved in distilled water, and gadolinium chloride (0.045 g) was added. The pH of the solution was gradually increased to 6.0 by the addition of 0.1 M NaOH during 1 h. The excess of gadolinium was removed by dialysis using a Visking dialysis tube with a cut off of 3.5 kDa for 48 h in water, and the polymer-gadolinium complex was lyophilized. The yield was 0.41 g of the complex. The gadolinium content in the polymer complexes was 5.2 ± 0.3 wt-%, as determined by inductively coupled plasma-mass spectrometry (ICP-MS).

2.4. Determination of the thermic stability

A total of 1 mol of the Gd-containing HPMA copolymers and 100 mol of tri-sodium-citrate were diluted in 11 mL of PBS (pH 7.4). Samples of the stock solution with 1 mL each were incubated at 60 °C for 1, 5, and 25 h, respectively. At each time point, 100 µL were removed and diluted with 900 µL of PBS, and filtered to remove free gadolinium (5 kDa MW filter; Millipore, Billerica, USA). The citrate complexed Gd-content was determined by plasma mass spectrometry.

2.5. Gd-DTPA-human serum albumin (Gd-DTPA-HSA)

Gadolinium-DTPA-labeled albumin was synthesized at the German Cancer Research Center as described previously [13], i.e. by covalently binding gadolinium-DTPA to albumin.

2.6. In vitro determination of cell toxicity

Human fibroblasts (MSU) and human hepatoma cells (HEP-G2) were used. MSU and HEP-G2 cell lines were obtained from the German Cancer Research Center, Heidelberg, Germany. Cells were grown in 75 cm^2 plastic culture flasks (TPP, Switzerland) in 10 mL of medium at 37 C and in a humidified 5% CO_2 atmosphere. Human fibroblasts were maintained in Dulbecco's MEM-medium (Biochrom. AG, Berlin) supplemented with 10% fetal bovine serum (FBS), 1% sodium pyruvate, and 100 U penicillin/streptomycin. HEP-G2 cells were grown in RPMI 1640-medium (GIBCO, UK) with 5% FBS, 1% glutamine, and 100 U penicillin/streptomycin. Media were replaced every 4 days, and cells were split upon confluence at a split ratio of 1:5. For incubations, 24-bottom well plates with plastic cover slips of 13-mm diameter (Nalge Nunc International, Denmark) were used. A total of 500 µL of cell suspension was added to each well. To investigate toxicity, cells were incubated with either HE-24.8 or Gd-DTPA-BMA (Omniscan, Amersham Health, Princeton, USA) in equimolar gadolinium concentrations (0.05 and 0.5 mmol of Gd/L) for 24 and 48 h. Cells grown in unmodified medium served as controls. Viability was determined by Trypan blue exclusion following the manufacturer's instructions (GIBCO, Gland Island, NY). The fraction of nonviable cells was determined using a Neubauer counting chamber by analyzing five vision fields and calculating means and standard deviations (SD). Cell survival was compared using the Student's t-test and $p < 0.05$ was considered to represent statistical significance.

2.7. Animal model

All experiments were approved by a governmental review committee on animal care. Four healthy Copenhagen rats were used to study kinetics, biodistribution, and tolerability of HE-24.8. To perform tumor micro-angiographies, five Copenhagen rats with subcutaneous Dunning R3327-AT1 prostate tumors were used. Tumors were induced in the right upper thigh by injection of $2*10^5$ cells in 1 mL of 0.9% NaCl. Tumors were grown for 3 weeks prior to analysis.

2.8. Kinetics, biodistribution and in vivo Toxicity.

To assess circulation time, organ accumulation and elimination, an HPMA copolymer-Gd complex analogous to HE-24.8 was synthesized. The tyrosinamide groups incorporated in this copolymer were radiolabeled with ^{131}I (HE-radiolabel). The radiolabeled conjugate was injected into the tail vein of four healthy Copenhagen rats. Blood samples and scintigraphic images were taken

at indicated time points. Two weeks after intravenous injection, the animals were sacrificed and their organs were removed for quantification. Residual activity was corrected for radioactive decay. During the two-week follow-up period, the animals were monitored for signs of toxicity.

2.9. MR imaging

Magnetic resonance imaging (MRI) was performed on a clinical 1.5 T whole-body MR system (Siemens Symphony, Erlangen, Germany) using a custom-made radio frequency-(RF) coil for RF excitation and signal reception. The RF coil was designed as a cylindrical volume resonator with an inner diameter of 83 mm and a useable length of 120 mm. To optimize the available signal-to-noise ratio, manual tuning and matching of the coil's resonance circuitry was performed for each measurement individually.

Determination of the Relaxivity of HE-24.8, Gd-DTPA-HSA, and Gd-DTPA-BMA. Relaxivity measurements of HE-24.8, Gd-DTPA-HSA, and Gd-DTPA-BMA were performed using a 1.5 T MR scanner (Magnetom Vision, Siemens Erlangen, Germany) and a standard head coil (Siemens Erlangen, Germany). Increasing concentrations of contrast medium (0.0, 0.01, 0.05, 0.1, 0.5, 1.0 mmol of Gd/L of 0.9% NaCl) were transferred to phantom vials and placed in the isocenter of the coil. T_1 times were determined with a saturation-recovery turbo FLASH-sequence (TR/TE = 10 ms / 4 ms, flip-angle: 12, T_{rec} = 53-9000 ms). The relaxation rates were plotted against concentrations and fitted by linear regression to analyze relaxivities.

High-Resolution MR Angiography. For MR examination and catheterization, rats were anaesthetized by inhalation with a mixture of isofluorane (1.5%), N_2O (35%), and O_2 (60%). Tail veins were catheterized using a 24 G indwelling cannula (Introcan; Braun Melsungen AG, Melsungen, Germany), which was connected to a 1 mL syringe (Braun Melsungen AG, Melsungen, Germany) filled with 1 mL of the contrast agent (i.e. 0.05 mmol of Gd/kg of body weight for both HE-24.8 and Gd-DTPA-HSA). MR examinations of the rats were initiated by a T_2 weighted turbo spin-echo sequence: TR = 4000 ms, TE = 96 ms, 1 acquisition, echo train length = 7, TA = 1 min 49 s, field of view = 50 x 37.5 mm, matrix = 140 x 256, slice thickness = 2 mm, voxel size = 2.0 x 0.36 x 0.15 mm^3. Four animals were examined with HE-24.8-enhanced scans, one after administration of Gd-DTPA-HSA. The contrast agent was injected before the first MR

angiography scan. In three of four rats which were examined with HE-24.8-enhanced scans, and in the animal injected with Gd-DTPA-HSA, tumors were initially investigated using a three-dimensional gradient echo pulse sequence (TR/TE = 28.0/8.6 ms, flip-angle = 70, field of view = 12.8 x 30 x 50 mm^3, matrix = 128 x 317 x 512, reconstructed voxel size = 100 x 98 x 98 m^3, 2 acquisitions, total scan time = 24 min). Subsequently, the chest was imaged using again a three-dimensional gradient echo pulse sequence with the following parameters: TR/TE = 10.2/3.8 ms, flip-angle = 70, field of view = 30 x 55 x 110 mm^3, matrix = 60 x 256 x 512, reconstructed voxel size = 500 x 215 x 215 m^3, 4 acquisitions, total scan time = 5.18 min. In the remaining animal, which was scanned with HE-24.8, a high resolved examination of the brain was performed using the first of the abovementioned gradient echo pulse sequences. Afterward, the tumor was investigated as described previously.

Comparison of Vessel Contrast in HE-24.8- and Gd-DTPA-HSA-Enhanced Scans. To compare the in vivo contrast of vessels in HE-24.8- and Gd-DTPA-HSA-enhanced scans, circular ROIs (regions of interest; n = 5) were placed in the left ventricle of the heart, the aorta, the caval vein, the brachial vein, and the neck musculature. Signal intensities (SI) of vessels and heart were normalized to the mean SI of the muscle. Data were compared using the Student's t-test, and $p < 0.05$ was considered to represent statistical significance.

2.10. Histological and immunofluorescence analysis.

For histological analysis, tumors were dissected, covered with "tissue tek" (Sacura, Zoeterwoude, Netherlands), and frozen in liquid nitrogen vapor. Five µm thick sections were cut with a Reichert-Jung Frigocut 2700 microtome. For histology, sections were stained with hematoxilin and eosin (HE). Blood vessels were visualized by means of immunofluorescence, using a polyclonal primary antibody against collagen IV (Progen, Heidelberg, Germany) and a Cy3-labeled secondary antibody against anti-rabbit IgG (Dianova, Hamburg, Germany). Tissue sections were visualized by fluorescence microscopy using an Olympus AX-70 microscope. Images were captured with a digital camera and analyzed using the Soft-Imaging-System analysis software. From the immunofluorescence images, the mean diameters of the 10 largest vessels in the tumor periphery and center were analyzed, in order to obtain information about the minimal vessel diameters which can be resolved by MR-angiography using HE-24.8 and Gd-DTPA-HSA.

3. Results

3.1. In vitro experiments: thermic stability, relaxivity, and toxicity

Chemical Characterization of the Polymers. New polymeric MRI contrast agents based on HPMA copolymers bearing in the side chains aspartic acid residues complexed with gadolinium were prepared. Structures and characteristics of the HPMA copolymer-Gd complexes synthesized are presented in Figure 1 and Table 1.

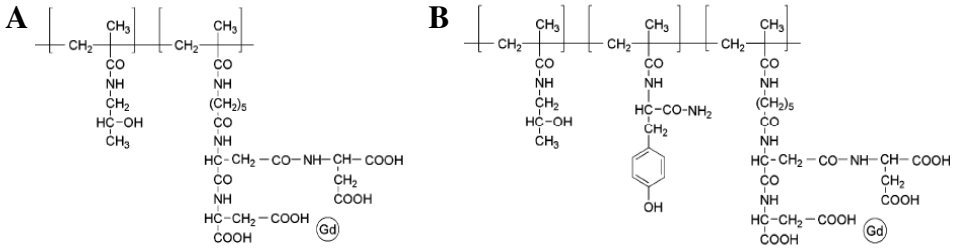

Figure 1. Chemical structures of the 24.8 kDa HPMA copolymer-based contrast agent HE-24.8 (A) and HE-radiolabel (B), the latter being used for the scintigraphic pharmacokinetic analysis in vivo.

Sample	Comonomer[a] in monomer mixture (mol%)	Ma-Tyr-NH_2 in monomer mixture (mol%)	Comonomer[a] in polymer (mol%)	Ma-Tyr-NH_2 in polymer (mol%)	M_W (kDa)	PD (M_W/M_n)
HE-24.8	5	0	3.3	0	24800	1.92
HE-radiolabel	5	2	3.2	0.8	26900	1.76

Table 1: Characteristics of HPMA copolymer-Gd complexes. M_W: Weight average molecular weight. PD: polydispersity. [a]: Ma-Acap-Asp-[Asp-$(OMe)_2$]$_2$

Thermic Stability of HE-24.8. The gadolinium content of nonfiltered samples containing the Gd-HPMA polymers in PBS was 11.6 ± 0.1 µg of Gd/mL. After the polymers were removed by filtration with a 5 kDa MW filter, 0.07 ± 0.01 µg of Gd/mL were left in the probe. Incubation of the polymer at 60 °C did not increase the amount of filtered gadolinium. A constant level of 0.05 ± 0.01 µg of Gd/mL was determined after 1, 5, and 25 h, respectively.

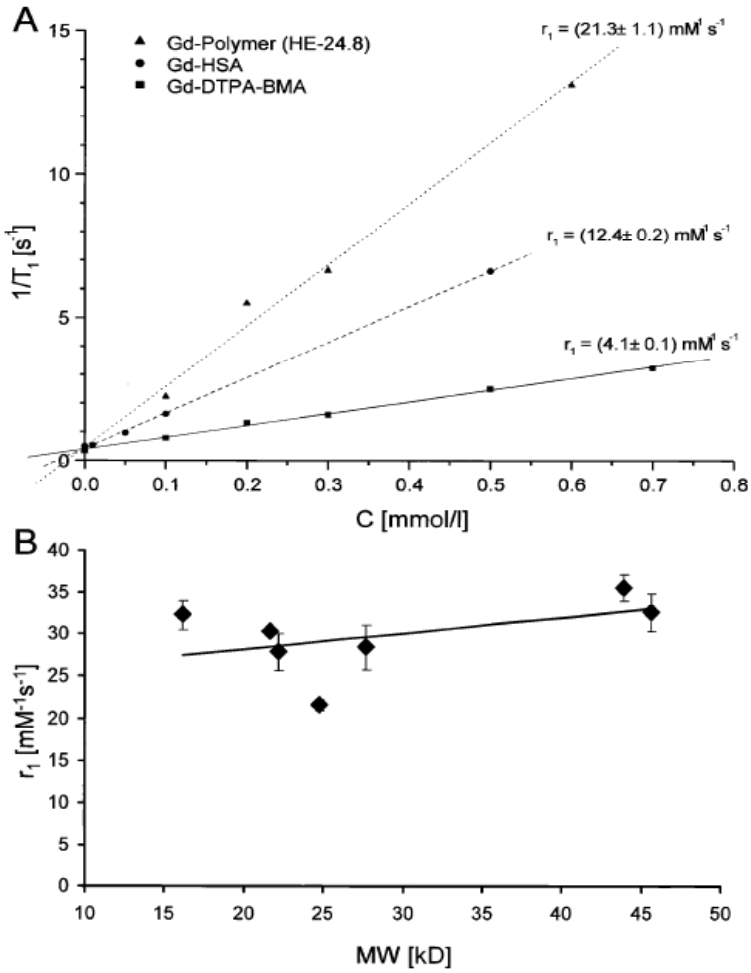

Figure 2. A: Results of the T_1 relaxivity (r_1) measurements of Gd-DTPA-BMA, Gd-DTPA-HSA and HE-24.8 measured at 1.5 T. B: T_1 relaxivity (r_1) of HPMA copolymer-Gd complexes with different sizes (16.2, 21.7, 22.2, 24.8, 27.7, 43.9 and 45.6 kDa). Values represent average ± SD (n=5).

Relaxivity. HE-24.8 showed a T_1 relaxivity of 21.3 ± 1.1 mM^{-1} s^{-1} at 1.5 T, which was higher than the relaxivity of Gd-DTPA-HSA (12.4 ± 0.2 mM^{-1} s^{-1}) and Gd-DTPA-BMA (4.1 ± 0.1 mM^{-1} s^{-1}). As a consequence, a higher T_1 contrast was achieved in MR angiography (Figure 2A). The T_2 relaxivity of HE-24.8 at 1.5 T was 29.4 ± 0.3 mM^{-1} s^{-1}. When comparing Gd-labeled HPMA copolymers of different sizes, it was observed that the T_1 relaxivity of the different compounds was similar in the used molecular size range (Figure 2B), which is advantageous when intending to use such substances for studying vessel permeability in vivo.

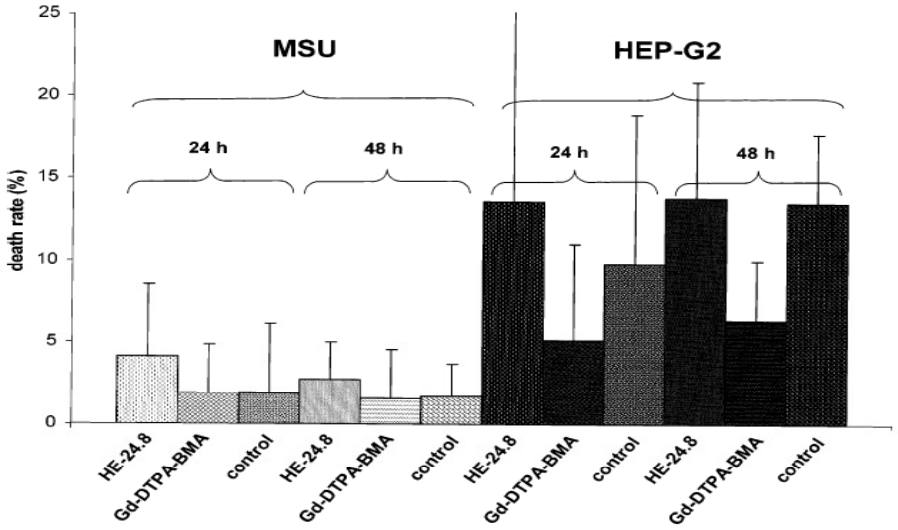

Figure 3. Cytotoxicity induced in human fibroblasts (MSU) and hepatocarcinoma cells (Hep-G2) after incubation with HE-24.8 and Gd-DTPA-BMA at a dose of 0.5 mmol of Gd/L. Incubation times were 24 and 48 h. Values represent average ± SD (n=10).

Cell Toxicity. Cell survival experiments were performed to study toxicity and the stability of the HPMA copolymer-Gd complex HE-24.8. No increased rates of cell death were observed upon incubation of the cells with HE-24.8 or Gd-DTPA-BMA at concentrations of 0.05 and 0.5 mmol of Gd/L. After 24 h of incubation of the cells with 0.5 mmol of Gd/L, the relative number of nonviable MSU cells was lower than 5% for both contrast agents and was comparable to that observed for control cells. Also after incubation times of 48 h, the average amounts of dead cells were always lower than 5% (Figure 3). The excellent tolerance of HE-24.8 was underlined by toxicity experiments with HEP-G2 cells, where also no significantly increased death rates were observed, although the baseline rates of cell death were higher for all experimental conditions (Figure 3).

3.2. Kinetics, biodistribution, and in vivo toxicity

Lack of toxicity in cell culture experiments encouraged us to initiate animal studies. As shown in Figure 4, the radiolabeled tyrosinamide-modified HPMA-Gd copolymer (HE-radiolabel) circulates for prolonged periods of time. At 15 min post intravenous injection (p.i.), for instance, approximately 45% of the injected dose (ID) was left in the systemic circulation, and at 4 h p.i., the concentration in the systemic circulation was ~20% ID. At 24, 168, and 336 h p.i., ~4.5, 0.4, and 0.1% ID could be attributed to the vascular compartment, respectively (Figure 4).

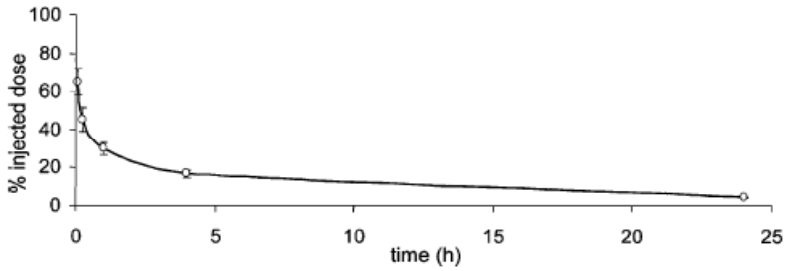

Figure 4. Blood levels of HE-radiolabel (^{131}I) in rats upon i.v. injection. Values represent average ± SD (n=4).

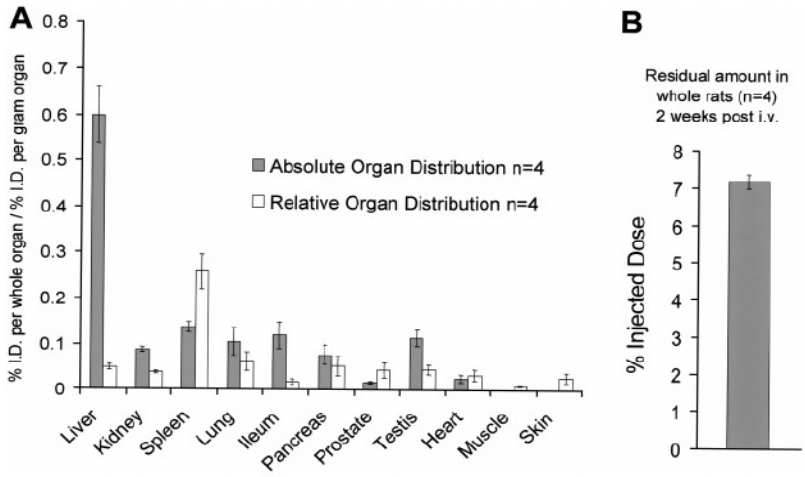

Figure 5. Radioactive counts representing the absolute and relative organ concentrations of HE-radiolabel in rats 14 days after i.v. administration (A). The mean absolute concentration in whole animals is shown in B. Values represent average ± SD (n=4).

Two weeks after intravenous injection of HE-radiolabel, animals were sacrificed, organs were removed, and radioactive counts were analyzed. HE-radiolabel did not accumulate in any organ specifically, when expressed as a percentage of ID. Relatively, the largest fraction of contrast agent accumulated in the spleen, with 0.25% ID/g of tissue (Figure 5). In most other tissues, concentrations approximately were 0.05% ID/g. Absolutely, i.e., when taking organ weight into account, at 336 h post injection, most of the conjugate ended up in the liver. Hepatic uptake was very acceptable, with only 0.6% ID in the whole organ. At the entire organism level, 37.6, 20.0, and 8.0% ID were still detected by scintigraphic imaging at 4, 24, and 336 h post injection, respectively (Figure 6). No decreased overall activity, no reduction in food intake, and no substantial signs of weight loss were observed during the course of these experiments.

3.3. MR angiography

To evaluate the in vivo contrast characteristics of HE-24.8, micro-MR angiographies of rats and experimental tumors were obtained, and they were compared with images obtained using Gd-DTPA-HSA. Both contrast agents showed an excellent display of the larger veins of the chest and the brain, as well as of the heart with its ventricles (Figure 7). However, as expected from the higher T_1 relaxivity, the contrast of the heart ventricles, and of the larger arteries and veins was more than 70% higher in HE-24.8-enhanced scans (Figures 7 and 8). For smaller peripheral veins, such as the brachial vein, no significant differences in vessel contrast was observed (Figure 8). In subcutaneous tumors, both contrast agents showed the potential to visualize the small and fragile tumor neo-vasculature (Figure 9). However, the vessel architecture of tumors could not be displayed in higher detail using HE-24.8, which was most probably resulted from the limited spatial resolution and signal-to-noise ratio of the clinical 1.5 T MR scanner. Predominantly larger vessels localized at the tumor periphery were visualized by MR angiography and they were reconstructed three-dimensionally. Determining the mean diameters of peripheral tumor blood vessels on histological images, it was shown that these vessels had diameters of 96 ± 51 µm, which is in line with vessel sizes resolved by other groups using 1.5 T MR angiography [18,19]. The small vessels found in the tumor center with a mean diameter of 12 ± 5 µm could not be visualized using MRI, neither using Gd-DTPA-HAS, nor using HE-24.8.

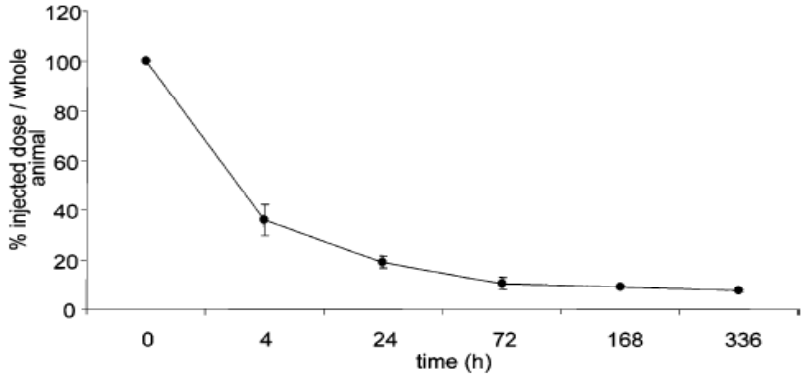

Figure 6. Retention of radioactivity at the whole organism level. The mean relative number of counts observed during a two-week follow up (detected using scintigraphic analysis of ^{131}I-labeled HPMA copolymer-Gd complex) is shown. The total number of counts detected after 1 h (in rats which were kept under continuous anesthesia) was set at 100%. Values represent average ± SD (n=4).

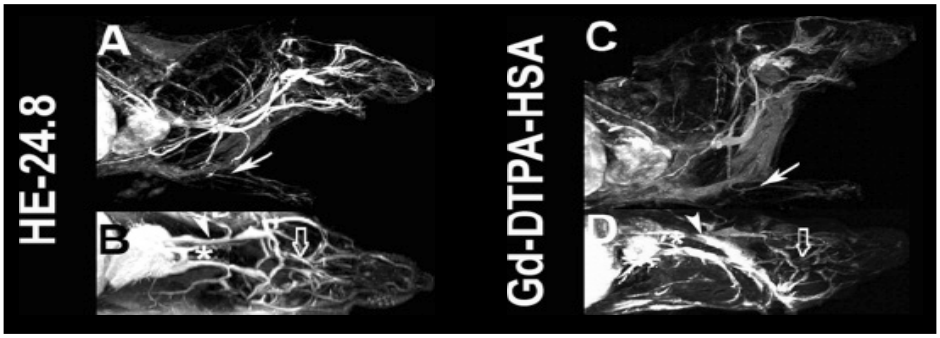

*Figure 7. MR angiography scans of the chest of rats using HE-24.8 (A and B) and Gd-DTPA-HSA (C and D). Images represent sagittal (A and C) and coronal (B and D) views of the animal. Both contrast agents give an excellent display of larger veins of the chest (arrowheads) and the brain (open arrow: jugular vein), as well as of the heart with its ventricles. While the contrast of larger vessels is better in HE-24.8-enhanced scans, it is comparable in smaller vessels, such as the brachial vein (arrow). *: aortic arc.*

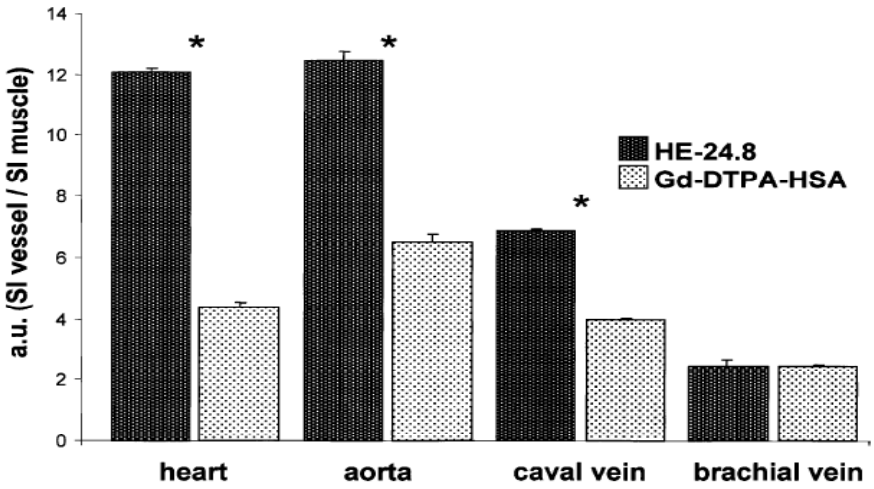

Figure 8. Comparison of vessel contrast in HE-24.8- and Gd-DTPA-HSA-enhanced scans. Using HE-24.8, significantly higher vessel contrast was observed in the heart, aorta and caval vein. Vessel contrast in the brachial vein was not significantly different. Values represent average ± SD of 5 ROI analyses ($p<0.05$).*

Also in the brain, HE-24.8 proved its potential as an excellent experimental angiographic contrast agent, by clearly visualizing the vascular network with the feeding carotic artery, the draining jugular vein, and the basal cerebral arteries of the circulus arteriosus cerebri. Even the middle cerebral artery and some of its branches could be detected at 1.5 T using HE-24.8 (Figure 10).

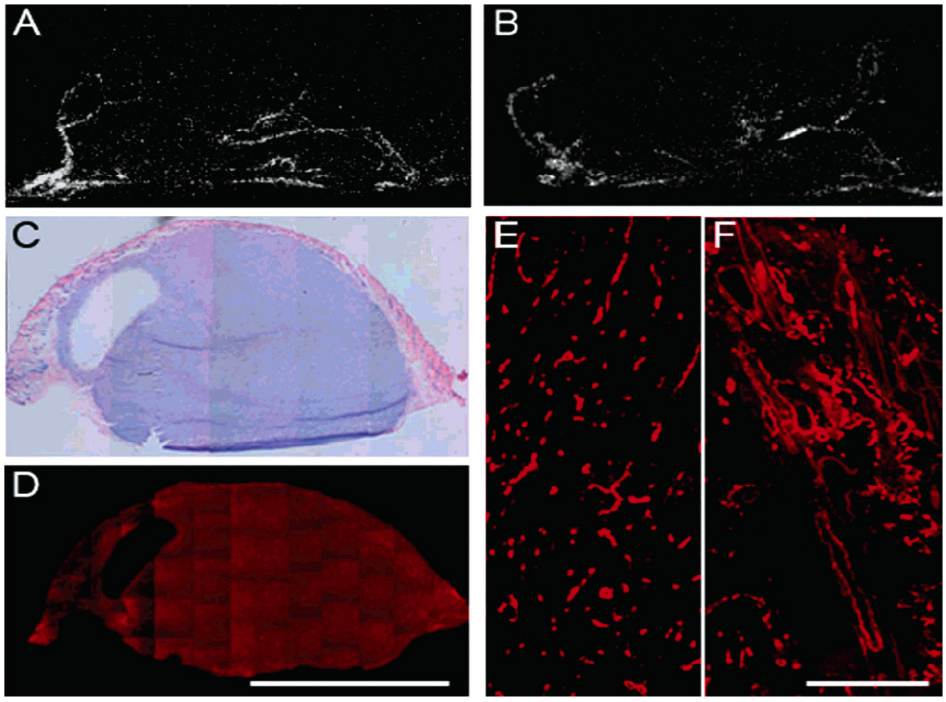

Figure 9. Maximum intensity projections (MIP) of a subcutaneous Dunning AT1 tumor in rats using HE-24.8 (A) and Gd-DTPA-HSA (B). Histological compilations of the tumor shown in A were prepared using hematoxilin and eosin staining (C), and collagen type IV staining (D). Magnifications of the immunofluorescence image taken from representative areas of the tumor center (E) and periphery (F) exemplify the differences in vessel architecture between larger vessels in the tumor periphery (91 ± 51 µm) and smaller capillary vessels in the center (12 ± 5 µm). Bars: 5 mm (D), 0.4 mm (F). See page 228.

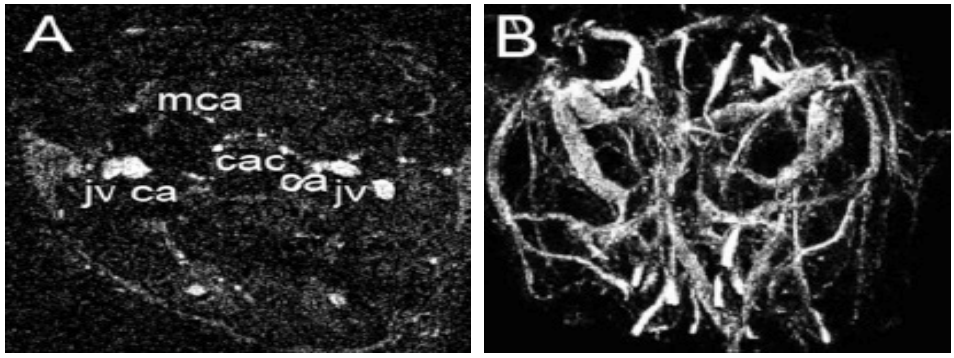

Figure 10. Coronal image (A) and MIP (B) of HE-24.8-enhanced scans of the rat head. The carotic artery (ca) and the jugular vein (jv) are clearly shown on both images. Also smaller vessels such as those of the circulus arteriosus cerebri (cac) or the middle cerebral artery (mca) could be nicely visualized.

4. Discussion

In this chapter, a novel long-circulating MR contrast based on an HPMA copolymer-Gd complex is presented. In this context, the synthesis of a new monomer Ma-Acap-Asp-[(Asp-$(OMe)_2$]$_2$ is described. This monomer and methodology enables the preparation of a broad range of copolymers differing in molecular weight and copolymer composition. The copolymers (after deprotection of carboxylic groups) form complexes with gadolinium and exhibit an excellent thermostability in aqueous solutions (temperatures up to 60 °C were evaluated). The copolymer HE-radiolabel contains a small amount of tyrosinamide, enabling radiolabeling and the use of this copolymer for pharmacokinetic studies. Copolymer HE-24.8 consists of HPMA and Ma-Acap-Asp-[(Asp-$(OH)_2$]$_2$-Gd units. In both polymer complexes, Gd was embedded in the side chains of the copolymer by means of three aspartic acid residues extending four carboxylic groups for complexation. As a basis for further studies, the biological behavior of HE-24.8 was examined in vitro and in vivo. Furthermore, initial results are presented using this contrast agent to visualize tumor and brain microvasculature, and contrast enhancement was compared to Gd-DTPA-HSA.

Complexing gadolinium atoms to HPMA copolymers results in a high T_1 relaxivity, which is superior to that of Gd-DTPA-BMA and of Gd-DTPA-HSA. This high T_1 relaxivity can be attributed to the new type of structure of the Gd complex, leading to an improved interaction of gadolinium with surrounding protons. This improved T_1 relaxivity might might also (at least in part) be due to the integration of gadolinium into a highly hydrophilic polymeric matrix, which is also known to result in increases in the T_1 relaxivity of contrast agents, in line with what has been found for proteins [38-40] and other tracers [11,15,20]. The relaxivity of Gd-DTPA-HSA may also increase by binding more Gd-DTPA molecules to albumin, or by modifying the method of binding [41]. However, the low number of Gd-DTPA molecules bound to HSA was chosen to reduce hepatic elimination, which is highly influenced by the loading rate of albumin [42]. It is a further advantage of the HPMA copolymer-Gd complexes that the T_1 relaxivities of the compounds with different molecular sizes (between 15 and 46 kDa) were not significantly different. This predetermines HPMA copolymer-Gd complexes for studies on blood vessel permeability, using e.g. copolymers of different sizes to characterize vascular leakiness in response to anti-angiogenic therapy.

There were no indications for release of gadolinium in the in vitro experiments, which would have resulted cell death. In line with this, also in vivo, no toxic effects were observed. However, studies with higher animal numbers and longer follow-up times are necessary to confirm this notion. In spite of the fact that the polymers themselves are known to be non-immunogenic, it is furthermore also important to address immunogenic reactions. These could e.g. be caused by the chelating side chain groups, and have been reported for Gd-DOTA.

For visualizing the (tumor) microvasculature using a clinical 1.5 T MR scanner, long acquisition times are required, in order to achieve a sufficiently high signal-to-noise ratio. In this study, because of the longer intravascular persistence of HE-24.8 as compared to the clinically used small Gd-chelates, extended acquisition times can be easily realized.

However, long circulation times are accompanied by slow elimination. In line with previous reports on parental and drug-functionalized HPMA copolymers [30, 31], and with studies on other long-circulating carrier materials, like PEG, we did not observe accumulation of the gadolinium-containing copolymer in any organ specifically. Given a size below ~45 kDa, polymeric drug carriers are generally initially cleared by means of renal filtration, and later on predominantly by the reticuloendothelial system. This notion is confirmed by the fact that the highest uptake of HE-24.8 per gram of tissue was found in the spleen, where the construct accumulated because of phagocytosis by macrophages.

When comparing HE-24.8 with other macromolecular carrier materials [13,20], it is a great advantage that the liver does not accumulate HE-24.8 in high amounts. Only 0.6% of the injected dose was found in the liver two weeks after i.v. administration. Thus, we conclude that the hydrophilic nature of the HPMA polymer chain, the neutral loading, the absence of structural inhomogeneities (as present e.g. in liposomes), and the random coil configuration, reduce the immunological detection of HE-24.8.

We are aware of the fact that for clinical application, the intracorporal persistence of more than 7% of the injected dose of HE-24.8 at 14 days p.i. is still too high. The molecular weight of approximately 25 kDa was chosen for the synthesis of HE-24.8 to be in the size range of HPMA copolymer-based anticancer agents. Currently, at least six HPMA-based polymer therapeutics of comparable size have been evaluated clinically [44]. The aim of such polymeric

prodrugs, however, is to increase the circulation time and the tumor accumulation of the attached active agent, and to attenuate its localization to healthy tissues. Consequently, the properties of the copolymers have been optimized for therapeutic purposes, and not (yet) for imaging purposes. The versatile nature of HPMA copolymers enable us to tailor size, structure and stability of the complexes, indicating that there still is much room for improvements. Currently, we are evaluating several conjugates of significantly smaller size, and in the near future, we will try to establish comparable but biodegradable contrast agents [44,45], to initially retain the prolonged circulation (and acquisition) times, but to boost elimination in the first two weeks after i.v. administration.

MR angiographies showed a detailed display of rat and tumor vasculature even for vessels with relatively slow blood flow, like for most of the tumor blood vessels. For these vessels, the signal enhancement by flow effects is considerably low, and as a consequence, the vessel contrast is more dependent on the contrast agent. Compared with Gd-DTPA-HSA, the contrast of vessels was higher, while the amount of vessels was not increased. The lack of displaying smaller vessels, however, can be attributed to the voxel sizes, which could not be chosen smaller at an acceptable signal-to-noise ratio with the clinical 1.5 T MR-scanner. In the extremities, the difference in vessel contrast between HE-24.8- and Gd-DTPA-HSA-enhanced scans was reduced as compared with larger central vessels of the chest. This may be because if only part of the voxel contains the vessel, the signal intensity change after contrast agent application becomes lower. Thus, the signal enhancement, which is achieved with contrast agents with higher or lower T_1 relaxivity, equalizes. The advantages of HE-24.8 to image smaller vessels would most probably become more evident at higher field strength (>1.5 T), where differences in T_1 relaxivity between Gd-DTPA-BMA, Gd-DTPA-HSA and HE-24.8 become more important (own unpublished results), and where smaller voxel sizes can be chosen.

In summary, we here report a novel macromolecular contrast agent with flexible size and structure. Besides its suitability for experimental MR angiography, the independence of the T_1 relaxivity on polymer size suggests that this polymeric contrast agent might be an interesting tool for studying blood vessel permeability in tumors. For potential clinical applications, further chemical refinements are necessary, assuring e.g. a more rapid clearance from the body.

References

1. Felix, R., Semmler, W., Schorner, W., and Laniado, M. (1985) Contrast media in magnetic resonance tomography. A review. 1. Physicochemical and pharmacological bases of MR contrast media using gadolinium-DTPA as an example. Rofo 142, 641-646.
2. Wolf, G. L., Burnett, K. R., Goldstein, E. J., and Joseph, P. M. (1985) Contrast agents for magnetic resonance imaging. Magn. Reson. Annu. 231-266
3. Semelka, R. C., and Helmberger, T. K. (2001) Contrast agents for MR imaging of the liver. Radiology 218, 27-38
4. Padhani, A. R. (2002) Dynamic contrast-enhanced MRI in clinical oncology: current status and future directions. J. Magn. Reson. Imaging 16, 407-422
5. Roberts, T. P., Chuang, N., and Roberts, H. C. (2000) Neuroimaging: do we really need new contrast agents for MRI? Eur. J. Radiol. 34, 166-178
6. Krinsky, G. (1998) Gadolinium-enhanced three-dimensional magnetic resonance angiography of the thoracic aorta and arch vessels. A review. Invest. Radiol. 33, 587-605
7. Rofsky, N. M., and Adelman, M. A. (2000) MR angiography in the evaluation of atherosclerotic peripheral vascular disease. Radiology 214, 325-338
8. Spinosa, D. J., Kaufmann, J. A., and Hartwell, G. D. (2002) Gadolinium chelates in angiography and interventional radiology: a useful alternative to iodinated contrast media for angiography. Radiology 223, 319-325
9. Kiessling, F., Farhan, N., Lichy, M. P., Vosseler, S., Heilmann, M., Krix, M., Bohlen, P., Miller, D. W., Mueller, M. M., Semmler, W., Fusenig, N. E., and Delorme, S. (2004) Dynamic contrast-enhanced magnetic resonance imaging rapidly indicates vessel regression in human squamous cell carcinomas grown in nude mice caused by VEGF receptor 2 blockade with DC101. Neoplasia 6, 213-223
10. Turetschek, K., Preda, A., Novikov, V., Brasch, R. C., Weinmann, H. J., Wunderbaldinger, P., and Roberts, T. P. (2004) Tumor microvascular changes in antiangiogenic treatment: Assessment by magnetic resonance contrast media of different molecular weights. J. Magn. Reson. Imaging 20, 138-144
11. Kobayashi, H., and Brechbiel, M. W. (2003) Dendrimer-based macromolecular MRI contrast agents: characteristics and application. Mol. Imaging 2, 1-10
12. Brasch, R., and Turetschek, K. (2000) MRI characterization of tumors and grading angiogenesis using macromolecular contrast media: status report. Eur. J. Radiol. 34, 148-155
13. Kiessling, F., Fink, C., Hansen, M., Bock, M., Sinn, H., Schrenk, H. H., Krix, M., Egelhof, T., Fusenig, N. E., and Delorme, S. (2002) Magnetic resonance imaging of nude mice with heterotransplanted high-grade squamous cell carcinomas: use of a low-loaded, covalently bound Gd-Hsa conjugate as contrast agent with high tumor affinity. Invest. Radiol. 37, 193-198
14. Dafni, H., Gilead, A., Nevo, N., Eilam, R., Harmelin, A., and Neeman, M. (2003) Modulation of the pharmacokinetics of macromolecular contrast material by avidin chase: MRI, optical, and inductively coupled plasma mass spectrometry tracking of triply labeled albumin. Magn. Reson. Med. 50, 904-914. [ChemPort] [Medline] [CrossRef]
15. Misselwitz, B., Schmitt-Willich, H., Ebert, W., Frenzel, T., and Weinmann, H. J. (2001) Pharmacokinetics of Gadomer-17, a new dendritic magnetic resonance contrast agent. MAGMA 12, 128-134
16. Lauffer, R. B., Parmelee, D. J., Dunham, S. U., Ouellet, H. S., Dolan, R. P., Witte, S., McMurry, T. J., and Walovitch, R. C. (1998) MS-325: albumin-targeted contrast agent for MR angiography. Radiology 207, 529-538
17. Marzola, P., Farace, P., Calderan, L., Crescimanno, C., Lunati, E., Nicolato, E., Benati, D., Degrassi, A., Terron, A., Klapwijk, J., Pesenti, E., Sbarbati, A., and Osculati, F. (2003) In vivo mapping of fractional plasma volume (fpv) and endothelial transfer coefficient (Kps) in solid tumors using a macromolecular contrast agent: correlation with histology and ultrastructure. Int. J. Cancer 104, 462-468
18. Fink, C., Kiessling, F., Bock, M., Lichy, M. P., Misselwitz, B., Peschke, P., Fusenig, N. E., Grobholz, R., and Delorme, S. (2003) High-resolution three-dimensional MR angiography of rodent tumors: morphologic characterization of intratumoral vasculature. J. Magn. Reson. Imaging 18, 59-65
19. Kobayashi, H., Sato, N., Kawamoto, S, Saga, T., Hiraga, A., Ishimori, T., Konishi, J., Togashi, K., and Brechbiel, M. W. (2001) 3D MR angiography of intratumoral vasculature using a novel macromolecular MR contrast agent. Magn. Reson. Med. 46, 579-585.

20. Weissleder, R., Bogdanov, A., Tung, C. H., and Weinmann, H. J. (2001) Size optimization of synthetic graft copolymers for in vivo angiogenesis imaging. Bioconjugate Chem. 12, 213-219
21. Callahan, R. J., Bogdanov, A., Fischman, A. J., Brady, T. J., and Weissleder, R. (1998) Preclinical evaluation and phase I clinical trial of a 99mTc-labeled synthetic polymer used in blood pool imaging. Am. J. Roentgenol. 171, 137-143
22. Bremer, C., Tung, C. H., and Weissleder, R. (2001) In vivo molecular target assessment of matrix metalloproteinase inhibition. Nat. Med. 7, 743-748
23. Rihova, B., Strohalm, J., Kubakova, K., Jelinkova, M., Rozprimova, L., Sirova, M., Plocova, D., Mrkvan, T., Kovar M., Pokorna, J., Etrych, T., and Ulbrich, K. (2003) Drug-HPMA-HuIg conjugates effective against human solid cancer. Adv. Exp. Med. Biol. 519, 125-143
24. Caiolfa, V. R., Zamai, M., Fiorino, A., Frigerio, E., Pellizzoni, C., d'Argy, R., Ghiglieri, A., Castelli, M. G., Farao, M., Pesenti, E., Gigli, M., Angelucci, F., and Suarato, A. (2000) Polymer-bound camptothecin: initial biodistribution and antitumour activity studies. J. Control. Release 65, 105-119
25. Meerum-Terwogt, J. M., ten Bokkel Huinink, W. W., Schellens, J. H., Schot, M., Mandjes, I. A., Zurlo, M. G., Rocchetti, M., Rosing, H., Koopman, F. J., and Beijnen, J. H. (2001) Phase I clinical and pharmacokinetic study of PNU166945, a novel water-soluble polymer-conjugated prodrug of paclitaxel. Anti-Cancer Drugs 12, 315-323
26. Gianasi, E., Buckley, R. G., Latigo, J., Wasil, M., and Duncan, R. (2002) HPMA copolymers platinates containing dicarboxylato ligands. Preparation, characterisation and in vitro and in vivo evaluation. J. Drug Targeting 10, 549-556
27. Rihova, B., and Kubackova, K. (2004) Clinical implications of N-(2-hydroxypropyl)methacrylamide copolymers. Curr. Pharm. Biotechnol. 4, 311-322
28. Searle, F., Gac-Breton, S., Keane R., Dimitrijevic, S., Brocchini, S., Sausville, E. A., and Duncan, R. (2001) N-(2-hydroxypropyl)methacrylamide copolymer-6-(3-aminopropyl)-ellipticine conjugates. Synthesis, in vitro, and preliminary in vivo evaluation. Bioconjugate Chem. 12, 711-718
29. Noguchi, Y., Wu, J., Duncan, R., Strohalm, J., Ulbrich, K., Akaike, T., and Maeda, H. (1998) Early phase tumor accumulation of macromolecules: a great difference in clearance rate between tumor and normal tissues. Jpn. J. Cancer Res. 89, 307-314
30. Shiah, J. G., Dvorak, M., Kopeckova, P., Sun, Y., Peterson, C. M., and Kopecek, J. (2001) Biodistribution and antitumour efficacy of long-circulating N-(2-hydroxypropyl)methacrylamide copolymer-doxorubicin conjugates in nude mice. Eur. J. Cancer 37, 131-139
31. Kissel, M., Peschke, P., ubr, V., Ulbrich, K., Schuhmacher, J., Debus, J., and Friedrich, E. (2001) Synthetic macromolecular drug carriers: biodistribution of poly[(N-2-hydroxypropyl)methacrylamide] copolymers and their accumulation in solid rat tumors. PDA J. Pharm. Sci. Technol. 55, 191-201
32. Mitra, A., Nan, A. J., Ghandehari, H., McNeill, E., Mulholland, J., and Line, B. R. (2004) Technetium-99m-labeled N-(2-hydroxypropyl) methacrylamide copolymers: Synthesis, characterization, and in vivo biodistribution. Pharm. Res. 21, 1153-1159
33. Huang, Y., Nan, A. J., and Rosen, G. M. (2003) N-(2-hydroxypropyl)methacrylamide (HPMA) copolymer-linked nitroxides: Potential magnetic resonance contrast agents. Macromol. Biosci. 3, 647-652
34. Wang, D., Miller, S. C., Sima, M., Parker, D., Buswell, H., Doodrich, K., C., Kopeckova, P., and Kopecek J. (2004) The arthrotropism of macromolecules in adjuvant-induced arthritis rat model: a preliminary study. Pharm. Res. 21, 1741-1749
35. Ulbrich, K., ubr, V., Strohalm, J., Plocova, D., Jelinkova, M., and ihova, M. (2000) Polymeric drugs based on conjugates of synthetic and natural macromolecules I. Synthesis and physico-chemical characterisation. J. Control. Release 64, 63-79
36. Kissel, M., Peschke, P., ubr, V., Ulbrich, K., Strunz, A. M., Kuhnlein, R., Debus, J., and Friedrich, E. (2002) Detection and cellular localisation of the synthetic soluble macromolecular drug carrier pHPMA. Eur. J. Nucl. Med. 29, 1055-1062
37. Drobnik, J., Kopeek, J., Labsk, J., Reimanova, P., Exner, J., Saudek, V., and Kalal, J. (1976) Enzymatic cleavage of side chains of synthetic water-soluble polymers. Makromol. Chem. 177, 2833-2848
38. Stanisz, G. J., and Henkelman, R. M. (2000) Gd-DTPA relaxivity depends on macromolecular content. Magn. Reson. Med. 44, 665-667
39. McMurry, T. J., Parmelee, D. J., Sajiki, H., Scott, D. M., Ouellet, H. S., Walovitch, R. C., Tyeklar, Z., Dumas, S., Bernard, P., Nadler, S., Midelfort, K., Greenfield, M., Troughton, J., and Lauffer, R. B. (2002) The effect of a phosphodiester linking group on albumin binding,

blood half-life, and relaxivity of intravascular diethylenetriaminepentaacetato aquo gadolinium(III) MRI contrast agents. J. Med. Chem. 45, 3465-3474

40. Aime, S., Chiaussa, M., Digilio, G., Gianolio, E., and Terreno, E. (1999) Contrast agents for magnetic resonance angiographic applications: 1H and 17O NMR relaxometric investigations on two gadolinium(III) DTPA-like chelates endowed with high binding affinity to human serum albumin. J. Biol. Inorg. Chem. 4, 766-774
41. Stehle, G., Sinn, H., Wunder, A., Schrenk, H. H., Schutt, S., Maier-Borst, W., and Heene, D. L. (1997) The loading rate determines tumor targeting properties of methotrexate-albumin conjugates in rats. Anti-Cancer Drugs 8, 677-685.
42. Caravan, P., Greenfield, M. T., Li, X., and Sherry, A. D. (2001) The Gd(3+) complex of a fatty acid analogue of DOTP binds to multiple albumin sites with variable water relaxivities. Inorg. Chem. 40, 6580-6587
43. Duncan, R. (2003) The dawning era of polymer therapeutics. Nat. Rev. Drug Discov. 2, 347-360
44. Jabbari, E., Wang, S., Lu, L., Gruetzmacher, J. A., Ameenuddin, S., Hefferan, T. E., Currier, B. L., Windebank, A. J., and Yaszemski, M. J. (2005) Synthesis, material properties, and biocompatibility of a novel self-cross-linkable poly(caprolactone fumerate) as an injectable tissue engeneering scaffold. Biomacromolecules 6, 2503-2511
45. Mohs, A. M., Wang, X., Goodrich, K. C., Zong, Y., Parker, D. L., and Lu, Z. R. (2004) PEG-g-poly(GdDTPA-co-L-cystine): a biodegradable macromolecular blood pool contrast agent for MR imaging. Bioconjugate Chem. 15, 1424-1430

Chapter 5

Effect of intratumoral injection on the biodistribution and the therapeutic potential of HPMA copolymer-based drug delivery systems

Twan Lammers[a,b], Peter Peschke[a], Rainer Kühnlein[a], Vladimir Subr[c], Karel Ulbrich[c], Peter Huber[a], Wim Hennink[b], Gert Storm[b]

[a] Department of Innovative Cancer Diagnosis and Therapy, Clinical Cooperation Unit Radiotherapeutic Oncology, German Cancer Research Center, Im Neuenheimer Feld 280, 69120 Heidelberg, Germany
[b] Department of Pharmaceutics, Utrecht Institute for Pharmaceutical Sciences, Utrecht University, Sorbonnelaan 16, 3584 CA Utrecht, The Netherlands
[c] Institute of Macromolecular Chemistry, Academy of Sciences of the Czech Republic, Heyrovsky Square 2, 162 06 Prague 6, Czech Republic

Neoplasia 8: 788-795 (2006)

Abstract

The direct intratumoral injection of anticancer agents has been evaluated extensively in the past few decades. Thus far, however, it has failed to become established as an alternative route of administration in routine clinical practice. In the present report, the impact of i.t. injection on the biodistribution and the therapeutic potential of HPMA copolymer-based drug delivery systems was investigated. It was found that as compared to i.v. injection, i.t. injection improved both the tumor concentrations and the tumor-to-organ ratios of the copolymers substantially. In addition, as compared to i.v. and i.t. applied free doxorubicin and to i.v. applied poly(HPMA)-GFLG-doxorubicin, the i.t. administered polymeric prodrug presented with a significantly increased antitumor efficacy, as well as with an improved therapeutic index. Based on these findings, we propose intratumorally injected carrier-based chemotherapy as an interesting alternative to the routinely used chemotherapy regimens and routes of administration.

1. Introduction

Even though the direct intratumoral (i.t.) injection of anticancer agents has been evaluated extensively in the past few decades [1-5], it has failed to become established as an alternative route of administration in routine clinical practice. This is generally considered to be due to the invasive nature of i.t. injection, to the relatively rapid clearance of locally administered drugs from tumors, and to the development of dose-limiting toxicities in the tissues surrounding the site of application. In addition, those types of tumors that would, in principle, be readily accessible for i.t. injection, are generally being treated with more standardized (and more effective) locoregional treatment modalities, such as surgery and radiotherapy.

Alongside the advances in establishing novel antitumor therapeutics, a large number of drug delivery systems have been developed over the years, both for parenteral and for local administration [6-10]. Thus far, however, even though several highly innovative drug delivery systems have been designed specifically for locoregional application, only very few have managed to progress into clinical trials. Taking this notion into account, we have here set out to evaluate the impact of i.t. injection on the biodistribution and the therapeutic potential of HPMA copolymer-based drug delivery systems. Copolymers of *N*-(2-hydroxypropyl)methacrylamide (HPMA) are prototypic and well-characterized polymeric drug carriers that have been broadly implemented in the delivery of anticancer therapeutics, and that have been tested in several phase I and II clinical trials [11-15].

In the first set of experiments, the circulation kinetics, the organ distribution and the tumor accumulation of i.v. and i.t. applied HPMA copolymers were investigated in rats bearing subcutaneously transplanted Dunning AT1 tumors. Subsequently, the impact of i.t. injection on the biodistribution of poly(HPMA)-GFLG-doxorubicin was assessed, in order to evaluate if the effects observed for chemically unmodified HPMA copolymers also hold for a clinically relevant HPMA copolymer carrying a chemotherapeutic drug. And finally, the antitumor efficacy, the toxicity and the therapeutic index of i.v. and i.t. applied poly(HPMA)-GFLG-doxorubicin were analyzed, and they were compared to those of i.v. and i.t. applied free doxorubicin.

2. Materials and Methods

2.1. Chemicals

Methacryloyl chloride, methacrylic acid, 1-aminopropan-2-ol, tyrosinamide, glycylglycine, glycylphenylalanine, leucylglycine, 4-nitrophenol, dimethylsulfoxide (DMSO) and doxorubicin hydrochloride (Dox.HCl) were obtained from Fluka and were of appropriate analytical grade.

2.2. Synthesis and characterization of the copolymers

The HPMA copolymers used in this study were synthesized as described previously [16]. Briefly, poly(HPMA-co-MA-TyrNH_2) was prepared by solution radical copolymerization of the monomers HPMA and MA-TyrNH_2 in methanol. The weight- and number-average molecular weights (M_w and M_n) and the polydispersity (M_w/M_n) of the copolymers after their fractionation (on Superose 4B/6B columns) were determined by size exclusion chromatography on an Äkta Explorer (Amersham Biosciences), equipped with UV, a differential refractometer (Shodex R-72) and a multiangle light scattering detector (DAWN DSP-F; Wyatt Technology Corp.). The average molecular weights of the two parental HPMA copolymers were 30.5 kD and 64.5 kD, their polydispersities were 1.3 and 1.2, and the relative amounts of tyrosinamide, included to allow for radiolabeling, were 0.8 mol% and 0.3 mol%. The precursor for poly(HPMA)-GFLG-doxorubicin, i.e. poly(HPMA)-co-MA-TyrNH_2-co-MA-Gly-DL-PheLeuGly-ONp, was prepared by precipitation radical terpolymerization of HPMA, MA-TyrNH_2 and MA-GFLG-ONp in acetone. After purification, doxorubicin was conjugated to this precursor in DMSO, in the presence of Et_3N. The reaction mixture was stirred for 4 h, 1-aminopropan-2-ol was added and the mixture was precipitated into a mixture of acetone and diethylether (3:1). The resulting doxorubicin-containing conjugate was then filtered off, dried in vacuum, purified on a Sephadex LH-20 column (to remove free doxorubicin), and purified on a Sephadex LH-60 column (to obtain a narrow distribution of the molecular weight). The molecular weight of the conjugate was 27.9 kD, its polydispersity was 1.5, the amount of tyrosinamide was 1.3 mol% and the amount of doxorubicin was 6.5 wt%.

2.3. Radiolabeling

Iodine-131 was obtained from Amersham (Freiburg, Germany). The tyrosinamide groups incorporated into the copolymers were radiolabeled using the mild oxidizing agent 1,3,4,6-tetrachloro-3 alpha,6 alpha-diphenyl glycoluril (i.e. by means of the Iodogen method [17]). Upon 10 minutes of incubation, the mixture of iodine-131, Iodogen and the copolymer was applied to a Biogel-P6 column and it was eluted with 30 ml of PBS. The eluate was recovered in 1 ml fractions and the radioactivity of each of these fractions was determined by means of a scintillation counter. The radiolabeled copolymer was retrieved in the fifth to seventh ml of the eluate, while free (i.e. unbound) iodine-131was eluted in the fourteenth to eighteenth ml. As this methodology allowed us to concentrate the copolymer-associated fraction, no additional purification was required. The efficacy of radiolabeling was quantified by dividing the amount of radioactivity collected in the fifth to seventh ml of the eluate by the total amount of radioactivity retrieved, i.e. by the sum of the activities detected in all thirty 1 ml fractions. The labeling efficacies for 31 kD poly(HPMA), 65 kD poly(HPMA) and 28 kD poly(HPMA)-GFLG-doxorubicin were 95.2%, 96.2% and 86.3%, respectively.

2.4. Animal model

All experiments involving animals were approved by an external committee for animal welfare and were performed according to the guidelines for laboratory animals established by the German government. Experiments were performed on 6-12 month old male Copenhagen rats (Charles River, Germany), using the syngeneic Dunning R3327-AT1 prostate carcinoma model [18]. During all experimental procedures, the animals were anaesthetized using Ethrane. Fresh pieces of AT1 tumor tissue were prepared from an AT1 donor tumor and they were transplanted subcutaneously into the right hind limbs of the rats. Tumors were grown for 12-18 days, until they reached an average diameter of ~12 mm.

2.5. Biodistribution

For analyzing the biodistrution of the copolymers, 500 µl of a 0.1 mM solution (based on copolymer concentration; corresponding to a radioactivity of 150 to 300 µCi) were injected i.v. into the lateral tail vein of the animals. The biodistribution of the copolymers upon i.t. injection was evaluated upon administrating a substantially smaller volume (50-100 µl) containing the same amount of copolymer (i.e. 0.1 mmol; 150 to 300 µCi) directly into the center of

the tumors. Immediately after i.t. injection, the application site was covered and washed twice with absorbing paper, in order to retrieve radiolabeled copolymer leaking out of the tumor. At 0.1, 0.25, 1, 4 and 24 h post injection (p.i.), the concentrations of the copolymers in systemic circulation were determined by withdrawing 50 µl of blood from the tail vein of the rats, and by assuming that the complete blood pool equals 6% of their body weight. At 0.5 (obtained after keeping the animals under general anesthesia for 30 minutes), 4 and 24 h p.i., the biodistribution of the copolymers was monitored two-dimensionally using a Searle-Siemens scintillation camera. At 24 h p.i., the animals were sacrificed, and their tumors and organs were harvested for quantification. The residual amounts of radioactivity were determined using a gamma counter, they were corrected for radioactive decay and they were expressed as percent of the injected dose per gram tissue.

2.6. In vitro toxicity

The cytotoxicity of free and HPMA copolymer-bound doxorubicin was determined by seeding 200 Dunning AT1 cells into 6-well plates. Four hours later, the cells were treated with 0.001-10 µMol of free doxorubicin, with 0.001-1000 µMol of poly(HPMA)-GFLG-doxorubicin and with 0.001-1000 µMol of a drug-free control copolymer. After 8-10 days, the cells were fixed and stained, and the number of surviving colonies was counted.

2.7. Antitumor efficacy

Rats bearing 10-15 mm AT1 tumors were randomly assigned to various treatment groups. Free and HPMA copolymer-bound doxorubicin were administered by means of a single i.v. or i.t injection at a (doxorubicin-equivalent) dose of 5 mg/kg. Tumor volumes were calculated using the formula $V = (a*(b*b))/2$, with a being the largest and b being the smallest diameter, and they were expressed relative to the tumor volume determined at the first day of therapy. The toxicity of the four regimens was assessed by measuring the relative body weight (loss) of the animals.

2.8. Statistical analysis

All values are expressed as average ± standard deviation. In the experiments addressing the kinetics, the biodistribution and the tumor localization of the copolymers, the standard student's t-test was used. In the experiments evaluating the efficacy and the toxicity of the various treatment regimens, the Mann-Whitney U test was used. In both cases, $p<0.05$ was considered to represent statistical significance.

3. Results

3.1. Effect of i.t. injection on the kinetics of HPMA copolymers

First, the impact of i.t. injection on the circulation kinetics of two chemically unmodified HPMA copolymers (i.e. without spacer and drug) was investigated. Hereto, 31 kD and 65 kD poly(HPMA) were radiolabeled, and they were administered to the rats either as an i.v. bolus injection, or directly into the center of the tumors. Figure 1A shows that up to 24 h post injection (p.i.), the blood concentrations of i.t. applied 31 kD poly(HPMA) were significantly lower than those of i.v. applied 31 kD poly(HPMA). At 1 h and 24 h p.i., for instance, 30.1±5.2 % and 4.9±0.7 % of the injected dose (ID) were found in blood for i.t. administration, as compared to 67.4±3.3 %ID ($p<0.0001$) and 11.2±0.7 %ID ($p<0.0001$) for i.v. administration.

Figure 1B shows that also for 65 kD poly(HPMA), the levels in systemic circulation were significantly lower upon i.t. injection. At 1 h and 24 h p.i., 17.2±11.6 %ID and 20.5±3.7 %ID were found for i.t. administration, versus 78.8±3.4 %ID ($p<0.0001$) and 24.0±0.8 %ID ($p<0.05$) for i.v. administration, respectively. As compared to 31 kD poly(HPMA), a different pharmacokinetic pattern was observed for 65 kD poly(HPMA). For the smaller copolymer, the concentrations in blood were found to be relatively high immediately upon i.t. injection (~50 %ID at 5 min p.i.), and they then gradually decreased over time. For the larger copolymer, on the other hand, the initial levels were relatively low (~10 %ID at 5 min p.i.), and they tended to remain constant over time. This indicates that larger HPMA copolymers are retained in tumors more effectively than smaller copolymers.

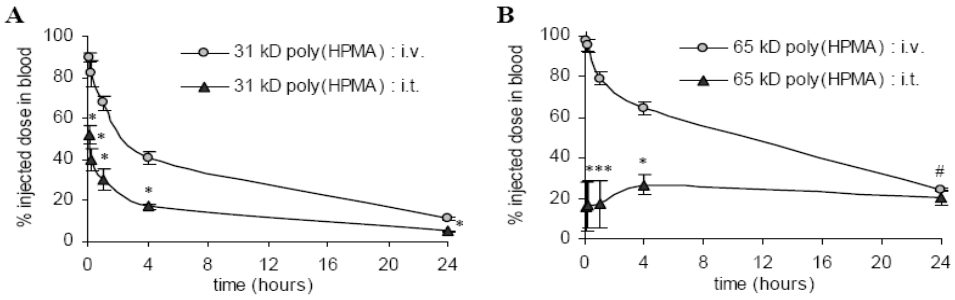

*Figure 1. Effect of intratumoral injection on the circulation kinetics of HPMA copolymers. The blood concentrations of 31 kD (A) and 65 kD poly(HPMA) (B) after intravenous (i.v.) and intratumoral (i.t.) injection are plotted against time. Values represent average ± standard deviation of 4-6 animals per experimental group. * Indicates $p<0.0001$ vs. i.v. injection, # indicates $p<0.05$ vs. i.v. injection.*

3.2. Effect of i.t. injection on the biodistribution of HPMA copolymers

Next, the tumor localization and the organ distribution of i.v. and i.t. applied HPMA copolymers were compared. As shown in the scintigrams in Figure 2A, at 4 and 24 h post i.v. injection, alongside a substantial accumulation in AT1-sc tumors, significant amounts of the copolymers were also found in heart (i.e. in circulation), in spleen and in liver. Upon i.t. application, on the other hand, only localization to tumor could be observed over the first 24 h after administration.

In addition, the scintigrams in Figure 2A also pointed towards an accumulation of radioactivity in the thyroid. This is due to the release of iodine-131 from the copolymers. Under physiological conditions, a small amount of the radiolabel is liberated from the tyrosinamide groups (~2% per 24 h). Most of this released iodine-131 is eliminated rapidly by means of renal filtration, a significant portion, however, is also always taken up by thyroid cells, as these cells specifically express the sodium-iodide symporter (NIS).

At 24 h p.i., tumors and organs were then harvested, and the concentrations of the copolymers were quantified. Figures 2B and 2C show that upon i.v. injection, the highest amounts of copolymer were always detected in spleen, followed by lung and by tumor. For 31 kD poly(HPMA), the levels localizing to tumor were 0.38±0.03 %ID/g for i.v. injection, and 1.42±0.52 %ID/g for i.t. injection ($p=0.0023$). In spleen, lung and liver, the concentrations of i.v. applied 31 kD poly(HPMA) were 0.52±0.04, 0.39±0.06 and 0.19±0.03 %ID/g, respectively, as compared to 0.38±0.06, 0.26±0.04 and 0.15±0.04 %ID/g for i.t. applied 31 kD poly(HPMA). These findings indicate that in addition to increasing the tumor concentrations of this copolymer, i.t. injection also decreases its localization to healthy tissues. Overall, however, the differences were less obvious than predicted by the scintigrams, and they were only found to be significant for spleen ($p=0.0043$), for lung ($p=0.0039$) and for heart ($p=0.0026$).

For 65 kD poly(HPMA), an identical biodistributional pattern was observed. As shown in Figure 2C, 24 h after i.v. injection, the highest concentrations of the copolymer were found in spleen (1.67±0.06 %ID/g), in lung (1.06±0.15 %ID/g), in tumor (0.87±0.06 %ID/g) and in liver (0.80±0.05 %ID/g). Upon i.t. injection, its levels in these tissues were 1.12±0.37 ($p=0.0059$), 0.86±0.35 ($p=0.2314$), 11.9±9.5 ($p=0.0195$) and 0.66±0.19 %ID/g ($p=0.0971$), respectively. Thus, as for 31 kD poly(HPMA), i.t. injection not only increased the tumor accumulation of 65 kD poly(HPMA), but it also attenuated its localization to certain healthy tissues.

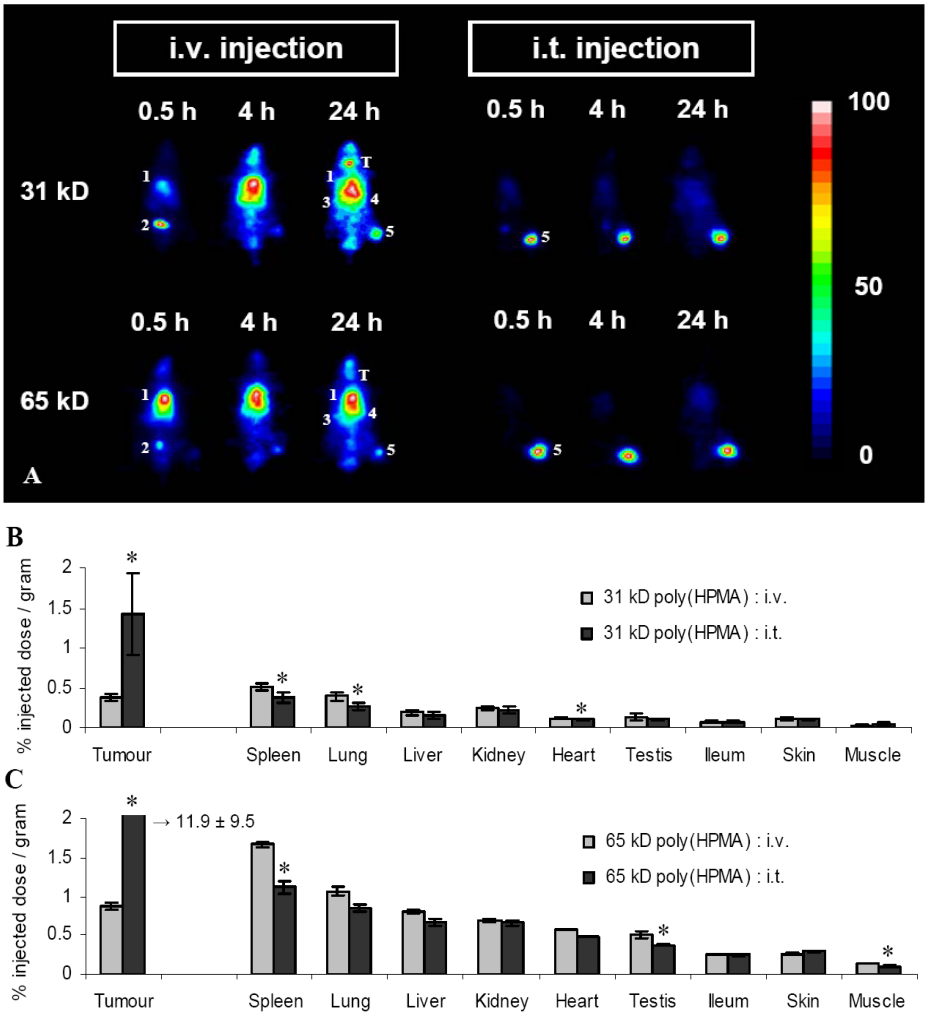

*Figure 2. Effect of intratumoral injection on the biodistribution of HPMA copolymers. A: Scintigraphic analysis of the effect of i.t. injection on the biodistribution of 31 kD and 65 kD poly(HPMA) in rats bearing subcutaneous Dunning AT1 tumors. In the images obtained at 0.5 h after i.v. administration, the accumulation of the radiolabeled copolymers was most prominent in heart (i.e. in circulation; 1) and in bladder (2). In the images obtained at 4 and 24 h, the highest amounts of copolymer were found in heart/lung (1), in spleen (3), in liver (4) and in tumor (5). In addition, at the two latter time points, an accumulation of released radioactive iodine in thyroid (T) was noted. Upon i.t. injection, only localization to tumor (5) could be observed over the first 24 h after administration. B and C: Quantification of the effect of i.t. injection on the tumor and organ concentrations of 31 kD poly(HPMA) (B) and 65 kD poly(HPMA) (C) at 24 h p.i. Values represent average ± standard deviation of 4-6 animals per experimental group. * Indicates p<0.05 vs. i.v. injection (Student's t-test). See page 229.*

In order to more directly assess the effects of i.t. injection on the biodistribution of the copolymers, tumor-to-organ ratios were calculated. Hereto, the tumor concentrations of 31 kD and 65 kD poly(HPMA) at 24 h p.i. were divided by their respective organ concentrations at 24 h p.i. As shown in Table 1, the tumor-to-organ ratios of i.t. applied 31 kD poly(HPMA) were on average a 4-fold higher than those of i.v. applied 31 kD poly(HPMA). For 65 kD poly(HPMA), i.t. injection improved the tumor-to-organ ratios by a factor 15-20. These findings indicate that the (positive) impact of i.t. injection correlates to the molecular weight of the copolymers.

	31 kD pHPMA		**65 kD pHPMA**		**28 kD pHPMA-GFLG-Dox**	
	i.v.	**i.t.**	**i.v.**	**i.t.**	**i.v.**	**i.t.**
Tumour	1	1	1	1	1	1
Spleen	0.7	3.8	0.5	10.6	0.2	1.9
Lung	1.0	5.5	0.8	13.8	1.2	8.5
Liver	2.0	9.4	1.1	18.0	1.3	8.1
Kidney	1.6	6.3	1.3	18.1	0.1	0.5
Heart	3.2	14.1	1.5	24.6	3.2	15.6
Testis	2.8	13.7	1.7	32.0	2.8	14.8
Skin	5.0	19.7	3.5	49.0	1.6	9.4
Ileum	3.5	13.6	3.3	40.3	2.5	19.3
Muscle	12.0	36.6	6.2	120.7	7.6	45.7

Table 1. Evaluation of the tumor-to-organ ratios of i.v. and i.t. applied HPMA copolymers. Tumor-to-organ ratios were calculated at 24 hours post i.v. and i.t. injection. Hereto, the tumor concentrations of 31 kD poly(HPMA), 65 kD poly(HPMA) and 28 kD poly(HPMA)-GFLG-doxorubicin at 24 hours p.i. were divided by the respective organ concentrations at 24 hours p.i. A tumor-to-organ ratio >1 (thus) indicates a preferred localization to tumor tissue, a ratio <1 indicates a more selective localization to the corresponding healthy tissue. The tumor-to-organ ratios allow for a more direct evaluation of the impact of i.t. injection on the biodistribution of the copolymers.

3.3. Effect of i.t. injection on the biodistribution of poly(HPMA)-GFLG-doxorubicin

To evaluate if the effects observed for the two chemically unmodified copolymers also hold for a clinically relevant HPMA copolymer carrying a chemotherapeutic drug, we next analyzed the impact of i.t. injection on the biodistribution of poly(HPMA)-GFLG-doxorubicin. As shown in the scintigrams in Figure 3A, the biodistribution of i.v. applied poly(HPMA)-GFLG-doxorubicin appeared to be very different from that observed for the two parental copolymers (Figure 2A). In a previous study, however, we have shown that as a result of the incorporation of drug and/or spacer moieties, the kidney concentrations of the copolymers are always induced significantly (~ 5-10 fold), while their relative levels in the majority of other tissues are affected only moderately [16]. The scintigrams in Figure 3A furthermore exemplify that as for the two parental HPMA copolymers, i.t. injection substantially improved the tumor localization of poly(HPMA)-GFLG-doxorubicin. Quantification at 24 h p.i. confirmed this notion, showing that for i.t. administration, 2.00±0.28 %ID was found per gram tumor tissue, as compared to 0.36±0.02 %ID/g ($p=0.0006$) for i.v. administration (Figure 3B). Figure 3B also shows that i.t. injection reduced the amount of poly(HPMA)-GFLG-doxorubicin accumulating in spleen ($p=0.0018$), in kidney ($p=0.0261$) and in skin ($p=0.0091$). As a result, the tumor-to-organ ratios of i.t. applied poly(HPMA)-GFLG-doxorubicin were found to be substantially higher than those of i.v. applied poly(HPMA)-GFLG-doxorubicin, on average, they were improved by more than 500% (Table 1).

3.4. In vitro efficacy of free and HPMA copolymer-bound doxorubicin

Subsequently, the cytotoxicity of poly(HPMA)-GFLG-doxorubicin was compared to that of free doxorubicin. As shown in Figure 4, and as could be expected, free doxorubicin was found to be significantly more effective in inhibiting the clonogenic survival of AT1 cells than was poly(HPMA)-GFLG-doxorubicin. In line with the literature [19, 20], the IC_{50} value of the free drug (~ 0.3 µMol) was approximately a 100-fold lower than that of the copolymer-bound drug (~ 30 µMol). For a drug-free control copolymer, no cytotoxic effects were observed.

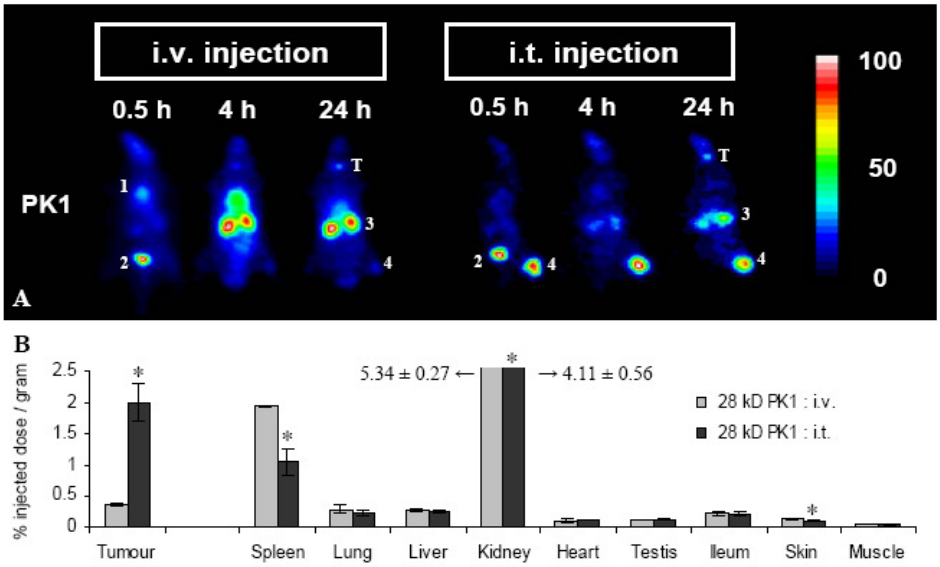

*Figure 3. Effect of intratumoral injection on the biodistribution of poly(HPMA)-GFLG-doxorubicin (PK1). A: Scintigraphic analysis of the effect of i.t. injection on the biodistribution of PK1 in rats bearing subcutaneous Dunning AT1 tumors. In the images obtained at 0.5 h post i.v. injection, the accumulation of the radiolabeled conjugate was most prominent in heart (i.e. in circulation; 1) and in bladder (2), at 4 and 24 h, most of the conjugate was found in kidney (3) and in tumor (4). Released radioactive iodine was again found to accumulate in thyroid (T). Upon i.t. injection, the highest amounts of PK1 were found in kidney (3) and in tumor (4). B: Quantification of the effect of i.t. injection on the tumor and organ concentrations of PK1 at 24 h p.i. Values represent average ± s.d. of 3-4 animals. * Indicates p<0.05 vs. i.v. injection (Student's t-test). See page 229.*

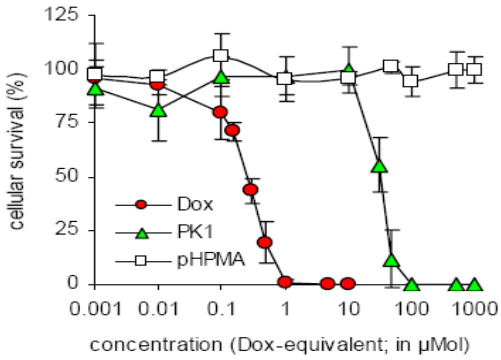

Figure 4. In vitro efficacy of free and HPMA copolymer-bound doxorubicin.The cytotoxicity of free doxorubicin, of poly(HPMA)-GFLG-doxorubicin and of a drug-free control copolymer was evaluated by assessing the ability of the agents to inhibit the colony formation of AT1 rat prostate carcinoma cells. Values represent average ± standard deviation of three independent experiments.

3.5. Effect of i.t. injection on the efficacy and the toxicity of free and HPMA copolymer-bound doxorubicin

Finally, the therapeutic efficacy of i.v. and i.t. applied poly(HPMA)-GFLG-doxorubicin (PK1) was compared to that of i.v. and i.t. applied free doxorubicin. As shown in Figure 5A, neither a single i.v. injection of free doxorubicin, nor a single i.v. injection of PK1 was able to inhibit the growth of aggressively growing and relatively chemoresistant Dunning AT1 tumors. When free doxorubicin was applied directly into the tumors, it was only found to be significantly more effective than control (p=0.02). I.t. applied PK1, on the other hand, was not only found to be significantly more effective than control (p=0.004), but also than i.v. applied free doxorubicin (p=0.005), than i.t. applied free doxorubicin (p=0.03) and than i.v. applied PK1 (p=0.008).

In addition to evaluating the effect of i.t. injection on the antitumor efficacy of free and HPMA copolymer-bound doxorubicin, we also investigated its impact on the toxicity of the two chemotherapeutic agents. Hereto, the body weight loss of the animals was monitored throughout the course of the experiment. As shown in Figure 5B, i.v. and i.t. applied PK1 turned out to be better tolerated than i.v. and i.t. applied free doxorubicin; whereas the toxicity resulting from the two regimens involving PK1 was comparable to that of control, both regimens involving free doxorubicin were found to be significantly more toxic than control (p=0.01).

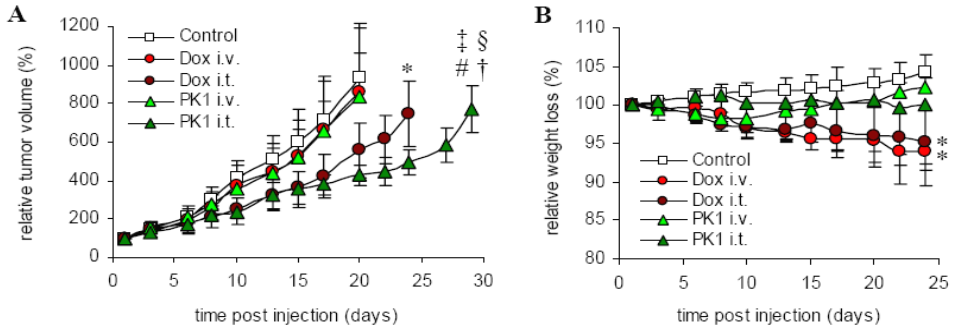

*Figure 5. Effect of intratumoral injection on the efficacy and the toxicity of free and HPMA copolymer-bound doxorubicin. A: Growth inhibition of subcutaneous AT1 tumors induced by a single i.v. injection of saline (Control; n=12), by a single i.v. injection of 5 mg/kg of free doxorubicin (Dox i.v.; n=9), by a single i.t. injection of 5 mg/kg of doxorubicin (Dox i.t.; n=4), by a single i.v. injection of 5 mg/kg doxorubicin-equivalent of poly(HPMA)-GFLG-doxorubicin (PK1 i.v.; n=7) and by a single i.t. injection of 5 mg/kg doxorubicin-equivalent of poly(HPMA)-GFLG-doxorubicin (PK1 i.t.; n=4). * Indicates p<0.05 vs. control, # indicates p<0.005 vs. control, † indicates p<0.01 vs. Dox i.v., ‡ indicates p<0.01 vs. PK1 i.t. and § indicates p<0.05 vs. DOX i.t. (Mann-Whitney U test). B: Weight loss induced by the four chemotherapy regimens mentioned above. * Indicates p<0.05 vs. control and vs. PK1 i.v. (Mann-Whitney U test).*

In order to be able to more directly compare the overall therapeutic potential of i.v. and i.t. applied PK1 to that of i.v. and i.t. applied free doxorubicin, therapeutic indices were attributed to the four chemotherapy regimens. Hereto, the relative increases in efficacy, i.e. in tumor growth inhibition (as compared to control), were divided by the relative increases in toxicity, i.e. in body weight loss (as compared to control). At day 10 p.i., for instance, the relative tumor volumes for control and for i.t. applied PK1 were 417 % and 238 %, respectively (Figure 5A). The relative body weights for these two regimens at this time point were 102 % and 100 %, respectively (Figure 5B). Thus, the resulting therapeutic index for i.t. applied PK1 at day 10 is 1.72, i.e. (417/238) / (102/100). As shown in Table 2, when simultaneously addressing the efficacy and the toxicity of a single dose of chemotherapy, i.t. applied PK1 turned out to be the most optimal regimen for treating Copenhagen rats bearing chemoresistant Dunning AT1 tumors: throughout follow-up, its therapeutic indices were always well above 1 (i.e. better than saline controls), and they were also always substantially higher than the therapeutic indices determined for the other three chemotherapy regimens.

Time (days)	1	3	6	8	10	13	15	17	20
Control	1	1	1	1	1	1	1	1	1
Dox i.v.	1	1.12	1.09	1.14	1.06	1.07	1.07	1.00	1.00
Dox i.t.	1	1.00	1.19	1.30	1.56	1.50	1.58	1.59	1.56
PK1 i.v.	1	0.95	0.97	1.06	1.13	1.14	1.12	1.06	1.08

Table 2. Evaluation of the therapeutic index of i.v. and i.t. applied free and HPMA copolymer-bound doxorubicin. Therapeutic indices were determined for each of the four chemotherapy regimens throughout the course of the experiment. For quantifying the therapeutic indices, the relative increases in efficacy, i.e. in tumor growth inhibition (as compared to saline-treated controls), were divided by the relative increases in toxicity, i.e. in body weight loss (as compared to controls; see text for details). The assessment of the therapeutic indices is intended to allow for a more direct and cross-sectional comparison of the overall therapeutic potential of the four chemotherapy regimens.

4. Discussion

Besides being the standard route of administration for most ((pre)clinical) gene therapy applications [21,22], i.t. injection has also been evaluated relatively extensively for improving the therapeutic index of standard anticancer agents [1-5,23-25]. The obvious rationale behind this approach is that the local administration of chemotherapeutic drugs increases the concentrations of the agents at the target site, while lowering their localization to healthy tissues. As a result, i.t. injection is generally considered to be able to improve the antitumor efficacy of the agents, while lowering the incidence and the intensity of their side effects.

In principle, the rationale behind the implementation of drug delivery systems is identical to that of i.t. injection: to improve the therapeutic index of chemotherapeutic agents by increasing their tumor concentrations and by decreasing their accumulation in healthy tissues [6-10]. It therefore seems mere logic that the combination of these two approaches, i.e. the i.t. injection of drug delivery systems, holds significant potential for further enhancing the efficacy of anticancer therapy. Thus far, however, this combination has been largely neglected and only very few reports have evaluated the impact of i.t. injection on the biodistribution and the therapeutic index of carrier-based chemotherapeutics. Those reports that did investigate the efficacy of the combination have convincingly confirmed its potential: carmustine-containing polymeric wafers designed specifically for (intraoperative) intracerebral administration, for instance, have been shown to be able to improve both the efficacy and the tolerability of chemotherapy, and they have consequently been FDA approved for the treatment of glioblastoma [26-28].

Surely, drug delivery systems designed specifically for local administration can be expected to be more suitable for i.t. administration than are delivery systems designed for parenteral administration (e.g. HPMA copolymers). Based on the notion, however, that HPMA copolymers are clinically relevant drug carriers, and that they are known to posses a proper biocompatability and an enhanced tumor retention [8,11-16], we decided to use HPMA copolymers to demonstrate that even by implementing drug delivery systems designed specifically for parenteral administration, the therapeutic index of locoregionally applied chemotherapy can be improved substantially. On the one hand, this was done to urge oncologists

considering intra- or postoperative chemotherapy to use carrier-based chemotherapeutics instead of standard chemotherapeutics. One the other hand, this study should serve as a starting point for intensifying the evaluation and the implementation of drug delivery systems designed specifically for locoregional application.

In the present report, several lines of evidence are provided indicating that the direct intratumoral injection of carrier-based chemotherapeutics is a promising approach for improving the efficacy of anticancer therapy. First, the blood concentrations of i.t applied drug delivery systems were found to be significantly lower than those of i.v. applied delivery systems. This indicates that the systemic toxicity of i.t. applied (carrier-based) chemotherapy can be expected to be lower than that of i.v. applied (carrier-based) chemotherapy. Second, in line with the experimental evidence provided by Harrington and colleagues, who showed that the i.t. administration of colloidal drug carriers substantially increases their tumor concentrations [29], we found that i.t. injection also substantially improves the biodistribution of polymeric drug delivery systems (Figures 2 and 3). As compared to i.v. injection, the tumor-to-organ ratios resulting from i.t. injection were increased by up to 2000 % (Table 1). And third, most likely as a direct result of this improved tumor localization, the antitumor efficacy of i.t. applied poly(HPMA)-GFLG-doxorubicin was found to be significantly higher than that of i.v. applied poly(HPMA)-GFLG-doxorubicin, and also than that of i.v. and i.t. applied free doxorubicin (Figure 5A). At the same time, the toxicity of this regimen turned out to be attenuated (Figure 5B), resulting in a substantial improvement in the overall therapeutic index of the intervention (Table 2). These findings indicate that when advanced solid malignancies are easily accessible (e.g. intraoperatively), the intratumoral injection of HPMA copolymer-based chemotherapeutics, and likely of all carrier-based chemotherapeutics, should be considered as an interesting alternative to the routinely used chemotherapy regimens and routes of administration.

References

1. Brincker H. Direct intratumoral chemotherapy. *Crit Rev Oncol Hematol* 1993, **15**, 91-98.
2. Walter KA, Tamargo RJ, Olivi A, Burger PC, and Brem H. Intratumoral chemotherapy. *Neurosurgery* 1995, **37**, 1128-1145.
3. Voulgaris S, Partheni M, Karamouzis M, Dimopoulos P, Papadakis N, and Kalofonos HP. Intratumoral doxorubicin in patients with malignant brain gliomas. *Am J Clin Oncol* 2002, **1**, 60-64.
4. Goldberg EP, Hadba AR, Almond BA, and Marotta JS. Intratumoral cancer chemotherapy and immunotherapy: opportunities for nonsystemic preoperative drug delivery. *J Pharm Pharmacol* 2002, **54**, 159-180.
5. Duvillard C, Romanet P, Cosmidis A, Beaudouin N, and Chauffert B. Phase 2 study of intratumoral cisplatin and epinephrine treatment for locally recurrent head and neck tumors. *Ann Otol Rhinol Laryngol* 2004, **113**, 229-233.
6. Allen TM. Ligand-targeted therapeutics in anticancer therapy. *Nat Rev Cancer* 2002, **2**, 750-763.
7. Moses MA, Brem H, and Langer R. Advancing the field of drug delivery: taking aim at cancer. *Cancer Cell* 2003, **4**, 337-341.
8. Duncan R. The dawning era of polymer therapeutics. *Nat Rev Drug Discov* 2003, **2**, 347-360.
9. Zamboni WC. Liposomal, nanoparticle, and conjugated formulations of anticancer agents. *Clin Cancer Res* 2005, **11**, 8230-8234.
10. Braun K, Pipkorn R, and Waldeck W. Development and characterization of drug delivery systems for targeting mammalian cells and tissues: a review. *Curr Med Chem* 2005, **12**, 1841-1858.
11. Kopecek J, Kopeckova P, Minko T, and Lu Z. HPMA copolymer-anticancer drug conjugates: design, activity, and mechanism of action. *Eur J Pharm Biopharm* 2000, **50**, 61-81.
12. Meerum Terwogt JM, ten Bokkel Huinink WW, Schellens JH, Schot M, Mandjes IA, Zurlo MG, Rocchetti M, Rosing H, Koopman FJ, and Beijnen JH. Phase I clinical and pharmacokinetic study of PNU166945, a novel water-soluble polymer-conjugated prodrug of paclitaxel. *Anticancer Drugs* 2001, **12**, 315-323.
13. Bilim V. Technology evaluation: PK1, Pfizer/Cancer Research UK. *Curr Opin Mol Ther* 2003, **5**, 326-330.
14. Rihova B, and Kubackova K. Clinical implications of N-(2-hydroxypropyl) methacrylamide copolymers. *Curr Pharm Biotechnol* 2003, **4**, 311-322.
15. Rademaker-Lakhai JM, Terret C, Howell SB, Baud CM, De Boer RF, Pluim D, Beijnen JH, Schellens JH, and Droz JP. A Phase I and pharmacological study of the platinum polymer AP5280 given as an intravenous infusion once every 3 weeks in patients with solid tumors. *Clin Cancer Res* 2004, **10**, 3386-3395.
16. Lammers T, Kuhnlein R, Kissel M, Subr V, Etrych T, Pola R, Pechar M, Ulbrich K, Storm G, Huber P, and Peschke P. Effect of physicochemical modification on the biodistribution and tumor accumulation of HPMA copolymers. *J Control Release* 2005, **110**, 103-118.
17. Salacinski PR, McLean C, Sykes JE, Clement-Jones VV, and Lowry PJ. Iodination of proteins, glycoproteins, and peptides using a solid-phase oxidizing agent, 1,3,4,6-tetrachloro-3 alpha,6 alpha-diphenyl glycoluril (Iodogen). A*nal Biochem* 1981, **117**, 136-146
18. Lubaroff DM, Canfield L, Feldbush TL, and Bonney WW. R3327 adenocarcinoma of the Copenhagen rat as a model for the study of the immunologic aspects of prostate cancer. *J Natl Cancer Inst* 1977, **58**, 1677-1689.
19. Demoy M, Minko T, Kopeckova P, and Kopecek J. Time- and concentration-dependent apoptosis and necrosis induced by free and HPMA copolymer-bound doxorubicin in human ovarian carcinoma cells. *J Control Release* 2000, **69**, 185-196.
20. Kovar M, Kovar L, Subr V, Etrych T, Ulbrich K, Mrkvan T, Loucka J, and Rihova B. HPMA copolymers containing doxorubicin bound by a proteolytically or hydrolytically cleavable bond: comparison of biological properties in vitro. *J Control Release* 2004, **99**, 301-314.
21. Akporiaye ET, and Hersh E. Clinical aspects of intratumoral gene therapy. *Curr Opin Mol Ther* 1999, **4**, 443-453.
22. Neyns B, and Noppen M. Intratumoral gene therapy for non-small cell lung cancer: current status and future directions. *Monaldi Arch Chest Dis* 2003, **59**, 287-295.
23. Aigner KR, Gailhofer S, and Kopp S. Regional versus systemic chemotherapy for advanced pancreatic cancer: a randomized study. *Hepatogastroenterology* 1998, **45**, 1125-1129.

24. Wientjes MG, Zheng JH, Hu L, Gan Y, and Au JL. Intraprostatic chemotherapy: distribution and transport mechanisms. *Clin Cancer Res* 2005, **11**, 4204-4211.
25. Lesniak MS, Upadhyay U, Goodwin R, Tyler B, and Brem H. Local delivery of doxorubicin for the treatment of malignant brain tumors in rats. *Anticancer Res* 2005, **25**, 3825-3831.
26. Valtonen S, Timonen U, Toivanen P, Kalimo H, Kivipelto L, Heiskanen O, Unsgaard G, and Kuurne T. Interstitial chemotherapy with carmustine-loaded polymers for high-grade gliomas: a randomized double-blind study. *Neurosurgery* 1997, **41**, 44-49.
27. Westphal M, Hilt DC, Bortey E, Delavault P, Olivares R, Warnke PC, Whittle IR, Jaaskelainen J, and Ram Z. A phase III trial of local chemotherapy with biodegradable carmustine wafers (Gliadel wafers) in patients with primary malignant glioma. *Neuro-oncol* 2003, **5**, 79-88.
28. Guerin C, Olivi A, Weingart JD, Lawson HC, and Brem H. Recent advances in brain tumor therapy: local intracerebral drug delivery by polymers. *Invest New Drugs* 2004, **22**, 27-37.
29. Harrington KJ, Rowlinson-Busza G, Syrigos KN, Uster PS, Vile RG, and Stewart JS. Pegylated liposomes have potential as vehicles for intratumoral and subcutaneous drug delivery. *Clin Cancer Res* 2000, **6**, 2528-2537.

Chapter 6

Effect of radiotherapy and hyperthermia on the tumor accumulation of HPMA copolymer-based drug delivery systems

Twan Lammers[a,b], Peter Peschke[a], Rainer Kühnlein[a], Vladimir Subr[c], Karel Ulbrich[c], Jürgen Debus[d], Peter E. Huber[a], Wim E. Hennink[b], Gert Storm[b]

[a] Department of Innovative Cancer Diagnosis and Therapy, Clinical Cooperation Unit Radiotherapeutic Oncology, German Cancer Research Center, Im Neuenheimer Feld 280, 69120 Heidelberg, Germany

[b] Department of Pharmaceutics, Utrecht Institute for Pharmaceutical Sciences, Utrecht University, Sorbonnelaan 16, 3584 CA Utrecht, The Netherlands

[c] Institute of Macromolecular Chemistry, Academy of Sciences of the Czech Republic, Heyrovsky Square 2, 162 06 Prague 6, Czech Republic

[d] Department of Radiation Oncology and Radiotherapy, Heidelberg University Medical School, Im Neuenheimer Feld 110, 69120 Heidelberg, Germany

J. Control. Release 117: 333-341 (2007)

Abstract

Copolymers of *N*-(2-hydroxypropyl)methacrylamide (HPMA) are prototypic and well-characterized polymeric drug carriers that have been broadly implemented in the delivery of anticancer therapeutics. In an attempt to improve the tumor accumulation of HPMA copolymer-based drug delivery systems, their in vivo application was combined with radiotherapy and with hyperthermia. As the effects of radiotherapy and hyperthermia were considered to depend significantly on the tumor model used, we first analyzed the accumulation of two differently sized HPMA copolymers in three different types of tumors, based on the syngeneic Dunning rat prostate carcinoma model. Subsequently, in these three models, the effects of different doses of radiotherapy and hyperthermia on the tumor accumulation of 31 kD poly(HPMA), 65 kD poly(HPMA) and 28 kD poly(HPMA)-GFLG-doxorubicin were evaluated. It was found that the polymeric drug delivery systems accumulated effectively in all three tumor models. In addition, as opposed to hyperthermia, radiotherapy was found to improve the concentrations of the copolymers independent of the tumor model used. Based on these findings, we conclude that radiotherapy is an effective means for increasing the tumour accumulation of (polymeric) drug delivery systems, and we propose that the combination of carrier-based chemotherapy with radiotherapy might hold significant potential for improving the treatment of advanced solid malignancies.

1. Introduction

Copolymers of *N*-(2-hydroxypropyl)methacrylamide (HPMA) are prototypic and well-characterized polymeric drug carriers that have been broadly implemented in the delivery of anticancer therapeutics [1-3]. Upon i.v. injection, HPMA copolymers circulate for prolonged periods of time, an by means of the enhanced permeability and retention (EPR) effect [4,5], they localize to tumors both effectively and selectively [6-8]. Based on this notion, several different HPMA copolymer-based anticancer agents have been designed and evaluated, carrying not only classical chemotherapeutics, like doxorubicin [9,10] and platinum [11,12], but also more recently discovered drugs, like the heat shock protein inhibitor geldanamycin [13,14] and the angiogenesis inhibitor TNP-470 [15,16].

Over the years, various attempts have been made to improve the tumor accumulation of HPMA copolymer-based drug delivery systems: the molecular weight of the copolymers was increased [8,17,18], star-like copolymers were prepared [19,20], and targeting moieties, like antibodies [21-23], peptides [24-26], sugars [27-29] and sugar-binding proteins [30-31] were included, in order to improve not only the efficacy, but also the specificity of the delivery systems. Thus far, however, even though several of these variants have presented with a clearly improved tumour targeting potential, only one of them has managed to progress into clinical trials [32].

In the present report, we have therefore set out to evaluate an alternative strategy for improving the tumor localization of HPMA copolymer-based drug delivery systems, i.e. by combining them with radiotherapy and hyperthermia. Taking into account, however, that the effects of radiotherapy and hyperthermia are likely significantly depend on the tumor model used, we first analyzed the tumor accumulation of two differentially sized HPMA copolymers in three different types of tumors, based on the syngeneic Dunning rat prostate carcinoma model [33]. Subsequently, in these three models, the effects of different doses of radiotherapy and hyperthermia on the tumor localization of the copolymers were investigated. And finally, the impact of radiotherapy and hyperthermia on the tumor accumulation of poly(HPMA)-GFLG-doxorubicin was assessed, in order to evaluate if the effects observed for chemically unmodified HPMA copolymers also hold for a clinically relevant HPMA copolymer carrying a chemotherapeutic drug.

2. Materials and methods

2.1. Synthesis and characterization of the copolymers

The HPMA copolymers used in this study were synthesized as described previously [8]. Briefly, poly(HPMA-co-MA-TyrNH_2) was prepared by solution radical copolymerization of the monomers HPMA and MA-TyrNH_2. The average molecular weights of the two parental HPMA copolymers (as determined by size exclusion chromatography) were 30.5 kD and 64.5 kD, their polydispersities were 1.3 and 1.2, and the relative amounts of tyrosinamide (TyrNH_2), included to allow for radiolabeling, were 0.8 mol-% and 1.1 mol-%. The precursor for poly(HPMA)-GFLG-doxorubicin, i.e. poly(HPMA-co-MA-TyrNH_2-co-MA-GFLG-ONp), was prepared by precipitation radical copolymerization of HPMA, MA-TyrNH_2 and MA-GFLG-ONp. After purification, doxorubicin was conjugated to this precursor in DMSO, in the presence of Et_3N. The resulting doxorubicin-containing conjugate was then filtered off, dried in vacuum, purified on a Sephadex LH-20 column (to remove free doxorubicin), and fractionated on an LH-60 column (to obtain a narrow distribution of the molecular weight). The average molecular weight of poly(HPMA)-GFLG-doxorubicin was 27.9 kD, its polydispersity was 1.5, the amount of tyrosinamide was 1.3 mol-%, and the amount of doxorubicin was 6.5 wt-%.

2.2. Radiolabeling

Iodine-131 was obtained from Amersham. The tyrosinamide groups incorporated into the copolymers were radiolabeled using the mild oxidizing agent 1,3,4,6-tetrachloro-3 alpha,6 alpha-diphenyl glycoluril (i.e. by means of the Iodogen-method) [34]. Upon 10 min of incubation, the mixture of iodine-131, Iodogen and the copolymer was applied to a Biogel-P6 column and it was eluted with 30 ml of PBS. The eluate was recovered in 1 ml fractions and the radioactivity of each of these fractions was determined by means of a scintillation counter. The radiolabeled copolymer was retrieved in the 5^{th} to 7^{th} ml of the eluate, while free (i.e. unbound) iodine-131 was eluted in the 14^{th} to 18^{th} ml. As this methodology allowed us to concentrate the copolymer-associated fraction, no additional purification was required. The efficacy of radiolabeling was quantified by dividing the amount of radioactivity collected in the 5^{th} to 7^{th} ml of the eluate by the total amount of radioactivity retrieved, i.e. by the sum of the activities detected in all thirty 1 ml fractions. Labeling efficacies were ~ 95% for 31 kD poly(HPMA) and 65 kD poly(HPMA), and ~ 85% for 28 kD poly(HPMA)-GFLG-doxorubicin.

2.3. Tumor models

All experiments involving animals were approved by an external committee for animal welfare and were performed according to the guidelines for laboratory animals established by the German government. During all experimental procedures, the animals were anaesthetized using Ethrane. Three different types of tumors were used, based on the syngeneic Dunning R-3327 prostate carcinoma model [33]. Hormone-independent and aggressively growing Dunning AT1 tumors were induced both subcutaneously (AT1-sc) and intramuscularly (AT1-im), and hormone-dependent and slowly growing Dunning H tumors were induced subcutaneously (H-sc). Tumours were grown until they reached an average diameter of 12 mm (range: 9-15 mm), and the animals were subdivided in such a way that the tumor sizes did not vary too much between the various experimental groups

2.4. Immunohistochemistry

For histological and immunofluorescence analyses, 6 µm sections of AT1-sc, AT1-im and H-sc tumors were prepared. Haematoxylin and eosin staining was performed according to standard procedures. Vascular endothelial cells were stained in methanol/acetone-fixed cryosections using a 1:50 dilution of a mouse monoclonal antibody directed against rat CD31 (MAB1393; Chemicon Int., Chandlers Ford, UK). To assess the degree of differentiation of the tumor blood vessels, the cryosections were simultaneously stained with a 1:100 dilution of a rabbit polyclonal antibody directed against alpha smooth muscle actin (AB5694; Biozol, Eching, Germany). The sections were counterstained using DAPI and imaged under a Nikon Eclipse E600 fluorescence microscope.

2.5. Biodistribution and tumor accumulation

For analyzing the biodistrution of the copolymers, 500 µl of a 0.1 mM solution (based on copolymer concentration; corresponding to a radioactivity of 150 to 300 µCi) were injected i.v. into the lateral tail vein of the rats. At several time points post injection (p.i.), the biodistribution and the tumor accumulation of the copolymers were monitored two-dimensionally using a Searle-Siemens scintillation camera. At 24 and 168 h p.i., the animals were sacrificed, and their tumors and organs were harvested for quantification. The residual amounts of radioactivity were determined using a scintillation counter, they were corrected for radioactive decay and they were expressed as percent of the injected dose per gram tissue.

2.6. Radiotherapy and hyperthermia

Radiotherapy was applied by exposing the tumor-bearing limbs of the animals to cobalt-60 γ-radiation. Radiation was delivered by means of the Siemens Gammatron S, at a dose rate of 0.45 Gy/min. Single doses of 2 Gy and 20 Gy were administered, 1 h and 24 h before the injection of the copolymers. Hyperthermia was performed by submerging the right hind limbs of the animals for 1 h in a water bath heated to temperatures of 41.0, 42.0 and 42.5 ºC. The radiolabeled copolymers were injected 5 min after the initiation of hyperthermia.

2.7. Statistical analysis

All values are expressed as average ± standard deviation. The two-tailed t-test was used to assess if the difference in tumor concentration between the treated group and the untreated control group was significant. $P<0.05$ was considered to represent statistical significance.

3. Results

3.1. Characterization of the three tumor models

To properly assess the effects of radiotherapy and hyperthermia on the tumor accumulation of the polymeric drug carriers, analysis in more than one tumor model was considered to be required. We therefore initially investigated the accumulation of two chemically unmodified (i.e. drug-free) HPMA copolymers in three different types of tumors. Dunning AT1 tumors transplanted subcutaneously (AT1-sc) were used as a reference model and as a positive control, as it has been previously shown that these tumors accumulate the copolymers relatively effectively over time [8]. Dunning AT1 tumors inoculated intramuscularly (AT1-im) were used to reduce the impact of subcutaneous tumor encapsulation. Because of the increase in tumor-muscle surface area (Figure 1), the clearance of the copolymers from AT1-im tumors was expected to be less unidirectional and, therefore, to be more substantial than for AT1-sc tumors. Dunning H tumors transplanted subcutaneously (H-sc) were used to investigate the impact of the morphology of tumor blood vessels on the accumulation of HPMA copolymers. H-sc tumors grow much slower than AT1-sc tumors. As a result, they present a slowly matured and well-differentiated vasculature, which

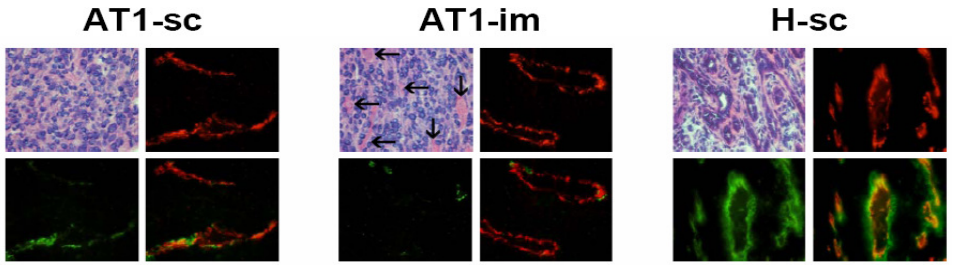

Figure 1. Characterization of the three tumor models used. Immunohistochemical analysis of subcutaneously transplanted Dunning AT1 tumors (AT1-sc), intramuscularly inoculated Dunning AT1 tumors (AT1-im) and subcutaneously transplanted Dunning H tumors (H-sc). Methanol / acetone-fixed cryosections were stained using H&E, CD31 (red) and alpha-smooth muscle actin (green), and imaged at magnifications of 400x (H&E) and 600x (CD31 and αSMA). The arrows indicate muscle fibers. *See page 230.*

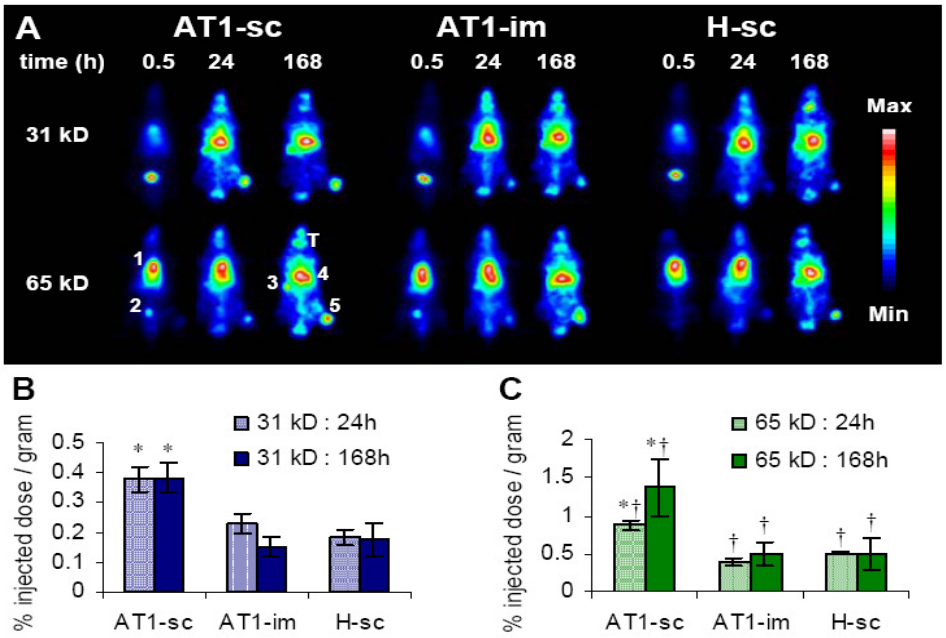

*Figure 2. Accumulation of HPMA copolymers in three different tumor models. A: Scintigraphic analysis of the biodistribution and the tumor accumulation of two differently sized radiolabeled HPMA copolymers in Copenhagen rats bearing AT1-sc, AT1-im and H-sc tumors. In the scintigrams obtained at 0.5 h p.i., localization to heart (i.e. in circulation; 1) and to bladder (2) was observed. In the images obtained at 24 h and 168 h p.i., the accumulation of the copolymers was most prominent in spleen (3), in liver (4) and in tumor (5). In addition, at the latter two time points, an accumulation of released radioactive iodine in thyroid (T) was noted. B and C: Quantification of the amounts of 31 kD poly(HPMA) (B) and 65 kD poly(HPMA) (C) per gram dissected tumor tissue at 24 h and 168 h p.i. Values represent average ± standard deviation of 3-6 animals per experimental group. * Indicates p<0.05 vs. AT1-im and H-sc tumors, † indicates p<0.05 vs. 31 kD poly(HPMA) (Student's t-test).* *See page 231.*

is exemplified by the high degree of colocalization of CD31 and alpha-smooth muscle actin (Figure 1). Based on this notion, the number and the size of the interendothelial gaps that allow for the extravasation of the copolymers were expected to be reduced significantly, and as for AT1-im tumors, it was hypothesized that their concentrations would be lower in H-sc tumors than in AT1-sc tumors.

3.2. Accumulation of HPMA copolymers in different tumor models

As shown in the scintigrams in Figure 2A, as expected, both 31 kD and 65 kD poly(HPMA) indeed accumulated most effectively in AT1-sc tumors. As compared to the other two tumor models, the levels of the radiolabeled copolymers in AT1-sc tumors were always approximately twice as high (Figures 2B and 2C). At 24 h post i.v. injection (p.i.), for instance, the levels of 31 kD poly(HPMA) in AT1-sc, AT-im and H-sc tumors were 0.38±0.04, 0.23±0.03 and 0.18±0.03 %ID/g, respectively (Figure 2B). For 65 kD poly(HPMA), 0.87±0.06, 0.39±0.05 and 0.50±0.02 %ID/g were found in these tumors at this time point, respectively (Figure 2C).

In line with several previous reports [8,17,18], the scintigrams in Figure 2A also demonstrate that the higher the molecular weight of an HPMA copolymer is, the more effectively it is retained in circulation; both at 30 min and at 24 h p.i., the signal coming from heart, representing the amount of radiolabeled copolymer still residing in systemic circulation, was found to be much more pronounced for 65 kD poly(HPMA). Paralleled by this increase in circulation time, the tumor concentrations of the larger copolymer were always found to be significantly higher than those of the smaller copolymer (Figures 2B and 2C).

The scintigrams in Figure 2A furthermore indicate that in all three tumor models, the concentrations of the two copolymers had increased over time. When quantified at 24 and 168 h p.i., however, their concentrations were only found to be increased for 65 kD poly(HPMA), and only when it was injected into animals bearing AT1-sc tumors (0.87±0.06 vs. 1.37±0.31 %ID/g; $p=0.0113$). In AT1-im tumors, a trend towards an increase was observed for 65 kD poly(HPMA), but the difference could not be confirmed statistically ($p=0.40$). For 31 kD poly(HPMA), on the other hand, even though the scintigrams had indicated otherwise, not even a trend towards an increase could be observed: in AT1-sc and H-sc tumors, its levels were comparable at both time points, and in AT1-im

tumors, its levels had even decreased over time (0.23±0.03 vs. 0.15±0.03 %ID/g; p=0.001), likely as a result of the abovementioned, more multidirectional drainage of the copolymers from these tumors. These findings indicate that the increases over time that were observed in the scintigrams should be attributed to decreases in the concentrations of the copolymers in blood and in healthy tissues, rather than to actual increases in tumor concentration.

3.3. Effect of radiotherapy on the tumor accumulation of HPMA copolymers

Next, in order to investigate how radiotherapy reflects on the tumor concentrations of the copolymers, the tumor-bearing limbs of the animals were exposed to 2 Gy and 20 Gy of cobalt-60 γ-radiation, 1 h and 24 h before their i.v. injection. Based on the abovementioned observation that the concentrations of the copolymers were comparable at 24 and 168 h p.i., we focused on the first 24 h after i.v. administration. As indicated in the scintigrams in Figure 3A, a 20 Gy dose of radiotherapy applied 24 h prior to i.v. injection increased the tumor accumulation of 31 kD poly(HPMA) both at 4 and at 24 h p.i., and both in the AT1-sc and in the H-sc tumor model. When the concentrations of 31 kD and 65 kD poly(HPMA) were subsequently quantified at 24 h p.i, radiotherapy was indeed found to improve the tumor accumulation of the copolymers independent of the tumor model used (Figures 3B and 3C). A 20 Gy dose of radiotherapy applied 24 h prior to i.v. injection, for instance, increased the concentration of 31 kD poly(HPMA) in AT1-sc tumors from 0.38±0.04 to 0.47±0.06 %ID/g (p=0.029), in AT1-im tumors from 0.23±0.03 to 0.34±0.10 %ID/g (p=0.011), and in H-sc tumors from 0.18±0.03 to 0.25±0.04 %ID/g (p=0.041). For 65 kD poly(HPMA), 20 Gy of radiotherapy applied 24 h prior to i.v. injection increased the concentration of the copolymer in AT1-sc tumors from 0.87±0.06 to 1.28±0.18 %ID/g (p=0.0013), and in H-sc tumors from 0.50±0.02 to 1.03±0.23 %ID/g (p=0.0095). As exemplified in Table 1, all radiotherapy regimens evaluated improved the tumor accumulation of the copolymers. On average, the concentrations of the smaller copolymer were improved by 11% in AT1-sc tumors, by 32% in AT1-im tumors and by 36% in H-sc tumors, and those of the larger copolymer by 26% in AT1-sc tumors, and by 105% in H-sc tumors.

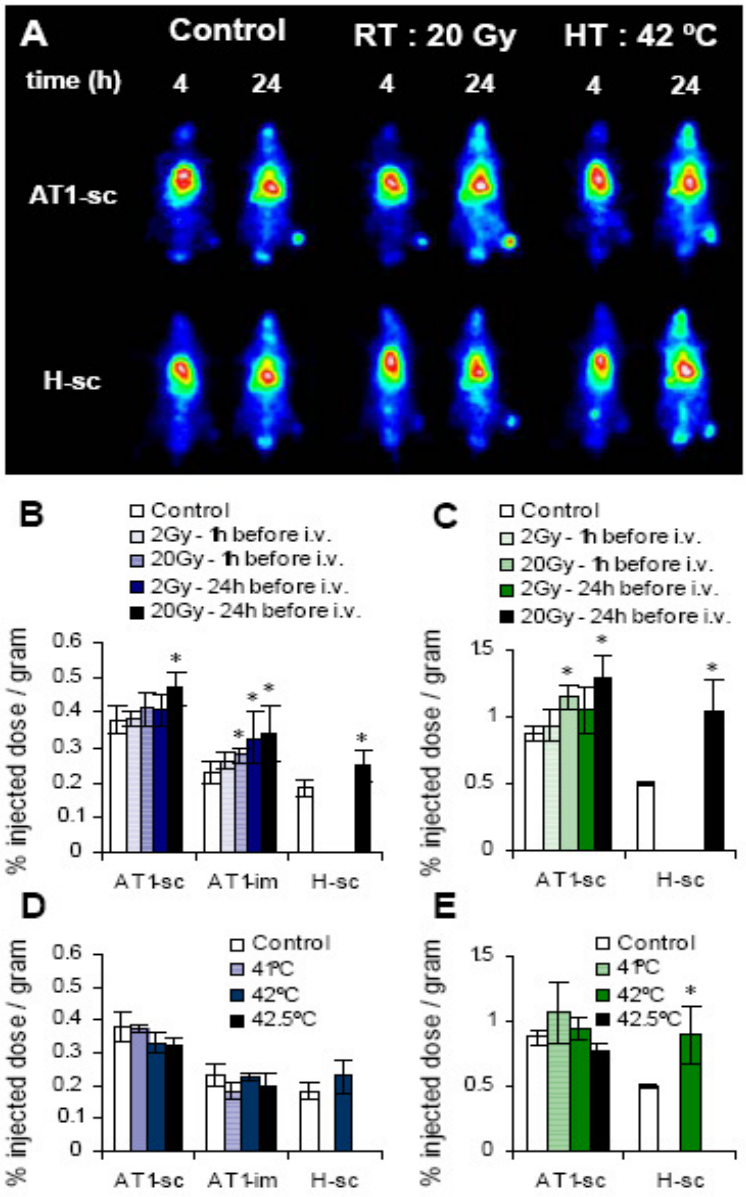

*Figure 3. Effect of radiotherapy and hyperthermia on the tumor accumulation of HPMA copolymers. A: Scintigraphic analysis of the effects of radiotherapy (20 Gy, applied 24 h prior to i.v. injection) and hyperthermia (42 ºC, applied for 1 h, concomitant to i.v. injection) on the tumor accumulation of 31 kD poly(HPMA) in rats bearing AT1-sc and H-sc tumors. B - E: Quantification of the effects of radiotherapy and hyperthermia on the tumor accumulation of 31 kD poly(HPMA) (B and D) and 65 kD poly(HPMA) (C and E) at 24 h p.i. Values represent average ± standard deviation of 3-6 animals per experimental group. * Indicates p<0.05 vs. control (Student's t-test). See page 231.*

3.4. Effect of hyperthermia on the tumor accumulation of HPMA copolymers

Subsequently, the two radiolabeled copolymers were injected i.v. into animals undergoing local tumor hyperthermia. Hyperthermia was applied for 1 h, concomitant to i.v. injection, using a water bath heated to 41, 42 and 42.5 °C. As shown in the scintigrams in Figure 3A, a 42 ºC dose of hyperthermia only increased the tumor accumulation of 31 kD poly(HPMA) in H-sc tumors. Quantification at 24 h p.i., however, indicated that this increase was not statistically significant (0.18±0.03 %ID/g for control vs. 0.23±0.05 %ID/g for 42 ºC of HT; p=0.19; Figure 3D). Only for 65 kD poly(HPMA), a significant increase in the amount of copolymer localizing to H-sc tumors was found (0.50±0.02 %ID/g for control vs. 0.90±0.22 %ID/g for 42 ºC of HT; p=0.036). In AT1-sc and AT1-im tumors, the concentrations of the copolymers were not affected (Figures 3D and 3E). As exemplified in Table 1, in the latter two tumor models, the accumulation of 31 kD poly(HPMA) even tended to decrease upon the implementation of hyperthermia.

	31 kD poly(HPMA)			65 kD poly(HPMA)		28 kD PK1
	AT1-sc	AT1-im	H-sc	AT1-sc	H-sc	AT1-sc
RT: 2Gy-1h	+ 1	+ 15	ND	+ 8	ND	ND
RT: 2Gy-24h	+ 8	+ 43*	ND	+ 20	ND	ND
RT: 20Gy-1h	+ 9	+ 22*	ND	+ 31*	ND	ND
RT: 20Gy-24h	+ 24*	+ 48*	+ 36*	+ 46*	+ 105*	+ 34*
HT: 41°C	0	- 20	ND	+ 22	ND	ND
HT: 42°C	- 13	- 1	+ 24	+ 9	+ 80*	- 7
HT: 42.5°C	- 16	- 13	ND	- 12	ND	ND

Table 1. Summary of the effects of radiotherapy and hyperthermia on the tumor accumulation of HPMA copolymers. The relative increases (in %; as compared to untreated control tumors) in the tumor accumulation of 31 kD poly(HPMA), 65 kD poly(HPMA) and 28 kD poly(HPMA)-GFLG-doxorubicin (PK1) upon treatment with the indicated doses of radiotherapy and hyperthermia are displayed. The asterisks (*) indicate statistical significance (p<0.05). ND: not determined.

3.5. Effect of radiotherapy and hyperthermia on the tumor accumulation of poly(HPMA)-GFLG-doxorubicin

Finally, in order to evaluate if the effects observed for the two chemically unmodified HPMA copolymers also hold for a clinically relevant HPMA copolymer carrying a chemotherapeutic drug, we investigated the impact of radiotherapy and hyperthermia on the tumor accumulation of poly(HPMA)-GFLG-doxorubicin (PK1). As shown in the scintigrams in Figure 4A, the biodistribution of PK1 appeared to be very different from that observed for the two parental copolymers (Figures 2A and 3A). In a previous study, however, we have shown that the incorporation of drug and/or spacer moieties only increases the kidney concentrations of the copolymers significantly (~ 5-10 fold), while affecting their relative levels in the majority of other tissues only moderately [8]. Even though these high kidney concentrations interfere substantially with a proper scintigraphic interpretation of the effects of the two treatment modalities on the tumor accumulation of PK1, the images in Figure 4A do indicate that in the AT1-sc tumor model, radiotherapy is more effective in increasing the tumor localization of the polymer-drug conjugate than is hyperthermia. In line with this observation, when the concentrations of PK1 were quantified at 24 h p.i., only radiotherapy turned out to be able to improve its tumor accumulation. As shown in Figure 4B, 0.48±0.03 %ID was found per gram pre-irradiated tumor, as compared to 0.36±0.02 %ID/g for control (p=0.0041), corresponding to an increase of 34% (Table 1). For tumors treated with hyperthermia, 0.34±0.07 %ID/g was found (p=0.61 vs. control).

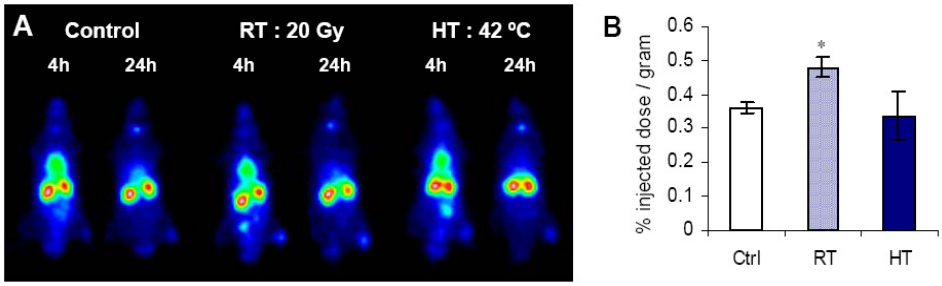

*Figure 4. Effect of radiotherapy and hyperthermia on the tumor accumulation of poly(HPMA)-GFLG-doxorubicin. A: Scintigraphic analysis of the effects of radiotherapy (20 Gy, applied 24 h prior to i.v. injection) and hyperthermia (42 ºC, applied for 1 h, concomitant to i.v. injection) on the tumor accumulation of poly(HPMA)-GFLG-doxorubicin in rats bearing AT1-sc tumors. B: Quantification of the effects of radiotherapy and hyperthermia on the tumor accumulation of poly(HPMA)-GFLG-doxorubicin at 24 h p.i. Values represent average ± standard deviation of 3-4 animals per experimental group. * Indicates p<0.05 vs. control (Student's t-test).* *See page 231.*

4. Discussion

In the present study, we have evaluated the possibility of improving the tumor accumulation of HPMA copolymer-based drug delivery systems by combining their in vivo application with radiotherapy and hyperthermia. As the effects of these two treatment modalities were expected to depend significantly on the tumor model used, we first analyzed the tumor accumulation of two differently sized HPMA copolymers in three different tumor models. As hypothesized, it was found that the tumor concentrations of 31 kD and 65 kD poly(HPMA) were highest in subcutaneously transplanted Dunning AT1 tumors (AT1-sc), which are known to possess a leaky vasculature, and which have previously been shown to accumulate the copolymers relatively effectively by means of the EPR effect [8]. In intramuscularly inocculated Dunning AT1 tumors (AT1-im), as well as in subcutaneously transplanted Dunning H tumors (H-sc), the levels of the copolymers were found to be approximately 50% lower than in AT1-sc tumors (Figure 2). For AT1-im tumors, this was assumed to be due to a reduction of the impact of tumor encapsulation. The increase in tumor-muscle surface area in these tumors (Figure 1) likely leads to a more multidirectional drainage of the copolymers and, thus, to significantly lower tumor concentrations. For H-sc tumors, the accumulation of the copolymers was also found to be reduced by half, in this case most likely as a result of a difference in the morphology of the tumor blood vessels. The fact that the endothelial lining is properly differentiated in slowly growing H-sc tumors indicates that it is largely intact and fully functional (Figure 1). As a consequence, as compared to AT1-sc tumors, the extravasation of HPMA copolymer-based drug delivery systems into the interstitium of these tumors was found to be hindered substantially, resulting in significantly lower tumor concentrations, both at 24 and at 168 h post i.v. injection (Figure 2).

Upon having demonstrated that the tumor concentrations of the polymeric drug carriers depend significantly on the tumor model used, we went on to assess the effects of radiotherapy on their tumor accumulation. It was found that radiotherapy increased the concentration of the 31 kD copolymer in all three tumor models that were tested, and the concentration of the 65 kD copolymer in both tumor models that were tested (Figure 3 and Table 1). This finding is in line with several previous reports addressing the impact of radiotherapy on the tumor localization of drug delivery systems. A single dose of 15 Gy of radiotherapy, for instance, has been shown to improve both the overall tumor accumulation as

well as the intratumoral distribution of a poly(L-glutamic acid)-paclitaxel conjugate [35]. In addition, it has recently been reported that a single dose of 8 Gy, as well as three (fractionated) doses of 3.6 Gy, applied 24 h after the i.v. administration of liposomal doxorubicin, increased the concentrations of the drug both in subcutaneous and in orthotopic osteosarcoma xenografts [36]. And furthermore, by designing drug delivery systems that are able to selectively bind to radiotherapy-induced membrane receptors, Hallahan and colleagues have proposed the concept of 'radiation-guided drug delivery' [37]. Based on the notion that $\alpha_{2b}\beta_3$ integrins (i.e. fibrinogen receptors) were found to be upregulated in response to ionizing radiation, they prepared fibrinogen-conjugated nanoparticles, and they showed that the concomitant administration of radiotherapy increased the tumor accumulation of these nanoparticles substantially.

According to the results presented here, besides being an attractive means for improving the tumor accumulation of actively targeted drug delivery systems (e.g. the abovementioned fibrinogen-modified nanoparticles), radiotherapy also seems to hold significant potential for improving the tumor localization of passively targeted drug delivery systems. Most important in this respect seems to the observation that as opposed to hyperthermia, radiotherapy increased the concentrations of the copolymers independent of the tumor model used (Figure 3 and Table 1), which indicates that radiotherapy affects the permeability of tumor blood vessels through one or more general physiological mechanisms. It is, for instance, known that radiotherapy upregulates the expression of vascular endothelial growth factor (VEGF) [38,39]. VEGF is also known as VPF, i.e. as vascular permeability factor, and its upregulation has been associated with an increased vascular permeability towards macromolecules [40,41]. The same holds for basic fibroblast growth factor (bFGF), which is also upregulated in response to radiotherapy [42] and which also increases vascular permeability [43-45]. In addition, radiotherapy has been shown to decrease the interstitial fluid pressure (IFP) within tumors [46]. The IFP is a pathophysiological characteristic of solid malignancies that contributes to an outward-bound pressure gradient across tumors and that is, at least in part, responsible for the poor penetration of blood-borne agents into tumors [47,48]. Furthermore, even within a 24-hour time frame, radiotherapy has been shown to reduce the tumor cell density in tumors [49], which is also known to be an important (negative) determinant of the degree of drug penetration into solid malignancies [50,51].

And finally, especially at higher doses of ionizing radiation (exceeding 8 Gy, i.e. only for 20 Gy-1h and for 20Gy-24h), endothelial cell apoptosis can also be expected to play a role in determining the degree of extravasation [52,53]. Taking the abovementioned notions into account, it seems to be reasonable to assume that the positive effects of radiotherapy on the tumor accumulation of (polymeric) drug delivery systems are guided by several physiological mechanisms: I) by increasing the production of VEGF and FGF, II) by lowering the interstitial fluid pressure, III) by lowering the tumor cell density and IV) by inducing endothelial cell apoptosis.

As opposed to radiotherapy, hyperthermia was only found to be able to improve the concentrations of the copolymers in one tumor model. In principle, this finding is in line with the observations made by Kong and colleagues, who have shown that hyperthermia increases the pore cutoff size of the vasculature, and that it improves the tumor accumulation of liposomal drug delivery systems [54,55]. In addition, it is in line with the data published by Dewhirst, Bigner, Zalutsky and coworkers, who have shown that hyperthermia increases the tumor localization of antibodies and antibody fragments [56-59]. The results presented here also convincingly demonstrate, however, that the effects of hyperthermia depend significantly on the tumor model used: in AT1-sc and AT1-im tumors, which already possess a relatively leaky vasculature, hyperthermia had no obvious effect on the amount of copolymer localizing to tumors (Figure 3 and Table 1). In H-sc tumors, on the other hand, which possess a properly differentiated endothelial lining (Figure 1), it did increase the concentrations of the copolymers (Figure 3 and Table 1), which seems to point towards a hyperthermia-induced increase in the pore cutoff size of the vasculature in these tumors [54,55]. Taking into account that it has been repetitively reported that the effects of hyperthermia on tumor blood flow, on tumor blood vessels and on the (micro)vascular permeability in tumors are multifaceted [60-62], it is indeed reasonable to assume that the impact of hyperthermia on the tumor accumulation of drug delivery systems varies from tumor model to tumor model.

5. Conclusion

Taken together, the results presented here show that HPMA copolymer-based drug delivery systems accumulate effectively in different types of tumors. In addition, they demonstrate that hyperthermia increases the tumor accumulation of the copolymers depending on the tumor model used, and that radiotherapy increases their tumor concentrations independent of the tumor model used. Based on these findings, we conclude that radiotherapy is an effective means for improving the tumour accumulation of (polymeric) drug delivery systems, and we propose that the combination of carrier-based chemotherapy with radiotherapy might hold significant potential for improving the efficacy of combined modality anticancer therapy.

References

1. R. Duncan, The dawning era of polymer therapeutics, Nat. Rev. Drug Discov. 2 (2003) 347-360.
2. J. Kopecek, P. Kopeckova, T. Minko, Z. Lu, HPMA copolymer-anticancer drug conjugates: design, activity, and mechanism of action, Eur. J. Pharm. Biopharm. 50 (2000) 61-81.
3. B. Rihova, K. Kubackova, Clinical implications of N-(2-hydroxypropyl)- methacrylamide copolymers, Curr. Pharm. Biotechnol. 4 (2003) 311-322.
4. H. Maeda, Y. Matsumura, A new concept for macromolecular therapeutics in cancer chemotherapy: mechanism of tumoritropic accumulation of proteins and the antitumor agent Smancs, Cancer Res. 46 (1986) 6387-6392.
5. H. Maeda, J. Wu, T. Sawa, Y. Matsumura, K. Hori, Tumor vascular permeability and the EPR effect in macromolecular therapeutics, J. Control. Release 65 (2000) 271-284.
6. Y. Noguchi, J. Wu, R. Duncan, J. Strohalm, K. Ulbrich, T. Akaike, H. Maeda, Early phase tumor accumulation of macromolecules: a great difference in clearance rate between tumor and normal tissues, Jpn. J. Cancer Res. 89 (1998) 307-314.
7. J. Kopecek, P. Kopeckova, T. Minko, Z.R. Lu, C.M. Peterson, Water soluble polymers in tumor targeted delivery, J. Control. Release 74 (2001) 147-158.
8. T. Lammers, R. Kuhnlein, M. Kissel, V. Subr, T. Etrych, R. Pola, M. Pechar, K. Ulbrich, G. Storm, P. Huber, P. Peschke, Effect of physicochemical modification on the biodistribution and tumor accumulation of HPMA copolymers, J. Control. Release 110 (2005) 103-118.
9. P.A. Vasey, S.B. Kaye, R. Morrison, C. Twelves, P. Wilson, R. Duncan, A.H. Thomson, L.S. Murray, T. Hilditch, T. Murray, S. Burtles, D. Fraier, E. Frigerio, J. Cassidy, Cancer Research Campaign Phase I/II Committee, Phase I clinical and pharmacokinetic study of PK1 [N-(2-hydroxypropyl)methacrylamide copolymer doxorubicin]: first member of a new class of chemotherapeutic agents-drug-polymer conjugates, Clin. Cancer Res. 5 (1999) 83-94.
10. V. Bilim, Technology evaluation: PK1, Pfizer/Cancer Research UK, Curr. Opin. Mol. Ther. 5 (2003) 326-330.
11. E. Gianasi, M. Wasil, E.G. Evagorou, A. Keddle, G. Wilson, R. Duncan, HPMA copolymer platinates as novel antitumour agents: in vitro properties, pharmacokinetics and antitumour activity in vivo, Eur. J. Cancer 35 (1999) 994-1002.
12. J.M. Rademaker-Lakhai, C. Terret, S.B. Howell, C.M. Baud, R.F. De Boer, D. Pluim, J.H. Beijnen, J.H. Schellens, J.P. Droz, Phase I and pharmacological study of the platinum polymer AP5280 given as an intravenous infusion once every 3 weeks in patients with solid tumors, Clin. Cancer Res. 10 (2004) 3386-3395.

13. Y. Kasuya, Z.R. Lu, P. Kopeckova, T. Minko, S.E. Tabibi, J. Kopecek, Synthesis and characterization of HPMA copolymer-aminopropylgeldanamycin conjugates, J. Control. Release 74 (2001) 203-211.
14. N. Nishiyama, A. Nori, A. Malugin, Y. Kasuya, P. Kopeckova, J. Kopecek J, Free and N-(2-hydroxypropyl)methacrylamide copolymer-bound geldanamycin derivative induce different stress responses in A2780 human ovarian carcinoma cells, Cancer Res. 63 (2003) 7876-7882
15. R. Satchi-Fainaro, M. Puder, J.W. Davies, H.T. Tran, D.A. Sampson, A.K. Greene, G. Corfas, J. Folkman, Targeting angiogenesis with a conjugate of HPMA copolymer and TNP-470, Nat. Med. 10 (2004) 255-261.
16. R. Satchi-Fainaro, R. Mamluk, L. Wang, S.M. Short, J.A. Nagy, D. Feng, A.M. Dvorak, H.F. Dvorak, M. Puder, D. Mukhopadhyay, J. Folkman, Inhibition of vessel permeability by TNP-470 and its polymer conjugate, caplostatin, Cancer Cell 3 (2005) 251-261.
17. L.W. Seymour, Y. Miyamoto, H. Maeda, M. Brereton, J. Strohalm, K. Ulbrich, R. Duncan, Influence of molecular weight on passive tumour accumulation of a soluble macromolecular drug carrier, Eur. J. Cancer 31 (1995) 766-770.
18. J.G. Shiah, M. Dvorak, P. Kopeckova, Y. Sun, C.M. Peterson, J. Kopecek, Biodistribution and antitumour efficacy of long-circulating N-(2-hydroxypropyl)methacrylamide copolymer-doxorubicin conjugates in nude mice, Eur. J. Cancer 37 (2001) 131-139.
19. D. Wang, J.P. Kopeckova, T. Minko, V. Nanayakkara, J. Kopecek, Synthesis of starlike N-(2-hydroxypropyl)methacrylamide copolymers: potential drug carriers, Biomacromolecules 1 (2000) 313-319.
20. M. Kovar, J. Strohalm, T. Etrych, K. Ulbrich, B. Rihova, Star structure of antibody-targeted HPMA copolymer-bound doxorubicin: a novel type of polymeric conjugate for targeted drug delivery with potent antitumor effect, Bioconjug. Chem. 13 (2002) 206-215.
21. L.W. Seymour, P.A. Flanagan, A. al-Shamkhani, V. Subr, K. Ulbrich, J. Cassidy, R. Duncan, Synthetic polymers conjugated to monoclonal antibodies: vehicles for tumour-targeted drug delivery, Sel. Cancer Ther. 7 (1991) 59-73.
22. J.G. Shiah, Y. Sun, P. Kopeckova, C.M. Peterson, R.C. Straight, J. Kopecek, Combination chemotherapy and photodynamic therapy of targetable N-(2-hydroxypropyl)methacrylamide copolymer-doxorubicin/mesochlorin e(6)-OV-TL 16 antibody immunoconjugates, J. Control. Release 74 (2001) 249-253.
23. K. Ulbrich, T. Etrych, P. Chytil, M. Jelinkova, B. Rihova, Antibody-targeted polymer-doxorubicin conjugates with pH-controlled activation, J. Drug Target. 12 (2004) 477-489.
24. A. Tang, P. Kopeckova, J. Kopecek, Binding and cytotoxicity of HPMA copolymer conjugates to lymphocytes mediated by receptor-binding epitopes, Pharm. Res. 20 (2003) 360-367.
25. A. Mitra, J. Mulholland, A. Nan, E. McNeill, H. Ghandehari, B.R. Line, Targeting tumor angiogenic vasculature using polymer-RGD conjugates, J. Control. Release 102 (2005) 191-201.
26. H. Ding, W.M. Prodinger, J. Kopecek, Identification of CD21-binding peptides with phage display and investigation of binding properties of HPMA copolymer-peptide conjugates, Bioconjug. Chem. 17 (2006) 514-523.
27. R. Duncan, J. Kopecek, P. Rejmanova, J.B. Lloyd, Targeting of N-(2-hydroxypropyl)methacrylamide copolymers to liver by incorporation of galactose residues, Biochim. Biophys. Acta 755 (1983) 518-521.
28. A. David, P. Kopeckova, T. Minko, A. Rubinstein, J. Kopecek, Design of a multivalent galactoside ligand for selective targeting of HPMA copolymer-doxorubicin conjugates to human colon cancer cells, Eur. J. Cancer 40 (2005) 148-157.
29. Y. Luo, N.J. Bernshaw, Z.R. Lu, J. Kopecek, G.D. Prestwich, Targeted delivery of doxorubicin by HPMA copolymer-hyaluronan bioconjugates, Pharm. Res. 19 (2002) 396-402.
30. S. Wroblewski, M. Berenson, P. Kopeckova, J. Kopecek, Potential of lectin-N-(2-hydroxypropyl)methacrylamide copolymer-drug conjugates for the treatment of pre-cancerous conditions, J. Control. Release 74 (2001) 283-293.
31. B. Rihova, M. Jelinkova, J. Strohalm, M. St'astny, O. Hovorka, D. Plocova, M. Kovar, L. Draberova, K. Ulbrich, Antiproliferative effect of a lectin- and anti-Thy-1.2 antibody-targeted HPMA copolymer-bound doxorubicin on primary and metastatic human colorectal carcinoma and on human colorectal carcinoma transfected with the mouse Thy-1.2 gene, Bioconjug. Chem. 11 (2002) 664-673.
32. L.W. Seymour, D.R. Ferry, D. Anderson, S. Hesslewood, P.J. Julyan, R. Poyner, J. Doran, A.M. Young, S. Burtles, D.J. Kerr, Cancer Research Campaign Phase I/II Clinical Trials committee, Hepatic drug targeting: phase I evaluation of polymer-bound doxorubicin, J. Clin. Oncol. 20 (2002) 1668-1676.

33. D.M. Lubaroff, L. Canfield, T.L. Feldbush, W.W. Bonney, R3327 adenocarcinoma of the Copenhagen rat as a model for the study of the immunologic aspects of prostate cancer, J. Natl. Cancer Inst. 58 (1977) 1677-1689.
34. P.R. Salacinski, C. McLean, J.E. Sykes, V.V. Clement-Jones, P.J. Lowry, Iodination of proteins, glycoproteins, and peptides using a solid-phase oxidizing agent, 1,3,4,6-tetrachloro-3 alpha, 6 alpha-diphenyl glycoluril (Iodogen), Anal. Biochem. 117 (1981) 136-146.
35. C. Li, S. Ke, Q.P. Wu, W. Tansey, N. Hunter, L.M. Buchmiller, L. Milas, C. Charnsangavej, S. Wallace, Tumor irradiation enhances the tumor-specific distribution of poly(L-glutamic acid)-conjugated paclitaxel and its antitumor efficacy, Clin. Cancer Res. 6 (2000) 2829-2834.
36. C.L. Davies, L.M. Lundstrom, J. Frengen, L. Eikenes, O.S. Bruland, O. Kaalhus, M.H. Hjelstuen, C.R. Brekken, Radiation improves the distribution and uptake of liposomal doxorubicin (caelyx) in human osteosarcoma xenografts, Cancer. Res 64 (2004) 547-553.
37. D. Hallahan, L. Geng, S. Qu, C. Scarfone, T. Giorgio, E. Donnelly, X. Gao, J. Clanton, Integrin-mediated targeting of drug delivery to irradiated tumor blood vessels, Cancer Cell 3 (2003) 63-74.
38. J.S. Park, L. Qiao, Z.Z. Su, D. Hinman, K. Willoughby, R. McKinstry, A. Yacoub, G.J. Duigou, C.S. Young, S. Grant, M.P. Hagan, E. Ellis, P.B. Fisher, P. Dent, Ionizing radiation modulates vascular endothelial growth factor expression through multiple mitogen activated protein kinase dependent pathways, Oncogene 25 (2001) 3266-3280.
39. Y.L. Chung, J.J. Jian, S.H. Cheng, S.Y. Tsai, V.P. Chuang, T. Soong, Y.M. Lin, C.F. Horng, Sublethal irradiation induces vascular endothelial growth factor and promotes growth of hepatoma cells: implications for radiotherapy of hepatocellular carcinoma, Clin. Cancer Res. 12 (2006) 2706-2715.
40. H.F. Dvorak, L.F. Brown, M. Detmar, A.M. Dvorak, Vascular permeability factor/vascular endothelial growth factor, microvascular hyperpermeability, and angiogenesis, Am. J. Pathol. 146 (1995) 1029-1039.
41. D. Feng, J.A. Nagy, K. Pyne, I. Hammel, H.F. Dvorak, A.M. Dvorak, Pathways of macromolecular extravasation across microvascular endothelium in response to VPF/VEGF and other vasoactive mediators, Microcirculation 6 (1999) 23-44.
42. Y.J. Lee, S.S. Galoforo, C.M. Berns, G. Erdos, A.K. Gupta, D.K. Ways, P.M. Corry, Effect of ionizing radiation on AP-1 binding activity and basic fibroblast growth factor gene expression in drug-sensitive human breast carcinoma MCF-7 and multidrug-resistant MCF-7/ADR cells, J. Biol. Chem. 270 (1995) 28790-28796.
43. F. Samaniego, P.D. Markham, R. Gendelman, Y. Watanabe, V. Kao, K. Kowalski, J.A. Sonnabend, A. Pintus, R.C. Gallo, B. Ensoli, Vascular endothelial growth factor and basic fibroblast growth factor present in Kaposi's sarcoma (KS) are induced by inflammatory cytokines and synergize to promote vascular permeability and KS lesion development, Am. J. Pathol. 152 (1998) 1433-1443.
44. E. Toschi, G. Barillari, C. Sgadari, I. Bacigalupo, A. Cereseto, D. Carlei, C. Palladino, C. Zietz, P. Leone, M. Sturzl, S. Butto, A. Cafaro, P Monini, B. Ensoli, Activation of matrix-metalloproteinase-2 and membrane-type-1-matrix-metalloproteinase in endothelial cells and induction of vascular permeability in vivo by human immunodeficiency virus-1 Tat protein and basic fibroblast growth factor, Mol. Biol. Cell 12 (2001) 2934-2946.
45. T.T. Rissanen, J.E. Markkanen, K. Arve, J. Rutanen, M.I. Kettunen, I. Vajanto, S. Jauhiainen, L. Cashion, M. Gruchala, O. Narvanen, P. Taipale, R.A. Kauppinen, G.M. Rubanyi, S. Yla-Herttuala, Fibroblast growth factor 4 induces vascular permeability, angiogenesis and arteriogenesis in a rabbit hindlimb ischemia model, FASEB J. 17 (2003) 100-102.
46. C.A. Znati, M. Rosenstein, Y. Boucher, M.W. Epperly, W.D. Bloomer, R.K. Jain, Effect of radiation on interstitial fluid pressure and oxygenation in a human tumor xenograft, Cancer Res. 56 (1996) 964-968.
47. P.A. Netti, L.T. Baxter, Y Boucher, R. Skalak, R.K. Jain, Time-dependent behavior of interstitial fluid pressure in solid tumors: implications for drug delivery, Cancer Res. 55 (1995) 5451-5458.
48. P.A. Netti, L.M. Hamberg, J.W. Babich, D. Kierstead, W. Graham, G.J. Hunter, G.L. Wolf, A. Fischman, Y. Boucher, R.K. Jain, Enhancement of fluid filtration across tumor vessels: implication for delivery of macromolecules, Proc. Natl. Acad. Sci. USA 96 (1999) 3137-3142.
49. P. Peschke, V. Klein, G. Wolber, E. Friedrich, E.W. Hahn, Morphometric analysis of bromodeoxyuridine distribution and cell density in the rat Dunning prostate tumor R3327-AT1 following treatment with radiation and/or hyperthermia, Histol. Histopathol. 14 (1999) 461-469.
50. J.L. Au, S.H. Jang, J. Zheng, C.T. Chen, S. Song, L. Hu, M.G. Wientjes, Determinants of drug delivery and transport to solid tumors, J. Control. Release 74 (2001) 31-46.

51. S.H. Jang, M.G. Wientjes, D. Lu, J.L. Au, Drug delivery and transport to solid tumors, Pharm. Res. 20 (2003) 1337-1350.
52. R.E. Langley, E.A. Bump, S.G. Quartuccio, D. Medeiros, S.J. Braunhut, Radiation-induced apoptosis in microvascular endothelial cells, Br. J. Cancer 75 (1997) 666-672.
53. M. Garcia-Barros, F. Paris, C. Cordon-Cardo, D. Lyden, S. Rafii, A. Haimovitz-Friedman, Z. Fuks, R. Kolesnick, Tumor response to radiotherapy regulated by endothelial cell apoptosis, Science 300 (2003) 1155-1159.
54. G. Kong, R.D. Braun, M.W. Dewhirst, Hyperthermia enables tumor-specific nanoparticle delivery: effect of particle size, Cancer Res. 60 (2000) 4440-4445.
55. G. Kong, R.D. Braun, M.W. Dewhirst, Characterization of the effect of hyperthermia on nanoparticle extravasation from tumor vasculature, Cancer Res. 61 (2001) 3027-3032.
56. D.A. Cope, M.W. Dewhirst, H.S. Friedman, D.D. Bigner, M.R. Zalutsky, Enhanced delivery of a monoclonal antibody F(ab')2 fragment to subcutaneous human glioma xenografts using local hyperthermia, Cancer Res. 50 (1990) 1803-1809.
57. J.M. Schuster, M.R. Zalutsky, M.A. Noska, R. Dodge, H.S. Friedman, D.D. Bigner, M.W. Dewhirst, Hyperthermic modulation of radiolabelled antibody uptake in a human glioma xenograft and normal tissues, Int. J. Hyperthermia 11 (1995) 59-72.
58. M.L. Hauck, M.W. Dewhirst, D.D. Bigner, M.R. Zalutsky, Local hyperthermia improves uptake of a chimeric monoclonal antibody in a subcutaneous xenograft model, Clin. Cancer Res. 3 (1997) 63-70.
59. M.L. Hauck, M.R. Zalutsky, Enhanced tumour uptake of radiolabelled antibodies by hyperthermia: Part I: Timing of injection relative to hyperthermia, Int. J. Hyperthermia 21 (2005) 1-11.
60. T.E. Dudar, R.K. Jain, Differential response of normal and tumor microcirculation to hyperthermia, Cancer Res. 44 (1984) 605-612.
61. L.E. Gerlowski, R.K. Jain, Effect of hyperthermia on microvascular permeability to macromolecules in normal and tumor tissues, Int. J. Microcirc. Clin. Exp. 4 (1985) 363-372.
62. P. Wust, B. Hildebrandt, G. Sreenivasa, B. Rau, J. Gellermann, H. Riess, R. Felix, P.M. Schlag, Hyperthermia in combined treatment of cancer, Lancet Oncol. 3 (2002) 487-497.

Chapter 7

Image-guided and passively tumor-targeted polymeric nanomedicines for radiochemotherapy

Twan Lammers[a,b], Vladimir Subr[c], Peter Peschke[a], Rainer Kühnlein[a], Wim E. Hennink[b], Karel Ulbrich[c], Fabian Kiessling[d], Melanie Heilmann[d], Jürgen Debus[e], Peter E. Huber[a,e], Gert Storm[b]

[a] Department of Innovative Cancer Diagnosis and Therapy, German Cancer Research Center, Im Neuenheimer Feld 280, 69120 Heidelberg, Germany
[b] Department of Pharmaceutics, Utrecht Institute for Pharmaceutical Sciences, Utrecht University, Sorbonnelaan 16, 3584 CA Utrecht, The Netherlands
[c] Institute of Macromolecular Chemistry, Academy of Sciences of the Czech Republic, Heyrovsky Square 2, 162 06 Prague 6, Czech Republic
[d] Department of Medical Physics in Radiology, German Cancer Research Center, Im Neuenheimer Feld 280, 69120 Heidelberg, Germany
[e] Department of Radiooncology and Radiotherapy, Heidelberg University, Im Neuenheimer Feld 110, 69120 Heidelberg, Germany

Brit. J. Cancer 99: 900-910 (2008)

Abstract

Drug targeting systems are nanometer-sized carrier materials designed for improving the biodistribution of systemically applied (chemo-) therapeutics. Reasoning that I) the temporal and spatial interaction between i.v. applied chemotherapy and clinically relevant fractionated radiotherapy is suboptimal, and that II) drug targeting systems are able to improve the temporal and spatial parameters of this interaction, we have here set out to evaluate the potential of 'carrier-based radiochemotherapy'. HPMA copolymers were used as a model drug targeting system, doxorubicin and gemcitabine as model drugs, and the syngeneic and radio- and chemoresistant Dunning AT1 rat prostate carcinoma as a model tumor model. Using MRI and γ-scintigraphy, the polymeric drug carriers were first shown to circulate for prolonged periods of time, to localize to tumors both effectively and selectively, and to improve the tumor-directed delivery of low molecular weight agents. Subsequently, they were then shown to interact synergistically with radiotherapy, with radiotherapy increasing the tumor accumulation of the copolymers, and with the copolymers increasing the therapeutic index of radiochemotherapy (both for doxorubicin and for gemcitabine). Based on these findings, and on the fact that its principles are likely broadly applicable, we propose carrier-based radiochemotherapy as a novel concept for treating advanced solid malignancies.

1. Introduction

The combination of radiotherapy and chemotherapy has been evaluated extensively in the past few decades [1,2]. Besides significantly increasing the efficacy of radiotherapy, however, the simultaneous application of chemotherapy also substantially increases its toxicity [3,4]. As external beam radiotherapy can nowadays be delivered with extremely high levels of spatial specificity [5,6], this is likely mostly due to the low degree of spatial specificity that chemotherapeutic agents generally present upon i.v. administration. Based on this notion, and on the fact that drug targeting systems are known to be able to improve both the temporal (circulation time, tumor residence time) and the spatial (tumor accumulation, tumor-to-organ ratio) parameters of drug therapy [7-10], we reasoned that the implementation of a drug targeting system might increase the therapeutic index of radiochemotherapy. The rationale for this novel combination regimen, which we have termed 'carrier-based radiochemotherapy', relies on the notion that on the one hand, radiotherapy improves drug targeting (i.e. the tumor accumulation of drug targeting systems), and that on the other hand, drug targeting improves radiochemotherapy (i.e. the temporal and spatial interaction between daily radiotherapy and weekly chemotherapy; see Figure 1).

Concerning the former aspect of carrier-based radiochemotherapy, several different mechanisms can be envisioned by which radiotherapy increases the tumor accumulation of drug targeting systems (Figure 1B). Besides reflecting, for instance, on the integrity and function of the tumor vasculature (V), and on the expression of certain cellular receptors (R), it is also known to affect several cell membrane-related (C), nuclear (N), mitochondrial (M) and signaling (S) processes. By eliciting such effects, radiotherapy has been shown to induce I) an increase in the production of VEGF [11] and FGF [12], II) an increase in apoptosis and endothelial cell apoptosis [13], III) a decrease in tumor cell density [14], and IV) a reduction in interstitial fluid pressure [15]. By means of the former phenomenon, radiotherapy is considered to be able to increase the permeability of the vasculature towards long-circulating nanomedicines [16,17], and by means of the latter three, it likely improves their penetration and their intratumoral distribution [18-20].

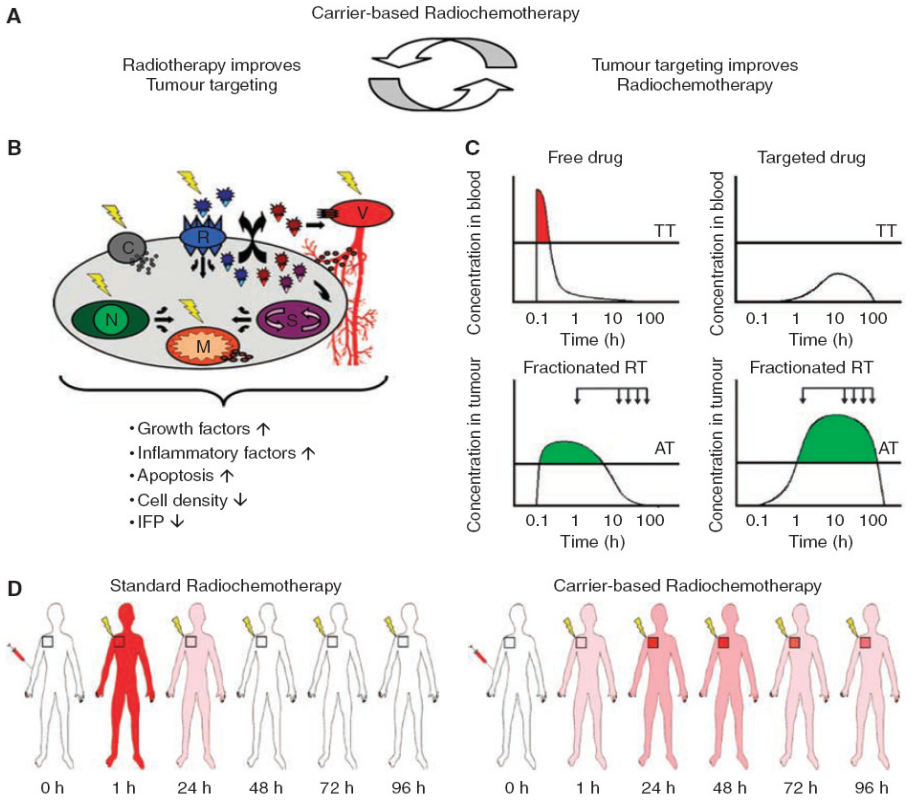

Figure 1. Rationale for carrier-based radiochemotherapy. A: Carrier-based radiochemotherapy is based on the notion that drug targeting and radiotherapy interact synergistically, with on the one hand, radiotherapy improving the tumor accumulation of drug targeting systems, and with on the other hand, drug targeting systems improving the therapeutic index of radiochemotherapy. B: Potential physiological mechanisms by which radiotherapy increases the tumor accumulation of drug targeting systems. See text for details. C: Schematic representation of the blood and tumor concentrations of an intravenously (i.v.) applied free drug (upper and lower left panels), and of a drug delivered to the tumor by means of an i.v. applied drug targeting system (upper and lower right panels). The arrows indicate the administration of fractionated radiotherapy, which is routinely applied on every weekday for several consecutive weeks. TT: toxicity threshold, AT: activity threshold. See text for details. D: Schematic representation of the in vivo interaction between radiotherapy and chemotherapy upon standard and upon carrier-based radiochemotherapy, exemplifying that in case of the latter, the temporal and spatial interaction between the two treatment modalities is improved. See page 232.

The rationale for the latter aspect of carrier-based radiochemotherapy, i.e. for the assumption that drug targeting systems are able to improve the interaction between radiotherapy and chemotherapy, is depicted in Figure 1C. Drug targeting systems are generally designed to be stable in circulation, and to release the conjugated or entrapped active agent only at the target site [8-10]. As a result, as compared to an i.v. applied free drug, the peak plasma concentration of a tumor-targeted agent tends to be reduced, and the degree of systemic toxicity can often be attenuated (Figure 1C; upper two panels). For doxorubicin, for instance, both polymeric [9,21] and liposomal [8,22], drug targeting systems have been shown to be able to reduce the incidence of cardiomyopathy. At the same time, by increasing the concentration of the active agent at the target site, drug targeting systems also tend to be able to improve the efficacy of the drug [7-10]. As a matter of fact, as depicted schematically in the lower two panels in Figure 1C, the implementation of a drug targeting system generally not only increases the concentration of the active agent at the target site, but it also improves its availability over time (i.e. its AUC; as a result of the Enhanced Permeability and Retention (EPR) effect [23]). When combining a clinically relevant regimen of weekly chemotherapy with a clinically relevant regimen of (daily) radiotherapy, it can therefore be expected that a drug delivered to the tumor by means of a drug targeting system interacts more effectively with radiotherapy than does a free, untargeted drug (Figure 1D). As will be outlined below, this was indeed found to be the case, and both for doxorubicin and for gemcitabine, it could be demonstrated that drug targeting systems increase the efficacy of radiochemotherapy without increasing its toxicity.

2. Materials and methods

2.1. Synthesis of the monomers

N-(2-hydroxypropyl)methacrylamide (HPMA) was synthesized by the reaction of methacryloyl chloride with 1-aminopropan-2-ol in dichloromethane in the presence of sodium carbonate. *N*-methacryloyl tyrosinamide (MA-TyrNH_2) was prepared by the reaction of methacryloyl chloride with tyrosinamide in distilled water. 6-Methacrylaminohexanoic acid (MA-AH-OH) and *N*-methacryloyl glycyl-DL-phenylalanylleucylglycine (MA-GFLG-OH) were prepared by Schotten-Baumann acylation of the amino acids and oligopeptides with methacryloyl chloride in an aqueous alkaline solution. MA-GFLG-ONp was synthesized by the

reaction of MA-GFLG-OH with 4-nitrophenol in the presence of *N,N'*-dicyclohexylcarbodiimide in tetrahydrofurane. 3-(6-Methacrylamidohexanoyl)-thiazolidine-2-thione (MA-AH-TT) and 3-(*N*-methacryloyl-GFLG)-thiazolidine-2-thione (MA-GFLG-TT) were prepared by the reaction of MA-AH-OH or MA-GFLG-OH with 4,5-dihydrothiazole-2-thiol in the presence of *N,N'*-dicyclohexylcarbodiimide and 4-(dimethylamino)pyridine.

2.2. Synthesis of the tyrosinamide- and gadolinium-containing copolymers

Poly(HPMA-co-MA-TyrNH_2) was prepared by solution radical copolymerization of the monomers HPMA and MA-TyrNH_2 in methanol [24]. The precursor for poly(HPMA-co-MA-AH-Asp-[(Asp-$(OH)_2]_2$) was prepared by alkaline hydrolysis of the copolymer poly(HPMA-co-MA-AH-Asp-[(Asp-$(O\text{-}CH_3)_2]_2$), which was itself synthesized by solution radical copolymerization of the monomers HPMA and Ma-AH-Asp-[(Asp-$(O\text{-}CH_3)_2]_2$, in methanol, using AIBN as an initiator [25]. After hydrolysis, dialysis and lyophilization, the conjugate it was dissolved in distilled water, and gadolinium chloride was added. The pH of the solution was gradually increased to 6.0 (by addition of 0.1 M NaOH), and the excess of gadolinium was removed by dialysis, using a Visking dialysis tube with a cut-off size of 3.5 kDa. Finally, the amount of gadolinium incorporated into the copolymer was determined by means of ICP-MS and the conjugate was lyophilized.

2.3. Synthesis of the doxorubicin-containing copolymers

The precursor for poly(HPMA)-GFLG-doxorubicin (PK1), i.e. poly(HPMA-co-MA-GFLG-ONp), was prepared by precipitation radical copolymerization of HPMA and MA-GFLG-ONp in acetone. The precipitated precursor was then filtered off, washed with acetone and diethyl ether, dried in vacuum, and conjugated to doxorubicin hydrochloride in DMSO, in the presence of triethylamine. The resulting polymer-drug conjugate was subsequently isolated by precipitation into a mixture of acetone-diethyl ether, filtered off, dried in vacuum, purified on a Sephadex LH-20 column in methanol (to remove free doxorubicin), and fractionated on a Sephadex LH-60 column (to obtain a narrow distribution of the molecular weight). For the preparation of IgG-poly(HPMA)-GFLG-doxorubicin (IgG-PK1), a comparable precursor, i.e. poly(HPMA-co-MA-GFLG-ONp), was used. This precursor, however, contained approximately twice as many ONp groups as the precursor used for synthesizing PK1, in order to allow for the binding of - besides doxorubicin - several IgG moieties. Upon the conjugation of doxorubicin, which was performed as described above, the precipitation-isolated

intermediate with remaining ONp reactive groups was incubated with human IgG in saline-borate buffer (pH=8.0). Finally, the conjugate was purified by gel filtration on a Sephadex G-25 column and lyophilized.

2.4. Synthesis of the gemcitabine-containing copolymers

Polymer conjugates of gemcitabine have not been prepared thus far, and their synthesis will therefore be described in a bit more detail. Precursors containing thiazolidine-2-thione imide (TT) reactive groups (i.e. poly(HPMA)-co-MA-AH-TT for A-Gem, and poly(HPMA)-co-MA-GFLG-TT for B-Gem) were prepared by solution radical copolymerization of HPMA and MA-AH-TT, and of HPMA and MA-GFLG-TT, in DMSO, respectively. The comonomer concentrations in the polymerization mixture were 12.5 wt%, and the concentration of the initiator AIBN was 2.0 wt%. After polymerization, the copolymers were precipitated into an acetone-diethyl ether mixture (3:1), the solvents were filtered off and the precipitate was dried in vacuum.

The precursor used for preparing A-Gem, i.e. poly(HPMA)-co-MA-AH-TT (1 g; 5.52 x 10^{-4} mol of TT reactive groups), was dissolved in a glass ampoule containing 10 ml of dry pyridine. Gemcitabine hydrochloride (0.248 g; 8.27 x 10^{-4} mol) was added, the solution was mixed (i.e. bubbled with argon) and the ampoule was sealed. The ampoule was then incubated in a water bath at 50 ºC for 28 h. The copolymer with bound gemcitabine was isolated by precipitation into a mixture of acetone-diethyl ether (2:1), the solvents were filtered off and the precipitate was dried in vacuum. The remaining TT reactive groups were aminolyzed by the addition of 20 µl of 1-amino-propan-2-ol in DMSO. The resulting conjugate (i.e. A-Gem; poly(HPMA-AH-Gem)) was subsequently purified from unbound gemcitabine by gel filtration on a Sephadex LH-20 column in methanol and lyophilized.

In principle, B-Gem (i.e. poly(HPMA)-GFLG-Gem) was synthesized according to an identical procedure: 1.0 g of poly(HPMA-co-MA-GFLG-TT) (4.60x10^{-4} mol of TT reactive groups) was dissolved in a glass ampoule containing 10 ml of dry pyridine and mixed with 0.207 g of gemcitabine hydrochloride (6.89x10^{-4} mol). The solution was then bubbled with argon, sealed and incubated at 50 ºC for 28 h. Subsequently, the precipitate was again isolated into a mixture of acetone-diethyl ether (2:1), it was dried in vacuum, the remaining TT reactive groups were aminolyzed using 1-amino-propan-2-ol, and the polymer-drug conjugate was purified from free gemcitabine by gel filtration on a Sephadex LH-20 column.

2.5. Characterization of the copolymers

The weight- and number-average molecular weights (M_w and M_n), and the polydispersity (M_w / M_n) of the copolymers were determined by size exclusion chromatography, and the amounts of doxorubicin and gemcitabine incorporated by means of spectrophotometry. The (weight-) average molecular weights of the two tyrosinamide-containing copolymers (i.e. poly(HPMA-co-MA-TyrNH_2)) were 30.5 and 64.5 kDa, their polydispersities were 1.3 and 1.2, and the amounts of tyrosinamide, included to allow for radiolabeling, were 0.8 and 1.1 mol%. The average molecular weight of the gadolinium-labeled copolymer (i.e. poly(HPMA-co-MA-AH-Asp-[(Asp-$(OH)_2]_2$)-Gd) was 24.8 kDa, its polydispersity was 1.9 and the amount of gadolinium was 5.2 wt% (as determined by ICP-MS). The average molecular weights of PK1 (i.e. poly(HPMA)-GFLG-doxorubicin) and IgG-PK1 (i.e. IgG-poly(HPMA)-GFLG-doxorubicin) were 27.9 and 900 kDa, their polydispersities were 1.5 and 4.0, and relative amounts of doxorubicin were 6.5 and 4.8 wt%, respectively. The average molecular weights of A-Gem (i.e. poly(HPMA)-AH-Gem; uncleavable) and of B-Gem (i.e. poly(HPMA)-GFLG-Gem; cleavable) were 20.2 and 24.0 kDa, their polydispersities were 1.5 and 1.6, and their drug contents were 6.8 and 10.9 wt%, respectively.

2.6. Drug release and in vitro efficacy of the gemcitabine-containing copolymers

The release of gemcitabine from A-Gem and from B-Gem was investigated at pH=7.4, at pH=6.0, and at pH=6.0 in the presence of the lysosomal cysteine protease cathepsin B. The temperature was set to resemble physiological conditions (i.e. 37 °C). The concentrations of the two polymeric prodrugs were 2.3×10^{-3} mol/l Gem-equivalent. The concentration of cathepsin B was 1.9×10^{-7} mol/l, and its activity was standardized using the substrate BzArgNAp. Drug release was quantified spectrophotometrically at 310 nm. The cytotoxicity of free and HPMA copolymer-bound gemcitabine was determined by seeding Dunning AT1 rat prostate carcinoma cells and A2780 human ovarian carcinoma cells into 6-well plates, and by incubating them with increasing concentrations of the free drug, the two polymeric prodrugs and a drug-free control copolymer. Eight to ten days later, the cells were fixed and stained with crystal violet, and the number of surviving colonies was counted.

2.7. MRI analysis

Magnetic resonance imaging was performed using a clinical 1.5 T whole-body MRI system (Siemens Symphony) and a custom-made radio frequency (RF) coil for RF excitation and signal reception. The RF coil was designed as a cylindrical volume resonator with an inner diameter of 83 mm and a useable length of 120 mm. To optimize the available signal-to-noise ratio, manual tuning and matching of the coil's resonance circuitry was performed prior to each measurement.

For MR angiography, four rats were anaesthetized by inhalation using a mixture of isofluorane, N_2O and O_2. The tail veins of the rats were catheterized using a 24 G indwelling cannula, which was connected to a syringe filled with ~1 ml of pHPMA-gadolinium (Gd concentration: 0.05 mmol per kg). Blood vessels AT1 tumors were imaged at 30 min p.i. using a 3D gradient echo pulse sequence (3 FLASH; TR/TE=28.0/8.6 ms, flip-angle=70°, field of view= 12.8x30x50 mm^3, matrix=128x317x512, reconstructed voxel size=100x98x98 μm^3; 2 acquisitions). Vessels in the head and chest region were visualized using a different 3D sequence: TR/TE=10.2/3.8 ms, flip angle=70°, field of view= 30x55x110 mm^3, matrix=60x256x512, reconstructed voxel size=500x215x215 μm^3; 4 acquisitions. For comparing the biodistribution of the 25 kDa pHPMA-gadolinium conjugate to that of a clinically relevant low molecular weight MR contrast agent (gadolinium-DTPA-BMA; Omniscan®; 0.5 kDa; Amersham Buchler), we first imaged the tumor localization morphology with a T_{2w}-Turbo-spinecho sequence (T_{2w}-TSE_i; TR/TE/Turbo-factor = 4000ms/96ms/7). In addition, the pre- and post-contrast (30 min p.i.) values of the longitudinal (T_1) and the transversal (T_2) relaxation time were measured in liver, kidney and tumor. At a slice thickness of 3 mm, the T_1 times were determined with a saturation-recovery turbo gradient echo pulse sequence ($CPMG_i$; TR/TE/α/T_{rec} = 8.3ms/4.1ms/12°/53ms-9s), whereas the T_2-measurements were performed with a 32-echo spinecho sequence (TR/TE = 2000ms/23ms-360ms). In this case, the concentrations of the contrast agents were equivalent to 0.1 mmol gadolinium per kg. Dynamic contrast-enhanced MRI was performed using a 3D-FLASH sequence (TR/TE/α = 45ms/8.3ms/45°; spatial resolution: Δx = 0.4 x 0.4 x 0.4 mm^3), and each 3D-FLASH measurement was followed by a T_1-determination (as described above). The T_1- and T_2-values were calculated with an IDL-based software using a least-square fit algorithm. On the one hand, T_1- and T_2-values were determined pixel-wise, in order to create color-coded parameter maps, and on the other hand, for assessing the contrast agent accumulation in tumors, a T_1-value was calculated for a region

covering the whole tumor. For kidney and for liver, contrast agent accumulation was analyzed analogously. The change of the longitudinal relaxation rate, $1/T_1$, over time was converted into contrast agent concentration using the formula $1/T_1 = 1/T_{1,0} + (r_1 \times C)$, and relaxivities ($r_1$) of 21.3 $mM^{-1}s^{-1}$ for pHPMA-gadolinium and 4.1 $mM^{-1}s^{-1}$ for gadolinium-DTPA-BMA [25].

2.8. Scintigraphic analyses

For the scintigraphic analyses, two differently sized poly(HPMA-co-MA-TyrNH_2) conjugates were radiolabeled with iodine-131 (by means of the Iodogen method). Labeling efficacies were always >95% [26]. Five hundred microliters of a 0.1 mM solution (based on copolymer concentration and corresponding to a radioactivity of 150 to 300 µCi) were injected i.v. into male Copenhagen rats bearing subcutaneous Dunning AT1 tumors. At several different time points post injection, blood samples were collected for kinetic analyses, and the biodistribution of the copolymers was visualized by means of a Searle-Siemens scintillation camera. At 24 and 168 h, animals were sacrificed, and tumors and organs were harvested for quantification. The residual amounts of radioactivity were determined using a gamma counter, they were corrected for radioactive decay and they were expressed as percent of the injected dose per gram tissue.

2.9. HPLC analysis

Rats bearing 8-12 mm AT1 tumors were i.v. injected with 5 mg/kg of free doxorubicin or with 77.0 mg of HPMA copolymer-bound doxorubicin (PK1; 6.5 wt-% doxorubicin). Twenty four hours later, tumors were harvested, frozen in liquid nitrogen and homogenized in saline. The total amount of doxorubicin in tumors was determined upon hydrolysis of the homogenate with 2 M HCl at 50 ºC for 1 h (i.e. as doxorubicinone; upon release from the copolymer). Free doxorubicinone was then extracted from the homogenate using chloroform, evaporated to dryness, dissolved in methanol, and subjected to HPLC analysis (Reverse Phase Column Chromolith® Performance RP-18e (Merck)). The amounts of doxorubicinone were analyzed using a fluorescence detector (RF10AXL; Shimadzu; excitation wavelength 484 nm; emission wavelength 560 nm), and they were quantified using a calibration curve.

2.10. Therapeutic analyses

All experiments involving animals were approved by an external committee for animal welfare and were performed according to the guidelines for laboratory animals established by the German government. Experiments were performed on 6-12 month old male Copenhagen rats, using the syngeneic and radio- and chemoresistant Dunning AT1 prostate carcinoma model. Fresh pieces (~10 mm^3) of an AT1 donor tumor were transplanted subcutaneously into both hind limbs of the animals. Prior to treatment, tumors were grown for 6 to 8 days, until they reached an average diameter of 6 mm. Free doxorubicin was administered at its maximum tolerated dose, i.e. at three doses of 2.5 mg/kg (day 1, 8 and 15). PK1 was applied at three (doxorubicin-equivalent) doses of 5 mg/kg, and IgG-PK1 at both the 2.5 and the 5 mg/kg regimen. Local external beam radiotherapy was delivered by means of the Siemens Gammatron S (cobalt-60 γ-irradiation; dose rate ~0.5 Gy/min) and it was applied at a regimen comparable to that routinely used in clinics: 2 Gy was given on every weekday for four consecutive weeks, i.e. for a total of 20 doses of 2 Gy (day 1-5, 8-12, 15-19 and 22-26). Gemcitabine and the gemcitabine-containing copolymers were administered four times, at a dose of 3 mg/kg (day 1, 8, 15 and 22). In this case, radiotherapy was delivered three times weekly for four weeks at a dose of 3 Gy, i.e. for a total of 12 doses of 3 Gy (day -1, 1, 3, 6, 8, 10, 13, 15, 17, 20, 22 and 24). Tumor volumes were calculated using the formula V=(a*(b*b))/2, and they were expressed relative to the volume determined on the first day of therapy. The toxicity of the combination regimens was assessed by determining the body weight loss of the animals and by analyzing the number of white blood cells, red blood cells and platelets (Bayer Advia 120 hematology analyzer).

2.11. Statistical analysis

Values are expressed as average ± s.d. or as average ± s.e.m. In the biodistributional analyses, the two-tailed t-test (for standard comparisons) or the paired t-test (for left vs. right comparisons) was used. In the therapeutic analyses, the Mann-Whitney U test (i.e. Wilcoxon Rank-Sum) was used. Bonferroni-Holm post-hoc analysis was used to correct for multiple comparisons. In all cases, $p<0.05$ was considered to represent statistical significance.

3. Results

3.1. Biodistributional analysis of HPMA copolymers

To assess the validity and the therapeutic potential of carrier-based radiochemotherapy, HPMA copolymers were selected as a model drug targeting system. Copolymers of *N*-(2-hydroxypropyl)methacrylamide (HPMA; Figure 2A) are prototypic and well-characterized polymeric drug carriers that have been broadly implemented in the delivery of anticancer therapeutics [9,10,27,28]. Figure 2B schematically depicts the different copolymers used in this study, functionalized e.g. with gadolinium and iodine-131 for imaging purposes, and with doxorubicin and gemcitabine for therapeutic purposes.

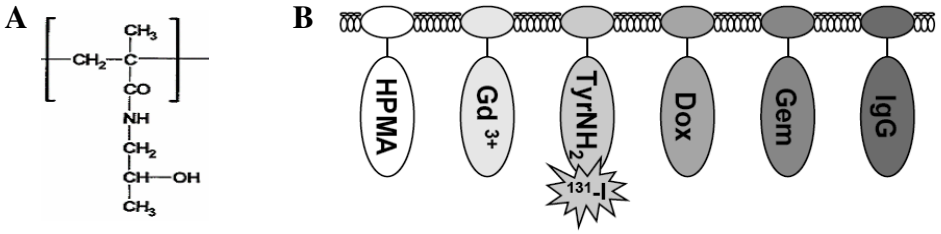

Figure 2. HPMA copolymers: Versatile and multifunctional drug carriers. A: Chemical structure of an HPMA (N-2-(hydroxypropyl)methacrylamide) monomer. B: Schematic representation of a functionalized HPMA copolymer and an overview over the functional groups introduced. Gd: Gadolinium. TyrNH2-^{131}I: Tyrosinamide-bound radioactive iodine. Dox: Doxorubicin. Gem: Gemcitabine. IgG: Human IgG (used as an unspecific targeting moiety [28]). Note that different (combinations of) functional groups were used in different experiments.

The biodistribution of the copolymers was evaluated by means of magnetic resonance imaging (MRI), γ-scintigraphy and HPLC. The MR angiography scans in Figure 3A show that at 0.5 h post i.v. injection (p.i.), a 25 kDa gadolinium-labeled HPMA copolymer was localized predominantly to the vascular compartment. The color-coded maximum intensity projection (MIP; right panel in Figure 3A) confirms the long-circulating properties of the copolymer, showing that also in tumors, the targeting system still resided predominantly within the vasculature at this time point. Up to 10 h p.i., the tumor, kidney and liver concentrations (i.e. whole organ levels) of the conjugate were then compared to those of gadolinium-DTPA-BMA (i.e. gadolinium-diethylenetriaminepentaacetic acid-bis-methylamide; Omniscan®; 0.5 kDa), which is a prototypic low molecular weight MR contrast agent that does not bind to plasma proteins and that is rapidly eliminated from blood by means of renal filtration. As shown in Figures

3B and 3C, it was found that the implementation of the targeting system attenuated the renal clearance of the gadolinium label (reducing the initial peak in kidney accumulation from 60.1±7.5 µM to 28.5±5.0 µM ($p<0.05$)), and that it consequently - i.e. as a result of the Enhanced Permeability and Retention effect (EPR; [23]) - enhanced its accumulation in tumors over time. Significant localization to liver was also noted (Figure 3C), but one needs to take into account that I) the weight (and volume) of a rat liver tends to be ~10 times higher than that of an average (10 x 10 mm) AT1 tumor, and that II) at such 'early' time points, the signal quantified does not necessarily reflect contrast agent accumulation, as significant amounts of the copolymer are still present in circulation up to 24 h (see below), and as the liver is a highly vascularized organ.

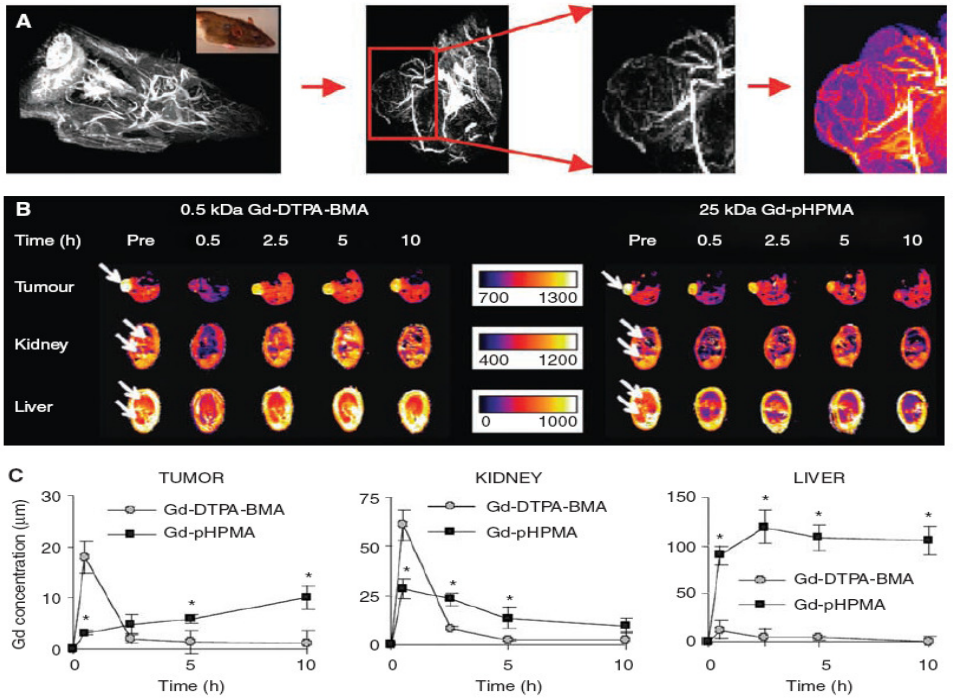

*Figure 3. Magnetic resonance imaging (MRI)-based biodistributional analysis of pHPMA-gadolinium (Gd). A: MR angiography scans of the chest and head region of a rat, of a tumor-bearing paw, and of an AT1 tumor, obtained at 0.5 h after the intravenous (i.v.) injection of 25 kDa pHPMA-Gd. A color-coded maximal intensity projection (MIP) of the polymer-visualised perfusion of the tumor is depicted in the right panel. B: Dynamic, color-coded MRI T1 determination obtained for AT1 tumor, for kidney and for liver before contrast agent administration and at various time points after the i.v. injection of a low (0.5 kDa Gd-DTPA-BMA) and high (25 kDa Gd-pHPMA) molecular weight MR contrast agent. Note that contrast agent accumulation corresponds to a decrease in the T1 signal. C: Quantification of the concentrations of gadolinium in AT1 tumor, kidney, and liver upon the i.v. injection of Gd-DTPA-BMA and pHPMA-Gd. Values represent average ± s.d. (n=3). * Indicates $P<0.05$ (paired t-test). See page 233.*

To more extensively evaluate the tumor and organ accumulation of the polymeric drug delivery system, and to do so at later time points, we next radiolabeled two differently sized tyrosinamide-containing HPMA copolymers with iodine-131, and we monitored their biodistribution scintigraphically. In line with the MR angiography data Figure 3A, the images in Figure 4A on the one hand again demonstrate that the polymeric drug carriers circulate for prolonged periods of time, with especially for the 65 kDa copolymer, substantial amounts still present in blood at 0.5 and 24 h p.i. (as exemplified by the high levels localized to heart). Quantification of the concentrations of the two copolymers in systemic circulation confirmed this observation, with at 24 h p.i., for instance, 11.2±0.7% and 23.7±1.2% of the injected dose still present in blood for 31 kDa and 65 kDa pHPMA, respectively (Figure 4B). The scintigrams in Figure 4A on the other hand also quite convincingly demonstrate that the polymeric drug delivery system presents with an acceptable biodistribution, with besides localization to tumors, only indications for an accumulation in organs of the reticuloendothelial system (RES; i.e. liver, spleen and lung), which is known to be involved in the clearance of long-circulating nanomedicines [8,9,23,27]. In line with this, when quantifying the tumor and organ concentrations of the smaller copolymer at 24 and 168 h p.i., actually only in spleen, levels were always significantly higher than in tumors (Figure 4C). In lung, comparable levels were found, and in all other organs, the concentrations of the copolymer were significantly lower than in tumors. For 65 kDa pHPMA, an identical pattern was observed, the only difference being that the targeting efficacy appeared to be lower at 24 h p.i., and higher at 168 h p.i. (Figure 4C). This can be explained by taking the basic principles of EPR and the prolonged circulation time of the larger copolymer into account, and is exemplified by the fact that levels in tumor and spleen substantially increased, and levels in healthy tissues substantially decreased over time. The tumor-to-organ ratios in Figure 4D confirm this observation, showing both higher overall values and larger increases over time for the 65 kDa copolymer, and they furthermore nicely illustrate that HPMA copolymers localize to tumors relatively selectively, with throughout follow-up, always higher levels in tumors than in 7 out of 9 healthy tissues. Using fluorescence microscopy and HPLC, it was finally also demonstrated that by means of their beneficial biodistributional properties, HPMA copolymers are able to improve the tumor-directed delivery of doxorubicin, increasing its target site accumulation at 24 h p.i. by more than a threefold (Figures 4E-F). Together, these findings show that HPMA copolymers are able to improve the temporal and spatial parameters of low molecular weight agents, and they thereby exemplify that HPMA copolymers are suitable targeting systems for assessing the validity and the therapeutic potential of carrier-based radiochemotherapy.

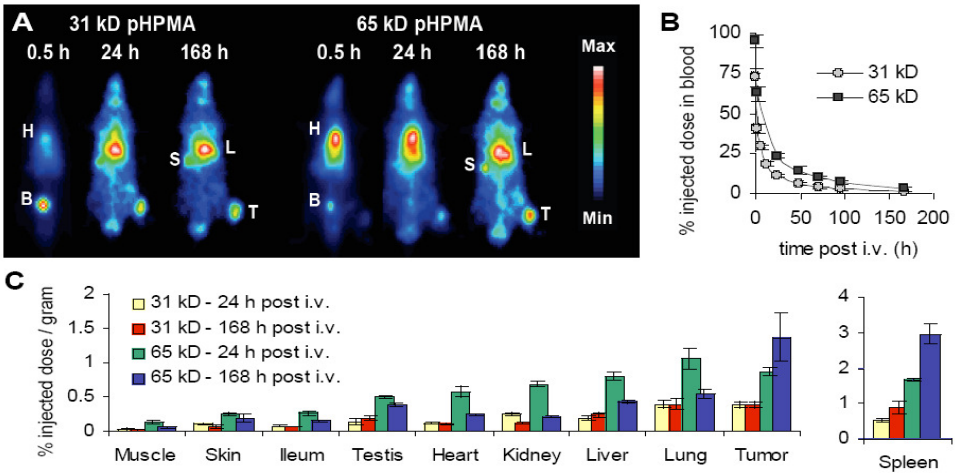

D

T/O Ratio	Muscle	Skin	Ileum	Testis	Heart	Kidney	Liver	Lung	Tumor	Spleen
31 kD-24 h	12,0	3,5	5,0	3,2	2,8	1,6	2,0	1,0	1	0,7
31 kD-168 h	20,1	5,5	5,7	3,5	2,0	3,3	1,6	1,0	1	0,4
65 kD-24 h	6,2	3,5	3,3	1,3	1,5	1,7	1,1	0,8	1	0,5
65 kD-168 h	23,1	9,1	7,3	6,6	5,7	3,5	3,2	2,5	1	0,5

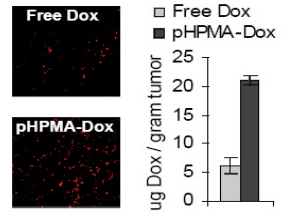

Figure 4. HPMA copolymers localise to tumors effectively and selectively. A: Scintigraphic analysis of the biodistribution of two differently sized iodine-131-labeled HPMA copolymers in Copenhagen rats bearing subcutaneously transplanted Dunning AT1 tumors, demonstrating prolonged circulation and effective tumor accumulation (H: heart (blood), B: bladder, S: spleen, L: liver, T: tumor). B: Analysis of the blood concentrations of the two radiolabeled copolymers. Values represent average ± s.d. (n=6). C: Quantification of the tumor and organ concentrations of the two radiolabeled copolymers at 24 and 168 h p.i. Values represent average ± s.d. (n=6). Except for lung and spleen, concentrations in tumors were always significantly higher than those in healthy organs (P<0.05; two-tailed t-test). D: Quantification of the tumor-to-organ ratios of the copolymers analysed in C, pointing out (in green) that they accumulate more selectively in tumors than in seven out of nine healthy tissues. E: Fluorescence microscopy analysis of the amount of doxorubicin localized to AT1 tumors at 24 h p.i. F: HPLC analysis of the amount of doxorubicin in tumors at 24 p.i., exemplifying the beneficial effect of drug targeting. Values represent average ± s.e.m. (n=5). See page 234.

3.2. Radiotherapy improves drug targeting

To address the former aspect of carrier-based radiochemotherapy, i.e. to evaluate if radiotherapy is able to improve the tumor accumulation of drug targeting systems (Figure 1B), we next visualized and quantified the concentrations of the iodine- and the gadolinium-labeled HPMA copolymers in tumors that were exposed to 20 Gy of ionizing radiation 24 h prior to i.v. injection. The scintigrams in Figure 5A show that as hypothesized, ionizing

radiation indeed significantly improved the tumor accumulation of the carrier systems. Quantifications at 24 and 168 h p.i. confirmed this notion, showing that for the radiolabeled 31 kDa copolymer, increases of 24% and 57% were found, and for the 65 kDa copolymer, increases of 46% and 48%, respectively (Figure 5B). Using the abovementioned 25 kDa gadolinium-containing copolymer and a 1.5 T clinical MR scanner, we subsequently also quantified the tumor accumulation of the targeting system at several earlier time points, i.e. between 0.5 and 24 h after i.v. administration. In this case, upon quantifying the T1 signal enhancements in irradiated vs. control tumors, increases ranging from 31% to 44% were observed (Figures 5C and 5D). Even though such increases may intuitively seem to be modest, in line with previous findings, using different doses, tumor models and carrier systems [29-31], they do convincingly demonstrate that the tumor accumulation of drug targeting systems can be improved by combining them with radiotherapy. This in contrast, for instance, to the majority of targeting ligands that have been evaluated for this purpose over the years, but that generally only tend to improve the internalization of the systems [32,33].

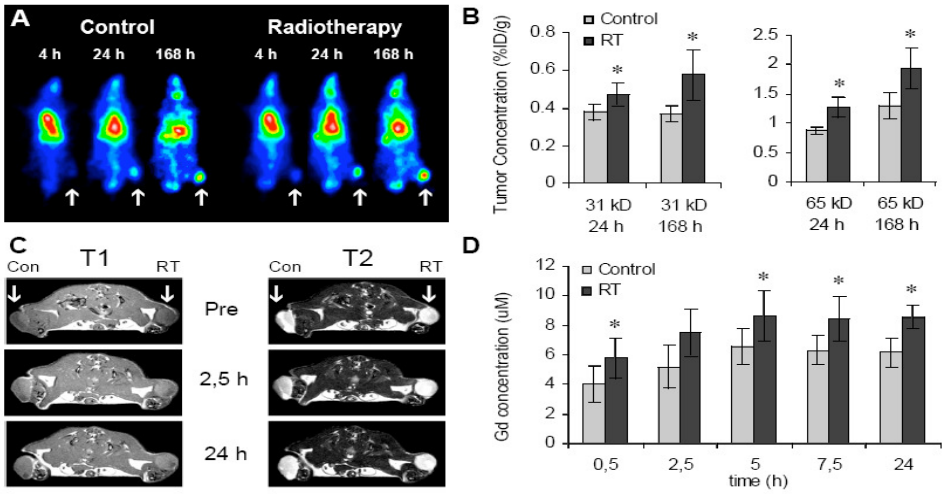

*Figure 5. Radiotherapy improves drug targeting. A: Scintigraphic analysis of the effect of 20 Gy of radiotherapy on the tumor accumulation of an iodine-131-labeled 31 kDa HPMA copolymer, demonstrating that radiotherapy beneficially affects tumor targeting. B: Quantification of the effect of radiotherapy (RT) on the tumor concentrations of the 31 kDa (left panel) and 65 kDa (right panel) copolymer at 24 and 168 h post intravenous injection. Values represent average ± s.d. (n=3–6). * Indicates P<0.05 (two-tailed t-test). C: Magnetic resonance imaging analysis of the effect of 20 Gy of radiotherapy on the tumor accumulation of the 25 kDa gadolinium-labeled HPMA copolymer. The T1 images correspond to contrast agent accumulation, the T2 images were used for positioning and for morphological analysis. D: Quantification of the effect of radiotherapy on the tumor accumulation of the 25 kDa gadolinium-labeled copolymer. Values represent average ± s.d. (n=3). * Indicates P<0.05 (paired t-test). See page 235.*

3.3. Drug targeting improves doxorubicin-based radiochemotherapy

To subsequently address the latter (and clinically much more relevant) aspect of carrier-based radiochemotherapy, i.e to investigate if drug targeting systems are able to improve the interaction between radiotherapy and chemotherapy (Figure 1D), two different versions of HPMA copolymer-bound doxorubicin were synthesized, i.e. PK1 (poly(HPMA)-GFLG-doxorubicin; 28 kDa) and IgG-PK1 (poly(HPMA)-GFLG-doxorubicin; 900 kDa). Both polymeric prodrugs have been tested in clinical trials, and both have been shown to be at least equally effective as free doxorubicin [9,27,28,34,35]. As the maximum tolerated dose (MTD) of PK1 is known to be 4-5 times higher than that of free doxorubicin (both in humans and in rodents [21,36]), in an attempt to simultaneously increase the efficacy and reduce the toxicity of the intervention, we chose to apply PK1 at three times 5 mg/kg (day 1, 8 and 15), i.e. at twice the dose used for free doxorubicin, which has a cumulative MTD of 7.5 mg/kg in rats. IgG-PK1 was applied at both the 2.5 and the 5 mg/kg regimen.

Treatment	n	T10-time (days)	DEF	P-value (vs. Control)	P-value (vs. Dox)
Control	12	20.7	—	—	—
Dox: 3x2.5 mg/kg	8	26.0	—	0.0016 *	—
PK1: 3x5 mg/kg	6	26.7	—	0.0066 *	0.75
IgG-PK1: 3x2.5 mg/kg	8	25.1	—	0.0087 *	0.28
IgG-PK1: 3x5 mg/kg	8	27.8	—	0.00037 *	0.76
Control: 20x2 Gy	10	39.5	1	—	—
Dox: 3x2.5 mg/kg + 20x2 Gy	10	50.5	1.28	0.0065 *	—
PK1: 3x5 mg/kg + 20x2 Gy	10	58.6	1.49	0.0010 *	0.013 *
IgG-PK1: 3x2.5 mg/kg + 20x2 Gy	8	59.1	1.50	0.0014 *	0.021 *
IgG-PK1: 3x5 mg/kg + 20x2 Gy	10	72.0	1.82	0.00016 *	0.00050 *

*Table 1. Summary of the details of the experiments assessing the efficacy of doxorubicin-based radiochemotherapy. N represents the number of tumors per experimental group. The T10-time is the time needed by the tumors to reach ten times the volume determined at the first day of therapy. DEF is the dose enhancement factor, which is calculated by dividing the T10-time for the respective radiochemotherapy regimen by the T10-time for radiotherapy alone, and which is a routinely used parameter for assessing the radiosensitizing potential of chemotherapeutic agents. The p-values versus control and versus the free drug are determined by means of the Mann-Whitney U test. * Indicates a significantly improved antitumor efficacy upon correcting for multiple comparisons using Bonferroni-Holm post-hoc analysis.*

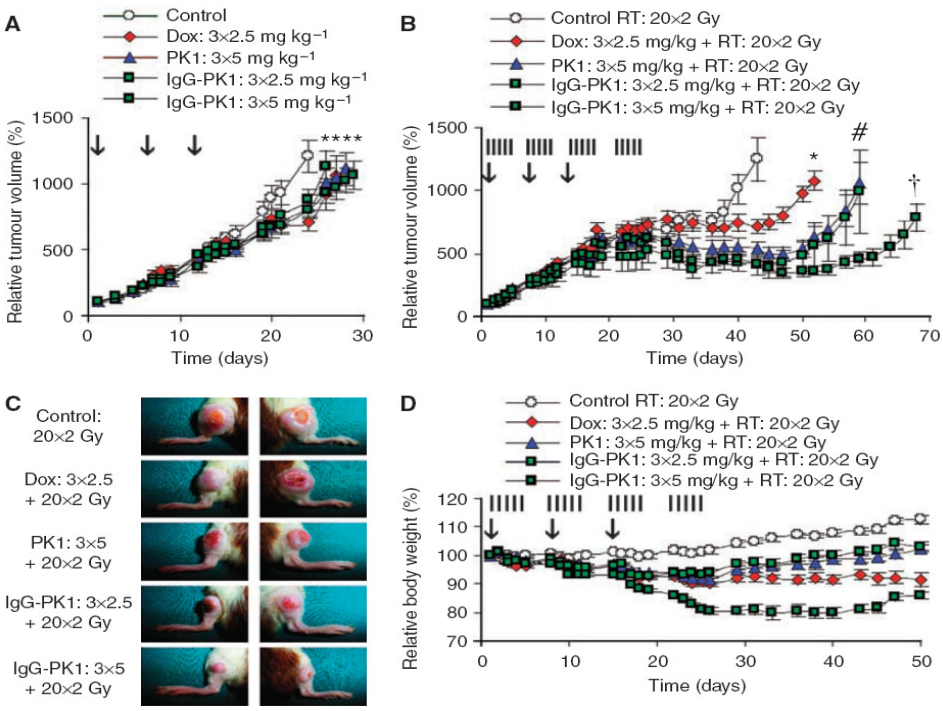

*Figure 6: Drug targeting improves doxorubicin-based radiochemotherapy. A: Growth inhibition of Dunning AT1 tumors induced by three i.v. injections (day 1, 8 and 15; vertical arrows) of saline, of free doxorubicin and of HPMA copolymer-bound doxorubicin. PK1: pHPMA-GFLG-doxorubicin. IgG-PK1: Human IgG-modified pHPMA-GFLG-doxorubicin. Values represent average ± s.e.m (n=6-12). * Indicates p<0.05 vs. control (Mann-Whitney U test; Bonferroni-Holm post-hoc analysis). B: Tumor growth inhibition induced by three i.v. injections of the abovementioned chemotherapeutic agents in combination with a clinically relevant regimen of fractionated radiotherapy (20x2 Gy; vertical lines). Values represent average ± s.e.m. (n=8-10). * Indicates p<0.05 vs. control, # indicates p<0.05 vs. free doxorubicin, and † indicates p<0.005 vs. free doxorubicin (Mann-Whitney U test; Bonferroni-Holm post-hoc analysis). C: Representative images (day 50) of tumors treated with the indicated combination regimens. D: Weight loss induced by doxorubicin-based combined modality therapy. Values represent average ± s.e.m. (n=4-5). See page 236.*

3.4. Preparation of gemcitabine-containing HPMA copolymers

To provide additional evidence for the validity of carrier-based radiochemotherapy, we next set out to synthesize pHPMA-gemcitabine. Gemcitabine is a well-known radiosensitizer [37], and it is used in the first-line treatment of various advanced solid malignancies. Two different gemcitabine-containing copolymers were prepared, termed A-Gem and B-Gem (Figures 7A and 7B). In A-Gem, the drug is conjugated to the copolymer by means of the uncleavable aminohexanoic acid spacer (AH => A-Gem). In B-Gem, gemcitabine is attached to the polymeric backbone by means of the GFLG spacer, which is

also used in PK1 and which is known to be cleaved by the lysosomal cysteine protease cathepsin B (=> B-Gem). Figure 7C shows that A-Gem does not release the drug in vitro: independent of the conditions used, less than 1% of the agent was liberated upon 8 h of incubation. B-Gem, on the other hand, was quite effective in releasing gemcitabine: at pH=6, ~10% was released after 8 h, at pH=7.4, ~30% was released, and upon incubation with physiologically relevant concentrations of cathepsin B (at pH=6; resembling endo- and lysosomal conditions), the total amount of drug conjugated to the copolymer was released within less than 6 h (Figure 7D). To demonstrate that the extent of drug release correlates with the cytotoxicity of the conjugates, clonogenic survival assays were performed. As shown in Figures 7E and 7F, as expected, both in AT1 rat prostate carcinoma cells and in A2780 human ovarian carcinoma cells, B-Gem was significantly more effective than A-Gem. In addition, also in line with our expectations, the two carrier-based agents were found to be less effective than the free drug. For a drug-free control copolymer, no cytotoxicity was observed.

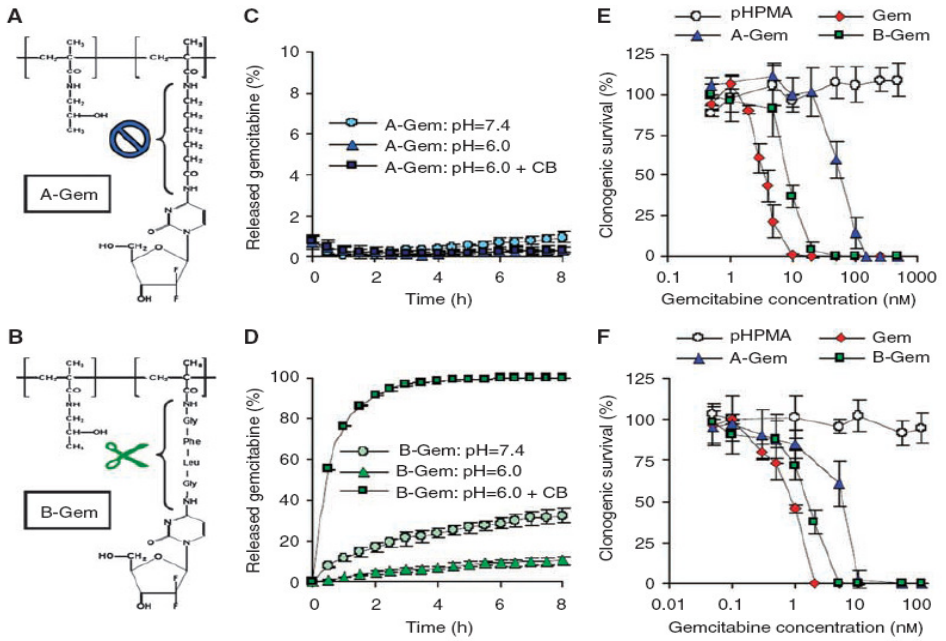

Figure 7. Characterization of the gemcitabine-containing HPMA copolymers. A and B: Chemical structure of A-Gem (poly(HPMA)-AH-gemcitabine) and B-Gem (poly(HPMA)-GFLG-gemcitabine). C and D: Release of gemcitabine from A-Gem and B-Gem at pH=7.4, at pH=6.0 and at pH=6.0 in the presence of the lysosomal cysteine protease cathepsin B (CB). Values are expressed relative to the total amount of drug conjugated to the copolymers, and represent average ± s.d. of three independent experiments. E and F: Cytotoxicity of free gemcitabine, of A-Gem, of B-Gem and of a drug-free control copolymer. Colony formation assays were performed using AT1 rat prostate carcinoma cells (E) and A2780 human ovarian carcinoma cells (F). Values are average ± s.d. (n=3).

3.5. Drug targeting improves gemcitabine-based radiochemotherapy

In the final set of experiments, we set out to investigate the in vivo potential of HPMA copolymer-bound gemcitabine. As shown in Figure 8A, it was again found that without radiotherapy, neither the free drug, nor its polymeric prodrugs were able to induce substantial growth inhibition in the therapy-resistant Dunning AT1 tumor model: B-Gem applied at four 3 mg/kg doses appeared to be the only regimen that was significantly more effective than control, but it was not more effective than free gemcitabine (Table 2). In line with our rationale (Figure 1), however, upon again combining the agents with a clinically relevant regimen of fractionated radiotherapy (12x3 Gy), it could again be observed that the targeted formulation was significantly more effective than the free drug (Figures 8B and 8C): for B-Gem, a DEF of 2.79 was found, as compared to a DEF of 'only' 2.14 for free gemcitabine (Table 2). Figures 8D and 8E finally show that the combination of B-Gem with fractionated radiotherapy was equally well-tolerated as the combination of free gemcitabine with fractionated radiotherapy, with both agents inducing an identical degree of weight loss and of bone marrow suppression. In line with the results obtained for doxorubicin (Figure 6), these notions exemplify that drug targeting systems are able to increase the efficacy of radiochemotherapy without increasing its toxicity.

Treatment	n	T10-time (days)	DEF	P-value (vs. Control)	P-value (vs. Gem)
Control	10	17.4	—	—	—
Gem: 4x3 mg/kg	10	20.0	—	0.19	—
A-Gem: 4x3 mg/kg	10	17.5	—	0.53	0.075
B-Gem: 4x3 mg/kg	10	23.1	—	0.011 *	0.22
Control RT: 12x3 Gy	12	25.1	1	—	—
Gem: 4x3 mg/kg + 12x3 Gy	10	53.7	2.14	0.00017 *	—
A-Gem: 4x3 mg/kg + 12x3 Gy	10	25.6	1.02	0.72	0.0015
B-Gem: 4x3 mg/kg + 12x3 Gy	12	70.0	2.79	0.000032 *	0.025 *

*Table 2. Summary of the details of the experiments assessing the efficacy of gemcitabine-based radiochemotherapy. N represents the number of tumors per experimental group. The T10-time is the time needed by the tumors to reach ten times the volume determined at the first day of therapy. DEF is the dose enhancement factor, which is calculated by dividing the T10-time for the respective radiochemotherapy regimen by the T10-time for radiotherapy alone, and which is a routinely used parameter for assessing the radiosensitizing potential of chemotherapeutic agents. The p-values versus control and versus the free drug are determined by means of the Mann-Whitney U test. * Indicates a significantly improved antitumor efficacy upon correcting for multiple comparisons using Bonferroni-Holm post-hoc analysis.*

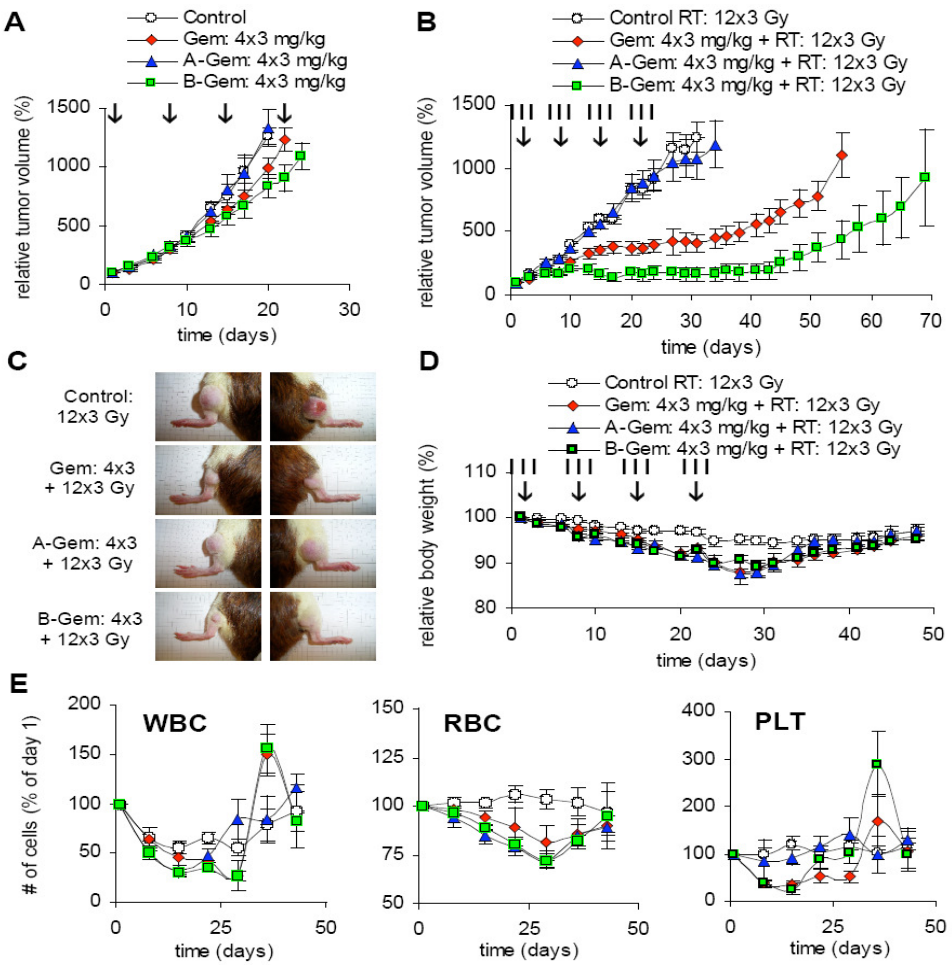

*Figure 8. Drug targeting improves gemcitabine-based radiochemotherapy. A: Growth inhibition of Dunning AT1 tumors induced by four i.v. injections (day 1, 8, 15 and 22; see vertical arrows) of saline, of free gemcitabine and of HPMA copolymer-bound gemcitabine. A-Gem: pHPMA-AH-gemcitabine (20 kDa). B-Gem: pHPMA-GFLG-gemcitabine (24 kDa). * Indicates p<0.05 vs. control (Mann-Whitney U test; Bonferroni-Holm post-hoc analysis). B: Tumor growth inhibition induced by four i.v. injections of the abovementioned chemotherapeutic agents in combination with a clinically relevant regimen of fractionated radiotherapy (12x3 Gy; see vertical lines). Values represent average ± s.e.m. (n=10-12). * Indicates p<0.005 vs. control, # indicates p<0.0005 vs. control, and † indicates p<0.05 vs. free gemcitabine (Mann-Whitney U test; Bonferroni-Holm post-hoc analysis). C: Representative images (day 45) of tumors treated with the indicated combination regimens. D: Weight loss induced by gemcitabine-based combined modality therapy. Values represent average ± s.e.m. (n=5-6). E: Hematological toxicity resulting from gemcitabine-based combined modality therapy. The numbers of white blood cells (WBC), red blood cells (RBC) and platelets (PLT) were determined at several different time points after the start of treatment, and are plotted relative to the number of cells at day 1. Values represent average ± s.d. (n=5-6). See page 237.*

4. Discussion

Over the years, a variety of different drug targeting systems have been developed, ranging in nature from simple polymers [9] and liposomes [8], to stimuli-sensitive polymeric micelles [38], bacterially derived Minicells [39] and temporally targeted Nanocells [40]. Thus far, however, not very many have managed to reach the final stages of clinical evaluation, and only about a handful have been approved by the responsible regulatory authorities. Consequently, hardly any information is available on the combination of tumor-targeted nanomedicines with other well-established treatment modalities. The potential of combining them with a clinically relevant regimen of fractionated radiotherapy, for instance, has not yet been properly evaluated, even though there is an obvious rationale for doing so (Figure 1).

We have here used the prototypic polymeric drug carrier poly(HPMA) to validate the potential of this targeted combination regimen. In line with the literature [27], HPMA copolymers were hereto first shown to be versatile and multifunctional drug carriers, that can be easily tracked in vivo, that circulate for prolonged periods of time, that localize to tumors both effectively and selectively, and that improve the tumor-targeted delivery of low molecular weight agents (Figures 3 and 4). Subsequently, they were then shown to interact synergistically with radiotherapy, with radiotherapy increasing the tumor accumulation of the copolymers (Figure 5), and with the copolymers increasing the therapeutic index of radiochemotherapy (Figures 6 and 8). Improvements were observed in a rapidly growing and therapy-resistant tumor model, and both for doxorubicin and for gemcitabine, together indicating that ‘carrier-based radiochemotherapy’ is indeed a promising approach for improving the efficacy of combined modality anticancer therapy.

This notion is in line with the results of a recently published phase I trial, in which 12 patients with localized esophageal and gastric cancer were treated with the combination of poly(l-glutamic acid)-bound paclitaxel (Xyotax; 6 doses; weekly) and fractionated radiotherapy (28 cycles; 1.8 Gy; daily), and in which 4 complete responses and an additional 7 partial responses (with reductions in tumor size of more than 50%) were achieved [41]. Prior to this trial, preclinical studies had already identified Xyotax as a highly potent radiosensitizer. When a single i.v. injection of Xyotax was combined with a single dose of radiotherapy, for

instance, the dose required to produce 50% tumor cure (TCD_{50}) could be reduced substantially, from 53.9 Gy to 7.5 Gy [42]. When radiotherapy was delivered as 5 daily fractions, the effect of Xyotax was even more pronounced, reducing the TCD_{50} from 66.6 Gy to 7.9 Gy. In a follow-up study in the same tumor model (i.e. C3Hf/KamLaw mice bearing ~7 mm syngeneic OCa-1 ovarian adenocarcinomas), similar results were reported for Abraxane, i.e. for albumin-based paclitaxel, which also beneficially combined both with single dose and with fractionated radiotherapy, and which did not increase normal tissue radiotoxicity [43].

In comparable analyses, Harrington et al. have demonstrated that also liposomes hold significant potential for combination with radiotherapy [44]. They combined both PEGylated liposomal doxorubicin and PEGylated liposomal cisplatin with both single dose (4.5 and 9 Gy) and fractionated (3 x 3 Gy) radiotherapy, and showed that animals treated with carrier-based radiochemotherapy survived for significantly longer periods of time than did animals treated with standard radiochemotherapy. Davies and colleagues recently confirmed and extended these findings, showing that PEGylated liposomal doxorubicin (Caelyx; Doxil) significantly improves the efficacy of both single dose (8 Gy) and fractionated (3 x 3.6 Gy) radiotherapy, and that it does so, at least in part, by improving the penetration and the intratumoral distribution of the agent [30]. In their studies on polymeric radiosensitizers, Li, Milas and colleagues had also already observed that radiotherapy increases the tumor accumulation of passively targeted nanomedicines, attributing at least part of the supra-additively improved efficacy of PGA-paclitaxel (Xyotax) and radiotherapy to a radiotherapy-induced increase in tumor localization [29]. It is interesting to note in this regard that the overall improvement in the tumor concentration of PGA-paclitaxel was virtually identical to that observed here for HPMA copolymers, with as compared to sham-irradiated controls, increases ranging from 25 to 50%. Also in line with our findings, Li and colleagues demonstrated that this radiotherapy-induced increase in tumor accumulation can already be observed almost immediately upon i.v. injection (i.e. at 1 h p.i.; vs. at 30 min p.i. here), and remains relatively constant over time. Together with Davies et al.'s findings on the enhanced penetration and the improved intratumoral distribution of PEGylated liposomal doxorubicin in response to radiotherapy, these observations suggest that radiotherapy beneficially affects both arms of the EPR effect: on the one hand, e.g. by enhancing the expression of VEGF [11,29], it likely increases the permeability of

the tumor blood vessels towards long-circulating nanomedicines, and on the other hand, e.g. by reducing the tumor cell density [14] and the interstitial fluid pressure [15], it likely enhances their retention and their intratumoral distribution. Though clinically clearly less important than the improved therapeutic indices resulting from carrier-based radiochemotherapy, these improvements in EPR-mediated drug targeting to tumors provide an additional rationale for combining tumor-targeted nanomedicines with radiotherapy.

In summary, using prototypic polymeric drug carriers, two different imaging techniques and two different chemotherapeutic agents, we here demonstrate that drug targeting systems and radiotherapy interact synergistically, with radiotherapy increasing the tumor accumulation of the targeting systems, and with the targeting systems increasing the therapeutic index of radiochemotherapy. We extend previous efforts by attempting to generalize the concept of 'carrier-based radiochemotherapy', by implementing clinically relevant regimens of radio- and chemotherapy, and by directly comparing the radiosensitizing potential of polymeric prodrugs to that of free chemotherapeutic agents. The results presented and the insights obtained strongly suggest that carrier-based radiochemotherapy holds significant potential for improving the treatment of advanced solid malignancies.

References

1. Vokes EE, Weichselbaum RR (1990) Concomitant chemoradiotherapy: rationale and clinical experience in patients with solid tumors. J Clin Oncol **8:** 911-934
2. Seiwert TY, Salama JK, Vokes EE (2007) The concurrent chemoradiation paradigm--general principles. *Nat Clin Pract Oncol* **4:** 86-100
3. Maduro JH, Pras E, Willemse PH, de Vries EG (2003) Acute and long-term toxicity following radiotherapy alone or in combination with chemotherapy for locally advanced cervical cancer. *Cancer Treat Rev* **29:** 471-488
4. Rowell NP, O'rourke NP (2004) Concurrent chemoradiotherapy in non-small cell lung cancer. *Cochrane Database Syst Rev* CD002140
5. Fuks Z, Leibel SA, Kutcher G, Mohan R, Ling C (1991) Three-dimensional conformal treatment: a new frontier in radiation therapy. *Important Adv Oncol* 151-172
6. Bernier J, Hall EJ, Giaccia A (2004) Radiation oncology: a century of achievements. *Nat Rev Cancer* **4:** 737-747
7. Moses MA, Brem H, Langer R (2003) Advancing the field of drug delivery: taking aim at cancer. *Cancer Cell* **4:** 337-341
8. Torchilin VP (2005) Recent advances with liposomes as pharmaceutical carriers. *Nat Rev Drug Discov* **4:** 145-160
9. Duncan R (2006) Polymer conjugates as anticancer nanomedicines. *Nat Rev Cancer* **6:** 688-701
10. Lammers T, Hennink WE, Storm G (2008) Tumor-targeted nanomedicines: Principles and Practice. *Br J Cancer* **99:** 392-397
11. Park JS, Qiao L, Su ZZ, Hinman D, Willoughby K, McKinstry R, Yacoub A, Duigou GJ, Young CS, Grant S, Hagan MP, Ellis E, Fisher PB, Dent P (2001) Ionizing radiation modulates vascular endothelial growth factor expression through multiple mitogen activated protein kinase dependent pathways. *Oncogene* **25:** 3266-3280
12. Lee YJ, Galoforo SS, Berns CM, Erdos G, Gupta AK, Ways DK, Corry PM (1995) Effect of ionizing radiation on AP-1 binding activity and basic fibroblast growth factor gene expression in drug-sensitive human breast carcinoma MCF-7 and multidrug-resistant MCF-7/ADR cells. *J Biol Chem* **270:** 28790-28796
13. Garcia-Barros M, Paris F, Cordon-Cardo C, Lyden D, Rafii S, Haimovitz-Friedman A, Fuks Z, Kolesnick R (2003) Tumor response to radiotherapy regulated by endothelial cell apoptosis. *Science* **300:** 1155-1159
14. Peschke P, Klein V, Wolber G, Friedrich E, Hahn EW (1999) Morphometric analysis of bromodeoxyuridine distribution and cell density in the rat Dunning prostate tumor R3327-AT1 following treatment with radiation and/or hyperthermia. *Histol Histopathol* **14:** 461-469
15. Znati CA, Rosenstein M, Boucher Y, Epperly MW, Bloomer WD, Jain RK (1996) Effect of radiation on interstitial fluid pressure and oxygenation in a human tumor xenograft. *Cancer Res* **56:** 964-968
16. Samaniego F, Markham PD, Gendelman R, Watanabe Y, Kao V, Kowalski K, Sonnabend JA, Pintus A, Gallo RC, Ensoli B (1998) Vascular endothelial growth factor and basic fibroblast growth factor present in Kaposi's sarcoma (KS) are induced by inflammatory cytokines and synergize to promote vascular permeability and KS lesion development. *Am J Pathol* **152:**1433-1443
17. Feng D, Nagy JA, Pyne K, Hammel I, Dvorak HF, Dvorak AM (1999) Pathways of macromolecular extravasation across microvascular endothelium in response to VPF/VEGF and other vasoactive mediators, *Microcirculation* **6:** 23-44
18. Jain RK (1994) Barriers to drug delivery in solid tumors. *Sci Am* **271:** 58-65
19. Netti P, Baxter L, Boucher Y, Skalak R, Jain R (1996) Time-dependent behavior of interstitial fluid pressure in solid tumors: implications for drug delivery. *Cancer Res* **55:** 5451-5458
20. Au JL, Jang SH, Zheng J, Chen CT, Song S, Hu L, Wientjes MG (2001) Determinants of drug delivery and transport to solid tumors. *J Control Release* **74:** 31-46
21. Yeung TK, Hopewell JW, Simmonds, RH, Seymour LW, Duncan R, Bellini O, Grandi M, Spreafico F, Strohalm J, Ulbrich K (1991) Reduced cardiotoxicity of doxorubicin given in the form of N-(2-hydroxypropyl)methacrylamide conjugates: and experimental study in the rat. *Cancer Chemother Pharmacol* **29:** 105-111
22. Ewer MS, Martin FJ, Henderson C, Shapiro CL, Benjamin RS, Gabizon AA (2004) Cardiac safety of liposomal anthracyclines. *Semin Oncol* **31:** 161-181
23. Maeda H, Wu J, Sawa T, Matsumura Y, Hori K (2000) Tumor vascular permeability and the EPR effect in macromolecular therapeutics: a review. *J Control Release* **65:** 271-284

24. Lammers T, Kuhnlein R, Kissel M, Subr V, Etrych T, Pola R, Pechar M, Ulbrich K, Storm G, Huber P, Peschke P (2005) Effect of physicochemical modification on the biodistribution and tumor accumulation of HPMA copolymers. *J Control Release* **110:** 103-118
25. Kiessling F, Heilmann M, Lammers T, Ulbrich K, Subr V, Peschke P, Waengler B, Mier W, Schrenk HH, Bock M, Schad L, Semmler W (2006) Synthesis and characterization of HE-24.8: a polymeric contrast agent for magnetic resonance angiography. *Bioconjug Chem* **17:** 42-51
26. Lammers T, Peschke P, Kühnlein R, Subr V, Ulbrich K, Huber P, Hennink W, Storm G (2006) Effect of intratumoral injection on the biodistribution and the therapeutic potential of HPMA copolymer-based drug delivery systems. *Neoplasia* **8:** 788-795
27. Kopecek J, Kopeckova P, Minko T, Lu Z (2000) HPMA copolymer-anticancer drug conjugates: design, activity, and mechanism of action. *Eur J Pharm Biopharm* **50:** 61-81
28. Rihova B, Kubackova K (2003a) Clinical implications of N-(2-hydroxypropyl)-methacrylamide copolymers. *Curr Pharm Biotechnol* **4:** 311-322
29. Li C, Ke S, Wu QP, Tansey W, Hunter N, Buchmiller LM, Milas L, Charnsangavej C, Wallace S (2000) Tumor irradiation enhances the tumor-specific distribution of poly(L-glutamic acid)-conjugated paclitaxel and its antitumor efficacy. *Clin Cancer Res **6:*** 2829-2834
30. Davies CdeL, Lundstrom LM, Frengen J, Eikenes L, Bruland SOS, Kaalhus O, Hjelstuen MH, Brekken C (2004) Radiation improves the distribution and uptake of liposomal doxorubicin (Caelyx) in human osteosarcoma xenografts, *Cancer Res* **64:** 47-53
31. Lammers T, Peschke P, Kühnlein R, Subr V, Ulbrich K, Debus J, Huber P, Hennink W, Storm G (2007) Effect of radiotherapy and hyperthermia on the tumor accumulation of HPMA copolymer-based drug delivery systems. *J Control Release* **117:** 333-341
32. Park JW, Benz CC, Martin FJ (2004) Future directions of liposome- and immunoliposome-based cancer therapeutics. *Semin Oncol* **31:** S13: 96-205
33. Kirpotin D, Drummond D, Shao Y, Shalaby M, Hong K, Nielsen U, Marks J, Benz C, Park J (2006) Antibody targeting of long-circulating lipidic nanoparticles does not increase tumor localization but does increase internalization in animal models. *Cancer Res* **66:** 6732-6740
34. Bilim V (2003) Technology evaluation: PK1, Pfizer/Cancer Research UK. *Curr Opin Mol Ther* **5:** 326-330
35. Rihova B, Strohalm J, Prausova J, Kubackova K, Jelinkova M, Rozprimova L, Sirova M, Plocova D, Etrych T, Subr V, Mrkvan T, Kovar M, Ulbrich K (2003b) Cytostatic and immunomobilizing activities of polymer-bound drugs: experimental and first clinical data. *J Control Release* **91:** 1-16
36. Vasey PA, Kaye SB, Morrison R, Twelves C, Wilson P, Duncan R, Thomson AH, Murray LS, Hilditch TE, Murray T (1995) Phase I clinical and pharmacokinetic study of PK1 [N-(2-hydroxypropyl)methacrylamide copolymer doxorubicin]: first member of a new class of chemotherapeutic agents-drug-polymer conjugates. Cancer Research Campaign Phase I/II Committee. *Clin Cancer Res* **5:** 83-94
37. Lawrence TS, Eisbruch A, Shewach DS (1997) Gemcitabine-mediated radiosensitization. *Semin Oncol* **24:** S7-28
38. Rapoport N, Gao Z, Kennedy A (2007) Multifunctional nanoparticles for combining ultrasonic tumor imaging and targeted chemotherapy. *J Natl Cancer Inst* **99:**1095-1106
39. MacDiarmid JA, Mugridge NB, Weiss JC, Phillips L, Burn AL, Paulin RP, Haasdyk JE, Dickson KA, Brahmbhatt VN, Pattison ST, James AC, Al Bakri G, Straw RC, Stillman B, Graham RM, Brahmbatt H (2007) Bacterially derived 400 nm particles for encapsulation and cancer cell targeting of chemotherapeutics. *Cancer Cell* **11:** 431-445
40. Sengupta S, Eavarone D, Capila I, Zhao G, Watson N, Kiziltepe T, Sasisekharan R (2005) Temporal targeting of tumor cells and neovasculature with a nanoscale delivery system. *Nature* **436:** 568-572
41. Dipetrillo T, Milas L, Evans D, Akerman P, Ng T, Miner T, Cruff D, Chauhan B, Iannitti D, Harrington D, Safran H (2006) Paclitaxel poliglumex (PPX-Xyotax) and concurrent radiation for esophageal and gastric cancer: a phase I study. *Am J Clin Oncol* **29:** 376-379
42. Milas L, Mason K, Hunter N, Li C, Wallace S (2003) Poly(l-glutamic acid)-paclitaxel conjugate is a potent enhancer of tumor radiocurability. *Int J Radiat Oncol Biol Phys* **55:** 707-712
43. Wiedenmann N, Valdecanas D, Hunter N, Hyde S, Buchholz TA, Milas L, Mason KA (2007) 130-nm albumin-bound paclitaxel enhances tumor radiocurability and therapeutic gain. *Clin Cancer Res* **13:**1868-1874
44. Harrington KJ, Rowlinson-Busza G, Syrigos KN, Vile RG, Uster PG, Peters AM, Stewart, JS (2000) Pegylated liposome-encapsulated doxorubicin and cisplatin enhance the effect of radiotherapy in a tumor xenograft model. *Clin Cancer Res* **6:** 4939-49

Chapter 8

Simultaneous delivery of doxorubicin and gemcitabine to tumors in vivo using prototypic polymeric drug carriers

Twan Lammers[a,b], Vladimir Subr[c], Karel Ulbrich[c], Peter Peschke[a], Peter E. Huber[a], Wim E. Hennink[b], Gert Storm[b]

[a] Department of Innovative Cancer Diagnosis and Therapy, Clinical Cooperation Unit Radiotherapeutic Oncology, German Cancer Research Center, Im Neuenheimer Feld 280, 69120 Heidelberg, Germany
[b] Department of Pharmaceutics, Utrecht Institute for Pharmaceutical Sciences, Utrecht University, Sorbonnelaan 16, 3584 CA Utrecht, The Netherlands
[c] Institute of Macromolecular Chemistry, Academy of Sciences of the Czech Republic, Heyrovsky Square 2, 162 06 Prague 6, Czech Republic

Biomaterials 30: 3466-3475 (2009)

Abstract

Copolymers of *N*-(2-hydroxypropyl)methacrylamide (HPMA) are prototypic and well-characterized polymeric drug carriers that have been broadly implemented in the delivery of anticancer therapeutics. To demonstrate that polymers, as liposomes, can be used for simultaneously delivering multiple chemotherapeutic agents to tumors in vivo, we have synthesized and evaluated an HPMA-based polymer-drug conjugate carrying 6.4 wt-% of gemcitabine, 5.7 wt-% of doxorubicin and 1.0 mol-% of tyrosinamide (to allow for radiolabeling). The resulting construct, i.e. poly(HPMA-co-MA-GFLG-gemcitabine-co-MA-GFLG-doxorubicin-co-MA-TyrNH_2), was termed P-Gem-Dox, and was shown to effectively kill cancer cells in vitro, to circulate for prolonged periods of time, to localize to tumors relatively selectively, and to inhibit tumor growth. As compared to control regimens, P-Gem-Dox increased the efficacy of the combination of gemcitabine and doxorubicin without increasing its toxicity, and it more strongly inhibited angiogenesis and induced apoptosis. These findings demonstrate that passively tumor-targeted polymeric drug carriers can be used for delivering two different chemotherapeutic agents to tumors simultaneously, and they thereby set the stage for more elaborate analyses on the potential of polymer-based multi-drug targeting.

1. Introduction

Drug targeting systems are nanometer-sized carrier materials designed for improving the biodistribution of systemically applied (chemo-) therapeutics. Various different drug targeting systems have been evaluated over the years, and clear evidence is currently available for substantial improvement of the therapeutic index of low molecular weight anticancer agents [1-4]. Promising results have recently also been obtained on the combination of tumor-targeted therapeutics with 'standard' chemotherapeutics: Doxil, for instance, i.e. PEGylated liposomal doxorubicin, has been successfully combined with gemcitabine, with cisplatin and with paclitaxel [5,6]; Myocet, i.e. non-PEGylated liposomal doxorubicin, with Herceptin and with paclitaxel [7]; and Abraxane, i.e. albumin-based paclitaxel, with Avastin and with gemcitabine [8,9].

Besides for such combination (i.e. 'co-administration') regimens, tumor-targeted nanomedicines have also been used for 'co-formulating' chemotherapeutics, i.e. for delivering two different pharmacologically active agents to tumors simultaneously. Sengupta and colleagues, for instance, recently demonstrated that treatment with a drug targeting system termed a 'Nanocell', which first releases the anti-angiogenic agent combrestatin (from the PEG-lipid shell) and subsequently the cytotoxic drug doxorubicin (from the polymeric core), was significantly more effective in inhibiting tumor growth than were all relevant control regimens [10]. They thereby extended the work of Mayer and coworkers, who co-encapsulated (optimal ratios of) doxorubicin and vincristine, irinotecan and floxuridine, and daunorubicin and cytarabine into liposomes [11-14], and who are currently evaluating the potential of the latter two formulations in clinical trials. Following up on this, Duncan and colleagues recently demonstrated that also polymeric drug carriers can be used for co-formulating (chemo-) therapeutics. They synthesized an HPMA (i.e. *N*-(2-hydroxypropyl)methacrylamide) -based polymer-drug conjugate carrying both doxorubicin and aminoglutethimide, and they demonstrated that treatment with this combination conjugate resulted in synergistic growth inhibition in vitro, as well as in advantageous interactions at the molecular level, as evidenced e.g. by the downregulation of (the anti-apoptotic protein) Bcl2 [15-17].

In spite of these promising in vitro findings, in vivo evidence for the potential of polymer-based multi-drug targeting has not yet been provided. Here, we have therefore synthesized an HPMA-based polymer-drug conjugate carrying both doxorubicin and gemcitabine, and we have evaluated its properties both in vitro and in vivo. HPMA copolymers were used because of their versatility, their biocompatibility and their beneficial biodistribution [3,18-22], and doxorubicin and gemcitabine were used because of the fact these two agents are also clinically routinely combined [23]. The newly generated construct, i.e. poly(HPMA-co-MA-GFLG-gemcitabine-co-MA-GFLG-doxorubicin-co-MA-TyrNH_2), was termed P-Gem-Dox, and it was shown to effectively kill cancer cells in vitro, to circulate for prolonged periods of time, to localize to tumors relatively selectively, and to inhibit tumor growth. These findings demonstrate that long-circulating and passively tumor-targeted polymeric drug carriers can be used for delivering multiple chemotherapeutic agents to tumors simultaneously.

2. Materials and methods

2.1. Materials

Methacryloyl chloride, 1-aminopropan-2-ol, 6-aminohexanoic acid, glycylphenylalanine, leucylglycine, 4,5-dihydrothiazole-2-thiol, 4-nitrophenol, *N,N'*-dicyclohexylcarbodiimide (DCC), 4-(dimethylamino)pyridine (DMAP), 2,2'-azobis(isobutyronitrile) (AIBN), *N,N*-dimethylformamide (DMF), dichloromethane (DCM), dimethyl sulfoxide (DMSO), doxorubicin hydrochloride (Dox.HCl), triethylamine (Et_3N), cathepsin B, ethylenediaminetetraacetic acid (EDTA) and reduced glutathione (GSH) were obtained from Fluka. Gemcitabine hydrochloride (Gem.HCl) was kindly provided by Eli Lilly. All chemicals and solvents were of appropriate analytical grade.

2.2. Synthesis of the monomers

N-(2-hydroxypropyl)methacrylamide (HPMA) was synthesized by reaction of methacryloyl chloride with 1-aminopropan-2-ol in DCM, in the presence of sodium carbonate [24]. *N*-Methacryloyl tyrosinamide (Ma-TyrNH_2) was prepared by reaction of methacryloyl chloride with tyrosinamide in distilled water [25]. *N*-methacryloyl glycyl-DL-phenylalanylleucylglycine (MA-GFLG-OH) was synthesized by Schotten-Baumann acylation of amino acids and oligopeptides

with methacryloyl chloride in an aqueous alkaline medium. *N*-methacryloyl glycyl-DL-phenylalanylleucylglycine 4-nitrophenyl ester (MA-GFLG-ONp) was prepared from this monomer as described in [26]. 3-(*N*-methacryloylglycyl-DL-phenylalanylleucylglycyl)thiazolidine-2-thione (MA-GFLG-TT) was synthesized by the reaction of MA-GFLG-OH with 4,5-dihydrothiazole-2-thiol in the presence of DCC and DMAP [27]. The monomer bearing thiazolidine-2-thione imide reactive groups (i.e. MA-GFLG-TT) was characterized by elemental analysis, by melting point analysis and by NMR. Elemental analysis (*calculated*/found): C=*55.60*/55.68, H=*6.28*/6.16, N=*12.46*/12.37 and S=*11.42*/10.81. Melting point: 136-138 °C. ^{1}H NMR [$(CD_3)_2SO$]: δ 0.84 d, 3H (CH_3-Leu); 0.89 d, 3H (CH_3-Leu); 1.30–1.70 m, 3H ($CHCH_2$-Leu); 1.84 s, 3H (CH_3); 2.70–3.10 m, 2H (β-Phe); 3.45 t, 2H (CH_2S); 3.50–3.75 m, 2H (Gly); 4.15–4.35 m, 1H (α-Leu); 4.45–4.75 m, 5H (CH_2N, Gly, α-Phe); 5.35 s, 1H (CH_2=); 5.69 s, 1H (CH_2=); 7.20 m, 5H (arom.); 8.01 d, 1H (NH-Phe); 8.10 m, 2H (NH-Gly); 8.25 t, 1H (NH-Leu).

2.3. Synthesis of the polymer precursors

The precursor containing tyrosinamide and thiazolidine-2-thione imide (TT) reactive groups, i.e. poly(HPMA-co-MA-TyrNH_2-co-MA-GFLG-TT), was prepared by solution radical copolymerization of HPMA, MA-TyrNH_2 and MA-GFLG-TT in DMSO at 60 °C for 6 h. The comonomer concentrations in the polymerization mixture were 12.5 wt-% and the concentration of AIBN was 2.0 wt-% [27]. After polymerization, the precursor was precipitated into a mixture of acetone : diethyl ether (3:1; v/v), the solvent mixture was filtered off, the precipitate was washed several times with acetone and diethyl ether, and it was dried in vacuum. Poly(HPMA-co-MA-GFLG-ONp), i.e. the precursor used for preparing P-Dox (i.e. poly(HPMA-co-MA-GFLG-doxorubicin)), was synthesized by precipitation radical copolymerization of HPMA and MA-GFLG-ONp in acetone [28]. The amounts of TT and ONp groups were determined spectrophotometrically, either in methanol (TT: ε_{305} = 10800 L.mol^{-1}.cm^{-1}) or in DMSO (ONp: ε_{274} = 9700 L.mol^{-1}.cm^{-1}).

2.4. Synthesis of P-Gem-Dox

P-Gem-Dox, i.e. the copolymer carrying both gemcitabine and doxorubicin, was synthesized from the precursor poly(HPMA-co-MA-TyrNH_2-co-MA-GFLG-TT) in two consecutive steps. Hereto, first, an appropriate amount of the precursor (0.6 g; 2.77 x 10^{-4} mol TT reactive groups; 1.0 mol-% tyrosinamide) was dissolved in an appropriate amount of dry pyridine (6 ml), and was added to a glass ampoule containing gemcitabine hydrochloride (0.083 g; 2.77 x 10^{-4} mol). The reaction

mixture was bubbled with argon and incubated in a water bath at 50 ºC for 18 h. The gemcitabine-containing precursor with remaining TT reactive groups (i.e. poly(HPMA-co-MA-TyrNH$_2$-co-MA-GFLG-gemcitabine-co-MA-GFLG-TT)), was then isolated by precipitation into a mixture of acetone : diethyl ether (3:1; v/v), the solvent mixture was filtered off, the copolymer was washed several times (with acetone and diethyl ether), and it was dried in vacuum. In the second step, this precursor was mixed with doxorubicin (0.045 g; 7.75 x 10^{-5} mol) in DMSO (3.5 ml), and Et_3N (30 µl) was added in three portions. The remaining TT reactive groups were then aminolyzed by the addition of 1-amino-propan-2-ol (10 µl), and the copolymer was precipitated into acetone : diethyl ether (2:1; v/v). Subsequently, the solvents were filtered off, and the reaction product (i.e. P-Gem-Dox; poly(HPMA-co-MA-GFLG-gemcitabine-co-MA-GFLG-doxorubicin-co-MA-TyrNH$_2$)) was washed, dried and purified (by gel filtration; on a Sephadex LH-20 column in methanol). The weight-average molecular weight of P-Gem-Dox was 23.5 kDa, its polydispersity was 1.6, and the amounts of gemcitabine and doxorubicin incorporated were 6.4 and 5.7 wt-%, respectively.

2.5. Synthesis of P-Gem, P-Dox and pHPMA

The conjugate carrying only gemcitabine (i.e. P-Gem; poly(HPMA-co-MA-GFLG-gemcitabine) was prepared using a comparable precursor and procedure as described above. In this case, however, the reaction time was prolonged (28 h vs. 18 h) and the gemcitabine concentration was increased (0.207 g; 6.89 x 10^{-4} mol) [21]. The weight-average molecular weight of P-Gem was 24.0 kDa, its polydispersity was 1.6, and its drug content was 10.9 wt-%. The conjugate carrying only doxorubicin (i.e. P-Dox; poly(HPMA-co-MA-GFLG-doxorubicin; also known as PK1) was synthesized by conjugating doxorubicin to poly(HPMA-co-MA-GFLG-ONp) in DMSO, in the presence of Et_3N [18,24,26]. The reaction product was isolated by precipitation into acetone : diethyl ether (2:1; v/v), washed several times, dried in vacuum, and purified by gel filtration. The weight-average molecular weight of P-Dox was 28.3 kDa, its polydispersity was 1.5, and its drug content was 8.7 wt-%. A drug-free control copolymer, used as a reference in the in vitro cytotoxicity and the in vivo biodistribution analyses, was synthesized by copolymerizing HPMA and MA-TyrNH$_2$ in DMSO, using AIBN as an initiator [25]. The weight-average molecular weight of this copolymer, i.e. poly(HPMA-co-MA-TyrNH$_2$), was 30.5 kDa, its polydispersity was 1.3, and the amount of tyrosinamide, included to allow for radiolabeling, was 0.8 mol-%.

2.6. Characterization of the copolymers

The weight-average molecular weight (M_w) and the polydispersity (M_w/M_n) of the copolymers (after aminolysis of TT and ONp reactive groups with 1-aminopropan-2-ol) were determined by size exclusion chromatography on a Shimadzu 10A HPLC system, equipped with a UV/VIS detector, an Optilab® rEX refractometer, and a DAWN® 8™ multiangle light scattering detector (Wyatt Technology Corp.), using a Superose 6™ column (Amersham Bioscience). Sodium acetate buffer (0.3 M; pH 6.5) containing 0.5 g/l sodium azide was used as the mobile phase. The flow rate was 0.5 ml/min. The amounts of gemcitabine and doxorubicin incorporated were determined spectrophotometrically, using molar extinction coefficients of ε_{299} = 5710 $l*mol^{-1}*cm^{-1}$ and ε_{484} = 13500 $l*mol^{-1}*cm^{-1}$, respectively.

2.7. Drug release

The release of gemcitabine and doxorubicin from P-Gem-Dox, P-Gem and P-Dox was investigated at pH 6, in the presence of cathepsin B (which cleaves GFLG-bonds [16,18,20]). The concentration of cathepsin B was 5.0 x 10^{-7} mol/l, and its activity was standardized using the standard substrate *N*-α-benzoyl-L-arginine 4-nitroanilide (BzArgNAp). Gemcitabine release was determined directly in the reaction mixture, and it was quantified by means of HPLC (UV detection). Doxorubicin release was determined after extraction of the incubation mixture into chloroform. Hereto, the sample (in buffer solution, i.e. 0.2 M Na_2CO_3/$NaHCO_3$ plus 4 M NaCl, pH=9.8) was mixed with chloroform, it was extracted into the organic phase, and the amounts of (released) doxorubicin were determined spectrophotometrically.

2.8. In vitro efficacy

The cytotoxicity of P-Gem-Dox, P-Gem, P-Dox, pHPMA, free gemcitabine and free doxorubicin was determined by seeding 200 Dunning AT1 rat prostate carcinoma cells into 6-well plates, and by continuously incubating the cells with increasing concentrations of the abovementioned agents. P-Gem-Dox, P-Gem and P-Dox were administered at doses equivalent to those used for the free agents. A drug-free control copolymer was used at concentrations normalized to the amounts of copolymer used for P-Gem and P-Dox After 8-10 days, i.e. as soon as sufficient numbers of colonies had formed in PBS treated control wells, the cells were fixed and stained (with crystal violet), and the number of surviving colonies was counted.

2.9. Biodistribution

The biodistribution of P-Gem-Dox was compared to that of a drug-free control copolymer (i.e. poly(HPMA-co-MA-TyrNH_2)). Both copolymers were radiolabeled with iodine-131 using the Iodogen method, as described in [29]. Five hundred microliters of 0.1 mM solution (based on copolymer concentration; corresponding to a radioactivity of ~150 µCi) were injected i.v. into male Copenhagen rats bearing subcutaneous Dunning AT1 tumors. At several time points post i.v. injection (p.i.), the concentrations of the copolymers in systemic circulation were determined by withdrawing 50 µl of blood from the tail veins of the rats, and by assuming that the complete blood pool equals 6% of their body weight. At 0.5 (obtained after keeping the animals under general anesthesia for 30 min), at 4 and at 24 h p.i., the biodistribution of the copolymers was visualized using a Searle-Siemens scintillation camera. At 24 h p.i., animals were then sacrificed, and tumors and organs were harvested for quantification. The residual amounts of radioactivity were determined using a gamma counter, they were corrected for radioactive decay and they were expressed as percent of the injected dose per gram tissue.

2.10. In vivo efficacy

All experiments involving animals were approved by an external committee for animal welfare and were performed according to the guidelines for laboratory animals established by the German government. Experiments were performed on 6-12 month old male Copenhagen rats, using the syngeneic and aggressively growing Dunning AT1 prostate carcinoma model. Fresh pieces (~10 mm^3) of an AT1 donor tumor were transplanted subcutaneously into both hind limbs of the animals, and prior to treatment, tumors were grown for 6 to 8 days, until they reached an average diameter of ~6 mm. All agents were applied once weekly for three weeks, at days 1, 8 and 15. Doses were based on half the maximum tolerated dose of free doxorubicin in rats (MTD = 7.5 mg/kg), as well as on the weight-ratio of both chemotherapeutic agents in P-Gem-Dox (6.4 wt-% Gem; 5.7 wt-% Dox). Therefore, the 50% MTD regimen of free doxorubicin plus free gemcitabine consisted of 3 x 1.25 mg/kg doxorubicin and 3 x 1.40 mg/kg gemcitabine. P-Dox and P-Gem, given their drug contents of 8.7 and 10.9 wt-%, were applied at 3 x 14.4 mg/kg and 3 x 12.8 mg/kg, respectively. P-Gem-Dox, which contains 6.4 wt-% gemcitabine and 5.7 wt-% doxorubicin, was applied at a dose equivalent to this regimen, i.e. at 3 x 21.9 mg/kg (which also corresponds to 3 x 1.25 mg/kg doxorubicin and 3 x 1.40 mg/kg gemcitabine). In addition to

this, P-Gem-Dox was also applied at 25% and 75% of the MTD of free doxorubicin, i.e. at 3 x 11.0 mg/kg and 3 x 32.9 mg/kg, respectively. Tumor volumes were calculated using the formula $V=(a*(b*b))/2$, and they were expressed relative to the tumor volume determined on the first day of therapy. The toxicity of the above regimens was determined by monitoring the (relative) weight loss of the animals.

2.11. Histological analysis

For the histological and fluorescence microscopy analyses, four representative tumors were harvested per experimental group (one week after the end of therapy; at day 22), and 6 µm cryosections were prepared. Blood vessels were stained in methanol/acetone-fixed cryosections, using a 1:50 dilution of a mouse monoclonal antibody against rat CD31 (MAB1393; Chemicon), and a 1:100 dilution of an Alexa-555-labeled goat anti-mouse antibody (A21424; Molecular Probes). Apoptotic cells were stained by means of TUNEL, i.e. by Terminal deoxynucleotidyl Transferase Biotin-dUTP Nick End Labeling (In situ cell death kit; Roche). Cryosections were counterstained with DAPI, and visualized under a Nikon Eclipse E600 fluorescence microscope. Images were obtained at a magnification of 200x, and were analyzed using Nikon Imaging Software.

2.12. Statistical analysis

Values are expressed as average ± s.d. (drug release, in vitro efficacy, biodistribution and histological analyses) or as average ± s.e.m. (in vivo efficacy analyses). In case of the former, the two-tailed Student's t-test was used to address statistical significance, and in case of the latter, the Mann-Whitney U (i.e. Wilcoxon Ranksum) test was used. Bonferroni-Holm post-hoc analysis was used to correct for multiple comparisons. In all cases, $p<0.05$ was considered to represent statistical significance.

3. Results

3.1. Synthesis and characterization of P-Gem-Dox

In the first reaction step, the monomers *N*-(2-hydroxypropyl)methacrylamide (HPMA; **1**), *N*-methacryloyl tyrosinamide (MA-TyrNH_2; **2**) and 3-(*N*-methacryloylglycyl-DL-phenylalanylleucylglycyl)thiazolidine-2-thione (MA-GFLG-TT; **3**) were polymerized in DMSO, using AIBN as an initiator (see Figure 1). This reaction yielded precursor copolymer **4**, i.e. poly(HPMA)-co-(MA-GFLG-TT)-co-(MA-TyrNH_2), which contained ~8 mol-% of thiazolidine-2-thione (TT) groups and ~1 mol-% of tyrosinamide (included to allow for radiolabeling). Subsequently, gemcitabine was conjugated to about two-thirds of the TT reactive groups in this precursor in pyridine, giving rise to copolymer **5.** Finally, doxorubicin was conjugated to the remaining TT reactive groups in copolymer **5** in DMSO, in the presence of Et_3N. The final product, i.e. poly(HPMA)-co-(MA-GFLG-gemcitabine)-co-(MA-GFLG-doxorubicin)-co-(MA-TyrNH_2), was termed P-Gem-Dox (**6**), and was found to have a weight-average molecular weight of 24 kDa and a polydispersity of 1.6 (Table 1). P-Gem-Dox was found to contain 6.4 wt-% of gemcitabine, 5.7 wt-% of doxorubicin and 1.0 mol-% of tyrosinamide. The copolymers containing only gemcitabine (i.e. P-Gem; poly(HPMA-co-MA-GFLG-gemcitabine)) and only doxorubicin (i.e. P-Dox; poly(HPMA-co-MA-GFLG-doxorubicin)) were used for control purposes, and were synthesized according to comparable procedures (see Methods section and Table 1).

Polymer	Chemical nature	MW	PD	Gem	Dox	TyrNH_2
pHPMA	poly(HPMA-co-MA-TyrNH2)	30.5	1.3	-	-	0.8 mol-%
P-Dox	poly(HPMA-co-MA-GFLG-doxorubicin)	28.3	1.5	-	8.7 wt-%	-
P-Gem	poly(HPMA-co-MA-GFLG-gemcitabine)	24.0	1.6	10.9 wt-%	-	-
P-Gem-Dox	poly(HPMA-co-MA-GLFG-gemcitabine-co-MA-GFLG-doxorubicin-co-MA-TyrNH2)	23.5	1.6	6.4 wt-%	5.7 wt-%	1.0 mol-%

Table 1: Characteristics of the copolymers used in this study. MW: Molecular weight (in kDa). PD: Polydispersity (M_w/M_n).

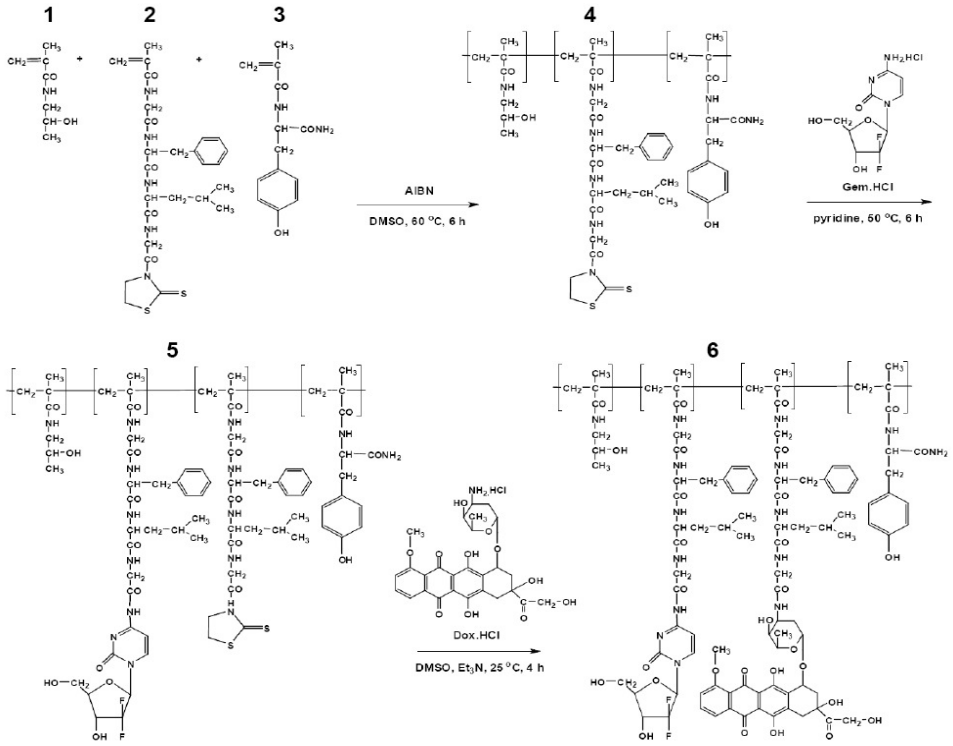

Figure 1: Synthesis and structure of P-Gem-Dox. P-Gem-Dox was synthesized in three steps. First, the monomers HPMA (1), MA-GFLG-TT (2) and MA-TyrNH$_2$ (3) were copolymerized in DMSO, using AIBN as an initiator. Subsequently, gemcitabine was conjugated to this precursor (4) in pyridine, yielding a copolymer containing besides gemcitabine several residual TT reactive groups (5). Finally, doxorubicin was conjugated to the remaining TT reactive groups in DMSO, in the presence of Et$_3$N. The resulting 24 kDa copolymer, i.e. poly(HPMA-co-MA-GFLG-gemcitabine-co-MA-GFLG-doxorubicin-co-MA-TyrNH$_2$) (6), was termed P-Gem-Dox, and was shown to contain 5.7 wt-% of gemcitabine, 6.4 wt-% of doxorubicin and 1.0 mol-% of tyrosinamide.

3.2. Release of gemcitabine and doxorubicin from P-Gem-Dox

To evaluate drug release from P-Gem-Dox, the conjugate was incubated with the lysosomal cysteine protease cathepsin B (which cleaves GFLG linkages) at pH 6, resembling endo- and lysosomal conditions. As shown in Figure 2, P-Gem-Dox effectively released both agents over time, in a manner corresponding closely to that observed for the two parental copolymers, i.e. for P-Gem and P-Dox. It should be noted, though, that especially at early time points, the release of gemcitabine from P-Gem-Dox was somewhat slower than its release from B-Gem (e.g. 75% vs. 95% at 3 h; $p<0.05$), which can likely be explained competition for the same enzyme. The release data in Figure 2 furthermore

demonstrate that gemcitabine is released from the copolymer much more rapidly than doxorubicin. This likely results from the fact that gemcitabine is substantially smaller than doxorubicin, and therefore likely causes less steric hindrance towards enzymatic cleavage.

3.3. In vitro efficacy

The in vitro efficacy of P-Gem-Dox was evaluated by subjecting Dunning AT1 rat prostate carcinoma cells to increasing concentrations of free and HPMA copolymer-bound chemotherapeutics, and by evaluating their clonogenic survival approximately one week later. Figure 3A shows that when administered at doxorubicin-equivalent concentrations, P-Gem-Dox was more than a hundred-fold more effective in inhibiting clonogenic survival than was the free drug (IC_{50} ~2 nM doxorubicin-equivalent, as compared to ~300 nM for free doxorubicin). This can be explained by taking into account that AT1 cells are much more sensitive to gemcitabine (IC_{50} ~3 nM; Figure 3B) than to doxorubicin (IC_{50} ~300 nM; Figure 3A). When subsequently comparing the in vitro efficacy of P-Gem-Dox to that of free and copolymer-bound gemcitabine, it was found to be slightly less effective than the free drug (IC_{50} ~5 nM gemcitabine-equivalent, as compared to ~3 nM for free gemcitabine), but to be more effective that P-Gem (IC_{50} ~5 nM vs. ~9 nM). This observation indicates that though moderately, the co-conjugation of doxorubicin enhances the in vitro efficacy of copolymer-bound gemcitabine, in spite of the fact that under these conditions, its relative levels are more than a hundred-fold lower than its IC_{50}.

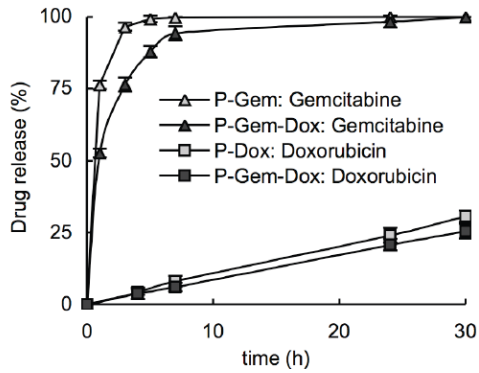

Figure 2: Drug release. The release of gemcitabine and doxorubicin from P-Gem-Dox was evaluated by incubating the conjugate with cathepsin B (which cleaves GFLG linkages) at pH=6, and by comparing its release rates to those of P-Dox and P-Gem. Values represent average ± s.d. (n=3).

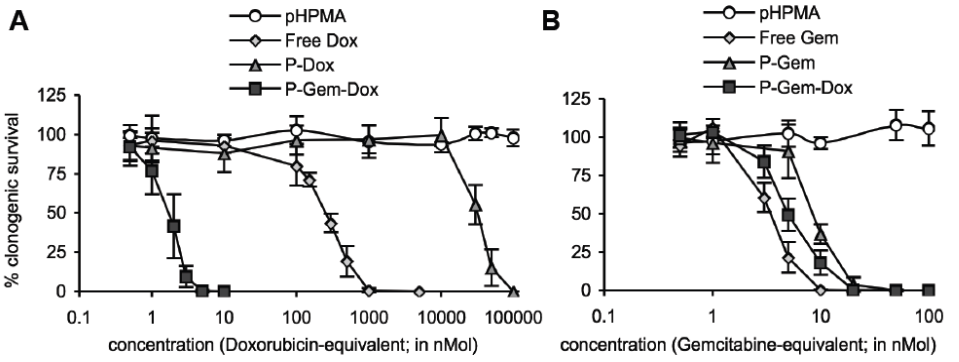

Figure 3: In vitro efficacy. A: Clonogenic survival of Dunning AT1 rat prostate carcinoma cells upon incubation with free doxorubicin, with P-Dox, with P-Gem-Dox and with a drug-free control copolymer. P-Dox (8.7 wt-% Dox) and P-Gem-Dox (5.7 wt-% Dox) were administered at doxorubicin-equivalent concentrations. Values are average ± s.d. (n=3). B: Clonogenic survival of Dunning AT1 cells upon incubation with free gemcitabine, with gemcitabine-equivalent concentrations of P-Gem (10.9 wt-% Gem) and of P-Gem-Dox (6.4 wt-% Gem), and with a drug-free control copolymer. Values are average ± s.d. (n=3).

3.4. Biodistributional analysis

To evaluate the in vivo behavior of P-Gem-Dox, the tyrosinamide groups incorporated into the copolymer were radiolabeled with iodine-131, and the conjugate was injected i.v. into rats bearing subcutaneous Dunning AT1 tumors. A 31 kD drug-free control copolymer (containing 0.8 % tyrosinamide) was used as a reference. At several different time points post i.v. injection (p.i.), scintigrams were obtained for visualizing the biodistribution of the copolymers (Figure 4A), and blood samples were collected for kinetic analyses (Figure 4B). When comparing the concentrations of the copolymers in blood, P-Gem-Dox was found to be cleared more rapidly than the drug-free control copolymer. It did, however, present with very acceptable long-circulating properties: at 4 and 24 h p.i., for instance, ~21 and ~9 % of the injected dose could still be detected in blood, respectively (Figure 4B). This observation is in line with the scintigrams in Figure 4A, which demonstrate that at 0.5 and 4 h p.i., significant amounts of P-Gem-Dox were still localized to the heart (which represents the amounts of copolymer still residing in systemic circulation). The scintigrams furthermore demonstrate that both pHPMA and P-Gem-Dox were primarily cleared by means of renal filtration, as evidenced by the high levels of radioactivity present in the bladder at 0.5 h p.i. (Figure 4A). At later time points, the control copolymer primarily localized in spleen, liver, lung and tumor, while P-Gem-Dox primarily

accumulated in kidney (Figure 4A). This phenomenon can be explained by taking into account that certain heavily modified (e.g. drug-functionalized) HPMA copolymers have a general tendency to accumulate in kidney [21,30,31]. At 24 h p.i., tumors and organs were harvested for quantification, and it was found that with 11.9% of the injected dose per gram tissue, the highest amount of P-Gem-Dox had indeed accumulated in kidney, followed by spleen (1.12±0.08 %ID/g) and by tumor (0.48±0.10 %ID/g; Figure 4C). In all other organs, the levels of the conjugate were lower than in tumors, in line with what was observed for the drug-free copolymer. This notion was confirmed by determining the tumor-to-organs ratios for pHPMA and for P-Gem-Dox at 24 h p.i., which showed that both unfunctionalized and functionalized HPMA copolymers localize to tumors relatively selectively, with higher levels in tumors than in 7 out of 9 healthy tissues (Figure 4D).

3.5. In vivo efficacy

The efficacy and the toxicity of P-Gem-Dox were compared to those of (dose-equivalent) combination regimens of free gemcitabine plus free doxorubicin, and of P-Dox and P-Gem. Agents were applied once weekly for three weeks, and doses were based on half the MTD of free doxorubicin (Maximum Tolerated Dose = 7.5 mg/kg), as well as on the weight-ratio of gemcitabine and doxorubicin in P-Gem-Dox (6.4 / 5.7 = 1.12; see Table 1). Thus, given a 50% MTD dose of 3.75 mg/kg for free doxorubicin, three 1.25 mg/kg doses of the drug were combined with three 1.40 (i.e. 1.12 x 1.25) mg/kg of free gemcitabine. Analogously, three 14.4 mg/kg doses of P-Dox (8.7 wt-%: 1.25 mg/kg doxorubicin) were combined with 12.8 mg/kg P-Gem (10.9 wt-%: 1.40 mg/kg gemcitabine). P-Gem-Dox, which contains 5.7 wt-% of doxorubicin and 6.4 wt-% of gemcitabine, was administered at three doses of 21.9 mg/kg, which also corresponds to 3 x 1.25 mg/kg of doxorubicin and to 3 x 1.40 mg/kg of gemcitabine. In addition to this 50% MTD regimen, P-Gem-Dox was also applied at doses equivalent to 25% and 75% of the MTD of free doxorubicin, i.e. at 3 x 11.0 and at 3 x 32.9 mg/kg, respectively.

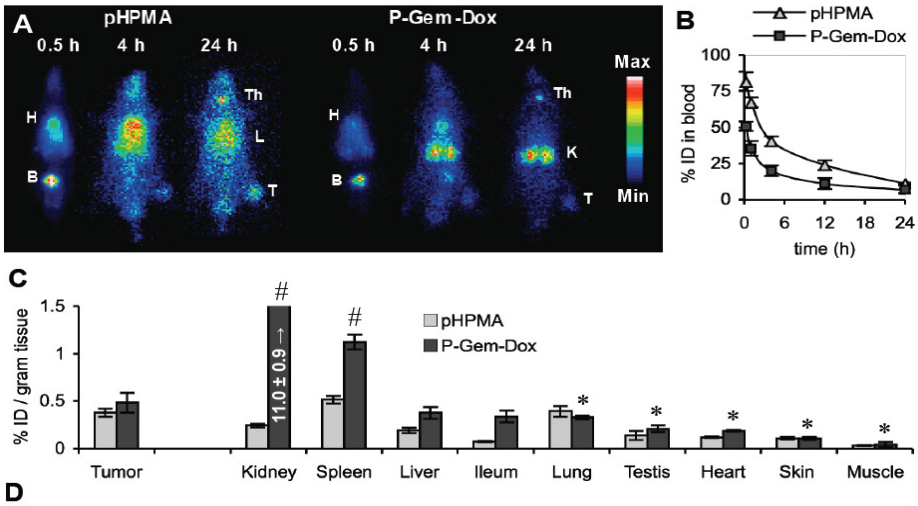

D

T/O Ratio	Tumor	Kidney	Spleen	Liver	Ileum	Lung	Testis	Heart	Skin	Muscle
pHPMA	1	1.55	0.73	1.97	4.97	0.96	2.76	3.17	3.49	12.04
P-Gem-Dox	1	0.04	0.43	1.29	1.43	1.47	2.31	2.58	4.52	11.53

*Figure 4: Biodistribution. A: Scintigraphic analysis of the biodistribution of iodine-131-labeled P-Gem-Dox (24 kDa) and of a radiolabeled drug-free control copolymer (31 kDa) upon i.v. injection into Copenhagen rats bearing subcutaneous Dunning AT1 tumors. At 0.5 h p.i., both copolymers primarily localized to heart (H; representative of the amount still present in circulation) and to bladder (B; confirming renal excretion). At 4 and 24 h p.i., P-Gem-Dox primarily localized to kidney (K), as well as to some extent to tumors (T), whereas the 31 kDa control copolymer primarily accumulated in tumors (T), and in liver, lung and spleen (collectively indicated by L). Note that accumulation in thyroid (Th) corresponds to released radioactive iodine. B: Analysis of the levels of P-Gem-Dox and of the drug-free control copolymer in blood. Values represent average ± s.d. (n=4-6). C: Quantification of the tumor and organ concentrations of the two radiolabeled copolymers at 24 h p.i. Values are expressed as percentages of the injected dose per gram tissue, and represent average ± s.d. (n=4-6). * Indicates significantly lower levels as in tumors (p<0.05), and # indicates significantly higher levels (p<0.05). D: Quantification of the tumor-to-organ ratios of the two copolymers at 24 h p.i., pointing out (in green) that they localize more selectively to tumors than to 7 out of 9 healthy tissues. See page 238.*

As shown in Figure 5A, all treatments except for the 25% MTD regimens of P-Gem-Dox, were found to be significantly more effective than saline in inhibiting AT1 tumor growth. One week after the end of therapy, for instance, free gemcitabine plus free doxorubicin had reduced tumor growth by ~30% as compared to controls ($p<0.05$); P-Gem plus P-Dox by ~40% ($p<0.05$); and P-Gem-Dox applied at the 50% MTD regimen by ~50% ($p<0.005$). P-Gem-Dox applied at 75% of the MTD of free doxorubicin was found to be even more effective, inhibiting tumor growth by ~60% ($p<0.005$). As compared to the

combination of free doxorubicin plus free gemcitabine, only the 50% and 75% MTD regimen of P-Gem-Dox significantly improved antitumor activity ($p<0.05$ and $p<0.005$, respectively), and as compared to the combination of P-Gem and P-Dox, only the 75% MTD regimen of P-Gem-Dox was found to be more effective ($p<0.05$; Figure 5A). Simultaneous monitoring of the body weight of the animals showed that all treatments were relatively well-tolerated: control animals and animals treated with the lowest dose of P-Gem-Dox did not show any weight loss, and animals treated with all other regimens lost at maximum ~5% of their initial weight ($p<0.05$; Figure 5B). These findings demonstrate that the simultaneous delivery of doxorubicin and gemcitabine increases the efficacy of combination chemotherapy without increasing its toxicity.

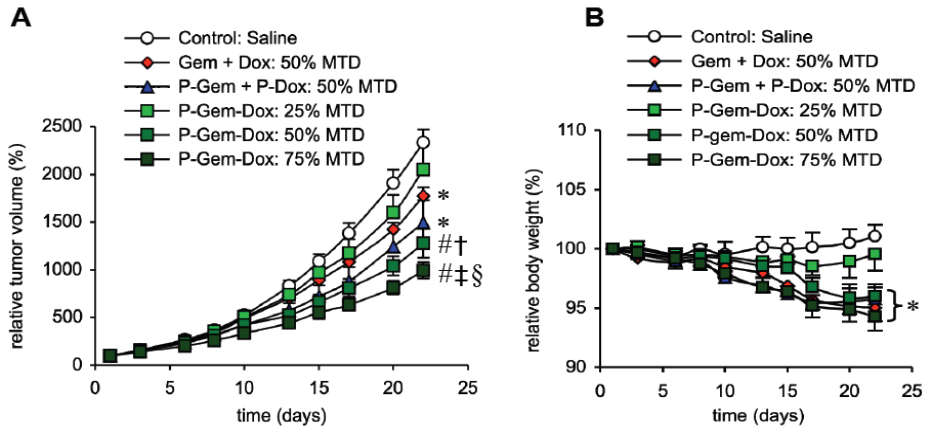

*Figure 5: In vivo efficacy. A: Growth inhibition of subcutaneously transplanted Dunning AT1 tumors induced by three i.v. injections (days 1, 8 and 15) of saline, of 1.4 mg/kg gemcitabine plus 1.25 mg/kg doxorubicin (Gem + Dox: 50% MTD), of 12.8 mg of P-Gem plus 14.4 mg/kg of P-Dox (10.9 wt-% and 8.7 wt-%, respectively; P-Gem + P-Dox: 50% MTD), and of 21.9 mg/kg of P-Gem-Dox (5.7 and 6.4 wt-%, respectively; P-Gem-Dox: 50% MTD). For the 25% and 75% MTD regimens, P-Gem-Dox was administered at 3 x 11.0 mg/kg and at 3 x 32.9 mg/kg, respectively. Values represent average ± s.e.m. (n-6). * Indicates $p<0.05$ vs. control, # indicates $p<0.005$ vs. control, † indicates $p<0.05$ vs. free gemcitabine plus free doxorubicin, ‡ indicates $p<0.005$ vs. free gemcitabine plus free doxorubicin, and § indicates $p<0.05$ vs. P-Gem plus P-Dox. B: Weight loss induced by the abovementioned treatment regimens. * Indicates $p<0.05$ vs. control.*

3.6. Effect of drug treatment on angiogenesis and apoptosis

To investigate how polymer-based multi-drug targeting reflects on angiogenesis and apoptosis, cryosections were prepared from four tumors per experimental group and were analyzed by means of fluorescence microscopy. CD31-staining was used to evaluate the impact of drug treatment on blood vessel density, and TUNEL-staining was used to assess apoptosis induction. As shown in Figure 6A,

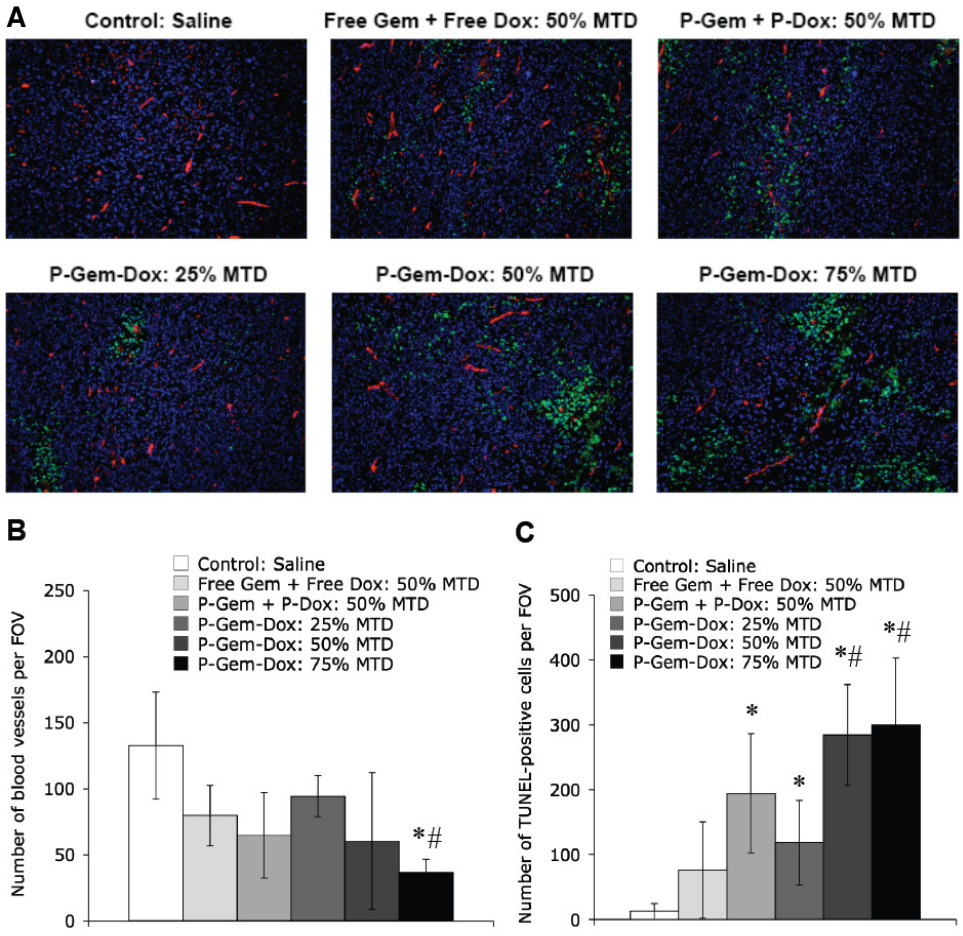

*Figure 6: Effect of drug treatment on angiogenesis and apoptosis. A: Cryosections were obtained one week after the end of therapy (i.e. at day 22; from four tumors per experimental group), and blood vessels and apoptotic cells were stained using antibodies against CD31 (red) and TUNEL (green), respectively. Images were counterstained with DAPI. B and C: Quantification of the number of CD31- and TUNEL-positive structures per 200x field of view (FOV). Values represent average ± s.d. (n=4). * Indicates p<0.05 vs. control, and # indicates p<0.05 vs. free gemcitabine plus free doxorubicin. See page 239.*

all treatments substantially affected the number of CD31- and TUNEL-positive cells. Figure 6A furthermore shows that targeted therapeutics were more effective in doing so than were free doxorubicine and gemcitabine, more strongly reducing the number of (neo-angiogenic) blood vessels, and more markedly inducing apoptosis. It should be noted, however, that the distribution of blood vessels and apoptotic cells was relatively heterogeneous, even within single

tumors and treatment groups (as evidenced by the large standard deviations in Figures 6B and 6C). In spite of this, several significant differences could be observed when quantifying the cryosections: the 75% MTD regimen of P-Gem-Dox significantly reduced blood vessel density as compared to saline and to the combination of free gemcitabine plus free doxorubicin ($p<0.05$; Figure 6B); all polymer-based agents significantly increased the number of apoptotic cells as compared to saline ($p<0.05$ for 25% MTD; $p<0.005$ for others; Figure 6C); and both the 50% and 75% MTD regimen of P-Gem-Dox significantly increased the number of apoptotic cells as compared to free doxorubicin plus free gemcitabine ($p<0.05$; Figure 6C). An additional interesting observation in the images in Figure 6A relates to the ratio of small (i.e. neoangiogenic) versus large (i.e. more mature, and generally better perfused) blood vessels, which decreased according to treatment response. The strongest effects were observed for P-Gem-Dox and for P-Gem plus P-Dox, which hints towards an enhanced 'vessel normalization' in tumors treated with targeted therapeutics [32,33].

4. Discussion

Copolymers based on *N*-(2-hydroxypropyl)methacrylamide (HPMA) are prototypic and well-characterized polymeric drug carriers that have been broadly implemented in the delivery of anticancer agents [18,19]. Over the years, various different types of drugs have been conjugated to HPMA copolymers, ranging from standard low molecular weight therapeutics, like doxorubicin [34], cisplatin [35] and paclitaxel [36], to more sophisticatedly acting agents, like the heat shock protein-inhibitor geldanamycin [37] and the anti-angiogenic agent TNP-470 [38]. Promising results have been obtained in a large number of animal experiments, and five different HPMA-based polymeric nanomedicines have entered clinical trials [3,18,19]. To date, however, none of these 'first-generation' polymer therapeutics has managed to gain FDA and/or EMEA approval.

Attempts to improve the efficacy of HPMA copolymer-based nanomedicines have focused on the incorporation of targeting moieties (like antibodies and peptides [39-41]), on the development of biodegradable high molecular weight grafts (prepared using semi-telechelic precursors [42,43]), and on the establishment of more optimal mechanisms for drug release (e.g. using pH-responsive hydrazones [20,44]). Additional efforts have elaborated on the

combination of HPMA-based polymeric nanomedicines with other treatment modalities, e.g. with radiotherapy [22,25], with photodynamic therapy [45,46], and with chemotherapy [47]. Furthermore, polymer therapeutics have been shown to combine well with each other, as evidenced e.g. by the synergistic growth inhibitory effects induced by the combination of HPMA copolymer-bound doxorubicin and HPMA copolymer-bound mesochlorin e_6 [48,49]. And finally, as an alternative to the abovementioned combination (i.e. co-administration) regimens, HPMA copolymers have recently been used for co-formulating chemotherapeutics, i.e. for delivering two different anticancer agents to tumor cells simultaneously. Doxorubicin and aminoglutethimide were co-conjugated to same copolymer, and the construct was shown to present with more optimal release rates, with an improved in vitro efficacy, and with beneficial interactions at the molecular level [15-17].

To extend the above efforts, and to provide in vivo evidence for the potential of polymer-based multi-drug targeting, we have here synthesized an HPMA-based polymer-drug conjugate carrying 6.4 wt-% gemcitabine and 5.7 wt-% doxorubicin (as well as 1 mol-% of tyrosinamide; to allow for radiolabeling). The resulting 24 kDa conjugate was termed P-Gem-Dox, and it was evaluated both in vitro and in vivo. In vitro, P-Gem-Dox was found to effectively release both agents over time, and to kill cancer cells at low nanomolar concentrations. Gemcitabine and doxorubicin were released from the copolymer at rates comparable to those observed for P-Gem and for P-Dox, and gemcitabine was found to be released much more rapidly than was doxorubicin. The former observation contrasts with the results obtained by Duncan and colleagues, who observed that the co-conjugation of doxorubicin enhanced aminoglutethimide release [15], and the latter is in line with their findings, demonstrating that smaller agents, like gemcitabine (299 Da) and aminoglutethimide (232 Da), are released from HPMA copolymers much more rapidly than are higher molecular weight drugs, like doxorubicin (543 Da) [15].

In vivo, using radiolabeled copolymers and 2D scintigraphic imaging, we subsequently showed that P-Gem-Dox circulates for prolonged periods of time, and localizes to tumors more effectively than to 7 out of 9 healthy tissues. The highest levels of the conjugate were found in the kidney, which is in line with previous findings on (heavily) functionalized HPMA copolymers [21,30,31]. This notion on the one hand underlines the importance of monitoring kidney function

when intending to treat patients with (HPMA-based) polymeric nanomedicines, but it on the other hand also suggests that polymer therapeutics might hold significant potential for treating kidney disorders, like renal fibrosis and renal cell carcinoma. Through in vivo efficacy analyses, we finally demonstrated that P-Gem-Dox more strongly inhibits the growth of Dunning AT1 tumors than do combinations of free and HPMA copolymer-bound drugs. Growth inhibition was achieved in a rapidly growing and therapy-resistant tumor model, and P-Gem-Dox increased the efficacy of the intervention without increasing its toxicity. These findings demonstrate that polymers, as liposomes, can be used for delivering multiple chemotherapeutic agents to tumors simultaneously, and they thereby set the stage for more elaborate analyses on the potential of polymer-based multi-drug targeting.

5. Conclusion

Using HPMA copolymers as a model drug delivery system, and doxorubicin and gemcitabine as model drugs, we here show that polymeric drug carriers can deliver multiple chemotherapeutic agents to tumors simultaneously. A polymer-drug conjugate carrying 6.4 wt-% of gemcitabine, 5.7 wt-% of doxorubicin and 1.0 mol-% of tyrosinamide was synthesized, and it was shown to kill cancer cells in vitro, to circulate for prolonged periods of time, to accumulate in tumors, and to inhibit tumor growth. These findings provide in vivo evidence for the potential of polymer-based multi-drug targeting, and they suggest that multifunctional polymer therapeutics might hold significant clinical potential.

References

1. Moses MA, Brem H, Langer R. Advancing the field of drug delivery: taking aim at cancer. Cancer Cell 2003;4:337-341.
2. Torchilin VP. Recent advances with liposomes as pharmaceutical carriers. Nat Rev Drug Discov 2005;4:145-160.
3. Duncan R. Polymer conjugates as anticancer nanomedicines. Nat Rev Cancer 2006;6:688-701.
4. Lammers T, Hennink WE, Storm G. Tumor-targeted nanomedicines: Principles and Practice. Br J Cancer 2008;99:900-910
5. Adamo V, Lorusso V, Rossello R, Adamo B, Ferraro G, Lorusso D, et al. Pegylated liposomal doxorubicin and gemcitabine in the front-line treatment of recurrent/metastatic breast cancer: a multicentre phase II study. Br J Cancer 2008;98:1916-1921.
6. Gibbs DD, Pyle L, Allen M, Vaughan M, Webb A, Johnston SR, et al. A phase I dose-finding study of a combination of pegylated liposomal doxorubicin (Doxil), carboplatin and paclitaxel in ovarian cancer. Br J Cancer 2002;86:1379-1384.
7. Trigo J, Climent MA, Lluch A, Gascon P, Hornedo J, Gil M, et al. Liposomal doxorubicin Myocet(R) in combination with Herceptin(R) and paclitaxel is active and well tolerated in patients with HER2-positive locally advanced or metastatic breast cancer: a phase II study. Breast Cancer Res Treat 2004;82 Suppl 1:S83.
8. Moreno-Aspitia A, Perez EA. North Central Cancer Treatment Group N0531: Phase II Trial of weekly albumin-bound paclitaxel (ABI-007; Abraxane) in combination with gemcitabine in patients with metastatic breast cancer. Clin Breast Cancer 2005;6:361-364.
9. C Lobo, G Lopes, O Silva, S Gluck. Paclitaxel albumin-bound particles (abraxane) in combination with bevacizumab with or without gemcitabine: early experience at the University of Miami/Braman Family Breast Cancer Institute. Biomed Pharmacother 2007;61:531-533.
10. Sengupta S, Eavarone D, Capila I, Zhao G, Watson N, Kiziltepe T, et al. Temporal targeting of tumour cells and neovasculature with a nanoscale delivery system. Nature 2005;436:568-572.
11. Mayer LD, Harasym TO, Tardi PG, Harasym NL, Shew CR, Johnstone SA, et al. Ratiometric dosing of anticancer drug combinations: controlling drug ratios after systemic administration regulates therapeutic activity in tumor-bearing mice. Mol Cancer Ther 2006;5:1854-1863.
12. Abraham SA, McKenzie C, Masin D, Ng R, Harasym TO, Mayer LD, et al. In vitro and in vivo characterization of doxorubicin and vincristine coencapsulated within liposomes through use of transition metal ion complexation and pH gradient loading. Clin Cancer Res 2004;10:728-738.
13. Tardi PG, Gallagher RC, Johnstone S, Harasym N, Webb M, Bally MB, et al. Coencapsulation of irinotecan and floxuridine into low cholesterol-containing liposomes that coordinate drug release in vivo. Biochim Biophys Acta 2007;1768:678-687.
14. Tardi P, Johnstone S, Harasym N, Xie S, Harasym T, Zisman N, et al. In vivo maintenance of synergistic cytarabine:daunorubicin ratios greatly enhances therapeutic efficacy. Leuk Res 2009;33:129-139.
15. Vicent MJ, Greco F, Nicholson RI, Paul A, Griffiths PC, Duncan R. Polymer therapeutics designed for a combination therapy of hormone-dependent cancer. Angew Chem Int Ed Engl 2005;44:4061-4066.
16. Greco F, Vicent MJ, Penning NA, Nicholson RI, Duncan R. HPMA copolymer-aminoglutethimide conjugates inhibit aromatase in MCF-7 cell lines. J Drug Target 2005;13:459-470.
17. Greco F, Vicent MJ, Gee S, Jones AT, Gee J, Nicholson RI, et al. Investigating the mechanism of enhanced cytotoxicity of HPMA copolymer-Dox-AGM in breast cancer cells. J Control Release 2007;117:28-39.
18. Kopecek J, Kopeckova P, Minko T, Lu Z. HPMA copolymer-anticancer drug conjugates: design, activity, and mechanism of action. Eur J Pharm Biopharm 2000;50:61-81.
19. Rihova B, Kubackova K. Clinical implications of N-(2-hydroxypropyl)-methacrylamide copolymers. Curr Pharm Biotechnol 2003;4:311-22.
20. Ulbrich K, Subr V. Polymeric anticancer drugs with pH-controlled activation. Adv Drug Deliv Rev 2004;56:1023-1050.
21. Lammers T, Kühnlein R, Kissel M, Subr V, Etrych T, Pola R, et al. Effect of physicochemical modification on the biodistribution and tumor accumulation of HPMA copolymers J Control Release 2005;110:103-18.

22. Lammers T, Subr V, Peschke P, Kühnlein R, Hennink WE, Ulbrich K, et al. Image-guided and passively tumour-targeted polymeric nanomedicines for radiochemotherapy. Br J Cancer 2008;99:900-910.
23. Pérez-Manga G, Lluch A, Alba E, Moreno-Nogueira JA, Palomero M, García-Conde J, et al. Gemcitabine in combination with doxorubicin in advanced breast cancer: final results of a phase II pharmacokinetic trial. J Clin Oncol 2000;18:2545-2552.
24. K. Ulbrich, V. Šubr, J. Strohalm, D. Plocová, M. Jelínková, B. Říhová. Polymeric drugs based on conjugates of synthetic and natural macromolecules. I. Synthesis and physico-chemical characterisation. J Control Release 2000;64:63-79.
25. Lammers T, Peschke P, Kühnlein R, Subr V, Ulbrich K, Debus J, et al. Effect of radiotherapy and hyperthermia on the tumor accumulation of HPMA copolymer-based drug delivery systems. J Control Release 2007;117:333-341.
26. B. Říhová, K. Ulbrich, J. Strohalm, V. Vetvička, M. Bilej, J. Kopeček, et al. Biocompatibility of N-(2-hydroxypropyl) methacrylamide copolymers containing adriamycin. Immunogenicity, and effect on haematopoietic stem cells in bone marrow in vivo and mouse splenocytes and human peripheral blood lymphocytes in vitro. Biomaterials 1989;10:335-342.
27. V. Šubr, K. Ulbrich. Synthesis and properties of new N-(2-hydroxypropyl)methacrylamide copolymers containing thiazolidine-2-thione reactive groups, React Funct Polymers 2006;66:1525-1538.
28. Strohalm J, Kopecek J. Poly N-(2-hydroxypropyl) methacrylamide. 4. Heterogeneous polymerization. Angew Makromol Chem 1978;70:109-118.
29. Lammers T, Peschke P, Kühnlein R, Subr V, Ulbrich K, Huber P, et al. Effect of intratumoral injection on the biodistribution and the therapeutic potential of HPMA copolymer-based drug delivery systems. Neoplasia 2006;8:788-795.
30. Borgman MP, Coleman T, Kolhatkar RB, Geyser-Stoops S, Line BR, Ghandehari H. Tumor-targeted HPMA copolymer-(RGDfK)-(CHX-A″-DTPA) conjugates show increased kidney accumulation. J Control Release 2008:132:193-198.
31. Wang Y, Ye F, Jeong EK, Sun Y, Parker DL, Lu ZR. Noninvasive visualization of pharmacokinetics, biodistribution and tumor targeting of poly[N-(2-hydroxypropyl)methacrylamide] in mice using contrast enhanced MRI. Pharm Res 2007;24:1208-1216.
32. Jain RK. Normalization of tumor vasculature: an emerging concept in antiangiogenic therapy. Science 2005;307:58-62.
33. Jain RK, Tong RT, Munn LL. Effect of vascular normalization by antiangiogenic therapy on interstitial hypertension, peritumor edema, and lymphatic metastasis: insights from a mathematical model. Cancer Res 2007;67:2729-2735.
34. P.A. Vasey, S.B. Kaye, R. Morrison, C. Twelves, P. Wilson, R. Duncan, et al. Phase I clinical and pharmacokinetic study of PK1 [N-(2-hydroxypropyl)methacrylamide copolymer doxorubicin]: first member of a new class of chemotherapeutic agents-drug-polymer conjugates, Clin Cancer Res 1999;5:83-94.
35. Rademaker-Lakhai JM, Terret C, Howell SB, Baud CM, De Boer RF, Pluim D, et al. A Phase I and pharmacological study of the platinum polymer AP5280 given as an intravenous infusion once every 3 weeks in patients with solid tumors. Clin Cancer Res 2004;10:3386-3395.
36. Meerum Terwogt JM, ten Bokkel Huinink WW, Schellens JH, Schot M, Mandjes IA, Zurlo MG, et al. Phase I clinical and pharmacokinetic study of PNU166945, a novel water-soluble polymer-conjugated prodrug of paclitaxel. Anticancer Drugs 2001;12:315-323.
37. Nishiyama N, Nori A, Malugin A, Kasuya Y, Kopecková P, Kopecek J. Free and N-(2-hydroxypropyl)methacrylamide copolymer-bound geldanamycin derivative induce different stress responses in A2780 human ovarian carcinoma cells. Cancer Res 2003;63:7876-7882.
38. Satchi-Fainaro R, Puder M, Davies JW, Tran HT, Sampson DA, Greene AK, et al. Targeting angiogenesis with a conjugate of HPMA copolymer and TNP-470. Nat Med 2004;10:255-261.
39. Říhová B. Antibody-targeted polymer-bound drugs. Folia Microbiol (Praha) 1995;40:367-384.
40. Lu ZR, Kopecková P, Kopecek J. Polymerizable Fab' antibody fragments for targeting of anticancer drugs. Nat Biotechnol 1999;17:1101-1104.
41. Mitra A, Mulholland J, Nan A, McNeill E, Ghandehari H, Line BR. Targeting tumor angiogenic vasculature using polymer-RGD conjugates. J Control Release 2005;102:191-201.
42. Wang D, Kopecková JP, Minko T, Nanayakkara V, Kopecek J. Synthesis of starlike N-(2-hydroxypropyl)methacrylamide copolymers: potential drug carriers. Biomacromolecules 2000;1:313-319.

43. Etrych T, Chytil P, Mrkvan T, Sírová M, Říhová B, Ulbrich K. Conjugates of doxorubicin with graft HPMA copolymers for passive tumor targeting. J Control Release 2008;132:184-192.
44. Ulbrich K, Etrych T, Chytil P, Jelínková M, Říhová B. HPMA copolymers with pH-controlled release of doxorubicin: in vitro cytotoxicity and in vivo antitumor activity. J Control Release 2003;87:33-47.
45. Peterson CM, Lu JM, Sun Y, Peterson CA, Shiah JG, Straight RC, et al. Combination chemotherapy and photodynamic therapy with N-(2-hydroxypropyl) methacrylamide copolymer-bound anticancer drugs inhibit human ovarian carcinoma heterotransplanted in nude mice. Cancer Res 1996;56:3980-3985.
46. Peterson CM, Shiah JG, Sun Y, Kopecková P, Minko T, Straight RC, et al. HPMA copolymer delivery of chemotherapy and photodynamic therapy in ovarian cancer. Adv Exp Med Biol 2003;519:101-123.
47. Hongrapipat J, Kopecková P, Prakongpan S, Kopecek J. Enhanced antitumor activity of combinations of free and HPMA copolymer-bound drugs. Int J Pharm 2008;351:259-70.
48. Shiah JG, Sun Y, Peterson CM, Straight RC, Kopecek J. Antitumor activity of N-(2-hydroxypropyl) methacrylamide copolymer-Mesochlorine e6 and adriamycin conjugates in combination treatments. Clin Cancer Res 2000;6:1008-1015.
49. Shiah JG, Sun Y, Kopecková P, Peterson CM, Straight RC, Kopecek J. Combination chemotherapy and photodynamic therapy of targetable N-(2-hydroxypropyl)methacrylamide copolymer-doxorubicin/mesochlorin e(6)-OV-TL 16 antibody immunoconjugates. J Control Release 2001;74:249-253.

Chapter 9

Discussion:
Drug targeting to tumors using HPMA copolymers

Twan Lammers[a,b]

[a] Department of Pharmaceutics, Utrecht Institute for Pharmaceutical Sciences, Utrecht University, Sorbonnelaan 16, 3584 CA Utrecht, The Netherlands
[b] Department of Innovative Cancer Diagnosis and Therapy, Clinical Cooperation Unit Radiotherapeutic Oncology, German Cancer Research Center, Im Neuenheimer Feld 280, 69120 Heidelberg, Germany

Expert Opin. Drug Deliv. (in preparation: 2010)

Abstract

Together, the work described in this thesis demonstrates that HPMA copolymers circulate for prolonged of time, that they localize to tumors both effectively and selectively, and that they are able improve the efficacy of combined modality anticancer therapy. Here, the insights provided and the evidence obtained are summarized and discussed, and several general conclusions are drawn.

The aim of the present thesis was to investigate, understand, improve and extend drug targeting to tumors using HPMA copolymers. Investigations have ranged from studies focusing on the copolymers themselves, evaluating the biodistributional consequences of functionalization (Chapter 3) and their potential for MR angiography (Chapter 4), to experiments in which HPMA copolymers were used as a model drug delivery system, to evaluate the potential of combining long-circulating and passively tumor-targeted nanomedicines with other treatment modalities (Chapters 5-8). Over 50 different copolymers have been evaluated over the past 5 years, and experiments have ranged from simple cytotoxicity and release studies, to extensive in vivo efficacy analyses, in which up to 40 animals were treated on every weekday for several consecutive weeks with clinically relevant regimens of radiochemotherapy.

HPMA copolymers were considered an appropriate model system for these investigations as they are easy to manufacture and modify, and non-immunogenic and non-toxic [1]. In addition, about a handful of HPMA copolymer-based chemotherapeutic agents have already been evaluated in patients, and a significant amount of clinical and preclinical evidence is available demonstrating that HPMA copolymers circulate for prolonged periods of time, and localize to tumors both effectively and selectively [2-6]. As will be described in more detail below, these insights not only illustrate that HPMA copolymers are an excellent model system for investigating drug targeting to tumors, but also that long-circulating and passively tumor-targeted polymeric drug carriers can be used to improve the efficacy of combined modality anticancer therapy.

In the present thesis, to investigate, understand, improve and extend drug targeting to tumors using HPMA copolymers, we I) confirm the beneficial biodistributional properties of HPMA copolymers, and we II) demonstrate that long-circulating and passively tumor-targeted polymeric prodrugs combine well with other treatment modalities. Regarding the former, i.e. confirming the beneficial biodistribution of HPMA copolymers, evidence is provided showing that a gadolinium-labeled copolymer circulates for prolonged periods of time, and can be used for MR angiography (i.e. for imaging blood vessels; Chapter 4). In addition, in Chapter 3, evidence is provided showing that the physicochemical modification of HPMA copolymers does not negatively affect their biodistribution, and that also charge-, drug-, spacer- and peptide-functionalized copolymers localize to tumors relatively selectively. Furthermore, in Chapter 6, HPMA copolymers are shown to be able to effectively accumulate in three different tumor models. And finally, in Chapter 7, HPMA copolymers are shown to be able to improve the tumor accumulation of doxorubicin.

Regarding the latter of the above aims, i.e. the combination of long-circulating and passively tumor-targeted polymeric prodrugs with other treatment modalities, evidence is provided showing that HPMA copolymers combine well with surgery, with radiotherapy and with chemotherapy. In Chapter 5, to provide some initial indications in favor of the combination of polymer-drug conjugates with surgery, HPMA copolymers are shown to be able to improve the retention of an i.t. applied active agent at the target site, and to enhance its efficacy and reduce its toxicity. In Chapter 6, evidence is provided showing that radiotherapy (and to a lesser extent also hyperthermia) increases the tumor accumulation of the copolymers, and that it does so independent of the tumor model used. In Chapter 7, efforts in this regard are extended, and both for doxorubicin and for gemcitabine, HPMA copolymers are shown to be able to improve the efficacy of radiochemotherapy. And finally, in Chapter 8, using an HPMA copolymer co-functionalized both with doxorubicin and with gemcitabine, evidence is provided showing that long-circulating and passively tumor-targeted polymeric drug carriers can be used to deliver two different drugs to tumors simultaneously, and to improve the efficacy of chemotherapy combinations. Below, the above insights and efforts are summarized and discussed.

1 - Investigating drug targeting to tumors using HPMA copolymers

As described in Chapters 1 and 2, passive drug targeting is a validated method for improving the delivery of low molecular weight (chemo-) therapeutic agents to tumors [7-11]. Various different types of passively tumor-targeted drug delivery systems have been evaluated over the years, including besides liposomes [12-14], polymers [2-6,15] and micelles [16-18], also more exotic carrier materials, like nanotubes [19-20], nanospheres [21], nanoshells [22], MiniCells [23] and NanoCells [24]. Given their versatility, their biocompatability and their beneficial biodistribution, we have here chosen to work with polymers. Several different polymer-based anticancer agents have been approved for clinical use, including e.g. Gliadel (i.e. carmustine-containing polymeric wafers; for surgical implantation in case of brain cancer), Lupron Depot (i.e. LHRH-containing polymeric microspheres; for local prostate cancer therapy) and Oncaspar (i.e. PEG-L-asparaginase; for the treatment of leukemia) [3,5,11,25]. For passive tumor targeting, however, essentially only Abraxane, i.e. albumin-based paclitaxel, has managed to gain FDA and EMEA approval (for metastatic

breast cancer) [5,11,26,27]. This in spite of the large number of passively tumor-targeted polymeric drug carriers that have been evaluated in animal models and in patients. Systems evaluated in patients include besides albumin and poly(ethylene glycol) also e.g. dextran, poly(L-glutamic acid) and poly(*N*-(2-hydroxypropyl)methacrylamide) [2-6,11,15]. The most advanced of these formulations currently is Xyotax, i.e. poly(L-glutamic acid)-based paclitaxel, which is in phase III trials for breast, ovarian and lung cancer [5,11,28,29].

The first clinical trial in which an i.v. applied passively tumor-targeted polymeric prodrug was evaluated in patients was initiated in 1994 [30]. The results of this trial, in which copolymers based on *N*-(2-hydroxypropyl)methacrylamide (i.e. HPMA) were used to improve the tumor-directed delivery of doxorubicin, were published in 1999, and they demonstrated that long-circulating and passively tumor-targeted polymeric drug carriers are able to beneficially affect the therapeutic index of doxorubicin-based chemotherapy: the maximum tolerated dose of poly(HPMA-co-MA-GFLG-doxorubicin) was found to be 4-5 times higher than that of free doxorubicin, no cardiotoxicity was detected (in spite of the relatively high overall doses administered), and several clear responses were observed, in patients with non-small cell lung cancer, with colon cancer and with doxorubicin-resistant breast cancer [31]. Following these not unpromising findings obtained for PK1 (i.e. 'Prague-Keele 1'; poly(HPMA-co-MA-GFLG-doxorubicin)), about a handful of other HPMA-based polymeric prodrugs entered clinical trials, including e.g. PK2 (i.e. galactosamine-targeted PK1), PNU166945 (i.e. polymer-bound paclitaxel), AP5280 (i.e. a polymer-bound cisplatin-derivative) and AP5346 (i.e. polymer-bound oxaliplatin) [32-35]. In addition to this, under the acronym PK3, also an HPMA-based diagnostic agent has been evaluated in patients [5,31,32,36]. This ~25 kDa-sized tyrosinamide-modified copolymer can be radiolabeled with iodine, and it can consequently be used for γ-scintigraphy, for PET and for SPECT. At the preclinical level, a large number of additional HPMA-based nano-diagnostics and nano-therapeutics have been evaluated over the years, functionalized besides with standard chemotherapeutics, like doxorubicin, cisplatin and paclitaxel, also with more recently developed (and more sophisticatedly acting) agents, such as the heat shock protein-inhibitor geldanamycin [37,38], and the anti-angiogenic agent TNP-470 [39,40]. Moreover, besides passively tumor-targeted polymer therapeutics, also a large number of actively targeted HPMA copolymers have been designed and evaluated [41-45]. Furthermore, both in animal models and in patients, certain antibody-targeted polymer-drug conjugates with

immunomodulating properties have been tested [46-50]. And finally, significant progress has also been made with respect to the development of novel drug linkers, like pH-sensitive hydrazone spacers, which are much more effective than GFLG spacers in releasing doxorubicin, and which consequently much more strongly inhibit tumor growth [51-55].

Together, the above insights and efforts, and the wealth of information available in the literature illustrate that HPMA copolymers are highly suitable systems for (investigating and understanding) drug targeting to tumors. In addition, they indicate that by improving the pharmacokinetic and biodistributional properties of the attached active agents, long-circulating and passively tumor-targeted polymeric drug carriers can assist in improving the efficacy of combined modality anticancer therapy.

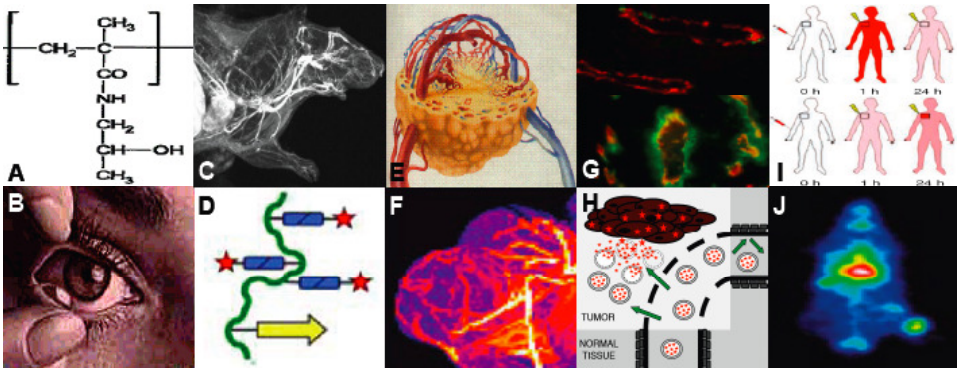

Figure 1: Rationale for investigating drug targeting to tumors using HPMA copolymers. Theoretical aspects are depicted in white, experimental evidence in black. Copolymers based on HPMA (i.e. N-(2-hydroxypropyl)methacrylamide: A) are closely related to poly(HEMA), which has been used in contact lenses (B), and which has been shown to be non-immunogenic and non-toxic. HPMA copolymers can be functionalized with different types of drugs, drug linkers, targeting moieties and imaging agents (D), and when injected intravenously, they circulate for prolonged periods of time (C+F). These prolonged circulation times, together with the fact that solid tumors tend to present with a dense (E) and highly leaky (G+H) vasculature, enable HPMA copolymers to effectively accumulate in tumors over time (J), by means of a mechanism known as the Enhanced Permeability and Retention effect (EPR: H+I). By improving the delivery of low molecular weight agents to tumors (I+J), HPMA copolymers assist in improving the efficacy of chemotherapy and of combined modality anticancer therapy. See page 240.

2 - Understanding drug targeting to tumors using HPMA copolymers

In several initial in vivo experiments, we have set out to better understand drug targeting to tumors using HPMA copolymers. Hereto, thirteen physicochemically different copolymers were synthesized, varying in size, in charge and in the nature and amount of functional groups introduced, and their circulation times, their tumor accumulation and their organ distribution were evaluated [56]. In line with the literature [57-60], it was found that larger HPMA copolymers circulated longer and accumulated in tumors stronger than did smaller copolymers. In addition, it was found that the tumor accumulation of copolymers with average molecular weights well below the renal clearance threshold of ~45 kDa peaked at about 24 h after i.v. injection, and remained relatively constant afterwards, whereas for larger copolymers, levels localizing to tumors continued to rise up until 168 h. The introduction of carboxyl and hydrazide groups, as well as that of spacer-, drug- and peptide-moieties, reduced the long-circulation properties of the copolymers, and it lowered their tumor concentrations. Interestingly, however, levels in the majority of healthy tissues were also found to be reduced, and when calculating tumor-to-organ ratios, hardly any difference was observed between functionalized and unfunctionalized HPMA copolymers. This is an important finding, as it demonstrates that also physicochemically modified HPMA copolymers localize to tumors relatively selectively, and as it illustrates that introducing functional groups into HPMA copolymers does not negatively affect their beneficial biodistribution.

The only organ for which a clear deviation from the above trend was observed was the kidney: all ten physicochemically modified HPMA copolymers accumulated in the kidney (much) more strongly than did size-matched non-modified controls [56]. Especially the introduction of peptide moieties was found to result in a strong increase in kidney accumulation, as exemplified by the high concentrations observed for both GFLG-containing copolymers, and for all three PHSCN-containing copolymers. Using HPMA copolymers modified with 3 and 8 mol-% of carboxyl and hydrazide groups, it could furthermore be demonstrated that the degree of functionalization correlates with the degree of kidney accumulation. This notion was confirmed in later experiments with P-Gem-Dox, in which relatively high amounts of doxorubicin and gemcitabine were co-conjugated to the same copolymer, and in which also very high kidney concentrations were observed [61]. It furthermore is in line with experiments in which HPMA copolymers were functionalized with different amounts of RGDfK

(i.e. a cyclic pentapeptide used for blood vessel targeting), and in which also a clear correlation between the degree of functionalization and the degree of kidney accumulation was observed [62].

Also in patients injected with radiolabeled PK1 [36], and in some of our own experiments with radiolabeled PK1 [63,64], indications for a more or less selective localization to the kidney were obtained. Strikingly however, when quantifying the levels of doxorubicin in the kidney, only relatively low levels of the drug were detected, and no tendency towards a more preferential localization to kidney was observed [65]. This either indicates that kidney accumulation takes place after the drug is released or, more likely, that the intact conjugate localizes to the kidney, and that doxorubicin is subsequently rapidly released and excreted (note that relatively high levels of cathepsin B are present in the kidney [66-68]). The finding that drug levels in the kidney are relatively low is substantiated by the fact that no major kidney-related side effects have been reported thus far, neither in animal models, nor in patients [1-5,31,36]. In spite of this important notion, however, it is advisable to always keep kidney accumulation in mind when working with polymer-drug conjugates, and to always monitor kidney function when treating patients with polymer therapeutics (especially in case of platins). Conversely, because of their strong tendency to accumulate in the kidney, one could also argue that certain densely modified and/or peptide-'targeted' HPMA copolymers could be used to improve drug delivery to the kidney, and to enhance the treatment of certain severe kidney disorders, such as renal fibrosis and renal cell carcinoma.

Other efforts with regard to understanding drug targeting to tumors using HPMA copolymers have elaborated on the establishment of a long-circulating gadolinium-containing contrast agent, which can be used for MR angiography (i.e. for visualizing blood vessels) [69]. Like iodine-labeled copolymers, this gadolinium-containing copolymer can be used for 'image-guided drug delivery'. Image-guided drug delivery refers to the combination of (cancer) diagnosis and therapy, and it not only aims to improve treatment outcome, but also to better understand (several important aspects of) the drug delivery process. Regarding the latter, image-guided drug delivery can be used to visualize the biodistribution of the conjugated or entrapped active agent, to monitor its tumor accumulation, to visualize drug release, to monitor its intratumoral distribution, and to non-invasively assess its therapeutic efficacy (e.g. in case of orthotopic tumors). Regarding the former, i.e. improving treatment outcome, image-guided drug

delivery can be used to monitor and to predict therapeutic responses. PK3, for instance, could have been used to pre-screen patients assigned to PK1, in order to identify which tumors are amenable to EPR-mediated drug targeting and which are not, and to predict which patients are likely to respond to PK1 therapy and which are not. By mixing in trace amounts of PK3 with (e.g. every second cycle of) PK1 during follow-up, and by continuously subjecting patients to 2D-scintigraphy or 3D-PET, it would furthermore be possible to visualize the efficacy of the intervention in real-time, and to provide important information for assisting in deciding whether or not to (dis-) continue therapy, and whether or not to adjust drug doses. Image-guided drug delivery might thereby assist in realizing the potential of 'personalized medicine', i.e. tailor-made therapy for individual patients, which besides on the study of genetic polymorphisms and biomarkers, also relies on the development of visual methods for measuring and predicting treatment outcome. An additional important aspect of image-guided drug delivery is that it substantially facilitates preclinical testing, enabling not only more informative and less invasive biodistribution studies, but also more elegant and more relevant efficacy analyses, in which e.g. genetically modified mice and orthotopic tumor models are used to study disease progression and treatment outcome in real-time. A final important consideration to take into account with regard to image-guided drug delivery relates to the fact that it can be used to better understand tumor physiology. Not only tumor perfusion and tumor blood vessel density can be visualized using image-guided nanomedicines, but e.g. also the extravasation of agents across tumor blood vessels, and their penetration into the (less well-vascularized areas in the) cores of the tumors.

We have here contributed to efforts in this regard by synthesizing several different image-guided (i.e. iodine- and gadolinium-labeled) polymer therapeutics. Iodine-labeled HPMA copolymers can be used for γ-scintigraphy, for PET and for SPECT, and they enable a highly detailed analysis of the pharmacokinetics and the biodistribution of the attached active agents. Gadolinium-labeled HPMA copolymers can be used both for biodistributional and for functional analyses, enabling e.g. MR angiography to study blood vessel status. Both iodine- and gadolinium-labeled copolymers are considered to be highly suitable systems for image-guided drug delivery: the former can be used for measuring tumor accumulation and predicting treatment outcome, and the latter for visualizing tumor penetration and tracking treatment efficacy (e.g. in case of antiangiogenic therapy). Interesting future directions in this regard relate to the use of an iodine-labeled hydrazone-based polymeric prodrug for predicting treatment efficacy in

patients, the use of a gadolinium-labeled HPMA copolymer for visualizing the antiangiogenic effects of (co-conjugated) TNP-470, and the use of polymer-based contrast agents for multimodality imaging (i.e. co-functionalized with two or three different MR-, PET-, SPECT- or NIR-probes). Together, the above insights demonstrate that HPMA copolymers are suitable systems for image-guided drug delivery, and they illustrate that iodine- and gadolinium-labeled HPMA copolymers can be used to better understand drug targeting to tumors.

3 - Improving drug targeting to tumors using HPMA copolymers

Attempts to improve drug targeting to tumors using HPMA copolymers have encompassed both passive and active targeting approaches. Regarding the latter, various different targeting ligands have been evaluated over the years (e.g. aminosugars, hormones, antibodies and peptides), and several different targeting strategies have been tested (e.g. cancer cell targeting, endothelial cell targeting and enhancing cellular uptake) [41-45]. Regarding the former, on the other hand, experiments have thus far essentially only aimed at establishing biodegradable high molecular weight grafts, which because of their large size and their prolonged circulation times accumulate in tumors significantly more effectively than do standard small HPMA copolymers (i.e. non-biodegradable polymer therapeutics, like PK1, with average molecular weights well below the renal clearance threshold of ~45 kDa) [65,70].

In the present thesis, as an alternative strategy for (actively) improving passive drug targeting, we have set out to combine HPMA copolymers with other treatment modalities. Both radiotherapy and hyperthermia were used for this purpose [64], and also agents known to affect tumor blood flow and tumor blood vessels were tested (i.e. angiotensin II and prostaglandin E2; data not shown). Regarding the latter, i.e. co-treatment with the vasoconstrictor ATII and the extravasation-enhancer PGE2, no indications for an improvement in tumor accumulation were observed, at least not for a 31 kDa-sized drug-free control copolymer, and not in the Dunning AT1-sc rat prostate carcinoma model. This can be explained by taking into account that blood vessels in AT1-sc tumors are poorly supported by pericytes and smooth muscle cells, and therefore already are relatively leaky, and likely do not respond well to treatment with vasoconstricting agents. As it seems obvious that other tumor models, in which blood vessels are less tortuous and less leaky (i.e. better differentiated), respond

very differently to treatment with such compounds, no definite conclusions can be drawn from these studies yet, and additional analyses are necessary to resolve this issue. Other interesting pharmacological means for improving passive drug targeting to tumors relate to the use of antiangiogenic agents, which normalize the tumor vasculature, and to the use of TNFα and inhibitors of TGFβ, which enhance extravasation.

The above notion of tumor heterogeneity was taken firmly into account when assessing the effects of radiotherapy and hyperthermia on the tumor accumulation of HPMA copolymers. Before actually combining the copolymers with radiotherapy and with hyperthermia, we therefore first evaluated the biodistribution and the tumor accumulation of two different HPMA copolymers in three different tumor models, i.e. AT1-sc, AT1-im and H-sc. Dunning AT1 tumors transplanted subcutaneously (AT1-sc) were used as a reference model and as a positive control, as they are known to possess relatively leaky blood vessels, and to accumulate HPMA copolymers relatively well. Dunning AT1 tumors inoculated intramuscularly (AT1-im) were used to reduce the impact of subcutaneous tumor encapsulation. Because of the more infiltrative growth and the substantial increase in tumor-muscle surface area, the clearance of HPMA copolymers from AT1-im tumors was expected to be less unidirectional and, therefore, to be more substantial than for AT1-sc tumors. Dunning H tumors transplanted subcutaneously (H-sc) were used to investigate the impact of the morphology of tumor blood vessels on the accumulation of HPMA copolymers. H-sc tumors grow much slower than AT1-sc tumors, and they consequently present with a slowly matured and well-differentiated vasculature, which is much less leaky than that in AT1-sc tumors (see Figure 1G). Two differently sized HPMA copolymers, i.e. a 31 kDa and a 65 kDa drug-free control copolymer containing ~1 mol-% of tyrosinamide (for radiolabeling), were used in these initial investigations, and in line with our expectations, it was found that HPMA copolymers accumulated most effectively in AT1-sc tumors. Levels in AT1-im and H-sc tumors were always approximately 50% lower, but in spite of this, evidence in favor of effective EPR-mediated passive drug targeting could be obtained in all cases, as exemplified e.g. by the fact that tumor concentrations were always substantially higher for the 65 kDa copolymer than for the 31 kDa copolymer [64]. This is an important finding, as it demonstrates that HPMA copolymers effectively accumulate in three different tumor models, and as it confirms the beneficial biodistributional properties of HPMA copolymers.

In these three models, we then set out to evaluate the effects of three different doses of hyperthermia (i.e. 41, 42 and 42.5 °C; applied for 1 h; concomitant to i.v. administration) and four different regimens of radiotherapy (i.e. 2 and 20 Gy; applied 1 and 24 h prior to i.v. injection) on the tumor accumulation of the copolymers. As opposed to hyperthermia, which only increased the tumor accumulation of the 65 kDa copolymer in H-sc tumors, 20 Gy of radiotherapy, applied 24 h prior to i.v. injection, improved the tumor accumulation of both copolymers in all three tumor models [64]. This notion suggests that radiotherapy affects the permeability of tumor blood vessels through one or more general (patho-) physiological mechanisms. It has been shown, for instance, that radiotherapy upregulates the expression of vascular endothelial growth factor (VEGF) [71] and fibroblast growth factor (FGF) [72], which are both known to be able to increase the permeability of (tumor) blood vessels towards nanosized materials [73,74]. Also by inducing apoptosis in endothelial cells, radiotherapy might enhance the extravasation of nanomedicines [75]. In addition to this, radiotherapy has been shown to be able to decrease the interstitial fluid pressure in tumors, i.e. the outward-bound pressure gradient that is typical of solid malignancies and that is, at least in part, responsible for the poor penetration of blood-borne agents into tumors [76-79]. And furthermore, radiotherapy has been shown to be able to reduce the cell density in tumors [80], which is also known to be an important (negative) determinant of drug penetration and drug distribution in solid malignancies [78,79].

Our findings are in line with the small number of other reports that have been published on the effects of radiotherapy on the tumor accumulation of passively targeted nanomedicines, and it is interesting to note that for similar systems, i.e. for PEGylated liposomal doxorubicin and for poly(L-glutamic acid)-based paclitaxel, similar levels of improvement have been observed (ranging from ~25% to ~100%; depending on polymer size and on the tumor model used) [81,82]. Together, these findings convincingly demonstrate that radiotherapy is an effective means for improving drug targeting to tumors. Interesting follow-up and future directions in this regard relate to the combination of passively tumor-targeted polymeric prodrugs with clinically relevant regimens of radiotherapy (see below), and to the development of fibrinogen- and RGD-modified actively targeted nanomedicines, which selectively bind to radiotherapy-induced membrane receptors, such as $\alpha_v\beta_3$ and $\alpha_{2b}\beta_3$ integrins.

As opposed to radiotherapy, hyperthermia was only found to be able to improve the concentration of one HPMA copolymer in one tumor model. In AT1-sc and AT1-im tumors, which already possess a relatively leaky vasculature, hyperthermia had no obvious effect on the amount of copolymer localizing to tumors [64]. In slowly growing H-sc tumors, on the other hand, which possess a properly differentiated endothelial lining, hyperthermia did increase the concentrations of the 31 kDa (~25%; not significant) and the 65 kDa (~80%; $p<0.05$) copolymer. In principle, these findings are in line with the results obtained for liposomes, for which it has been demonstrated that hyperthermia can increase the pore cut-off size of tumor blood vessels from less than 100 nm to values beyond 400 nm [83,84]. As compared to polymers, however, liposomes are relatively large (i.e. 2-10 nm vs. 100-200 nm, respectively). This implies that polymer therapeutics might already extravasate effectively at pore cut-off sizes of less than 10 nm, whereas for liposomes, pore cut-off sizes have to be at least 100 nm. It can consequently be reasoned that the more leaky tumors already are under non-hyperthermic conditions, the less likely it is that hyperthermia will have a beneficial effect on the tumor accumulation of polymeric prodrugs. As liposomes are much larger than polymers, and as liposomes therefore much more depend on pore cut-off size for effective extravasation, it seems as if hyperthermia might be more useful for improving the tumor accumulation of liposomes than for improving that of polymers. It should be noted in this regard, however, that in general, blood vessels in animal models tend to be (much) more leaky than blood vessels in human tumors, and it would therefore not be surprising if in patients, hyperthermia would turn out to be able to improve the tumor accumulation of polymers. These findings demonstrate, at least for HPMA copolymers, that the effects of hyperthermia depend significantly on the tumor model used, and they seem to suggest that tumor grade inversely correlates with responsiveness to hyperthermia. More promising progress with regard to the combination of tumor-targeted nanomedicines with hyperthermia has recently been made by developing temperature-sensitive drug delivery systems. By carefully optimizing lipid composition, for instance, doxorubicin-containing PEGylated liposomes can be prepared which effectively release the entrapped active agent upon heating to temperatures exceeding 38 °C. This formulation, i.e. ThermoDox, is currently under phase III evaluation for the treatment of patients with primary liver carcinomas, and the results of this trial are eagerly awaited.

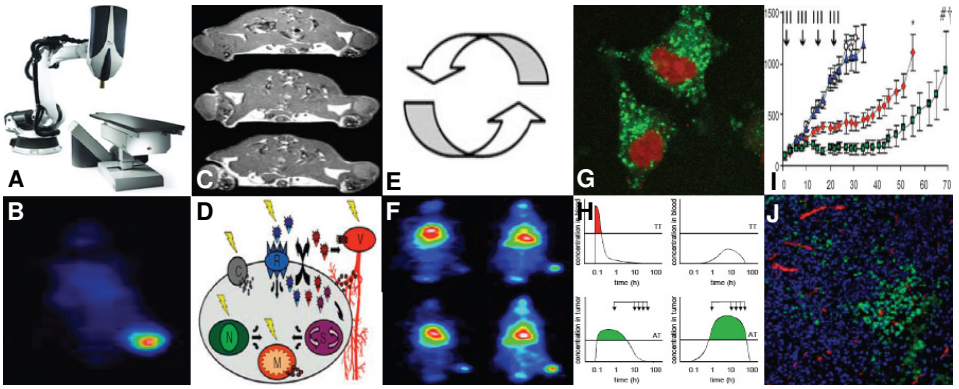

Figure 2: Improving and extending drug targeting to tumors using HPMA copolymers. In order to improve their tumor accumulation, HPMA copolymers were combined with radiotherapy (A) and with hyperthermia. Gamma-scintigraphy (B+F), magnetic resonance imaging (C) and fluorescence microscopy (G+J) were used to visualize the biodistribution of the copolymers. As opposed to hyperthermia, radiotherapy was found to be able to improve the tumor accumulation of the copolymers independent of the tumor model used (C+F). This was considered to be due to the fact that radiotherapy exerts several general physiological effects, such as an increase in the expression of VEGF and FGF, an induction of (endothelial cell) apoptosis, a reduction of the tumor cell density, and a reduction of the intestitial fluid pressure, which can all be expected to beneficially affect the tumor accumulation of HPMA copolymers (D). In addition, the copolymers were shown to be able to interact synergistically (E) with radiotherapy, with on the one hand radiotherapy increasing the tumor accumulation of the copolymers (C+F), and with on the other hand the copolymers increasing the therapeutic index of radiochemotherapy (H+I). Clinically relevant regimens of radiotherapy and chemotherapy were used (H), and promising results were obtained both for doxorubicin and for gemcitabine (I). Finally, to demonstrate that HPMA copolymers can be used to deliver two different drugs to tumors simultaneously, a polymeric prodrug carrying both doxorubicin and gemcitabine was synthesized, and this construct was shown to be effective both in vitro and in vivo (J). Together, these findings convincingly demonstrate that HPMA copolymer-based nanomedicine formulations hold significant potential for improving the efficacy of combined modality anticancer therapy. *See page 240.*

4 - Extending drug targeting to tumors using HPMA copolymers

Finally, efforts were undertaken to extend drug targeting to tumors using HPMA copolymers. Hereto, polymer therapeutics were combined with several other treatment modalities, i.e. with surgery, with radiotherapy and with chemotherapy. Regarding surgery, the effect of intratumoral injection on the biodistribution and the therapeutic potential of HPMA copolymer-based drug delivery systems was evaluated [63]. This was done to demonstrate that long-circulating and passively tumor-targeted polymeric drug carriers can be used to improve the retention of an i.t. applied low molecular weight drug at the target site. To assess the impact of i.t. injection on the biodistribution and the therapeutic potential of HPMA copolymers, three different copolymers were injected both i.v. and i.t., and their circulation kinetics, tumor concentrations, tumor-to-organ ratios, antitumor efficacy and toxicity were compared. It was found that as compared to i.v. injection, i.t. injection improved both the tumor concentrations and the tumor-to-organ ratios of the copolymers substantially. In addition, as compared to i.v. and i.t. applied free doxorubicin and to i.v. applied PK1 (i.e. poly(HPMA)-GFLG-doxorubicin), the i.t. administered polymeric prodrug was found to be significantly more effective, and to be less toxic. These findings suggest that when tumors are easily accessible, e.g. during surgery, intratumorally injected carrier-based chemotherapeutics should be considered as interesting alternatives for the routinely used chemotherapy regimens and routes of administration.

Following up on the abovementioned beneficial effects of radiotherapy on the tumor accumulation of HPMA copolymers, we have furthermore set out to evaluate the potential of ‘carrier-based radiochemotherapy’ [85]. Carrier-based radiochemotherapy is based on the notion that the temporal and spatial interaction between i.v. applied weekly chemotherapy and clinically relevant daily radiotherapy is suboptimal, and on the assumption that drug targeting systems are able to improve the temporal and spatial parameters of this interaction. HPMA copolymers were used as a model drug delivery system, doxorubicin and gemcitabine as model drugs, and the syngeneic and radio- and chemoresistant Dunning AT1 rat prostate carcinoma as a model tumor model. Using γ-scintigraphy, MRI, fluorescence microscopy and HPLC, the polymeric drug carriers were first shown to circulate for prolonged periods of time, to localize to tumors both effectively and selectively, and to improve the tumor-directed delivery of doxorubicin. Subsequently, they were then shown to interact

synergistically with radiotherapy, with radiotherapy increasing the tumor accumulation of the copolymers, and with the copolymers increasing the therapeutic index of radiochemotherapy (both for doxorubicin and for gemcitabine). Regarding the former, i.e. enhancing the tumor accumulation of HPMA copolymers, we have extended previous efforts by working both with iodine- and with gadolinium-labeled copolymers, and by evaluating their tumor concentrations both at 24 and at 168 h post i.v. injection. And regarding the latter, previous efforts were extended by attempting to generalize the concept of carrier-based radiochemotherapy, by implementing clinically relevant regimens of radio- and chemotherapy, by using a radio- and chemoresistant tumor model, and by directly comparing the radiosensitizing potential of polymeric prodrugs to that of free chemotherapeutic agents. Together, the insights provided and the evidence obtained strongly suggest that carrier-based radiochemotherapy holds significant potential for improving the treatment of advanced solid malignancies.

Some initial clinical proof-of-principle in favor of carrier-based radiochemotherapy has recently been provided by Dipetrillo and colleagues, who treated 12 patients with localized esophageal and gastric cancer with the combination of poly(L-glutamic acid)-bound paclitaxel (Xyotax; 6 doses; weekly) and fractionated radiotherapy (28 cycles; 1.8 Gy; daily), and who observed 4 complete responses and an additional 7 partial responses (with reductions in tumor size of more than 50%) [86]. Prior to this trial, preclinical studies had already identified Xyotax as a highly potent radiosensitizer: when a single i.v. injection of Xyotax was combined with a single dose of radiotherapy, for instance, the dose required to produce 50% tumor cures (i.e. the TCD_{50}) could be reduced substantially, from 53.9 to 7.5 Gy [87]. When radiotherapy was delivered as 5 daily fractions, the effect of Xyotax was even more pronounced, reducing the TCD_{50} from 66.6 to 7.9 Gy [87]. In line with this, in a follow-up study in the same tumor model, similar results were reported for Abraxane, i.e. for albumin-based paclitaxel, which also beneficially combined both with single dose and with fractionated radiotherapy, and which did not increase normal tissue radiotoxicity [88].

In comparable analyses, Harrington and colleagues have demonstrated that also liposomes hold significant potential for combination with radiotherapy [89]. They combined both PEGylated liposomal doxorubicin and PEGylated liposomal cisplatin with both single dose (4.5 and 9 Gy) and fractionated (3 x 3 Gy) radiotherapy, and they showed that animals treated with carrier-based radiochemotherapy survived for significantly longer periods of time than did

animals treated with standard radiochemotherapy. Davies and colleagues recently confirmed and extended these findings, showing that Doxil, i.e. PEGylated liposomal doxorubicin, significantly improves the efficacy of both single dose (8 Gy) and fractionated (3 x 3.6 Gy) radiotherapy, and that it does so, at least in part, by improving the penetration and the intratumoral distribution of the drug [82].

In experiments with Xyotax, it had also already been observed that radiotherapy increases the tumor accumulation of passively targeted nanomedicines, attributing at least part of the supra-additively improved efficacy of PGA-paclitaxel (i.e. Xyotax) and radiotherapy to a radiotherapy-induced increase in tumor localization [81]. It is interesting to note in this regard that the overall improvement in the tumor concentration of PGA-paclitaxel was virtually identical to that observed here for (size-matched) HPMA copolymers, with as compared to sham-irradiated controls, increases ranging from ~25 to 50%. Also in line with our findings, it was demonstrated that this radiotherapy-induced increase in the tumor accumulation of Xyotax could already be observed almost immediately upon i.v. injection (i.e. at 1 h p.i.; vs. at 30 min p.i. here), and that it remained relatively constant over time (i.e. up to 24 and up to 168 h p.i.). Together with the abovementioned findings on the enhanced penetration and the improved intratumoral distribution of PEGylated liposomal doxorubicin in response to radiotherapy [82], these observations suggest that radiotherapy beneficially affects both arms of the EPR effect: on the one hand, by enhancing the expression of VEGF and FGF [71-74], and by inducing endothelial cell apoptosis [75], it likely increases the permeability of tumor blood vessels towards long-circulating nanomedicines, and on the other hand, by reducing the tumor cell density [80] and the interstitial fluid pressure [76,77], it likely improves their retention and their intratumoral distribution. Though clinically clearly less important than the improved therapeutic indices resulting from carrier-based radiochemotherapy, these improvements in EPR-mediated drug targeting to tumors provide an additional indication for combining long-circulating and passively tumor-targeted (polymeric) nanomedicines with radiotherapy. Based on these findings, and on the fact that its principles are likely broadly applicable (and e.g. also hold for liposomes and for micelles), we propose carrier-based radiochemotherapy as a novel, a rational, a translational and a relatively straightforward approach for improving the treatment of advanced solid malignancies. Clinical trials in which nanomedicine formulations are combined with fractionated radiotherapy are therefore strongly encouraged.

To finally also extend drug targeting to tumors using HPMA copolymers with regard to chemotherapy, and to for the first time provide in vivo proof-of-principle for 'polymer-based multi-drug targeting', a polymer-drug conjugate carrying 6.4 wt-% of gemcitabine, 5.7 wt-% of doxorubicin and 1 mol-% of tyrosinamide (to allow for radiolabeling) was synthesized [61]. The resulting 24 kDa construct, i.e. poly(HPMA-co-MA-GFLG-gemcitabine-co-MA-GFLG-doxorubicin-co-MA-TyrNH_2), was termed P-Gem-Dox, and its properties were evaluated both in vitro and in vivo. In vitro, P-Gem-Dox was found to effectively release both agents over time, and to kill cancer cells at low nanomolar concentrations. In vivo, using 2D γ-scintigraphy, P-Gem-Dox was shown to circulate for prolonged periods of time, and to localize to tumors relatively selectively, with higher levels in tumors than in 7 out of 9 healthy tissues. In addition, P-Gem-Dox effectively inhibited tumor growth: as compared to control regimens, it increased the efficacy of the combination of gemcitabine and doxorubicin without increasing its toxicity, and it more strongly inhibited angiogenesis and induced apoptosis. These findings demonstrate that polymers, as e.g. liposomes, can be used to deliver two different drugs to tumors simultaneously, and they thereby set the stage for more elaborate analyses on the potential of polymer-based multi-drug targeting.

Together, the work described in this thesis demonstrates that HPMA copolymers
- are versatile and multifunctional drug carriers
- circulate for prolonged periods of time
- localize to tumors both effectively and selectively
- improve the tumor-directed delivery of low molecular weight agents
- are effectively internalized by cells
- hold potential for MR angiography and image-guided drug delivery
- hold potential for local application and combination with surgery
- interact synergistically with radiotherapy
- induce growth inhibition in rapidly growing and therapy-resistant tumors
- improve the efficacy of clinically relevant regimens of radiochemotherapy
- attenuate the toxicity of clinically relevant regimens of radiochemotherapy
- are suitable systems for 'carrier-based radiochemotherapy'
- are able to deliver two different drugs to tumors simultaneously
- are able to improve the efficacy of chemotherapy combinations
- are suitable systems for 'polymer-based multi-drug targeting'

These insights and efforts confirm the beneficial biodistributional properties of HPMA copolymers, and they demonstrate that long-circulating and passively tumor-targeted polymeric nanomedicines hold significant potential for improving the efficacy of combined modality anticancer therapy.

References

1. Kopecek J, Kopeckova P, Minko T, Lu Z (2000) HPMA copolymer-anticancer drug conjugates: design, activity, and mechanism of action, Eur J Pharm Biopharm **50**: 61-81
2. Kopecek J, Kopeckova P, Minko T, Lu ZR, Peterson CM (2001) Water soluble polymers in tumor targeted delivery, *J Control Release* **74**: 147-58
3. Duncan R (2003) The dawning era of polymer therapeutics, *Nat Rev Drug Discov* **2** 347-360
4. Rihova B, Kubackova K (2003) Clinical implications of N-(2-hydroxypropyl)-methacrylamide copolymers, *Curr Pharm Biotechnol* **4:** 311-322
5. Duncan R (2006) Polymer conjugates as anticancer nanomedicines, *Nat Rev Cancer* **6:** 688-701
6. Vicent MJ, Duncan R (2006) Polymer conjugates: nanosized medicines for treating cancer, Trends Biotechnol **24**: 39-47
7. Seymour LW (1992) Passive tumor targeting of soluble macromolecules and drug conjugates, *Crit Rev Ther Drug Carrier Syst* **9**: 135-187
8. Langer R (1998) Drug delivery and targeting, *Nature* **392**: S5-10
9. Torchilin VP (2000) Drug targeting, *Eur J Pharm Sci* **11**: S81-91
10. Allen TM, Cullis PR (2004) Drug delivery systems: entering the mainstream, Science **303**: 1818-1822
11. Lammers T, Hennink WE, Storm G (2008) Tumor-targeted nanomedicines: Principles and Practice, *Br J Cancer* **99**: 900-910
12. Torchilin VP (2005) Recent advances with liposomes as pharmaceutical carriers, *Nat Rev Drug Discov* **4**: 145-160
13. Drummond DC, Meyer O, Hong K, Kirpotin DB, Papahadjopoulos D (1999) Optimizing liposomes for delivery of chemotherapeutic agents to solid tumours, *Pharm Rev* **51**: 691-743
14. Storm G, Crommelin DJA (1998) Liposomes: Quo vadis? *Pharm Sci Tech Today* **1**: 19-31
15. Haag R, Kratz F (2006) Polymer Therapeutics: Concepts and applications, *Angew Chem Int Ed* **45**: 1198-1215
16. Kataoka K, Harada H, Nagasaki Y (2001) Block copolymer micelles for drug delivery: design, characterization and biological significance, *Adv Drug Deliv Rev* **41**: 113-131
17. Torchilin VP (2007) Micellar nanocarriers: Pharmaceutical perspectives*, Pharm Res* **24**: 1-16
18. Jones MC, Leroux JC (1999) Polymeric micelles - A new generation of colloidal drug carriers, *Eur J Pharm Biopharm* **48**: 101-111
19. Bianco A, Kostarelos K, Prato M (2005) Applications of carbon nanotubes in drug delivery, *Curr Opin Chem Biol* **9**: 674-679
20. Kam NW, O'Connell M, Wisdom JA, Dai H (2005) Carbon nanotubes as multifunctional biological transporters and near-infrared agents for selective cancer cell destruction, *Proc Natl Acad Sci USA* **102**: 11600-11605
21. Gref R, Minamitake Y, Peracchia MT, Trubetskoy V, Torchilin V, Langer R (1994) Biodegradable long-circulating polymeric nanospheres, *Science* **263**: 1600-160
22. Loo C, Lowery A, Halas N, West J, Drezek R (2005) Immunotargeted nanoshells for integrated cancer imaging and therapy, *Nano Lett* **5**: 709-711
23. MacDiarmid JA, Mugridge NB, Weiss JC, Phillips L, Burn AL, Paulin RP, Haasdyk JE, Dickson KA, Brahmbhatt VN, Pattison ST, James AC, Al Bakri G, Straw RC, Stillman B, Graham RM, Brahmbatt H (2007) Bacterially derived 400 nm particles for encapsulation and cancer cell targeting of chemotherapeutics, *Cancer Cell* **11:** 431-445
24. Sengupta S, Eavarone D, Capila I, Zhao G, Watson N, Kiziltepe T, Sasisekharan R (2005) Temporal targeting of tumor cells and neovasculature with a nanoscale delivery system, *Nature* **436:** 568-572
25. Moses MA, Brem H, Langer R (2003) Advancing the field of drug delivery: taking aim at cancer, *Cancer Cell* **4:** 337-341
26. Gradishar WJ, Tjulandin S, Davidson N, Shaw H, Desai N, Bhar P, Hawkins M, O'Shaughnessy J (2005) Phase III trial of nanoparticle albumin-bound paclitaxel compared with polyethylated castor oil-based paclitaxel in women with breast cancer, *J Clin Oncol* **23**: 7794–7803
27. Green MR, Manikhas GM, Orlov S, Afanasyev B, Makhson AM, Bhar P, Hawkins MJ (2006) Abraxane, a novel Cremophor-free, albumin-bound particle form of paclitaxel for the treatment of advanced non-small-cell lung cancer, *Ann Oncol* **17**: 1263-1268
28. Singer JW (2005) Paclitaxel poliglumex (XYOTAX, CT-2103): a macromolecular taxane, *J Control Release* **109**: 120-126

29. Paz-Ares L, Ross H, O'Brien M, Riviere A, Gatzemeier U, Von Pawel J, Kaukel E, Freitag L, Digel W, Bischoff H, García-Campelo R, Iannotti N, Reiterer P, Bover I, Prendiville J, Eisenfeld AJ, Oldham FB, Bandstra B, Singer JW, Bonomi P (2008) Phase III trial comparing paclitaxel poliglumex vs docetaxel in the second-line treatment of non-small-cell lung cancer, *Br J Cancer* **98**: 1608-1613
30. Vasey PA, Duncan R, Kaye SB, Cassidy J (1995) Clinical phase I trial of PK1 (HPMA co-polymer doxorubicin), *Eur J Cancer* **31**: S193
31. Vasey PA, Kaye SB, Morrison R, Twelves C, Wilson P, Duncan R, Thomson AH, Murray LS, Hilditch TE, Murray T, Burtles S, Fraier D, Frigerio E, Cassidy J (1999) Cancer Research Campaign Phase I/II Committee, Phase I clinical and pharmacokinetic study of PK1 [N-(2-hydroxypropyl)methacrylamide copolymer doxorubicin]: first member of a new class of chemotherapeutic agents-drug-polymer conjugates, *Clin Cancer Res* **5** 83-94
32. Seymour LW, Ferry DR, Anderson D, Hesslewood S, Julyan PJ, Poyner R, Doran J, Young AM, Burtles S, Kerr DJ; Cancer Research Campaign Phase I/II Clinical Trials committee (2002) Hepatic drug targeting: phase I evaluation of polymer-bound doxorubicin, *J Clin Oncol* **20**: 1668-1676
33. Rademaker-Lakhai JM, Terret C, Howell SB, Baud CM, De Boer RF, Pluim D, Beijnen JH, Schellens JH, Droz JP (2004) A Phase I and pharmacological study of the platinum polymer AP5280 given as an intravenous infusion once every 3 weeks in patients with solid tumors, *Clin Cancer Res* **10**: 3386-3395
34. Meerum Terwogt JM, ten Bokkel Huinink WW, Schellens JH, Schot M, Mandjes IA, Zurlo MG, Rocchetti M, Rosing H, Koopman FJ, Beijnen JH (2001) Phase I clinical and pharmacokinetic study of PNU166945, a novel water-soluble polymer-conjugated prodrug of paclitaxel, *Anticancer Drugs* **12**: 315-323
35. Campone M, Rademaker-Lakhai JM, Bennouna J, Howell SB, Nowotnik DP, Beijnen JH, Schellens JH (2007), Phase I and pharmacokinetic trial of AP5346, a DACH-platinum-polymer conjugate, administered weekly for three out of every 4 weeks to advanced solid tumor patients, *Cancer Chemother Pharmacol* **60**: 523-533
36. Seymour LW, Ferry DR, Kerr DJ, Rea D, Whitlock M, Poyner R, Boivin C, Hesslewood S, Twelves C, Blackie R, Schatzlein A, Jodrell D, Bissett D, Calvert H, Lind M, Robbins A, Burtles S, Duncan R, Cassidy J (2009) Phase II studies of polymer-doxorubicin (PK1, FCE28068) in the treatment of breast, lung and colorectal cancer, *Int J Oncol* **34**: 1629-1936
37. Kasuya Y, Lu ZR, Kopeckova P, Minko T, Tabibi SE, Kopecek J (2001) Synthesis and characterization of HPMA copolymer-aminopropylgeldanamycin conjugates, *J Control Release* **74**: 203-211
38. Nishiyama N, Nori A, Malugin A, Kasuya Y, Kopeckova P, Kopecek J (2003) Free and N-(2-hydroxypropyl)methacrylamide copolymer-bound geldanamycin derivative induce different stress responses in A2780 human ovarian carcinoma cells, *Cancer Res* **63**: 7876-7882
39. Satchi-Fainaro R, Puder M, Davies JW, Tran HT, Sampson DA, Greene AK, Corfas G, Folkman J (2004) Targeting angiogenesis with a conjugate of HPMA copolymer and TNP-470, *Nat Med* **10**: 255-261
40. Satchi-Fainaro R, Mamluk R, Wang L, Short SM, Nagy JA, Feng D, Dvorak AM, Dvorak HF, Puder M, Mukhopadhyay D, Folkman J (2005) Inhibition of vessel permeability by TNP-470 and its polymer conjugate, caplostatin, *Cancer Cell* **3**: 251-261
41. Omelyanenko V, Kopeckova P, Gentry C, Kopecek J (1998) Targetable HPMA copolymer-adriamycin conjugates. Recognition, internalization, and subcellular fate, *J Control Release* **53**: 25-37
42. Rihova B (1998) Receptor-mediated targeted drug or toxin delivery, Adv Drug Deliv Rev **29**: 273-289.
43. Lu ZR, Kopeckova P, Kopecek J (1999) Polymerizable Fab' antibody fragments for targeting of anticancer drugs, *Nat Biotech* **17**: 1101-1104
44. Mitra A, Mulholland J, Nan A, McNeill E, Ghandehari H, Line BR (2005) Targeting tumor angiogenic vasculature using polymer-RGD conjugates, *J Control Release* **102**: 191-201
45. Borgman MP, Ray A, Kolhatkar RB, Sausville EA, Burger AM, Ghandehari H (2009) Targetable HPMA copolymer-aminohexylgeldanamycin conjugates for prostate cancer therapy, *Pharm Res* **26**:1407-1418
46. Rihova B (2002) Immunomodulating activities of soluble synthetic polymer-bound drugs, Adv Drug Deliv Rev **12**: 653-674
47. Rihova B, Strohalm J, Kubackova K, Jelinkova M, Hovorka O, Kovar M, Plocova D, Sirova M, St'astny M, Rozprimova L, Ulbrich K, Acquired and specific immunological mechanisms co-responsible for efficacy of polymer-bound drugs, *J Control Release* **78**: 97-11

48. Rihova B, Strohalm J, Prausova J, Kubackova K, Jelinkova M, Rozprimova L, Sirova M, Plocova D, Etrych T, Subr V, Mrkvan T, Kovar K, Ulbrich K (2003) Cytostatic and immunomobilizing activities of polymer-bound drugs: experimental and first clinical data, *J Control Release* **91**: 1-16
49. Kovar M, Tomala J, Chmelova H, Kovar L, Mrkvan T, Joskova R, Zakostelska Z, Etrych T, Strohalm J, Ulbrich K, Sirova M, Rihova B (2008) Overcoming immunoescape mechanisms of BCL1 leukemia and induction of CD8+ T-cell-mediated BCL1-specific resistance in mice cured by targeted polymer-bound doxorubicin, *Cancer Res* **68**: 9875-9883
50. Sirova M, Strohalm J, Subr V, Plocova D, Rossmann P, Mrkvan T, Ulbrich K, Rihova B, Treatment with HPMA copolymer-based doxorubicin conjugate containing human immunoglobulin induces long-lasting systemic anti-tumour immunity in mice, *Cancer Immunol Immunother* **56**: 35-47
51. Etrych T, Jelinkova M, Rihova B, Ulbrich K (2001) New HPMA copolymers containing doxorubicin bound via pH-sensitive linkage: synthesis and preliminary in vitro and in vivo biological properties, *J Control Release* **73**: 89-102
52. Rihova B, Etrych T, Pechar M, Jelinkova M, Stastny M, Hovorka O, Kovar M, Ulbrich K (2001) Doxorubicin bound to a HPMA copolymer carrier through hydrazone, *J Control Release* **74**: 225-232
53. Ulbrich K, Etrych T, Chytil P, Pechar M, Jelinkova B, Rihova B (2004) Polymeric anticancer drugs with pH-controlled activation, *Int J Pharm* **277**: 63-72
54. Ulbrich K, Subr V (2004) Polymeric anticancer drugs with pH-controlled activation, Adv Drug Deliv Rev **56**: 1023-1050
55. Etrych T, Mrkvan T, Rihova B, Ulbrich K (2007) Star-shaped immunoglobulin-containing HPMA-based conjugates with doxorubicin for cancer therapy, *J Control Release* **122**: 31-38
56. Lammers T, Kühnlein R, Kissel M, Subr V, Etrych T, Pola R, Pechar M, Ulbrich K, Storm G, Huber P, Peschke P (2005) Effect of physicochemical modification on the biodistribution and tumor accumulation of HPMA copolymers, *J Control Release* **110**: 103-118
57. Seymour LW, Duncan R, Strohalm J, Kopecek J (1987) Effect of molecular weight (Mw) of N-(2-hydroxypropyl)methacrylamide copolymers on body distribution and rate of excretion after subcutaneous, intraperitoneal, and intravenous administration to rats, *J Biomed Mater Res* **21**: 1341-1358
58. Seymour LW, Miyamoto Y, Maeda H, Brereton M, Strohalm J, Ulbrich K, Duncan R (1995) Influence of molecular weight on passive tumour accumulation of a soluble macromolecular drug carrier, *Eur J Cancer* **31**: 766-770
59. Noguchi Y, Wu J, Duncan R, Strohalm J, Ulbrich K, Akaike T, Maeda H (1998) Early phase tumor accumulation of macromolecules: a great difference in clearance rate between tumor and normal tissues, *Jpn J Cancer Res* **89**: 307-314
60. Kissel M, Peschke P, Subr V, Ulbrich K, Schuhmacher J, Debus J, Friedrich E (2001) Synthetic macromolecular drug carriers: biodistribution of poly[(N-2-hydroxypropyl)-methacrylamide] copolymers and their accumulation in solid rat tumors, *PDA J Pharm Sci Technol* **55**: 191-201
61. Lammers T, Subr V, Ulbrich K, Peschke P, Huber PE, Hennink WE, Storm G (2009) Simultaneous delivery of doxorubicin and gemcitabine to tumors in vivo using prototypic polymeric drug carriers, *Biomaterials* **30**: 3466-3475
62. Borgman MP, Coleman T, Kolhatkar RB, Geyser-Stoops S, Line BR, Ghandehari H (2008) Tumor-targeted HPMA copolymer-(RGDfK)-(CHX-A''-DTPA) conjugates show increased kidney accumulation, *J Control Release* **132**: 193-199
63. Lammers T, Peschke P, Kühnlein R, Subr V, Ulbrich K, Huber P, Hennink W, Storm G (2006) Effect of intratumoral injection on the biodistribution and the therapeutic potential of HPMA copolymer-based drug delivery systems, *Neoplasia* **8:** 788-795
64. Lammers T, Peschke P, Kühnlein R, Subr V, Ulbrich K, Debus J, Huber P, Hennink W, Storm G (2007) Effect of radiotherapy and hyperthermia on the tumor accumulation of HPMA copolymer-based drug delivery systems, *J Control Release* **117:** 333-341
65. Shiah JG, Dvorak M, Kopeckova P, Sun Y, Peterson CM, Kopecek J (2001) Biodistribution and antitumour efficacy of long-circulating N-(2-hydroxypropyl)methacrylamide copolymer-doxorubicin conjugates in nude mice, *Eur J Cancer* **37**: 131-139
66. Kominami E, Tsukahara T, Bando Y, Katunuma N (1985) Distribution of cathepsins B and H in rat tissues and peripheral blood cells, *J Biochem* **98**: 87-93
67. Baricos WH, Zhou Y, Mason RW, Barrett AJ (1988) Human kidney cathepsins B and L. Characterization and potential role in degradation of glomerular basement membrane, *Biochem J* **252**: 301-304

68. Wang PH, Do YS, Macaulay L, Shinagawa T, Anderson PW, Baxter JD, Hsueh WA (1991) Identification of renal cathepsin B as a human prorenin-processing enzyme, *J Biol Chem* **266**: 12633-12638
69. Kiessling F, Heilmann M, Lammers T, Ulbrich K, Subr V, Peschke P, Waengler B, Mier W, Schrenk H, Bock M, Schad L, Semmler W (2006) Synthesis and characterization of HE-24.8: a polymeric contrast agent for magnetic resonance angiography, *Bioconjug Chem* **17:** 42-51
70. Etrych T, Chytil P, Mrkvan T, Sirova M, Rihova B, Ulbrich K (2008) Conjugates of doxorubicin with graft HPMA copolymers for passive tumor targeting, *J Control Rel* **132**: 184-192
71. Park JS, Qiao L, Su ZZ, Hinman D, Willoughby K, McKinstry R, Yacoub A, Duigou GJ, Young CS, Grant S, Hagan MP, Ellis E, Fisher PB, Dent P (2001) Ionizing radiation modulates VEGF expression through multiple MAPK-dependent pathways, *Oncogene* **25:** 3266-3280
72. Lee YJ, Galoforo SS, Berns CM, Erdos G, Gupta AK, Ways DK, Corry PM (1995) Effect of ionizing radiation on AP-1 binding activity and basic fibroblast growth factor gene expression in drug-sensitive human breast carcinoma MCF-7 and multidrug-resistant MCF-7/ADR cells, *J Biol Chem* **270:** 28790-28796
73. Samaniego F, Markham PD, Gendelman R, Watanabe Y, Kao V, Kowalski K, Sonnabend JA, Pintus A, Gallo RC, Ensoli B (1998) Vascular endothelial growth factor and basic fibroblast growth factor present in Kaposi's sarcoma (KS) are induced by inflammatory cytokines and synergize to promote vascular permeability and KS lesion development, *Am J Pathol* **152:**1433-1443
74. Feng D, Nagy JA, Pyne K, Hammel I, Dvorak HF, Dvorak AM (1999) Pathways of macromolecular extravasation across microvascular endothelium in response to VPF/VEGF and other vasoactive mediators, *Microcirculation* **6:** 23-44
75. Garcia-Barros M, Paris F, Cordon-Cardo C, Lyden D, Rafii S, Haimovitz-Friedman A, Fuks Z, Kolesnick R (2003) Tumor response to radiotherapy regulated by endothelial cell apoptosis, *Science* **300:** 1155-1159
76. Znati CA, Rosenstein M, Boucher Y, Epperly MW, Bloomer WD, Jain RK (1996) Effect of radiation on interstitial fluid pressure and oxygenation in a human tumor xenograft, *Cancer Res* **56:** 964-968
77. Netti P, Baxter L, Boucher Y, Skalak R, Jain R (1996) Time-dependent behavior of interstitial fluid pressure in solid tumors: implications for drug delivery, *Cancer Res* **55:** 5451-5458
78. Jain RK (1994) Barriers to drug delivery in solid tumors, *Sci Am* **271:** 58-65
79. Au JL, Jang SH, Zheng J, Chen CT, Song S, Hu L, Wientjes MG (2001) Determinants of drug delivery and transport to solid tumors, *J Control Release* **74:** 31-46
80. Peschke P, Klein V, Wolber G, Friedrich E, Hahn EW (1999) Morphometric analysis of bromodeoxyuridine distribution and cell density in the rat Dunning prostate tumor R3327-AT1 following treatment with radiation and/or hyperthermia, *Histol Histopathol* **14:** 461-469
81. Li C, Ke S, Wu QP, Tansey W, Hunter N, Buchmiller LM, Milas L, Charnsangavej C, Wallace S (2000) Tumor irradiation enhances the tumor-specific distribution of poly(L-glutamic acid)-conjugated paclitaxel and its antitumor efficacy, *Clin Cancer Res **6:*** 2829-2834
82. Davies CdeL, Lundstrom LM, Frengen J, Eikenes L, Bruland SOS, Kaalhus O, Hjelstuen MH, Brekken C (2004) Radiation improves the distribution and uptake of liposomal doxorubicin (Caelyx) in human osteosarcoma xenografts, *Cancer Res* **64:** 47-53
83. Kong G, Braun RD, Dewhirst MW (2000) Hyperthermia enables tumor-specific nanoparticle delivery: effect of particle size, *Cancer Res* **60**: 4440-4445
84. Kong G, Braun RD, Dewhirst MW (2001) Characterization of the effect of hyperthermia on nanoparticle extravasation from tumor vasculature, *Cancer Res* **61**: 3027-3032
85. Lammers T, Subr V, Peschke P, Kühnlein R, Hennink WE, Ulbrich K, Kiessling F, Heilmann M, Debus J, Huber PE, Storm G (2008) Image-guided and passively tumour-targeted polymeric nanomedicines for radiochemotherapy, *Br J Cancer* **99**: 900-910
86. Dipetrillo T, Milas L, Evans D, Akerman P, Ng T, Miner T, Cruff D, Chauhan B, Iannitti D, Harrington D, Safran H (2006) Paclitaxel poliglumex (PPX-Xyotax) and concurrent radiation for esophageal and gastric cancer: a phase I study, *Am J Clin Oncol* **29:** 376-379
87. Milas L, Mason K, Hunter N, Li C, Wallace S (2003) Poly(l-glutamic acid)-paclitaxel conjugate is a potent enhancer of tumor radiocurability, *Int J Radiat Oncol Biol Phys* **55:** 707-712
88. Wiedenmann N, Valdecanas D, Hunter N, Hyde S, Buchholz TA, Milas L, Mason KA (2007) 130-nm albumin-bound paclitaxel enhances tumor radiocurability and therapeutic gain, *Clin Cancer Res* **13:**1868-1874
89. Harrington KJ, Rowlinson-Busza G, Syrigos KN, Vile RG, Uster PG, Peters AM, Stewart, JS (2000) Pegylated liposome-encapsulated doxorubicin and cisplatin enhance the effect of radiotherapy in a tumor xenograft model. *Clin Cancer Res* **6:** 4939-49

Appendices

A. Summary

The aim of the present thesis was to investigate, understand, improve and extend drug targeting to tumors using HPMA copolymers. Hereto, the effects of physicochemical modification, drug-functionalization, intratumoral injection, radiotherapy and hyperthermia on the tumor accumulation of the copolymers were investigated, a novel polymeric contrast agent was developed, and long-circulating and passively tumor-targeted polymeric drug carriers were used to improve the efficacy of combined modality anticancer therapy.

To provide a proper theoretical framework for investigating drug targeting to tumors using HPMA copolymers, in **Chapters 1** and **2**, the basic principles of passive and active drug targeting were described. In addition, the most important classes of tumor-targeted nanomedicines were summarized, and several clinically relevant examples were highlighted. Furthermore, strategies for broadening the clinical applicability of tumor-targeted nanomedicines were addressed, related e.g. to the delivery of drugs other than standard chemotherapeutic agents (such as molecularly targeted therapeutics, anti-inflammatory agents and nucleic acids), and to the combination of tumor-targeted nanomedicines with other treatment modalities (such as with surgery, with radiotherapy and with chemotherapy). The insights provided in these two chapters illustrate that HPMA copolymers are suitable systems for improving the delivery of low molecular weight (chemo-) therapeutic agents to tumors, and they demonstrate that long-circulating and passively tumor-targeted polymeric drug carriers are able to improve the balance between the efficacy and the toxicity of systemic anticancer therapy.

In **Chapter 3**, to better understand drug targeting to tumors using HPMA copolymers, and to investigate the biodistributional consequences of functionalization, thirteen physicochemically different HPMA copolymers were synthesized, varying in molecular weight, in charge, and in the nature and amount of functional groups introduced. The copolymers were radiolabeled and injected i.v., and their circulation kinetics, their tissue distribution and their tumor accumulation were investigated in rats bearing subcutaneous Dunning AT1 tumors. Regarding size, in line with the literature, it was found that increasing the average molecular weight of the copolymers increased their circulation times, and that it (consequently) enhanced their tumor accumulation. The incorporation

of charged groups, as well as that of spacer, drug and peptide moieties, reduced the long-circulating properties of the copolymers, and as a result, lower levels were found in tumors and in all organs other than kidney. Interestingly, however, in spite of reduced absolute tumor concentrations, hardly any reduction in the relative levels localizing to tumors was observed, as exemplified by the fact that for the majority of physicochemically modified copolymers, tumor-to-organ ratios were comparable to those of unmodified controls. These findings demonstrate that HPMA copolymers circulate for prolonged periods of time, that they accumulate in tumors both effectively and selectively, and that their physicochemical modification does not negatively affect their biodistribution.

In **Chapter 4**, based on the notion that HPMA copolymers circulate for prolonged periods of time, we have set out to develop a novel polymeric contrast agent for MR angiography. The biological and physical properties of this gadolinium-containing HPMA copolymer (i.e. HE-24.8) were compared to those of an albumin-based macromolecular contrast agent (i.e. Gd-DTPA-HSA), as well as to those of a standard low molecular weight gadolinium complex (i.e. Gd-DTPA-BMA; Omniscan®). The T1 relaxivity of HE-24.8 was found to be a fivefold higher than that of Gd-DTPA-BMA, and twice as high as that of Gd-DTPA-HSA. No measurable release of gadolinium could be detected, and no cytotoxicity was observed. When injected i.v., HE-24.8 was retained in the circulation effectively, and an excellent display of chest, brain and tumor vasculature was achieved. The vessel contrast generated using HE-24.8 was found to be significantly higher than that resulting from the administration of Gd-DTPA-HSA. These findings demonstrate that gadolinium-modified HPMA copolymers are highly suitable systems for experimental MR angiography.

In **Chapter 5**, HPMA copolymers were injected intratumorally. This was done to demonstrate that long-circulating and passively tumor-targeted polymeric drug carriers can be used to improve the retention of i.t. applied chemotherapeutic agents at the target site. To assess the impact of i.t. injection on the biodistribution and the therapeutic potential of HPMA copolymer-based drug delivery systems, three different copolymers were injected both i.v. and i.t., and their circulation kinetics, their tumor concentrations, their tumor-to-organ ratios, their antitumor efficacy and their toxicity were compared. It was found that as compared to i.v. injection, i.t. injection improved both the tumor concentrations and the tumor-to-organ ratios of the copolymers substantially. In addition, as

compared to i.v. and i.t. applied free doxorubicin and to i.v. applied poly(HPMA)-GFLG-doxorubicin, the i.t. administered polymeric prodrug was found to be significantly more effective, and to be less toxic. These findings suggest that when tumor are easily accessible, e.g. during surgery, intratumorally injected carrier-based chemotherapeutics should be considered as interesting alternatives for the routinely used chemotherapy regimens and routes of administration.

In **Chapter 6**, to actively improve passive drug targeting, HPMA copolymers were combined with radiotherapy and with hyperthermia. As the effects of radiotherapy and hyperthermia were considered to depend significantly on the tumor model used, we first analyzed the accumulation of two different HPMA copolymers in three different types of tumors, based on the syngeneic Dunning rat prostate carcinoma model. Subsequently, in these three models, the effects of different doses of radiotherapy and hyperthermia on the tumor accumulation of 31 kDa poly(HPMA), 65 kDa poly(HPMA) and 28 kDa poly(HPMA)-GFLG-doxorubicin (PK1) were evaluated. It was found that as opposed to hyperthermia, which only increased the concentrations of the copolymers in subcutaneous Dunning H tumors, radiotherapy increased the concentrations of the copolymers in all three tumor models tested. Increases ranged from ~25% for 31 kDa poly(HPMA) in subcutaneous AT1 tumors, to more than 100% for 65 kDa poly(HPMA) in intramuscular AT1 tumors. These findings demonstrate radiotherapy is an effective means for improving the tumor accumulation of long-circulating and passively tumor-targeted polymeric drug delivery systems.

In **Chapter 7**, to extend drug targeting to tumors, HPMA copolymers were used to improve the efficacy of radiochemotherapy. The rationale for this novel combination regimen, which we have termed ‘carrier-based radiochemotherapy’, is based on the notion that the temporal and spatial interaction between i.v. applied (weekly) chemotherapy and clinically relevant (daily) radiotherapy is suboptimal, and on the assumption that drug targeting systems are able to improve the temporal and spatial parameters of this interaction. HPMA copolymers were used as a model drug targeting system, doxorubicin and gemcitabine as model drugs, and the syngeneic and radio- and chemoresistant Dunning AT1 rat prostate carcinoma as a model tumor model. MRI, γ-scintigraphy, fluorescence microscopy and HPLC were used to study the biodistribution of the copolymers, and clinically relevant regimens of daily radiotherapy and weekly chemotherapy to assess their efficacy-enhancing

effects. First, HPMA copolymers were shown to circulate for prolonged periods of time, to localize to tumors both effectively and selectively, and to improve the tumor-directed delivery of low molecular weight agents. Subsequently, they were then shown to interact synergistically with radiotherapy, with radiotherapy increasing the tumor accumulation of the copolymers, and with the copolymers increasing the therapeutic index of radiochemotherapy (both for doxorubicin and for gemcitabine). Based on these findings, and on the fact that its principles are likely broadly applicable, we propose 'carrier-based radiochemotherapy' as a novel concept for treating advanced solid malignancies.

In **Chapter 8**, to demonstrate that polymers, as e.g. liposomes, can be used to deliver two different drugs to tumors simultaneously, we have synthesized an HPMA-based polymer-drug conjugate carrying 6.4 wt-% of gemcitabine, 5.7 wt-% of doxorubicin and 1.0 mol-% of tyrosinamide (to allow for radiolabeling), and we have evaluated its properties both in vitro and in vivo. The newly generated construct, i.e. poly(HPMA-co-MA-GFLG-gemcitabine-co-MA-GFLG-doxorubicin-co-MA-TyrNH_2), was termed P-Gem-Dox, and it was shown to effectively kill cancer cells in vitro, to circulate for prolonged periods of time, to localize to tumors relatively selectively, and to inhibit tumor growth. As compared to control regimens, P-Gem-Dox increased the efficacy of the combination of gemcitabine and doxorubicin without increasing its toxicity, and it more strongly inhibited angiogenesis and induced apoptosis. These findings demonstrate that long-circulating and passively tumor-targeted polymeric drug carriers can deliver two different drugs to tumors simultaneously, and they thereby set the stage for more elaborate analyses on the potential of 'polymer-based multi-drug targeting'.

Finally, in **Chapter 9**, the insights provided and the evidence obtained are summarized and discussed, and several general conclusions are drawn. Together, the work described in this thesis demonstrates that HPMA copolymers are suitable systems for passive drug targeting to tumors, and that long-circulating and passively tumor-targeted polymeric nanomedicines are suitable systems for improving the efficacy of combined modality anticancer therapy.

B. Samenvatting in het Nederlands

Kanker is een ernstige en veel voorkomende ziekte, die vaak moeilijk te behandelen is. Kanker ontstaat doordat cellen snel en ongeremd groeien, en zo niet-repareerbare schade aanrichten in de weefsels waarin ze ontstaan en waarnaartoe ze uitzaaien. De therapie van kanker bestaat over het algemeen uit (combinaties van) chirurgie, radiotherapie en chemotherapie. Chemotherapeutica zijn cytostatische en/of cytotoxische stoffen die de celdeling remmen en schade aanrichten aan het DNA, en die er zo voor zorgen dat kankercellen minder snel groeien en/of dood gaan. Om zo veel mogelijk kankercellen te bereiken, en om tegelijkertijd schade aan het (erg gevoelige) maag-darm-kanaal te minimaliseren, worden chemotherapeutica over het algemeen niet in pil-vorm, maar intraveneus toegediend. Intraveneuze toediening leidt er echter toe dat chemotherapeutica zich over het hele lichaam verdelen, en behalve in tumoren, ook in vele gezonde weefsels belanden. Hierdoor kunnen er ernstige bijwerkingen ontstaan, die soms zelfs leiden tot de dood. Bovendien worden chemotherapeutica vaak vrij snel door de nieren geklaard en/of door de lever afgebroken, met als gevolg dat slechts een heel klein deel van de toegediende hoeveelheid de tumor bereikt, en dat de effectiviteit van chemotherapie laag is.

Om chemotherapeutica weg te houden uit gezonde weefsels, en om ze beter in tumoren te doen belanden, zijn er in de laatste drie à vier decennia heel wat tumor-gerichte geneesmiddeldragers ontwikkeld. De bekendste voorbeelden van dragersystemen zijn liposomen, polymeren en micellen. Wij hebben er hier voor gekozen te werken met polymeren, en meer specifiek, met polymeren gebaseerd op *N*-(2-hydroxypropyl)methacrylamide (i.e. HPMA). Polymeren gebaseerd op HPMA zijn gekozen omdat ze eenvoudig gesynthetiseerd en gemodificeerd kunnen worden, omdat ze niet-immunogeen en niet-toxisch zijn, omdat er vrij veel preklinische informatie beschikbaar is met betrekking tot HPMA copolymeren, en omdat er al vijf HPMA-gebaseerde chemotherapeutica in patienten getest zijn. Uit deze (pre-) klinische studies is duidelijk naar voren gekomen dat HPMA copolymeren – vanwege hun grootte (i.e. 50-2000 keer groter dan standaard geneesmiddelen) – vrij lang circuleren, dat ze effectief en selectief in tumoren accumuleren, en dat ze in staat zijn chemotherapeutica gericht naar tumoren te transporteren. Daarnaast bleken ze in staat chemotherapeutica weg te kunnen houden uit bepaalde gezonde weefsels, bijvoorbeeld uit het hart en uit de hersenen, die beide bijzonder gevoelig zijn voor de behandeling met bepaalde cytotoxische verbindingen.

Om tumor-gericht geneesmiddeltransport middels HPMA copolymeren beter te begrijpen, te verbeteren en uit te breiden, hebben we in dit proefschrift I) de goede tumoraccumulatie en de voordelige weefseldistributie van HPMA copolymeren onderzocht, en II) HPMA copolymeren gebruikt als een model geneesmiddeldrager, om aan te tonen dat lang-circulerende en passief getargete dragersystemen gebruikt kunnen worden om de effectiviteit van chirurgie, van radiotherapie en van chemotherapie te verbeteren.

Om een en ander in perspectief te plaatsen zijn hiertoe in **Hoofdstuk 1** en **2** de grondbeginselen van kanker, van kankertherapie, van tumor-gericht geneesmiddeltransport, en van tumor-gericht geneesmiddeltransport middels HPMA copolymeren samengevat. Naast polymere dragersystemen worden kort ook enkele andere klinisch relevante geneesmiddeldragers beschreven, en voorbeelden van tumor-gerichte nano-formuleringen die reeds op de markt zijn worden gebruikt om de principes van passief en actief geneesmiddeltransport uit te leggen. Verder worden in deze twee hoofdstukken enkele mogelijke toekomstperspectieven geschetst, die bijvoorbeeld verband houden met het tumor-gericht transport van niet-chemotherapeutica (zoals van anti-inflammatoire geneesmiddelen en van nucleïnezuren), met de ontwikkeling van temperatuur-gevoelige dragersystemen (die het geneesmiddel vrijzetten na hyperthermie), en met de combinatie van tumor-gerichte nano-formuleringen met andere therapeutische modaliteiten (zoals met chirugie, met radiotherapie en met chemotherapie). De inzichten beschreven in deze twee hoofdstukken illustreren dat HPMA copolymeren goede geneesmiddeldragers zijn, dat ze lang circuleren en sterk in tumoren accumuleren, en dat ze dientengevolge in staat zouden moeten zijn de effectiviteit van andere therapeutische modaliteiten te verbeteren.

Om tumor-gericht geneesmiddeltransport middels HPMA copolymeren beter te begrijpen, en om te onderzoeken hoe het veranderen van de fysisch-chemische eigenschappen van de polymeren zich vertaalt in een veranderde weefseldistributie en tumoraccumulatie, zijn in **Hoofdstuk 3** dertien verschillende HPMA copolymeren gesynthetiseerd en geëvalueerd. Zowel de grootte (23, 31 en 65 kDa) als de lading (3 en 8 mol-% positief en negatief geladen groepen) van de polymeren is gevarieerd, en ook polymeren gefunctionaliseerd met geneesmiddelen, met geneesmiddel-linkers en met peptiden zijn onderzocht. In lijn met reeds eerder gepubliceerde studies is er gevonden dat grote(re) polymeren langer circuleren dan kleine(re) polymeren,

en dat ze als gevolg hiervan sterker in tumoren accumuleren. Geladen polymeren, en met name positief geladen polymeren, werden duidelijk sneller uit de bloedsomloop geklaard, en hun concentraties in tumoren en in alle andere organen met uitzondering van de nier bleken duidelijk lager. Polymeren gemodificeerd met geneesmiddelen, met geneesmiddel-linkers en met peptiden bleken ook significant sneller uit het bloed te worden geklaard, en ook hun tumor- en orgaanconcentraties bleken duidelijk lager. In tegenstelling tot het feit dat de absolute tumorconcentraties van de geladen en de gefunctionaliseerde polymeren duidelijk lager waren dan die van niet-gemodificeerde polymeren, bleken de relatieve tumorconcentraties van de tien fysisch-chemisch verandere polymeren echter niet of nauwelijks veranderd: berekening van de tumor-orgaan-ratio's toonde aan dat er vrijwel geen verschillen waren in tumor-selectiviteit, en dat de polymeren in het gros van de gevallen effectiever in tumoren accumuleerden dan in zes tot acht van de gezonde organen die geëvalueerd werden. Deze bevindingen bewijzen dat HPMA copolymeren relatief lang circuleren, dat ze zowel effectief als selectief in tumoren accumuleren, en dat het veranderen van hun fysisch-chemische eigenschappen hun tumor-selectiviteit niet of nauwelijks verandert.

Gebaseerd op het feit dat HPMA copolymeren relatief lang circuleren, en in de eerste minuten tot uren na intraveneuze toediening in relatief hoge concentraties in het bloed aanwezig zijn, hebben we in **Hoofdstuk 4** een nieuw kontrastmiddel voor het visualiseren van bloedvaten gesynthetiseerd en geëvalueerd. De biologische en fysische eigenschappen van dit circa 25 kDa grote gadolinium-gemodificeerde polymeer, dat we HE-24.8 genoemd hebben, zijn vergeleken met die van een albumine-gebaseerd macromoleculair kontrastmiddel (i.e. Gd-DTPA-BSA), alsmede met die van een standaard klein kontrastmiddel (i.e. Gd-DTPA-BMA; Omniscan®). De sensitiviteit (i.e. de T1-relaxiviteit) van HE-24.8 was een factor vijf hoger dan die van Gd-DTPA-BMA, en twee keer zo hoog als die van Gd-DTPA-BSA. Geen meetbare vrijgifte van gadolinium kon worden vastgesteld, en de cytotoxiciteit van HE-24.8 bleek verwaarloosbaar. Na i.v. injectie bleef HE-24.8 vrij lang in de circulatie, en dientengevolge konden zowel de grote als de middelgrote bloedvaten in de borststreek, in de hersenen en in tumoren goed worden gevisualiseerd. Het bloedvat-contrast gegenereerd middels HE-24.8 bleek significant hoger dan dat gegenereerd middels Gd-DTPA-BSA. Deze bevindingen bevestigen het feit dat HPMA copolymeren goed en lang circuleren, en ze tonen aan dat HE-24.8 een interessant nieuw diagnosticum is voor experimentele MR angiografie.

Om de retentie van geneesmiddelen op de plek van toediening te verbeteren, en om aan te tonen dat polymere dragersystemen (in principe) gebruikt kunnen worden om de combinatie van chemotherapie en chirurgie te verbeteren, hebben we in **Hoofdstuk 5** het effect van intratumorale injectie op de biodistributie en de therapeutische effectiviteit van HPMA copolymeren onderzocht. Hiertoe zijn drie verschillende polymeren zowel intraveneus (i.v.) als intratumoraal (i.t.) toegediend, en zijn hun circulatietijden, hun tumoraccumulatie, hun orgaanverdeling, hun antitumor activiteit en hun toxiciteit onderzocht. In vergelijking met i.v. injectie bleken i.t. geïnjecteerde polymeren duidelijk lagere concentraties in het bloed en in gezonde weefsels te vertonen, en duidelijk hogere waarden in tumoren. Als gevolg hiervan waren de tumor-orgaan ratio's van i.t. ingespoten HPMA copolymeren een veelvoud hoger dan die van i.v. geïnjecteerde polymeren, en kon de therapeutische index significant worden verbeterd: in vergelijking met i.v. en i.t. geïnjecteerd vrij doxorubicine, en met i.v. geïnjecteerd poly(HPMA)-GFLG-doxorubicine, bleek i.t. ingespoten poly(HPMA)-GFLG-doxorubicine niet alleen duidelijk effectiever (i.e. in het remmen van de groei van AT1 tumoren), maar ook duidelijk minder toxisch (i.e. significant minder gewichtsverlies). Deze bevindingen impliceren dat als tumoren eenvoudig toegankelijk zijn, bijvoorbeeld tijdens operatieve ingrepen, intratumoraal geïnjecteerde nano-formuleringen overwogen dienen te worden als interessante alternatieven voor de standaard gebruikte geneesmiddelen en toedieningswegen.

In **Hoofdstuk 6** zijn HPMA copolymeren gecombineerd met radiotherapie en met hyperthermie. Dit om op een actieve manier passief geneesmiddeltransport naar tumoren te verbeteren. Aangezien we verwachtten dat de effecten van radiotherapie en van hyperthermie afhankelijk zouden zijn van het gebruikte tumormodel, en derhalve relatief sterk zouden kunnen variëren van model tot model, hebben we eerst de accumulatie van drie verschillende polymeren (i.e. 31 en 65 kDa poly(HPMA), en 28 kDa poly(HPMA)-GFLG-doxorubicine) in drie verschillende tumormodellen (i.e. subcutane en intramusculaire Dunning AT1 tumoren, en subcutane Dunning H tumoren) onderzocht. Na dit gedaan te hebben, en na te hebben aangetoond dat HPMA copolymeren effectief accumuleren in alle drie de gebruikte tumormodellen, zijn de effecten van drie verschillende doses hyperthermie en vier verschillende radiotherapie-doseringen onderzocht. In tegenstelling tot hyperthermie, dat slechts de accumulatie van één polymeer (i.e. 65 kDa poly(HPMA)) in één tumormodel (i.e. H-sc) verhoogde, bleek radiotherapie in staat de tumoraccumulatie van alle drie de

polymeren in alle drie de tumormodellen te verbeteren. Toenames in tumorconcentraties varieerden van circa 25% voor 31 kDa poly(HPMA) in AT1-sc tumoren, tot meer dan 100% voor 65 kDa poly(HPMA) in AT1-im tumoren. Deze bevindingen tonen aan dat radiotherapie (en in mindere mate ook hyperthermie) gebruikt kan worden om de tumoraccumulatie van lang-circulerende en passief getargete geneesmiddeldragers te verbeteren.

Om tumor-gericht geneesmiddeltransport middels HPMA copolymeren uit te breiden, en om aan te tonen dat lang-circulerende en passief getargete geneesmiddeldragers gebruikt kunnen worden om de effectiviteit van radiotherapie te verbeteren, hebben we in **Hoofdstuk 7** een nieuw therapeutische concept ontwikkeld, dat we 'drager-gebaseerde radiochemotherapie' (i.e. 'carrier-based radiochemotherapy') genoemd hebben. HPMA copolymeren zijn hierbij gebruikt als een voorbeeld geneesmiddeldrager, doxorubicine en gemcitabine als voorbeeld geneesmiddelen, en het syngene en radio- en chemoresistente AT1 tumormodel als een voorbeeld tumormodel. Magnetische resonantie tomografie, gamma-scintigrafie, fluorescentie microscopie en hoge druk vloeistof-chromatografie zijn gebruikt om de (effecten van radiotherapie op de) biodistributie en de tumoraccumulatie van de polymeren te onderzoeken, en klinisch relevante doseringsschema's (gebaseerd op dagelijkse bestraling en wekelijkse chemotherapie toediening) om de therapeutische effectiviteit van 'drager-gebaseerde radiochemotherapie' te evalueren. Als eerste is aangetoond dat HPMA copolymeren lang circuleren, dat ze effectief en selectief in tumoren accumuleren, en dat ze het tumor-gericht transport van diagnostica en therapeutica sterk verbeteren. Vervolgens is bewezen dat geneesmiddeldragers en radiotherapie synergistisch met elkaar interageren: enerzijds verbeterde radiotherapie de tumoraccumulatie van de polymeren, en anderzijds verbeterden de polymeren de therapeutische index van radiochemotherapie. Zowel voor (polymeer-gebonden) doxorubicine als voor (polymeer-gebonden) gemcitabine werd een duidelijk verbeterde effectiviteit gevonden, en ondanks het feit dat AT1 tumoren aggressief groeien, en radio- en chemoresistent zijn, kon de groei van deze tumoren sterk worden geremd. Deze bevindingen, alsmede het feit dat het aannemelijk is dat deze aanpak breed toepasbaar is (en niet alleen geldt voor polymeren, maar bijvoorbeeld ook voor liposomen en voor micellen), duiden erop dat 'drager-gebaseerde radiochemotherapie' een veelbelovend concept is voor het verbeteren van de behandeling van solide tumoren.

In **Hoofdstuk 8** hebben we getracht te bewijzen dat polymeren, net als liposomen, gebruikt kunnen worden om twee verschillende chemotherapeutica tegelijkertijd naar tumoren te transporteren. Hiertoe hebben we een conjugaat gesynthetiseerd dat zowel gemcitabine als doxorubicine bevat, en daarnaast ook nog een kleine hoeveelheid tyrosinamide (om het geheel te kunnen labelen met een radio-isotoop, en zo de biodistributie ervan te kunnen onderzoeken). Dit nieuwe construct, i.e. poly(HPMA-co-MA-GFLG-gemcitabine-co-MA-GFLG-doxorubicin-co-MA-TyrNH_2), hebben we P-Gem-Dox genoemd, en we hebben aangetoond dat het beide geneesmiddelen effectief vrijzet, en kankercellen doodt in nanomolaire concentraties. Tevens bleek het conjugaat lang te circuleren, en effectief en selectief in tumoren te accumuleren, met hogere concentraties in tumoren dan in zeven van de negen gezonde weefsels die we onderzocht hebben. Verder bleek P-Gem-Dox in staat de groei van tumoren te vertragen, angiogenese (i.e. bloedvat-groei) te remmen en apoptose (i.e. geprogrammeerde celdood) te induceren, zelfs in een aggresief groeiend en chemotherapie-resistent tumormodel, en zonder de toxiciteit (i.e. de gewichtsafname) van de interventie te laten toenemen. Deze bevindingen tonen aan dat polymeren in staat zijn meerdere chemotherapeutica tegelijkertijd naar tumoren te transporteren, en dat ze gebruikt kunnen worden om de effectiviteit van chemotherapie-combinaties te verbeteren.

In **Hoofdstuk 9** worden tenslotte de bovengenoemde bevindingen samengevat en bediscussieerd, en worden er enkele algemene conclusies getrokken. Alles tezamen toont dit proefschrift aan dat HPMA copolymeren geschikte systemen zijn voor tumor-gericht geneesmiddeltransport, en dat lang-circulerende en passief getargete polymere geneesmiddeldragers geschikte systemen zijn om de effectiviteit van combinatietherapieën te verbeteren.

C. Acknowledgements

None of the work described in this thesis would have been possible without the help of many different people and the support of several different funding agencies. The funding agencies that have enabled this work, and that I'd like to thank very much for their generous support, are the German Israeli Cooperation Program in Cancer Research (DKFZ-MOS; CA105), the Wieland-Stiftung and the European Commission (FP6: MediTrans). The people that have helped, assisted and supported me are summarized and acknowledged below.

First of all, I'd like to thank my two promotors, i.e. Gert Storm and Wim Hennink.

Gert: many thanks for giving me the opportunity to do a PhD under your guidance. Even though you (still...) tend to be very much in favor of liposomes, you were willing to supervise a thesis focusing exclusively on polymers, and even though your agenda has always been very full, you have always managed to make some time (sometimes a few minutes, sometimes a couple of hours) to discuss papers, problems and potential future projects. I furthermore very much appreciate the amount of freedom you have given me, both with regard to the experiments performed during my time as a PhD student in Heidelberg, and with regard to the tasks to be performed within the framework of MediTrans, during my time as a post-doc in Utrecht. I'd finally also like to thank you simply for being such a nice person, who is always willing answer questions, to listen to concerns and complaints, and to share some wise words, both from a professional and from a personal point of view. I sincerely hope that we can continue to cooperate for many more years to come, and I'd like to wish you all the best for the future.

Wim: I very much appreciate your guidance in the past few years, both from a scientific and from a leadership point of view. Even though I haven't experienced many yet, I'm practically sure you are the best department chair I will ever have: you're always there when people need help or advice, and your door is always open, and as a true captain, you can be both harsh and strict, and compassionate and caring, and you're always last to leave the ship (i.e. the 7th floor). I'd furthermore like to thank you for showing interest im my work, for your insightful and useful comments on my manuscripts, and for always delivering your comments within hours to days (as opposed to several others...). Finally, I've always enjoyed the time we spent together at conferences and meetings, and maybe even more, the time at hotel lobbies and bars afterwards, discussing

both professional and private things over one or two beers. I sincerely hope that you will manage to keep up the good work for many more years to come, and that we can continue to cooperate in the future.

Because of the fact that I did most (if not all) of the work described in this thesis in Heidelberg, and hardly spent any time in the labs on the 5th and the 6th floor, there officially are no other people at the Department of Pharmaceutics that need to be credited. In spite of this, however, without listing all of the names (I should maybe only mention Mies, as his name appears in all our of theses, and as he really is the hydrogel that holds the Department together, and the macro-initiator that keeps everything up and running), I do like to thank my colleagues in Utrecht, simply for being around, for sharing some thoughts every now and then, and for always being friendly. I'd like to apologize for hardly attending any coffeebreaks, birthday celebrations and borrels (I did attend all of the poker tournaments though...), and I'd like to wish all of you all the best for your future lifes and careers.

Next, I'd like to thank my colleagues at the German Cancer Research Center in Heidelberg, i.e. Rainer Kühnlein, Peter Peschke, Ditmar Greulich, Gabriele Becker, Volker Ehemann, Jochen Schumacher, Klaus Braun, Jürgen Jenne, Alexandra Tietz, Melanie Heilmann, Fabian Kiessling, Nicole Helker, Jürgen Debus and Peter Huber.

Rainer: you are definitely among the two or three people who deserve the most credit with regard to the realization of this thesis. There is hardly any figure on in vivo biodistribution and in vivo efficacy which has been generated without your help, and even working late nights and weekends (without me actually being there...) didn't seem to bother you. We spend many hours together, not only in the radioactive lab, at the gammatron and in the animal facilities, but also in the office, and occasionally on fairs and festivals in Heidelberg. I'm really very grateful for your efforts, your enthusiasm and your excellent technical assistance, and I sincerely hope that as a busy retiree, you will continue to do well in the years to come.

Peter: you essentially gave me the job, and you were my primary scientific adviser during my initial years at the DKFZ. You've accompanied me on my first scientific journeys (to Berlin, to Prague and to Tel Aviv), you've assisted me in finding funding to extend my stay in Heidelberg, and you've helped me to complete both the PP2C- and the HPMA-project. I really deeply appreciate the fact that you've always been there for me, in spite of the fact that you were often very busy with other things, and that you've always managed to make some time, both for answering questions, and for reading and writing reports. I sincerely hope that you will continue to be around for many more years to come, and that we can keep on cooperating (in one way or the other) in the future.

Ditmar: I've always enjoyed spending time with you, both in the cell culture lab and at the soccer pitch in Sandhausen (which in the meantime has turned into a real stadium...). I'm really very grateful to you for the large number of in vitro efficacy analyses you have performed, as well as for assisting me in preparing and staining cryosections. Given the fact that you're a great athlete and a passionate cycler, and that you ingest significant amounts of resveratrol every day, I'm sure that you will continue to do well for many more years to come.

Gabi: you're probably the one who learned me how to (properly) work with cells. You were always very critical with regard to the conditions to be used to assure reproducible results, and you always made sure that everything in the cell culture lab was running the way it should. In spite of the fact that hardly any of the cell cycle and FACS analyses you have performed have been included in this thesis, I'm very grateful to you for your help in this regard. I sincerely hope that you will continue to do well for many more years to come, and I'd like to wish you all the best for the future.

Volker: together with Gabi, you have performed a large number of cell cycle and FACS analyses. For several reasons, however, hardly any of these efforts have been included in the present thesis. With regard to the realization of the PP2C-project, on the other hand, your help has been very valuable, and without you, I probably wouldn't have been able to complete a thesis on PP2C. I'm really very grateful for your support, your enthusiam and your helpful suggestions, as well as for the numerous cups of coffee we have shared. I sincerely hope that you will continue to do well for many more years to come, and I'd like to wish you all the best for the future.

Jochen: you've radiolabeled practically all of the copolymers used in this thesis, and you've shared many thoughts on how to most effectively visualize their biodistribution. Without your help, I definitely wouldn't have been able to perform this many biodistribution analyses. I hope that you're enjoying your time as a retiree, and I'd like to wish you all the best for the future.

Klaus: in spite of the fact that you haven't been directly involved in the generation of this thesis, I'd like to thank you for sharing thoughts on a number of different issues, and simply for being around. You've taken me to several nice places and restaurants in Palatia, and you've regularly joined me to SV Sandhausen. I hope that you will continue to be around at the DKFZ for several more years, and that we can set up one or two things together in the future.

JJ: even though you haven't been directly involved in this thesis, I'd like to thank you for always helping me out with computer problems, and for discussing the physical bases of several different things (ranging from the application of ultrasound, to curveballs in soccer). I hope that you will remain to be around at the DKFZ for many more years, and that you will continue to do well in the future.

Alex: I'd like to thank you for helping both Rainer and me with transplanting large numbers of tumors into rats, for measuring their tumor volumes, and for replacing me whenever I wasn't in Heidelberg. I hope that you will continue to do well, and I'd like to wish you (and all of your animals) all the best for the future.

Melanie: we've cooperated both on the HE-24.8 and on the radiochemotherapy paper, and I'd like to thank you for sharing some thoughts and some of your data. I sincerely hope that you will continue to do well in Mannheim, and I'd like to wish you all the best for your future life and career.

Fabian: I'm very grateful to you for your interest in my work, and for your assistance with regard to the MRI experiments. In spite of the fact that you were always very busy with the large number of other projects you were running, you always managed to make some time to discuss how to set up things, how to report on them, and how to proceed. We've cooperated both on the HE-24.8 and on the radiochemotherapy paper, and we've also worked together on RGD-targeted iron oxide nanoparticles. I've always enjoyed working with you, and I'm sure I will continue to do so in the near and far future.

Nicole: you have helped me a lot with all of the administrative stuff that comes with working at a (German) research institute. Many thanks for always taking care of my questions and requests, and for always doing so in a timely manner. I sincerely hope that you will continue to enjoy your time at the DKFZ, and I'd like to wish you all the best for your future life and career.

Jürgen: I'd like to thank you very much for your involvement both in this and in the PP2C-thesis. In spite of the fact that you have always been tremendously busy, especially since you became director of the Radiotherapy Department at Heidelberg University, you have always managed to make some time for me, in order to discuss recent findings, and how to proceed. I sincerely hope that you will remain to be successful with regard to the realization of HIT and heavy-ion radiotherapy, and I'd like to wish you all the best for the future.

Peter: many thanks for supporting me during your time as chair of the Clinical Cooperation Unit Radiotherapeutic Oncology at the DKFZ. In spite of the fact that both PP2C and HPMA did not match very well with your own research interests, you have allowed me to keep on working on these two projects, and you have invested both time and money in making them work. I sincerely hope that you will continue to do well for many more years to come, and that we can set up one or two things together in the future.

Subsequently, I'd like to thank the people at the Institute of Macromolecular Chemistry at the Czech Academy of Sciences in Prague, i.e. Karel Ulbrich, Vladimir Subr, Michal Pechar, Robert Pola, Tomas Etrych and Blanka Rihova.

Karel: I've always had a good feeling about our cooperation. It felt right, right from the beginning, and it kept on going well for almost a decade now. I think you're a very nice and pleasant person, and a great boss, who always makes time for his people, and who really cares about his people (both at the institute and at home). I deeply appreciate the fact that you have never complained about the large number of emails and questions I have bothered you with, and that you have always responded in a timely manner, in spite of the fact that there were always many other things to be taken care of, especially during your time as director of the IMC. I sincerely hope that you will remain to be around for many more years, and that we can keep on cooperating in the future.

Mirek: you are definitely also among the two or three people who deserve the most credit with regard to the realization of this thesis. You've synthesized over a 100 copolymers over the past 10 years, you've performed a significant number of release studies, and you've arranged several HPLC analyses at Blanka's lab. And all of this without ever complaining for a single moment, and always with a smile on your face. I deeply appreciate your kind and pleasant nature, and the amount of time and effort you have invested in our cooperation, and I sincerely hope that we can keep on collaborating for many more years to come.

Michal, Robert and Tomas: many thanks for working with me on the peptide-targeted and the hydrazone-based copolymers. Even though our initial constructs didn't really work out the way we'd wanted them to, we did manage to publish some of the results obtained with them. I'd like to apologize for not having been able to test all of the constructs you have provided me with, but I promise that as soon as there is a possibility to do so, I will evaluate at least some of them, e.g. the RGD-targeted copolymers and the hydrazon-based polymeric prodrug of doxorubicin. Since we've already discussed several different things to do together in the years to come, I'm sure that we will remain to be in touch in the future.

Blanka: in spite of the fact that you haven't been directly involved in the generation of this thesis, I'd like to thank you for enabling us to perform several different HPLC analyses in your lab. I'd furthermore like to thank you for inviting me over to the ESCI congres in Prague in the beginning of 2006, giving me the opportunity to for the first time present my results at an international meeting. I'm sure that in spite of the fact that you're officially retired now, you will remain to be around in the field for many more years to come, and I look forward to setting up one or two things together in the future.

Finally, I'd like to thank my family and friends.

Mam: thank you very much for always having been there for me, either in person, or on the phone or via email. You've always helped and supported me wherever (and as good as) you could, and you've always shown interest in my work, even though you probably often had hardly any idea of what I was talking about. I am really very grateful to you for everything you have done for me, and I sincerely hope that you will be around for many, many more years.

Pap: you've probably shaped me to become the way I am, teaching me to always aim for the highest, and to always be very critical about things. I sincerely thank you for supporting me wherever you could, both mentally and financially, and for always guiding me with some wise words. I deeply appreciate the fact that you've always been there for me whenever I needed help, and I sincerely hope that you will remain to be around for many, many more years.

Willie: many thanks for always being there for me, for taking care of my sports career, and for taking care of my car. I guess both last aims didn't really work out the way you had planned them to (the car has been running for almost 15 years now though...), but I'm sure that you're happy with the way things have developed. I sincerely hope that you will remain to be around for many more years to come, and that we can start working on a next generation Wimbledon champion somewhere soon.

Elvira: you essentially taught me swimming when I was as little kid, and you've helped me realize what life is about in the years afterwards. I very much appreciate your kind and pleasant nature, and I've always enjoyed spending time with you. I sincerely hope that you will remain to be around for many more years, and that you will continue to enjoy life the way it is.

Nelly: as my third mother, you have always taken very good care of me. In the timeframe in which I've been working on this thesis, you were undoubtedly my number one mom, at least from a washing, ironing, cooking and cleaning up point of view (especially since we've moved to Maaseik). I really deeply appreciate your kind and uncomplicated nature, and I hope that you will remain to be around for many more years.

Herman: as a very devoted third father, you have always taken very good care of our huisje, our boompje and our beestje; you have essentialy (re-) built our house, you are still in charge of the garden (sorry...), and with great love, you've always taken very good care of our animals. I'm very grateful to you for all of this, and I sincerely hope that you will remain to be around for many more years.

With regard to my friends (and sincerely hoping not to forget anybody), I'd like to thank my soccer, poker and beer-drinking buddies: Ronny, Gert, Gary, Frank, Maurice, Jasper, Wouter, Tommy, Paul, Kenan, Bjorn, Ray, Roy, Jor and Roel,

as well as some of my female friends and some of my former teammates at Conventus and Juliana: thank you very much for listening to my stupid stories every now and then, for accepting me as who I am, and simply for being there, both when it's time to have fun, and when things aren't going that well. I've always very much enjoyed your friendship and companionship, and I sincerely hope that all of you will remain to be around for many more years to come. Let's all (try to) make the most of it!

Loes, lieverd: you really deserve a great lot of gratitude, and lots and lots of respect. Thank you very much for always having been there for me (even though I've hardly been there for you...), for being able to put up with my moods and mess (you can be quite moody and messy yourself though...), and for taking care of all of the things in and around the house (mostly together with your mom and dad though, and except for cooking...). I really deeply appreciate your kind and loving nature, and I've very much enjoyed the past 11 years with you. I think we go very well together, and I hope that we will remain to be a couple for many more years to come; until death (God) do us part...

D. Curriculum vitae

Twan Lammers was born in Vlodrop, in The Netherlands, in 1979. He attended the gymnasium at Serviam in Sittard from 1991 to 1997, and studied pharmacy in Utrecht from 1997 to 2002. From September 2001 until May 2002, he worked as a visiting graduate student at the Department of Pharmacology at Cornell University Medical College in New York, on a project focusing on serotonin-1A-signaling in anxious mice. In September 2002, he joined the German Cancer Research Center (DKFZ) in Heidelberg, to work on a project funded by the German-Israeli Cooperation Program in Cancer Research. The primary aim of this project was to use HPMA copolymers to improve the in vitro uptake and the in vivo delivery of Protein Phosphatase 2C-alpha (i.e. PP2Cα; a prototypic type 2C phosphatase known to be involved in p53 signaling). After about a year of efforts, in the beginning of 2004, this project was halted, as neither simple polymer-protein conjugates (based on PHPMA and PEG), nor more advanced systems (based on fusion proteins and on TAT- and R9-targeted polymer-protein conjugates) turned out to be able to deliver PP2Cα into the cytoplasm of cancer cells. It was decided to split up the project into two separate lines of research, one focusing on the role of PP2Cα in cell growth, in cellular stress signaling and in tumorigenesis (in cooperation with Sara Lavi from Tel Aviv University and Jürgen Debus from Heidelberg University), and one focusing on drug targeting to tumors using HPMA copolymers (in cooperation with Rainer Kühnlein, Peter Peschke and Peter Huber from the Department of Innovative Cancer Diagnosis and Therapy at the DKFZ in Heidelberg, with Vladimir Subr and Karel Ulbrich from the Institute of Macromolecular Chemistry at the Czech Academy of Sciences in Prague, and with Wim Hennink and Gert Storm from the Department of Pharmaceutics at Utrecht University). The former project has resulted in the completion of a DSc degree in Radiation Oncology at Heidelberg University in 2008, and the latter has provided the basis for the present PhD thesis. Since the beginning of 2007, Twan Lammers has been working as a post-doctoral fellow at the Department of Pharmaceutics in Utrecht, focusing primarily on the MediTrans project (FP6: 'Targeted Delivery of Nanomedicines'). His main research interests include drug targeting to tumors, image-guided drug delivery and combined modality anticancer therapy.

E: List of publications

1. Lammers T, Kühnlein R, Kissel M, Subr V, Etrych T, Pola R, Pechar M, Ulbrich K, Storm G, Huber P, Peschke P. Effect of physicochemical modification on the biodistribution and tumor accumulation of HPMA copolymers. *J Control Release* **110**: 103-118 (2005)

2. Lammers T, Peschke P, Kühnlein R, Subr V, Ulbrich K, Huber P, Hennink W, Storm G. Effect of intratumoral injection on the biodistribution and the therapeutic potential of HPMA copolymer-based drug delivery systems. *Neoplasia* **8**: 788-795 (2006)

3. Kiessling F, Heilmann M, Lammers T, Ulbrich K, Subr V, Peschke P, Wängler B, Mier W, Schrenk H, Bock M, Schad L, Semmler W. Synthesis and characterization of HE-24.8: a polymeric contrast agent for MR Angiography. *Bioconjug Chem* **17**: 42-51 (2006)

4. Lammers T, Subr V, Ulbrich K, Kiessling F, Huber P, Peschke P. HPMA copolymers for cancer diagnosis and therapy. *Eur J Clin Invest* **36**: S53 (2006)

5. Lammers T, Peschke P, Kühnlein R, Subr V, Ulbrich K, Debus J, Huber P, Hennink W, Storm G. Effect of radiotherapy and hyperthermia on the tumor accumulation of HPMA copolymer-based drug delivery systems. *J Control Release* **117**: 333-341 (2007)

6. Lammers T, Lavi S. Role of type 2C protein phosphatases in growth regulation and cellular stress signalling. *Crit Rev Biochem Mol Biol* **42**: 437-461 (2007)

7. Lammers T, Ehemann V, Debus J, Peschke P, Huber P, Lavi S. Role of PP2Cα in cell growth, in radio- and chemosensitivity, and in tumorigenicity. *Mol Cancer* **6**: 65 (2007)

8. Zhang C, Jugold M, Wönne E, Lammers T, Morgenstern B, Müller M, Zentgraf H, Bock M, Eisenhut M, Semmler W, Kiessling F. Specific targeting of tumor angiogenesis by RGD-conjugated APTMS-coated USPIO using a clinical 1.5 T MR-scanner. *Cancer Res* **67**: 1555-1562 (2007)

9. Lammers T, Hennink W, Storm G. Tumor-targeted nanomedicines: principles and practice. *Brit J Cancer* **99**: 392-397 (2008)

10. Lammers T, Subr V, Peschke P, Kühnlein R, Hennink W, Ulbrich K, Kiessling F, Heilmann M, Debus J, Huber P, Storm G. Image-guided and passively tumor-targeted polymeric nanomedicines for radiochemotherapy. *Brit J Cancer* **99**: 900-910 (2008)

11. Lammers T, Subr V, Ulbrich K, Peschke P, Kiessling F, Huber P, Hennink W, Storm G. Carrier-based radiochemotherapy. *J Control Release* **132**: e70 (2008)

12. Lammers T, Subr V, Ulbrich K, Peschke P, Huber P, Hennink W, Storm G. Simultaneous delivery of doxorubicin and gemcitabine to tumors in vivo using prototypic polymeric drug carriers. *Biomaterials* **30**: 3466-3475 (2009)

13. Talelli M, Rijcken C, Lammers T, Seevinck P, Storm G, van Nostrum C, Hennink W. Superparamagnetic Iron oxide nanoparticles encapsulated in biodegradable thermosensitive polymeric micelles: toward a targeted nanomedicine suitable for image-guided drug delivery. *Langmuir* **25**: 2060-2067 (2009)

14. Lammers T, Ulbrich K. HPMA copolymers: 30 years of advances. *Adv Drug Deliv Rev* (invited manuscript; 2010)

15. Lammers T. Using HPMA copolymer-based nanomedicine formulations to improve the efficacy of combined modality anticancer therapy. *Adv Drug Deliv Rev* (invited manuscript; 2010)

16. Lammers T. HPMA copolymers: Summarizing some recent advances. *Expert Opin Drug Deliv* (invited manuscript; 2010)

F: Color figures

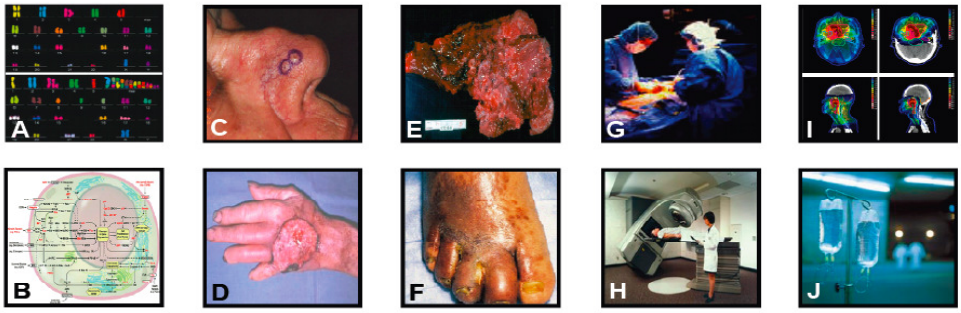

Chapter 1: Figure 1: Cancer and cancer therapy. Cancer is a complex disease, resulting from changes at the genetic (A: chromosomal aberrations in cancer cells (bottom panel) versus normal cells (top panel) visualized using fluorescent in-situ hybridization) and signaling level (B: schematic overview of key pathways deregulated in cancer (see [1] for details)). The phenotypic appearance of cancer can be very diverse, ranging from barely detectable malignant melanomas (C), to more obvious squamous cell carcinomas (D), lung carcinomas (E) and Kaposi Sarcomas (F). Treatments for cancer primarily rely on (combinations of) surgery (G), radiotherapy (H-I) and chemotherapy (J).

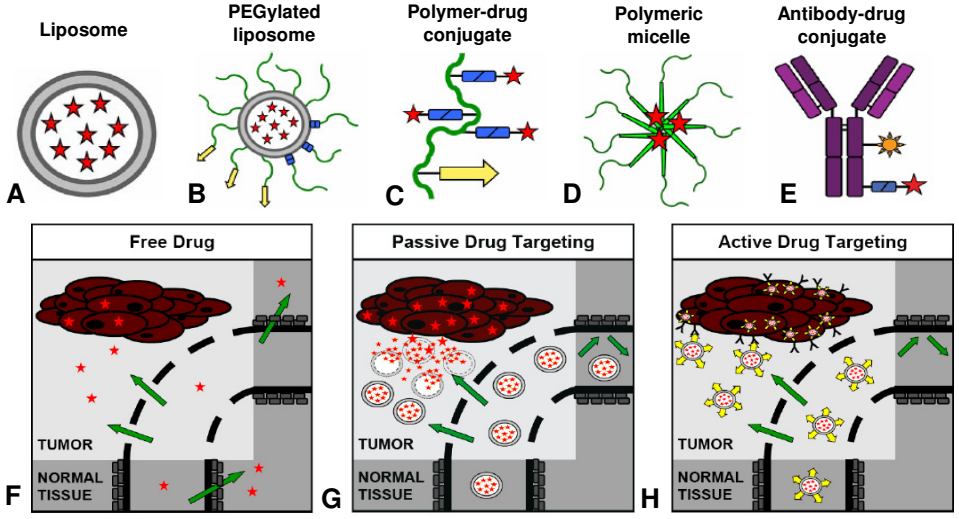

Chapter 1: Figure 2: Drug delivery systems and drug targeting strategies. A-E: Examples of clinically used tumor-targeted nanomedicines. Liposomes and liposomal bilayers are depicted in grey, polymers and polymer-coatings in green, linkers allowing for drug release and for sheddable stealth coatings in blue (rectangles), targeting ligands in yellow (arrows), antibodies and antibody fragment in purple, radionuclides in orange (suns) and conjugated or entrapped active agents in red (stars). F-H: Principles of passive and active drug targeting to tumors. F: Upon i.v. injection, a low molecular weight anticancer agent is generally rapidly cleared from the circulation, and only low levels of the drug accumulate in tumors and in tumor cells. At the same, due to its small size, high hydrophobicity and/or large volume of distribution, significant levels of the agent accumulate in healthy tissues. G: Upon encapsulation in (or conjugation to) a long-circulating and passively tumor-targeted drug delivery system, the concentration of the active agent in tumors can be increased substantially (by means of Enhanced Permeability and Retention (EPR)), while its accumulation in healthy tissues can be attenuated. H: Upon the incorporation of targeting ligands, like antibodies and peptides, the interaction between the drug and/or drug delivery system and cancer cells can be improved, resulting in a more selective target site localization and/or target cell uptake.

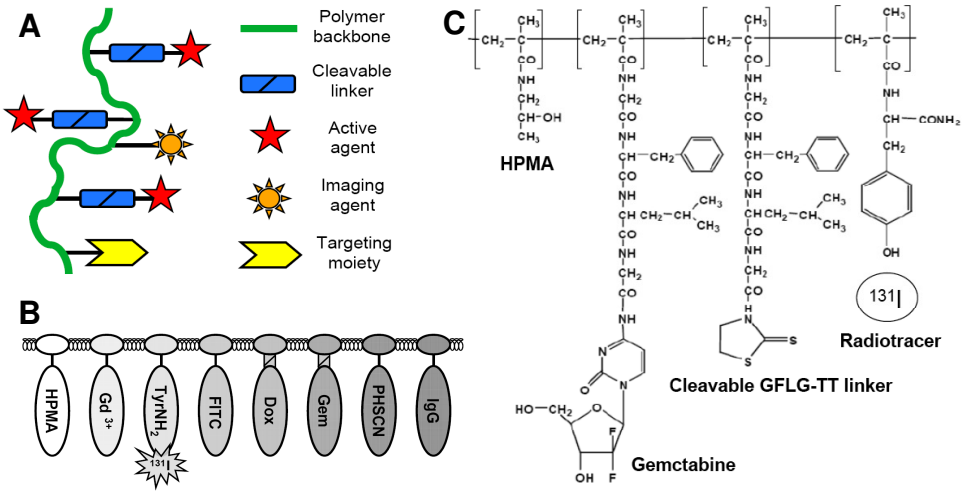

Chapter 1: Figure 3: Polymer-drug conjugates based on HPMA. A: Schematic overview of the components routinely used in polymer therapeutics. B: Examples of imaging agents (gadolinium and radioactive iodine), fluorophores (fluorescein isothiocyanate), drug molecules (doxorubicin and gemcitabine) and targeting ligands (oligopeptides and antibodies) incorporated into HPMA copolymers. C: Chemical structure of an exemplary HPMA copolymer, functionalized with tyrosinamide (for radiolabeling), with GFLG-gemcitabine (for drug delivery and release), and with remaining GFLG-TT reactive groups (for attaching additional components, like a targeting moiety). The chemical formula of this copolymer is poly(HPMA-co-MA-GFLG-gemcitabine-co-MA-GFLG-TT-co-MA-$TyrNH_2$). On average, HPMA copolymers contain 80-95 wt-% of HPMA, 5-10 wt-% of drug and 1-2 wt-% of tyrosinamide and imaging agent.

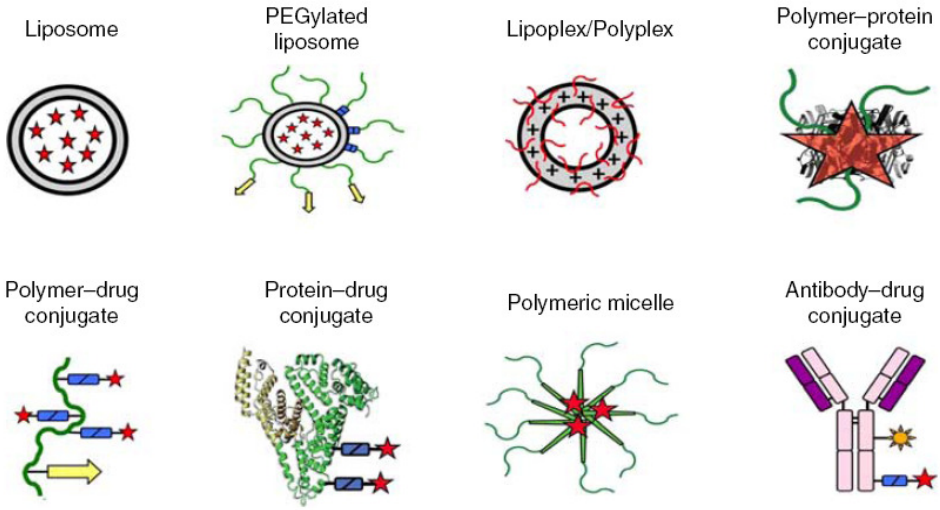

Chapter 2: Figure 1: Representative examples of clinically used tumour-targeted nanomedicines. Liposomal bilayers are depicted in grey, polymers and polymer-coatings in green, biodegradable linkers (for releasing drugs and polymer coatings) in blue, targeting ligands in yellow, antibody fragments in purple, radionuclides in orange, and conjugated or entrapped active agents in red.

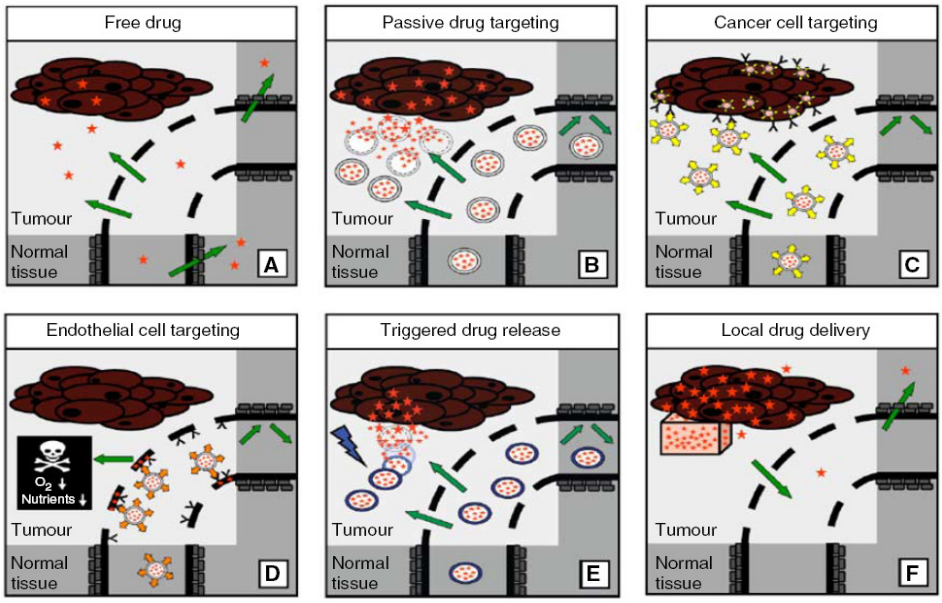

Chapter 2: Figure 2: Overview of the clinically most relevant drug targeting strategies. A: Upon the intravenous injection of a low molecular weight (chemo)therapeutic agent, which is often rapidly cleared from blood, only low levels of the drug accumulate in tumours and in tumour cells, whereas their localisation to certain healthy organs and tissues can be relatively high. B: Upon the implementation of a passively targeted drug delivery system, by means of the enhanced permeability and retention (EPR) effect, the accumulation of the active agent in tumours and in tumour cells can be increased substantially. C: Active drug targeting to internalisation-prone cell surface receptors (over)expressed by cancer cells generally intends to improve the cellular uptake of the nanomedicine systems, and is particularly useful for the intracellular delivery of macromolecular drugs, such as DNA, siRNA and proteins. D: Active drug targeting to receptors (over)expressed by angiogenic endothelial cells aims to reduce blood supply to tumours, thereby depriving tumour cells from oxygen and nutrients. E: Stimuli-sensitive nanomedicines, such as Thermodox, can be activated (i.e. induced to release their contents) by externally applied physical triggers, such as hyperthermia, ultrasound, magnetic fields and light. F: In cases in which tumours are easily accessible, e.g. during surgery, sustained-release delivery devices can be implanted or injected directly into tumours.

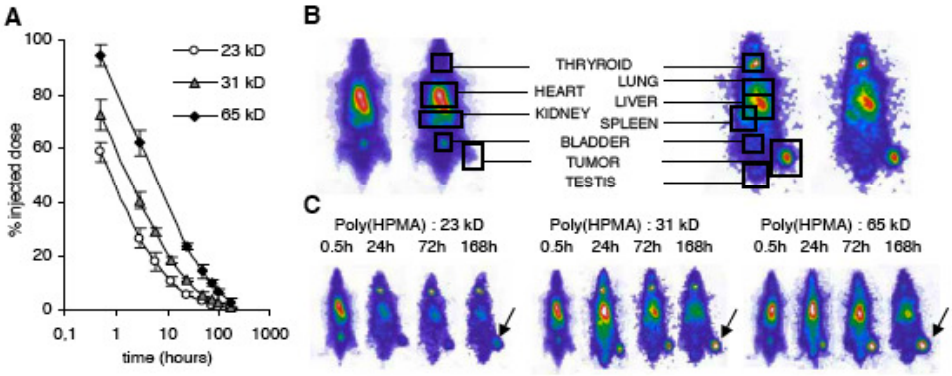

Chapter 3: Figure 2. Effect of (increasing) the average molecular weight of HPMA copolymers on their biodistribution. A: Percentage of the injected dose remaining in circulation after i.v. injection of radiolabeled HPMA copolymers with different molecular weights. B: Schematic representation of the regions of interest (and the corresponding organs) used in the scintigraphic analyses. C: Scintigraphic analysis of the biodistribution and the tumor (arrows) accumulation of the three copolymers.

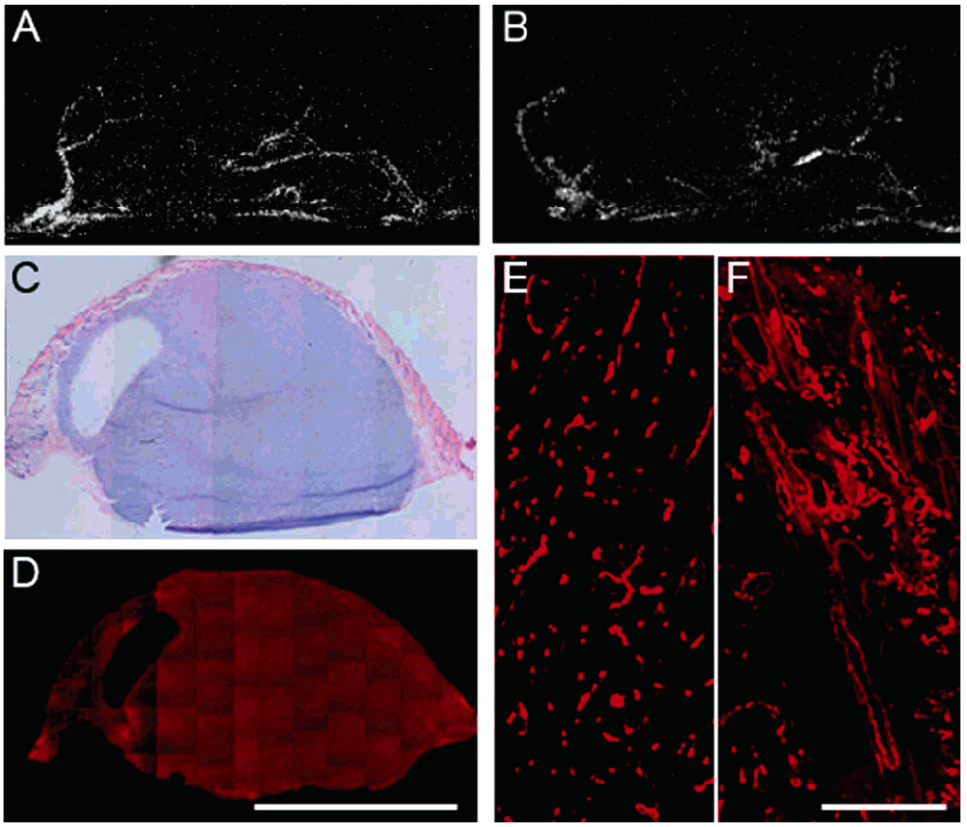

Chapter 4: Figure 9: Maximum intensity projections (MIP) of a subcutaneous Dunning prostate carcinoma in rats using HE-24.8 (A) and Gd-DTPA-HSA (B). Histological compound images of the tumor shown in A were prepared using hematoxilin and eosin staining (C), and collagen type IV staining (D). Magnifications of the immunofluorescence image taken from representative areas of the tumor center (E) and periphery (F) exemplify the differences in vessel architecture between larger vessels in the tumor periphery (91 ± 51 µm) and smaller capillary vessels in the center (12 ± 5 µm). Bars: 5 mm (D), 0.4 mm (F).

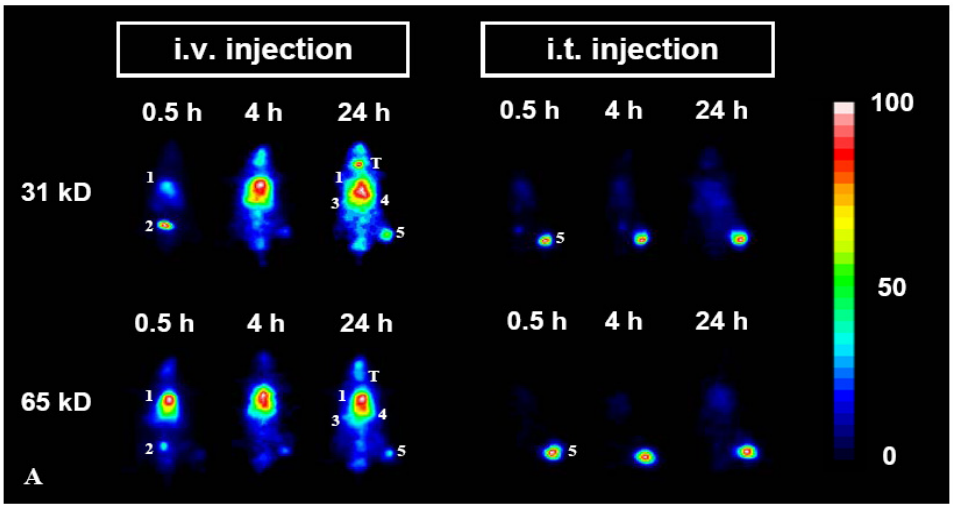

Chapter 5: Figure 2: Effect of intratumoral injection on the biodistribution of HPMA copolymers. A: Scintigraphic analysis of the effect of i.t. injection on the biodistribution of 31 kD and 65 kD poly(HPMA) in rats bearing subcutaneous Dunning AT1 tumors. In the images obtained at 0.5 h after i.v. administration, the accumulation of the radiolabeled copolymers was most prominent in heart (i.e. in circulation; 1) and in bladder (2). In the images obtained at 4 and 24 h, the highest amounts of copolymer were found in heart/lung (1), in spleen (3), in liver (4) and in tumor (5). In addition, at the two latter time points, an accumulation of released radioactive iodine in thyroid (T) was noted. Upon i.t. injection, only localization to tumor (5) could be observed over the first 24 h after administration.

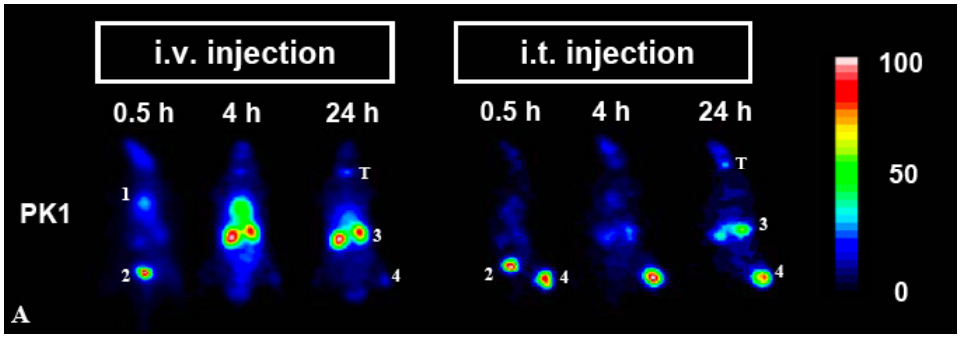

Chapter 5: Figure 3: Effect of intratumoral injection on the biodistribution of poly(HPMA)-GFLG-doxorubicin (PK1). A: Scintigraphic analysis of the effect of i.t. injection on the biodistribution of PK1 in rats bearing subcutaneous Dunning AT1 tumors. In the images obtained at 0.5 h post i.v. injection, the accumulation of the radiolabeled conjugate was most prominent in heart (i.e. in circulation; 1) and in bladder (2), at 4 and 24 h, most of the conjugate was found in kidney (3) and in tumor (4). Released radioactive iodine was again found to accumulate in thyroid (T). Upon i.t. injection, the highest amounts of PK1 were found in kidney (3) and in tumor (4). B: Quantification of the effect of i.t. injection on the tumor and organ concentrations of PK1 at 24 h p.i. Values represent average ± standard deviation of 3-4 animals. * Indicates $p<0.05$ vs. i.v. injection (Student's t-test).

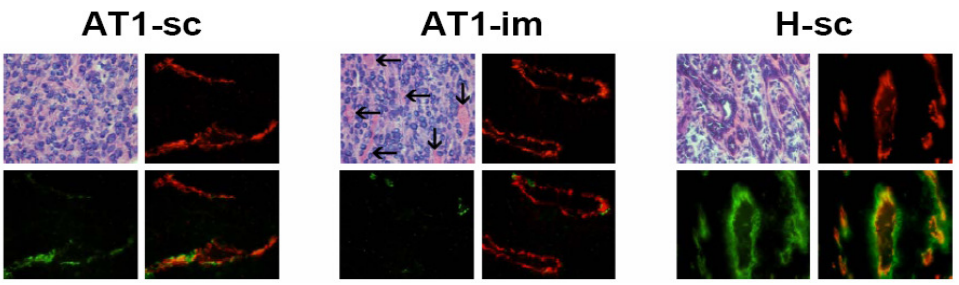

Chapter 6: Figure 1: Characterization of the three tumor models used. Immunohistochemical analysis of subcutaneously transplanted Dunning AT1 tumors (AT1-sc), intramuscularly inoculated Dunning AT1 tumors (AT1-im) and subcutaneously transplanted Dunning H tumors (H-sc). Methanol / acetone-fixed cryosections were stained using H&E, CD31 (red) and alpha-smooth muscle actin (green), and imaged at magnifications of 400x (H&E) and 600x (CD31 and α-SMA). Arrows indicate muscle fibers.

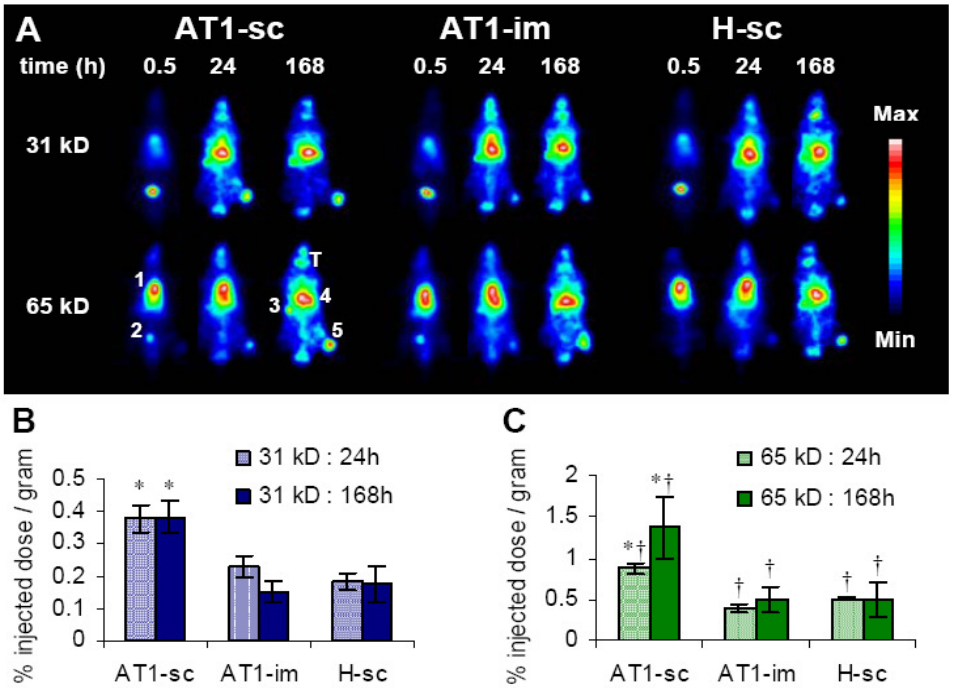

Chapter 6: Figure 2: Accumulation of HPMA copolymers in 3 different tumor models. A: Scintigraphic analysis of the biodistribution and the tumor accumulation of two differently sized radiolabeled HPMA copolymers in Copenhagen rats bearing AT1-sc, AT1-im and H-sc tumors. In the scintigrams obtained at 0.5 h p.i., localization to heart (i.e. in circulation; 1) and to bladder (2) was observed. In the images obtained at 24 h and 168 h p.i., the accumulation of the copolymers was most prominent in spleen (3), in liver (4) and in tumor (5). In addition, at the latter two time points, an accumulation of released radioactive iodine in thyroid (T) was noted. B and C: Quantification of the amounts of 31 kD poly(HPMA) (B) and 65 kD poly(HPMA) (C) per gram dissected tumor tissue at 24 h and 168 h p.i. Values represent average ± standard deviation of 3-6 animals per experimental group. * Indicates $p<0.05$ vs. AT1-im and H-sc tumors, † indicates $p<0.05$ vs. 31 kD poly(HPMA) (Student's t-test).

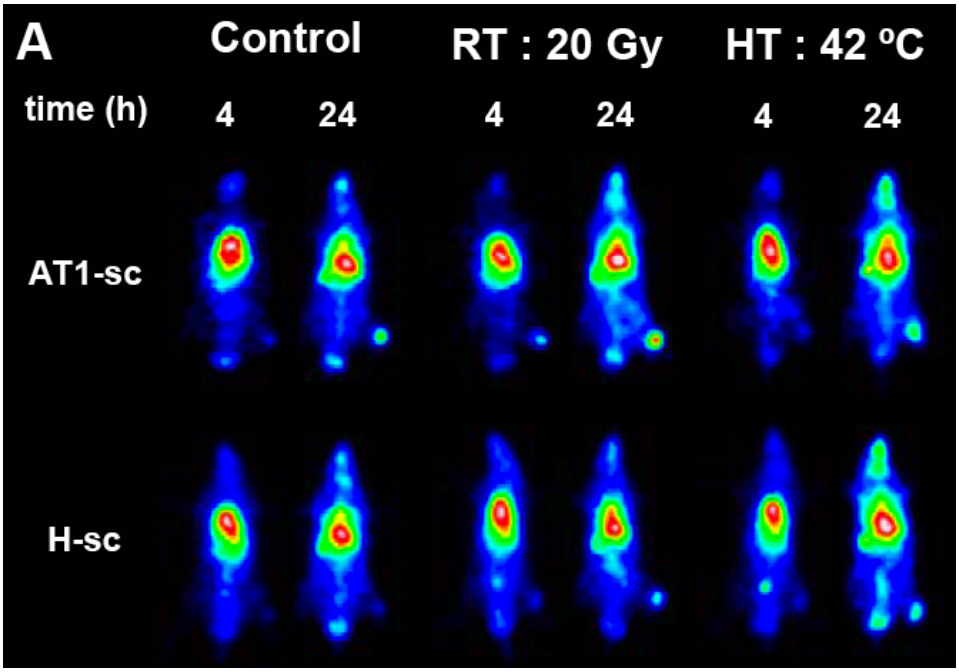

Chapter 6: Figure 3: Effect of radiotherapy and hyperthermia on the tumor accumulation of HPMA copolymers. A: Scintigraphic analysis of the effects of radiotherapy (20 Gy, applied 24 h prior to i.v. injection) and hyperthermia (42 ºC, applied for 1 h, concomitant to i.v. injection) on the tumor accumulation of 31 kD poly(HPMA) in rats bearing AT1-sc and H-sc tumors.

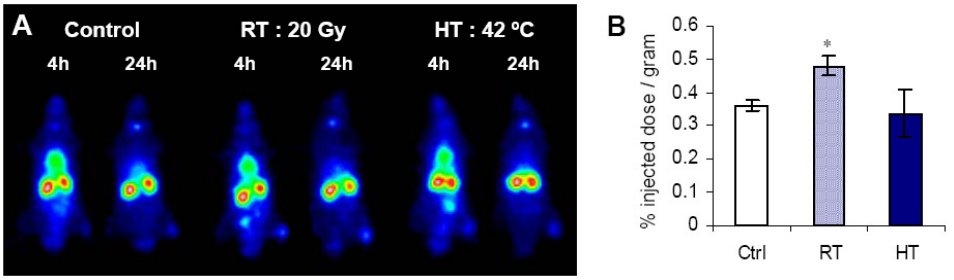

Chapter 6: Figure 4: Effect of radiotherapy and hyperthermia on the tumor accumulation of poly(HPMA)-GFLG-doxorubicin. A: Scintigraphic analysis of the effects of radiotherapy (20 Gy, applied 24 h prior to i.v. injection) and hyperthermia (42 ºC, applied for 1 h, concomitant to i.v. injection) on the tumor accumulation of poly(HPMA)-GFLG-doxorubicin in rats bearing AT1-sc tumors. B: Quantification of the effects of radiotherapy and hyperthermia on the tumor accumulation of poly(HPMA)-GFLG-doxorubicin at 24 h p.i. Values represent average ± standard deviation of 3-4 animals per experimental group. * Indicates $p<0.05$ vs. control (Student's t-test).

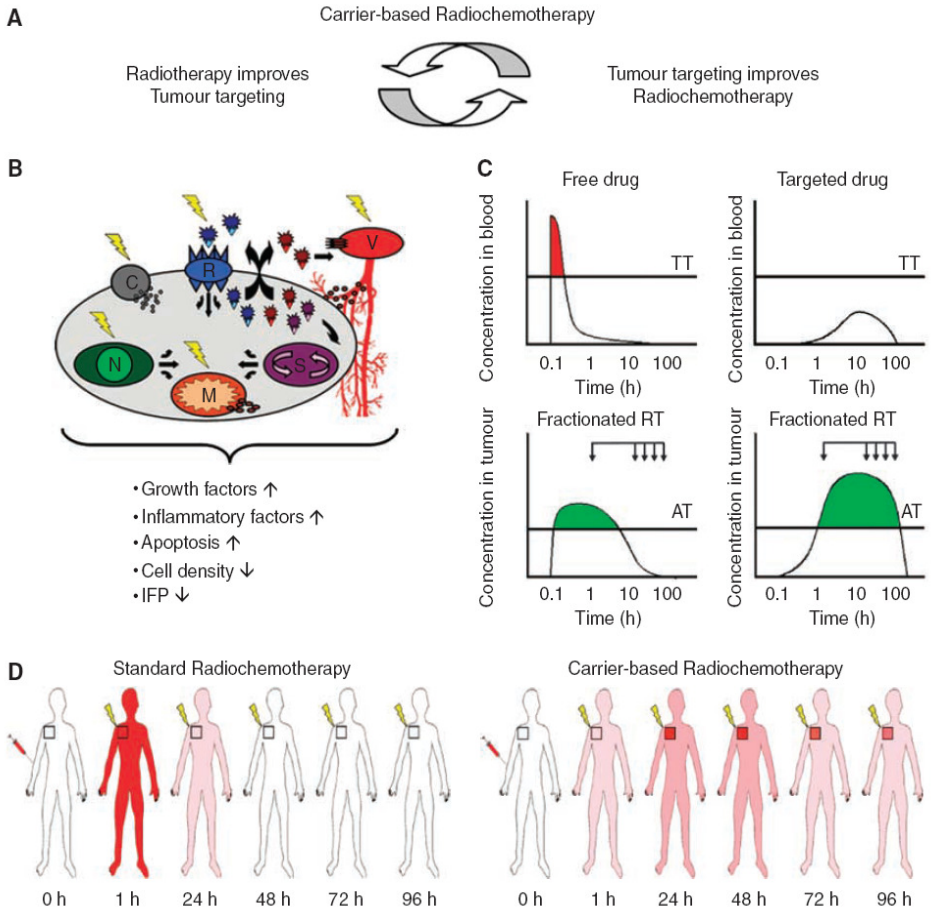

Chapter 7: Figure 1: Rationale for carrier-based radiochemotherapy. A: Carrier-based radiochemotherapy is based on the notion that drug targeting and radiotherapy interact synergistically, with on the one hand, radiotherapy improving the tumor accumulation of drug targeting systems, and with on the other hand, drug targeting systems improving the therapeutic index of radiochemotherapy. B: Potential physiological mechanisms by which radiotherapy increases the tumor accumulation of drug targeting systems. See text for details. C: Schematic representation of the blood and tumor concentrations of an intravenously (i.v.) applied free drug (upper and lower left panels), and of a drug delivered to the tumor by means of an i.v. applied drug targeting system (upper and lower right panels). The arrows indicate the administration of fractionated radiotherapy, which is routinely applied on every weekday for several consecutive weeks. TT: toxicity threshold, AT: activity threshold. See text for details. D: Schematic representation of the in vivo interaction between radiotherapy and chemotherapy upon standard and upon carrier-based radiochemotherapy, exemplifying that in case of the latter, the temporal and spatial interaction between the two treatment modalities is improved.

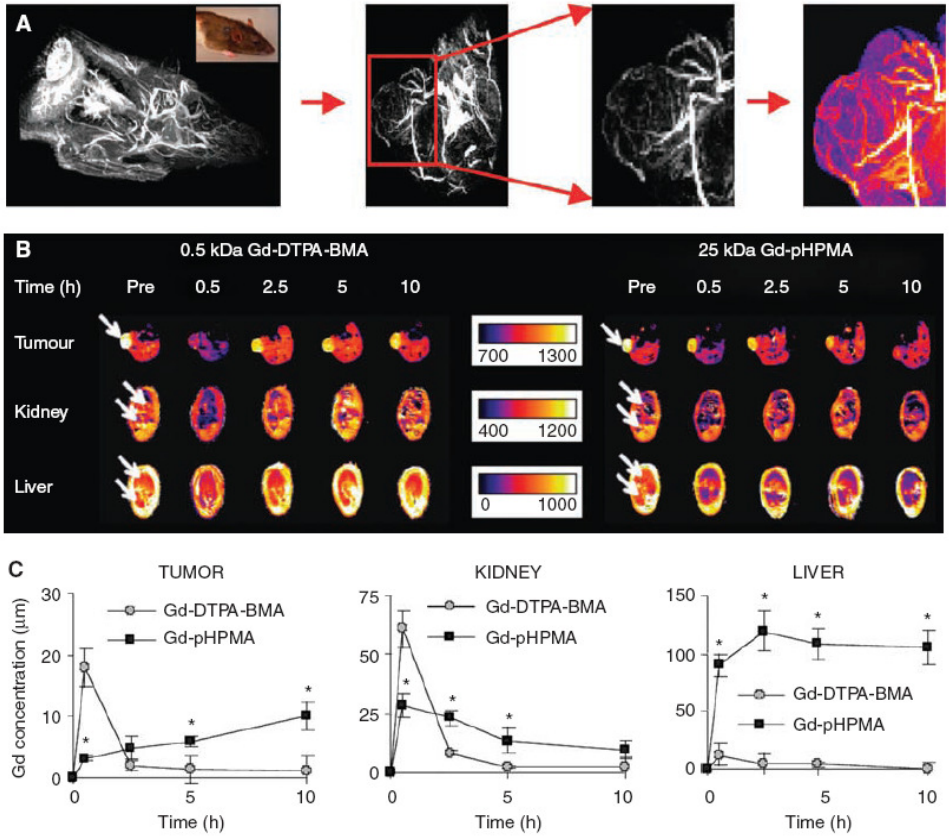

Chapter 7: Figure 3: Magnetic resonance imaging (MRI)-based biodistributional analysis of pHPMA-gadolinium (Gd). A: MR angiography scans of the chest and head region of a rat, of a tumor-bearing paw, and of an AT1 tumor, obtained at 0.5 h after the intravenous (i.v.) injection of 25 kDa pHPMA-Gd. A color-coded maximal intensity projection (MIP) of the polymer-visualised perfusion of the tumor is depicted in the right panel. B: Dynamic, color-coded MRI T1 determination obtained for AT1 tumor, for kidney and for liver before contrast agent administration and at various time points after the i.v. injection of a low (0.5 kDa Gd-DTPA-BMA) and high (25 kDa Gd-pHPMA) molecular weight MR contrast agent. Note that contrast agent accumulation corresponds to a decrease in the T1 signal. C: Quantification of the concentrations of gadolinium in AT1 tumor, kidney, and liver upon the i.v. injection of Gd-DTPA-BMA and pHPMA-Gd. Values represent average ± s.d. (n=3). * Indicates $P<0.05$ (paired t-test).

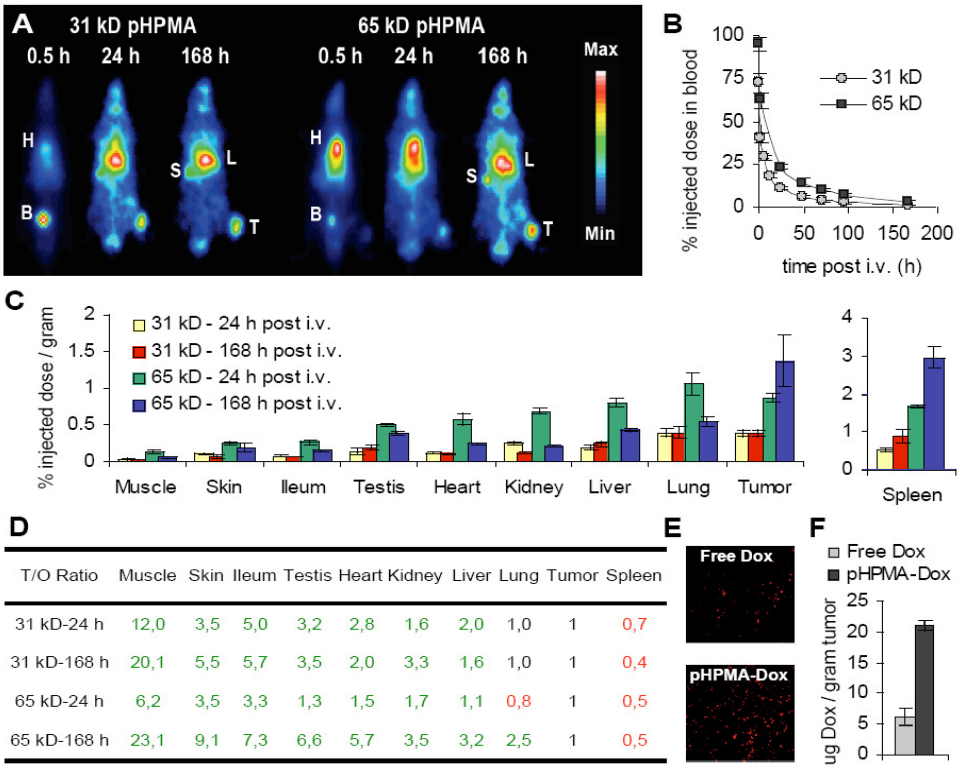

T/O Ratio	Muscle	Skin	Ileum	Testis	Heart	Kidney	Liver	Lung	Tumor	Spleen
31 kD-24 h	12,0	3,5	5,0	3,2	2,8	1,6	2,0	1,0	1	0,7
31 kD-168 h	20,1	5,5	5,7	3,5	2,0	3,3	1,6	1,0	1	0,4
65 kD-24 h	6,2	3,5	3,3	1,3	1,5	1,7	1,1	0,8	1	0,5
65 kD-168 h	23,1	9,1	7,3	6,6	5,7	3,5	3,2	2,5	1	0,5

Chapter 7: Figure 4: HPMA copolymers localise to tumors effectively and selectively. A: Scintigraphic analysis of the biodistribution of two differently sized iodine-131-labeled HPMA copolymers in Copenhagen rats bearing subcutaneously transplanted Dunning AT1 tumors, demonstrating prolonged circulation and effective tumor accumulation (H: heart (blood), B: bladder, S: spleen, L: liver, T: tumor). B: Analysis of the blood concentrations of the two radiolabeled copolymers. Values represent average±s.d. (n=6). C: Quantification of the tumor and organ concentrations of the two radiolabeled copolymers at 24 and 168 h p.i. Values represent average ± s.d. (n=6). Except for lung and spleen, concentrations in tumors were always significantly higher than those in healthy organs ($P<0.05$; two-tailed t-test). D: Quantification of the tumor-to-organ ratios of the copolymers analysed in C, pointing out (in green) that they accumulate more selectively in tumors than in seven out of nine healthy tissues. E: Fluorescence microscopy analysis of the amount of doxorubicin localized to AT1 tumors at 24 h p.i. F: HPLC analysis of the amount of doxorubicin in tumors at 24 p.i., exemplifying the beneficial effect of drug targeting. Values represent average ± s.e.m. (n=5).

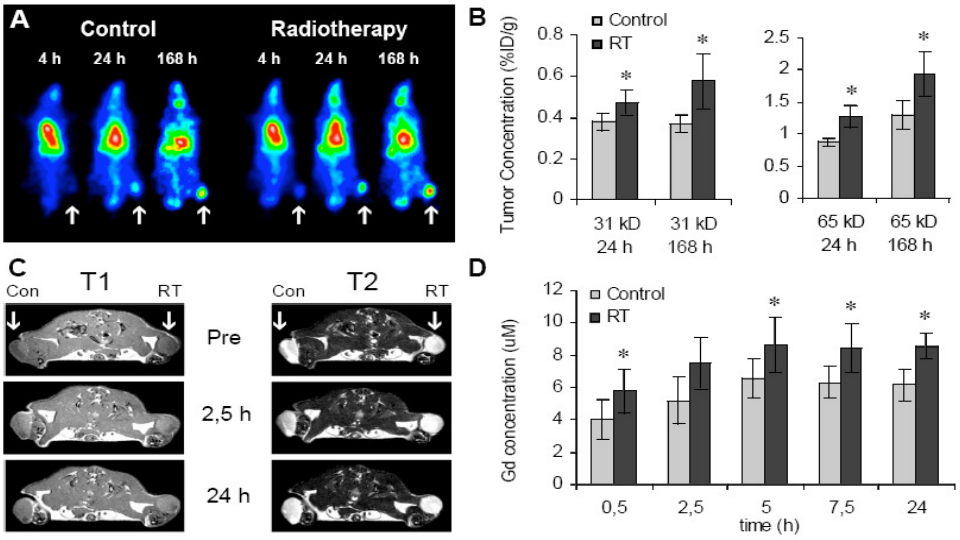

Chapter 7: Figure 5: Radiotherapy improves drug targeting. A: Scintigraphic analysis of the effect of 20 Gy of radiotherapy on the tumor accumulation of an iodine-131-labeled 31 kDa HPMA copolymer, demonstrating that radiotherapy beneficially affects tumor targeting. B: Quantification of the effect of radiotherapy (RT) on the tumor concentrations of the 31 kDa (left panel) and 65 kDa (right panel) copolymer at 24 and 168 h post intravenous injection. Values represent average s.d. (n=3–6). * Indicates P<0.05 (two-tailed t-test). C: Magnetic resonance imaging analysis of the effect of 20 Gy of radiotherapy on the tumor accumulation of the 25 kDa gadolinium-labeled HPMA copolymer. The T1 images correspond to contrast agent accumulation, the T2 images were used for positioning and for morphological analysis. D: Quantification of the effect of radiotherapy on the tumor accumulation of the 25 kDa gadolinium-labeled copolymer. Values represent average ± s.d. (n=3). * Indicates P<0.05 (paired t-test).

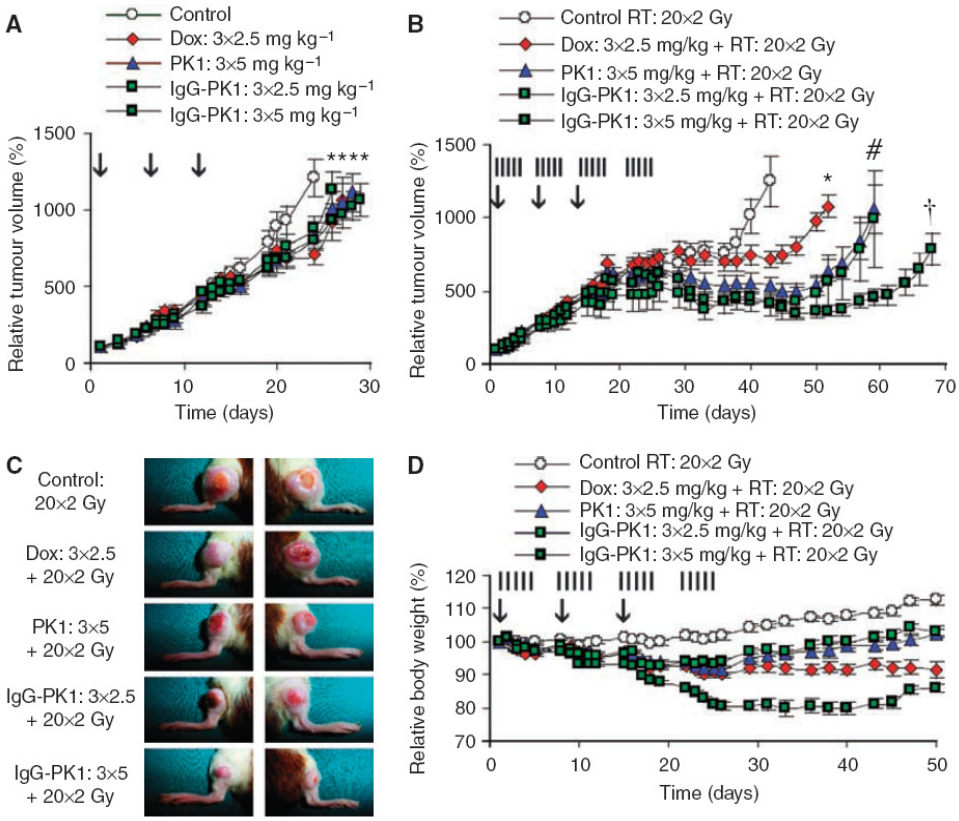

Chapter 7: Figure 6: Drug targeting improves doxorubicin-based radiochemotherapy. A: Growth inhibition of Dunning AT1 tumors induced by three i.v. injections (day 1, 8 and 15; vertical arrows) of saline, of free doxorubicin and of HPMA copolymer-bound doxorubicin. PK1: pHPMA-GFLG-doxorubicin. IgG-PK1: Human IgG-modified pHPMA-GFLG-doxorubicin. Values represent average ± s.e.m (n=6-12). * Indicates $p<0.05$ vs. control (Mann-Whitney U test; Bonferroni-Holm post-hoc analysis). B: Tumor growth inhibition induced by three i.v. injections of the abovementioned chemotherapeutic agents in combination with a clinically relevant regimen of fractionated radiotherapy (20x2 Gy; vertical lines). Values represent average ± s.e.m. (n=8-10). * Indicates $p<0.05$ vs. control, # indicates $p<0.05$ vs. free doxorubicin, and † indicates $p<0.005$ vs. free doxorubicin (Mann-Whitney U test; Bonferroni-Holm post-hoc analysis). C: Representative images (day 50) of tumors treated with the indicated combination regimens. D: Weight loss induced by doxorubicin-based combined modality therapy. Values represent average ± s.e.m. (n=4-5).

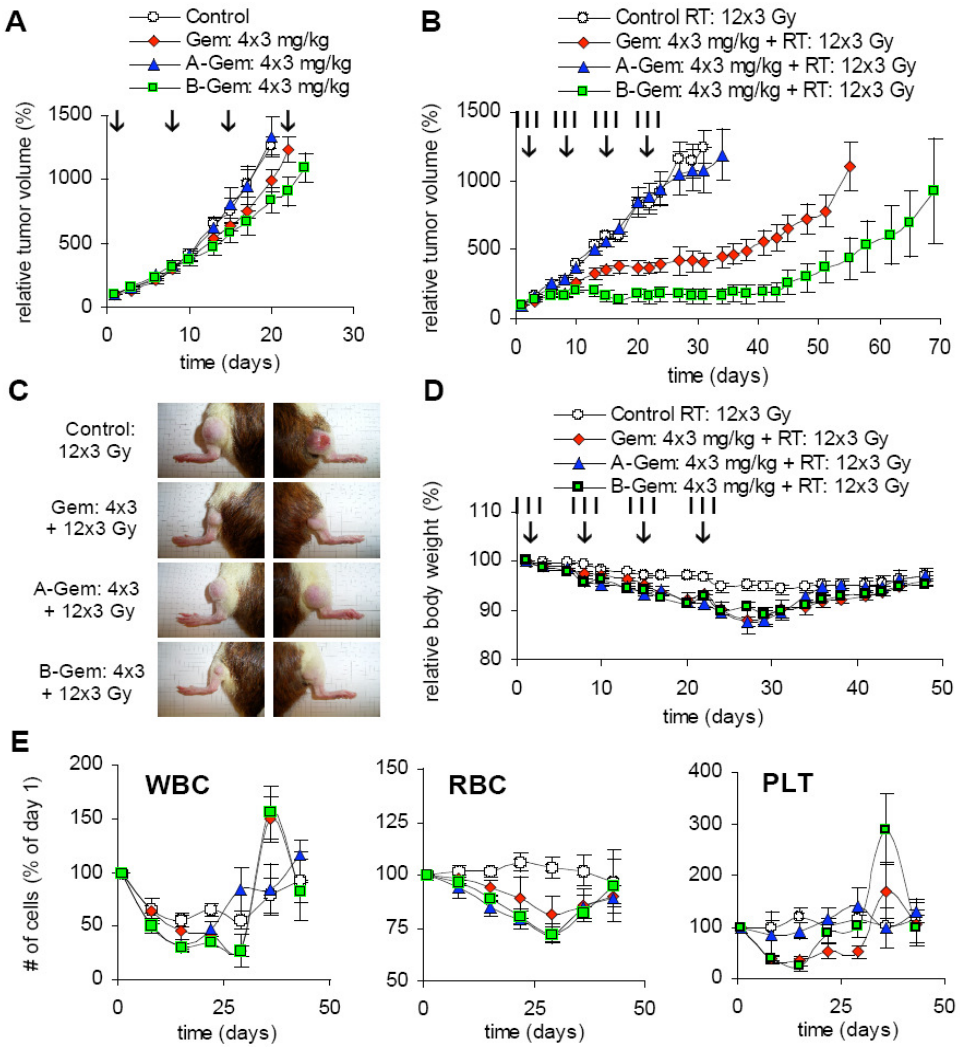

Chapter 7: Figure 8: Drug targeting improves gemcitabine-based radiochemotherapy. A: Growth inhibition of Dunning AT1 tumors induced by four i.v. injections (day 1, 8, 15 and 22; see vertical arrows) of saline, of free gemcitabine and of HPMA copolymer-bound gemcitabine. A-Gem: pHPMA-AH-gemcitabine (20 kDa). B-Gem: pHPMA-GFLG-gemcitabine (24 kDa). * Indicates $p<0.05$ vs. control (Mann-Whitney U test; Bonferroni-Holm post-hoc analysis). B: Tumor growth inhibition induced by four i.v. injections of the abovementioned chemotherapeutic agents in combination with a clinically relevant regimen of fractionated radiotherapy (12x3 Gy; see vertical lines). Values represent average ± s.e.m. (n=10-12). * Indicates $p<0.005$ vs. control, # indicates $p<0.0005$ vs. control, and † indicates $p<0.05$ vs. free gemcitabine (Mann-Whitney U test; Bonferroni-Holm post-hoc analysis). C: Representative images (day 45) of tumors treated with the indicated combination regimens. D: Weight loss induced by gemcitabine-based combined modality therapy. Values represent average ± s.e.m. (n=5-6). E: Hematological toxicity resulting from gemcitabine-based combined modality therapy. The numbers of white blood cells (WBC), red blood cells (RBC) and platelets (PLT) were determined at several different time points after the start of treatment, and are plotted relative to the number of cells at day 1. Values represent average ± s.d. (n=5-6).

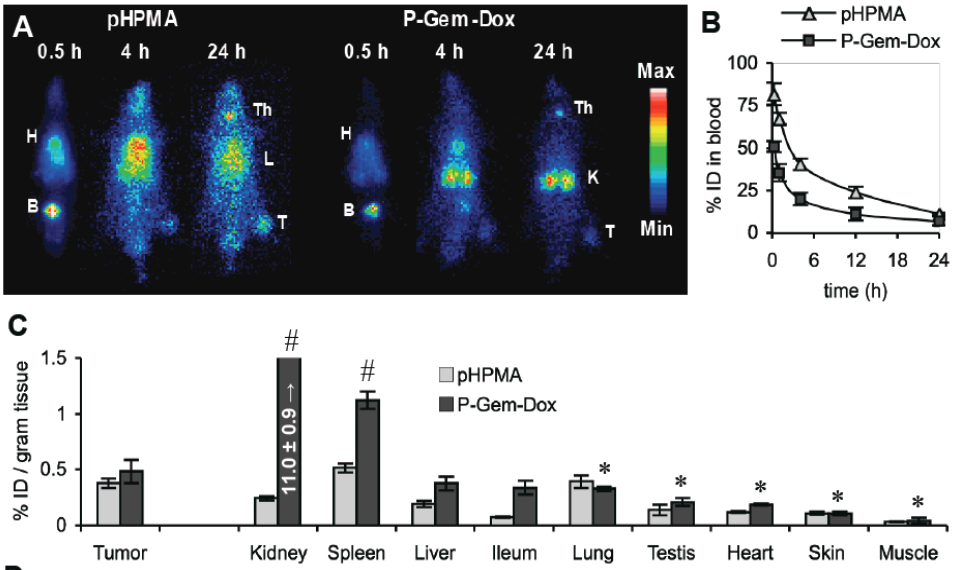

D

T/O Ratio	Tumor	Kidney	Spleen	Liver	Ileum	Lung	Testis	Heart	Skin	Muscle
pHPMA	1	1.55	0.73	1.97	4.97	0.96	2.76	3.17	3.49	12.04
P-Gem-Dox	1	0.04	0.43	1.29	1.43	1.47	2.31	2.58	4.52	11.53

Chapter 8: Figure 4: Biodistribution. A: Scintigraphic analysis of the biodistribution of iodine-131-labeled P-Gem-Dox (24 kDa) and of a radiolabeled drug-free control copolymer (31 kDa) upon i.v. injection into Copenhagen rats bearing subcutaneous Dunning AT1 tumors. At 0.5 h p.i., both copolymers primarily localized to heart (H; representative of the amount still present in circulation) and to bladder (B; confirming renal excretion). At 4 and 24 h p.i., P-Gem-Dox primarily localized to kidney (K), as well as to some extent to tumors (T), whereas the 31 kDa control copolymer primarily accumulated in tumors (T), and in liver, lung and spleen (collectively indicated by L). Note that accumulation in thyroid (Th) corresponds to released radioactive iodine. B: Analysis of the levels of P-Gem-Dox and of the drug-free control copolymer in blood. Values represent average ± s.d. (n=4-6). C: Quantification of the tumor and organ concentrations of the two radiolabeled copolymers at 24 h p.i. Values are expressed as percentages of the injected dose per gram tissue, and represent average ± s.d. (n=4-6). * Indicates significantly lower levels as in tumors ($p<0.05$), and # indicates significantly higher levels ($p<0.05$). D: Quantification of the tumor-to-organ ratios of the two copolymers at 24 h p.i., pointing out (in green) that they localize more selectively to tumors than to 7 out of 9 healthy tissues.

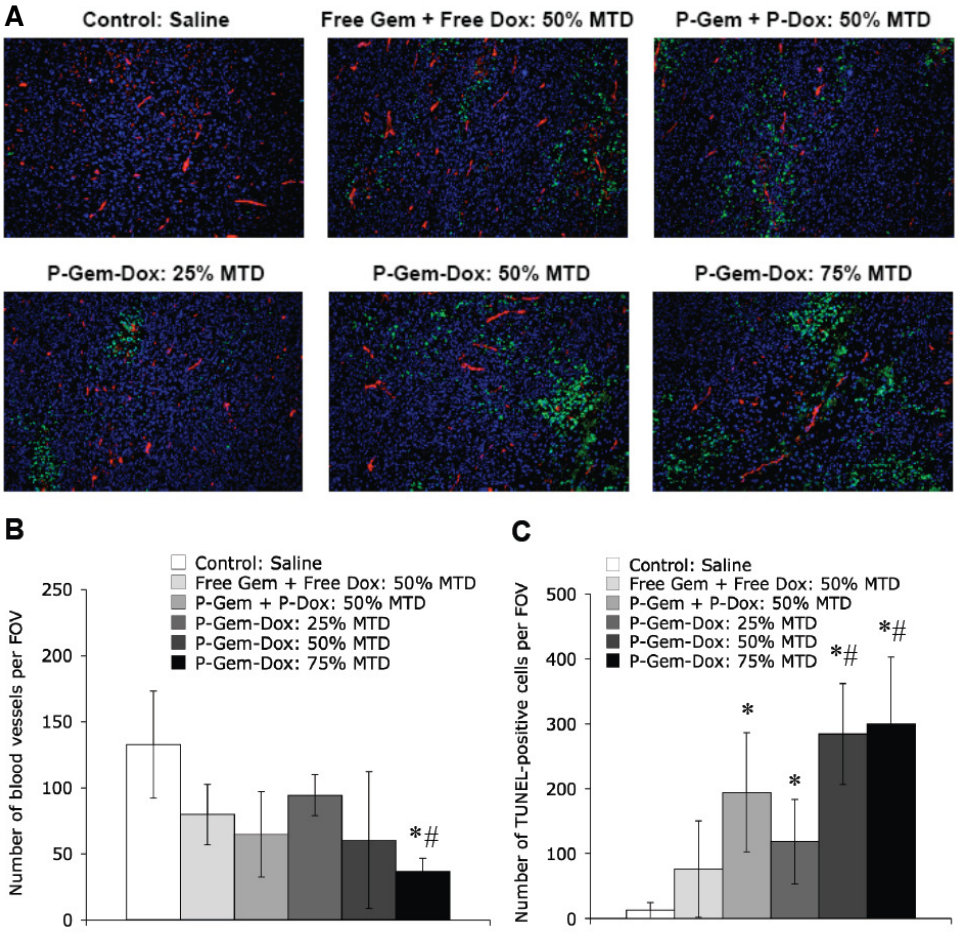

Chapter 8: Figure 6: Effect of drug treatment on angiogenesis and apoptosis. A: Cryosections were obtained one week after the end of therapy (i.e. at day 22; from four tumors per experimental group), and blood vessels and apoptotic cells were stained using antibodies against CD31 (red) and TUNEL (green), respectively. Images were counterstained with DAPI. B and C: Quantification of the number of CD31- and TUNEL-positive structures per 200x field of view (FOV). Values represent average ± s.d. (n=4). * Indicates $p<0.05$ vs. control, and # indicates $p<0.05$ vs. free gemcitabine plus free doxorubicin.

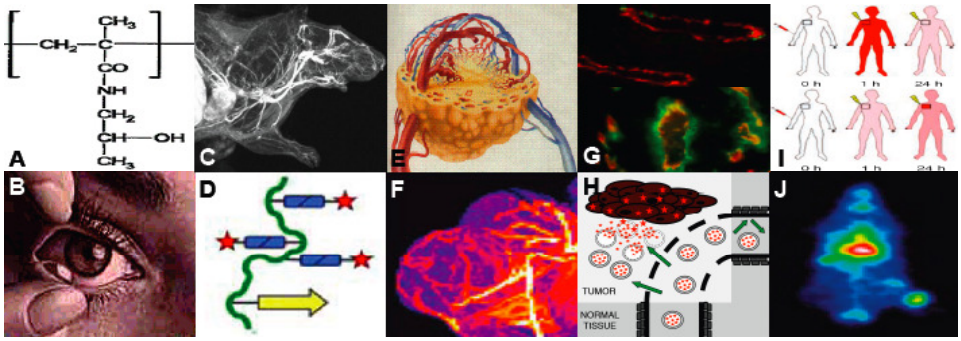

Chapter 9: Figure 1: Rationale for investigating drug targeting to tumors using HPMA copolymers. Theoretical aspects are depicted in white, experimental evidence in black. Copolymers based on HPMA (i.e. *N*-(2-hydroxypropyl)methacrylamide: A) are closely related to poly(HEMA), which has been used in contact lenses (B), and which has been shown to be non-immunogenic and non-toxic. HPMA copolymers can be functionalized with different types of drugs, drug linkers, targeting moieties and imaging agents (D), and when injected intravenously, they circulate for prolonged periods of time (C+F). These prolonged circulation times, together with the fact that solid tumors possess a dense (E) and leaky (G+H) vasculature, enable HPMA copolymers to effectively accumulate in tumors over time (J), by means of a mechanism known as the Enhanced Permeability and Retention effect (EPR: H+I). By improving the delivery of low molecular weight agents to tumors (I+J), HPMA copolymers assist in improving the efficacy of chemotherapy and of combined modality anticancer therapy.

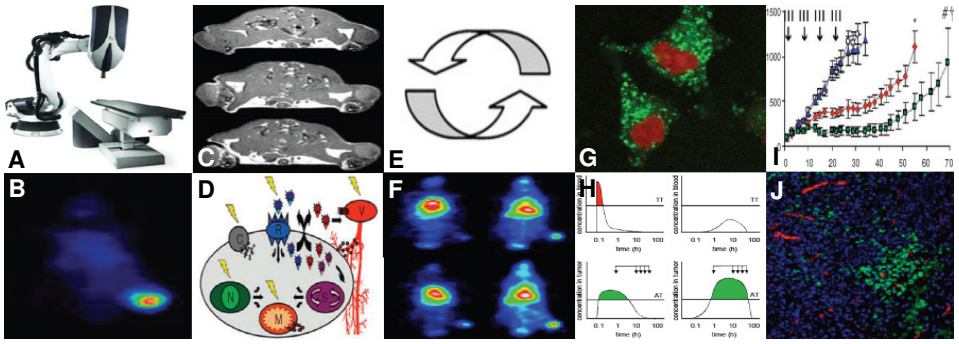

Chapter 9: Figure 2: Improving and extending drug targeting to tumors using HPMA copolymers. To improve their tumor accumulation, HPMA copolymers were combined with radiotherapy (A) and with hyperthermia. Gamma-scintigraphy (B+F), magnetic resonance imaging (C) and fluorescence microscopy (G+J) were used to visualize the biodistribution of the copolymers. As opposed to hyperthermia, radiotherapy was found to be able to improve the tumor accumulation of the copolymers independent of the tumor model used (C+F). This was considered to be due to the fact that radiotherapy exerts several general physiological effects, such as an increase in the expression of VEGF and FGF, an induction of (endothelial cell) apoptosis, a reduction of the tumor cell density, and a reduction of the interstitial fluid pressure, which can all be expected to beneficially affect the tumor accumulation of HPMA copolymers (D). In addition, the copolymers were shown to be able to interact synergistically (E) with radiotherapy, with on the one hand radiotherapy increasing the tumor accumulation of the copolymers (C+F), and with on the other hand the copolymers increasing the therapeutic index of radiochemotherapy (H+I). Clinically relevant regimens of radiotherapy and chemotherapy were used (H), and promising results were obtained both for doxorubicin and for gemcitabine (I). Finally, to demonstrate that HPMA copolymers can be used to deliver two different drugs to tumors simultaneously, a polymeric prodrug carrying both doxorubicin and gemcitabine was synthesized, and this construct was shown to be effective both in vitro and in vivo (J). Together, these findings convincingly demonstrate that HPMA copolymer-based nanomedicine formulations hold significant potential for improving the efficacy of combined modality anticancer therapy.